

THE BIOLOGICAL SIGNIFICANCE OF CANCER ANTIGEN 125

Daryn Michael Bsc Hons

Thesis presented for the Degree of Philosophiae Doctor

May 2006

**Institute of Nephrology
Wales College of Medicine
Cardiff University
Heath Park
Cardiff
CF14 4XN**

UMI Number: U584095

All rights reserved

INFORMATION TO ALL USERS

The quality of this reproduction is dependent upon the quality of the copy submitted.

In the unlikely event that the author did not send a complete manuscript and there are missing pages, these will be noted. Also, if material had to be removed, a note will indicate the deletion.



UMI U584095

Published by ProQuest LLC 2013. Copyright in the Dissertation held by the Author.
Microform Edition © ProQuest LLC.

All rights reserved. This work is protected against
unauthorized copying under Title 17, United States Code.



ProQuest LLC
789 East Eisenhower Parkway
P.O. Box 1346
Ann Arbor, MI 48106-1346

DEDICATION

For Mam and Dad.

ACKNOWLEDGEMENTS

I gratefully acknowledge the Medical Research Council (MRC) and Gambro Renal, Lund, Sweden, for funding the project.

A big thank-you goes to everyone at the Institute (both past and present) for their advice and support throughout the work. Thank you to John Martin, Jamie Monslow, Rachel McLoughlin, Dean Harris, Ruth Mackenzie and Ceri Fielding for providing guidance and support on a regular basis. Thanks also to all who offered useful and meaningful advice during departmental laboratory meetings.

A massive thank you to Dr Timothy Bowen for the support, patience, friendship and limitless supply of guidance he provided throughout this research. Thank you to Kathrine Craig for providing statistical expertise. Thank you to Professor John Williams for his encouragement and support during the project, for making me feel welcome as a member of the Institute and for his constructive criticism of the thesis.

An enormous thank you goes to Professor Nick Topley for his inspiring and optimistic attitude in the face of adversity, for his encouragement, friendship and for being an excellent supervisor over the past three and a half years.

Finally without the support of my family I would never have come this far. Mam, Dad, Rebecca and Liam, Thanks!

SUMMARY

Morphological changes including fibrosis, vascular degeneration and loss of mesothelium occur to the peritoneal membrane during peritoneal dialysis. The loss of mesothelium is thought to effect peritoneal homeostasis and host defence, as these cells play a pivotal role in these organs response to inflammation. Cancer antigen 125 (CA125), a mucilaginous high molecular weight glycoprotein, has been used as a marker of peritoneal mesothelial cells mass/turnover and membrane functional integrity in peritoneal dialysis patients. The use of new more biocompatible dialysis solutions is associated with an increase in CA125 effluent concentration, however it's precise molecular nature, function and regulation is poorly defined. This study investigates the transcriptional mechanisms regulating CA125 expression in human peritoneal mesothelial cells as well as CA125's regulation in response to inflammation. Additionally, CA125's function in the process of mesothelial cell repair is examined using a novel mesothelial wound healing system.

These investigations have:

- Successfully reconstructed the genomic structure of CA125 and characterised its proximal promoter region.
- Demonstrated regulation of CA125 cell surface expression and shedding in response to IL-1 β and IL-6 trans-signalling.
- Shown the retardation of human peritoneal mesothelial cell CA125 shedding in response to high levels of glucose degradation products present within peritoneal dialysis fluids.
- Shown the improved wound healing of mesothelial cells in response to elevated CA125 levels.

These investigations have clarified existing discrepancies regarding CA125 regulation during inflammation by demonstrating its altered expression at the cell surface, in response to inflammatory mediators. Additionally, this work has linked clinical observations regarding CA125 effluent levels during peritoneal dialysis to a potential role of CA125 in wound healing of the mesothelium.

PUBLICATIONS AND PRESENTATIONS ARISING FROM THIS THESIS

Peer-reviewed publications

Topley N, Michael DR, Bowen T (2005) CA125: Holy Grail or a poisoned chalice?
Nephron Clinical Practice:100(2)c52-c54.

Published abstracts

Daryn R. Michael, Timothy Bowen, John D Williams, Anders Wieslander and Nicholas Topley (2005). The functional significance and control of expression of CA125. *The 7th European Peritoneal Dialysis Meeting*, P-147.

Daryn R. Michael, Timothy Bowen, John D Williams, Anders Wieslander and Nicholas Topley (2003). The functional significance and control of expression of CA125. *The 19th Annual Postgraduate Research Day*. ISSN: 0967-7496 Issue: 11, PP-19.

Oral presentations

Daryn R. Michael, Timothy Bowen, John D Williams, Anders Wieslander and Nicholas Topley (2004). The functional significance and control of expression of CA125. *Presented at the 19th Annual Postgraduate Research Day, Wales College of Medicine, Cardiff University, Cardiff.*

Poster presentations

Daryn R. Michael, Timothy Bowen, John D Williams, Anders Wieslander and Nicholas Topley (2003). The functional significance and control of expression of CA125. *Presented at the 19th Annual Postgraduate Research Day, Wales College of Medicine, Cardiff University, Cardiff.*

Daryn R. Michael, Timothy Bowen, John D Williams, Anders Wieslander and Nicholas Topley (2005). The functional significance and control of expression of CA125. Presented at The 7th European Peritoneal Dialysis Meeting, Prague, Czech Republic.

ABBREVIATIONS

APS	Ammonium persulphate
AQP	Aquaporin
BLAST	Basic local alignment search tool
BM	Basement membrane
BRE	TFIIIB recognition element
BSA	Bovine serum albumin
CA125	Cancer antigen 125
CAPD	Continuous ambulatory peritoneal dialysis
cDNA	Coding deoxyribonucleic acid
CHO	Chinese hamster ovary cells
CNBr	Cyanogen Bromide
CPM	Counts per minute
CRP	C-reactive protein
DNA	Deoxyribonucleic acid
dNTP	Deoxyribonucleotide triphosphate
DPE	Downstream promoter element
DTT	Dithiothreitol
ECM	Extracellular matrix
EDTA	Ethylenediaminetetra (Acetic) acid
EGF	Epidermal growth factor
ELISA	Enzyme linked immuno-sorbant assay
ER	Oestrogen receptor
ERE	Oestrogen responsive element
ERF	Established renal failure
ERK	Extracellular response kinase
EST	Expressed sequence tag
FACS	Fluorescent activated cell sorting
FCS	Fetal calf serum
FITC	Fluorscein Isothiocyanate

GAPDH	Glyceraldehyde-3-phosphate dehydrogenase
gDNA	Genomic deoxyribonucleic acid
GDP	Glucose degradation product
GPI	Glycanphosphatidylinositol anchor
gp130	Glycoprotein 130
GRF	Glomerular filtration rate
HA	Hyaluronic Acid
HAS	Human hyaluronan synthase
HeLa	Human epithelial cells
HEPES	N-2-hydroxyethylpiperazine-N'-2ethanesulfonic acid
HK-2	Human kidney 2 cell
HLGP	Hypothetical luminal glycoprotein
HPMC	Human peritoneal mesothelial cell
IκB	Inhibitor of Nuclear factor kappa B
ICAM	Intracellular adhesion molecule 1
IFN	Interferon
IL	Interleukin
IL-1RacP	Interleukin 1 receptor accessory protein
IRAK-1	Interleukin receptor associated kinase-1
ITF	Intestinal trefoil factor
JAK	Janus kinase
LARII	Luciferase assay reagent II
M199	Medium 199
MAPK	Mitogen activated protein kinase
MCP	Monocyte chemoattractant protein
MMP	Matrix metalloproteinase
MPF	Megakaryocyte potentiating factor
mRNA	Messenger ribonucleic acid
NCBI	National centre for biotechnology information
NF-κB	Nuclear factor kappa B
NF-1	Nuclear factor 1

OC125	CA125 specific monoclonal antibody
ORF	Open reading frame
PA	Plasminogen activator
PAI	Plasminogen activator inhibitor
PBS	Phosphate buffered saline
PCR	Polymerase chain reaction
PD	Peritoneal dialysis
PDF	Peritoneal dialysis fluid
PMΦ	peritoneal macrophage
PMN	Polymorphonuclear cell (Neutrophil)
QPCR	Quantitative polymerase chain reaction
RA	Retinoic acid
RARE	Retinoic acid responsive element
RACE	Rapid amplification of cDNA ends
RANTES	Regulated upon activation normal T cell expressed
RAR	Retinoic acid receptor
RIA	Radioimmunoassay
RNA	Ribonucleic acid
RT	Room temperature
RT-PCR	Reverse transcriptase polymerase chain reaction
SDS	Sodium lauryl sulphate
SEA	a module first identified in Sea urchin sperm protein
sIL-6R	Soluble interleukin 6 receptor
siRNA	Small interfering ribonucleic acid
SNT	Supernatant
Sp1	Stimulating protein 1
Sp3	Stimulating protein 3
STAT	Signal transducer and activator of transcription
TAE	Tris acetate ethylenediaminetetra (Acetic) acid
Temed	N,N,N,N -Tetramethyl-ethylenediamine
TFBS	Transcription factor binding site

TGF	Transforming growth factor
TIR	Toll IL-1 receptor
TIS	Transcription initiation site
TLR	Toll-like receptor family
T_M	Annealing temperature
TNF	Tumour necrosis factor
TRAF	TNF receptor associated factor
Tris	Trisphosphate
UCSC	University of California Santa Cruz
UTR	Un-translated region
UV	Ultra-violet
VEGF	Vascular endothelial growth factor

CONTENTS**Page**

Title page	i
Declaration	ii
Dedication	iii
Acknowledgements	iv
Summary	v
Publications and presentations arising from this thesis	vi
Abbreviations	vii-xi

Chapter 1: Introduction	1
1.1 Established Renal Failure	2
1.2 Peritoneal Dialysis	2-6
1.2.1 Background	
1.2.2 The technique	
1.2.3 Complications of PD	
1.2.3.1 PDF biocompatibility	
1.2.3.2 Peritonitis	
1.3 The Peritoneal Cavity	7-14
1.3.1 Anatomy	
1.3.2 The peritoneal membrane	
1.3.3 The mesothelium	
1.3.4 Alterations in the peritoneal membrane	
1.4 Peritoneal Inflammation	15-20
1.4.1 Control of the peritoneal inflammatory response	
1.4.2 The cytokine network of the peritoneum	
1.4.3 Resolution of peritoneal inflammation	

1.5	Interleukin-1 – Role in inflammation and mechanism of action	20-21
1.6	Interleukin-6 – Role in inflammation and mechanism of action	21-22
1.7	Cancer Antigen 125	23-28
	1.7.1 CA125 in ovarian cancer	
	1.7.2 CA125 in peritoneal dialysis	
	1.7.3 PDF biocompatibility	
	1.7.4 CA125 in peritonitis	
1.8	The Molecular Status of CA125	28-31
	1.8.1 The protein	
	1.8.2 CA125 is a mucin type glycoprotein	
	1.8.3 CA125 proposed structure	
	1.8.4 Molecular weight	
	1.8.5 Cell surface secretion	
1.9	The Gene	31-32
	1.9.1 Initial characterization	
	1.9.2 Cloning of the CA125 gene	
1.10	Function of CA125	32-34
	1.10.1 Lubricating molecule	
	1.10.2 Mesothelin binding and cellular adhesion	
	1.10.3 Galectin binding and export	
1.11	Aim of Thesis	35-36
	1.11.1 Aim	
	1.11.2 Scope of the thesis	

Tables

1.1	Important functions of the mesothelium	11
-----	--	----

Figures

1.1	Thickness of the sub-mesothelial compact zone in PD	6
1.1	Structure of the peritoneal membrane	9
1.1	Alterations of the peritoneal membrane due to long term PD	14
1.1	The humoral and cellular components of the inflammatory response	15
1.1	CA125 levels during peritonitis	16
1.1	The cytokine network in peritoneal inflammation	18
1.1	The sequence of events leading to resolution of peritoneal infection by resident and recruited cell populations	19
1.8	Constitutive expression of CA125	25
1.9	Proposed structure of the CA125 antigen	30

Chapter 2:	Methods and Materials	37
-------------------	------------------------------	-----------

2.1	Computational Based Methods	38
------------	------------------------------------	-----------

2.1.1	CA125 <i>in silico</i> gene reconstruction	
2.1.2	Identification of putative transcription factor binding sites	

2.2	Cell Culture	39-43
------------	---------------------	--------------

2.2.1	Reagents	
2.2.2	Isolation and culture of human peritoneal mesothelial cells	
2.2.3	HPMC growth conditions	
2.2.4	Characterization of HPMC	
2.2.4.1	HPMC morphology	
2.2.4.2	Immunohistochemistry	
2.2.5	Human Kidney (HK) 2 cells	

2.2.6	HK-2 growth conditions	
2.2.7	Monolayer sub-culture	
2.2.8	Growth arrest	
2.2.9	Cell stimulation	
2.2.10	Oestrogen and retinoic acid stimulation	
2.3	RNA Analysis	43-48
2.3.1	Chloroform/Isopropanol RNA extraction	
2.3.2	Determination of DNA and RNA concentration	
2.3.3	RNA quantification	
2.3.4	Semi-quantitative RT-PCR	
2.3.5	5'-Rapid amplification of cDNA ends (5'-RACE)	
2.3.6	RNA interference	
	2.3.6.1 Plate layout	
	2.3.6.2 Total cell Count	
	2.3.6.3 siRNA transfection	
2.4	DNA Analysis	48-50
2.4.1	Polymerase Chain Reaction	
2.4.1	Quantitative Polymerase Chain Reaction	
2.4.3	Primer design	
2.4.4	Sizing of PCR products	
2.4.5	Purification of PCR products	
2.5	Cloning Techniques	50-53
2.5.1	Cloning of 5'-RACE products	
2.5.2	Generation of luciferase promoter constructs	
2.5.3	Transformation	
2.5.4	Purification of recombinant vectors	
2.5.5	Screening for presence of inserts	

2.5.6	Sequence analysis	
2.6	Luciferase Analysis	53-55
2.6.1	Plate set up	
2.6.2	Transient transfection	
2.6.3	Reporter gene analysis in HPMC	
2.6.4	Gene analysis in HK-2 cells	
2.7	Western Blot	55-57
2.7.1	Gel preparation	
2.7.2	Sample preparation and electrophoresis	
2.7.3	Supernatant sample preparation	
2.7.4	Cell lysate sample preparation	
2.7.5	Protein concentration estimation	
2.7.6	Transblotting	
2.7.7	Blocking and antibodies	
2.7.8	Detection	
2.8	FACS Analysis	58-59
2.8.1	CA125 HPMC surface expression	
2.9	Radioimmunoassay (RIA)	60
2.9.1	Determination of CA125 supernatant concentration	
2.10	Enzyme-Linked Immunoabsorbent Assays (ELISA)	61-62
2.10.1	MCP-1 ELISA	
2.10.2	IL-8 ELISA	
2.11	Time Lapse Photography	62-63
2.11.1	Scratch wounding of HPMC monolayer	
2.11.2	Assessment of wound closure by time-lapse photography	

Appendix I		64
Characterisation of HPMC		
Appendix II		65
1. 5'-RACE PCR protocol		
2. Standard PCR protocol		
Appendix III		66
1. pCR [®] 2.1 -TOPO [®] sequencing vector Map		
2. pCR [®] 2.1 -TOPO [®] Multiple cloning site		
Appendix IV		67
1. pGL3 Basic (Modified) Vector Map		
2. pGL3 basic (Modified) multiple cloning site		
Appendix V		68
1. LB Medium		
2. LB Agar plates		
Appendix VI		69
Optimisation of HPMC transfection conditions		
Tables		
2.1	Antibodies used for the characterization of HPMC	41
2.2	Restriction enzymes used in plasmid screening	52
2.3	Sequencing oligonucleotide primers	53
2.4	Western gel compositions	55
Figures		
2.1	RNA agarose gel showing the 18S and 28S ribosomal subunits of total RNA	44

2.2	5'-RACE Mechanism	46
2.3	Mechanism of gene knockdown by interference RNA	48
2.4	Calculation of percentage shift in positively stained cells	59
2.5	Calibration curve showing log of CPM versus log of CA125 concentration	60
Chapter 3: Elucidation of the genomic structure and analysis of the putative promoter region of the human CA125 gene		70
3.1	Introduction	71-73
3.2	Methods	74-79
3.2.1	<i>In silico</i> reconstruction of the human CA125 gene	
3.2.2	<i>In silico</i> analysis of the proximal promoter region for transcription factor binding sites	
3.2.3	Amplification of transcribed products from CA125 exon 1 and 2 from total RNA	
3.2.4	Analysis of CA125 terminal expressed sequences from purified mRNA	
3.2.5	Amplification and analysis of the putative CA125 proximal promoter transcriptional activity <i>in vitro</i>	
3.2.6	Analysis of CA125 promoter activity in response to retinoic acid and oestrogen stimulation	
3.2.7	Statistical analysis of luciferase assays	
3.3	Results	80-103
3.3.1	<i>In silico</i> reconstruction of the human CA125 gene	
3.3.2	<i>In silico</i> analysis of the proximal promoter region for transcription factor binding sites	
3.3.3	Amplification of the CA125 5' region	
3.3.4	Analysis of the 5' terminal expressed sequence	

3.3.5	Amplification and analysis of the putative CA125 proximal promoter transcriptional activity <i>in vitro</i>	
3.3.6	Analysis of CA125 promoter activity in response to retinoic acid and oestrogen stimulation	
3.4	Discussion	104-109
Appendix I		110-111
	5'-RACE Sequence data	
Appendix II		112
A.	The predicted composite sequence of CA125 (AF414442) and next upstream EST (AA633929)	
B.	Nucleotide sequence (5'-3') of RT-PCR band production using the RT-EST1 primers	
Appendix III		113
	CA125 Expression by HK-2 cells <i>versus</i> HPMC	
Tables:		
3.1	CA125 exon 1 and 2 oligonucleotide primers	74
3.2	CA125 mRNA termini oligonucleotide primers	75
3.3	5'-RACE oligonucleotide primers	75
3.4	CA125 upstream analysis oligonucleotide primers	77
3.5	EST analysis oligonucleotide primers	77
3.6	Nested CA125 promoter construct oligonucleotide primers	78
3.7	Predicted intronic and exonic structure of CA125	81
3.8	CA125 (5'-end) primer oligonucleotide specificity	85
Figures		
3.1	Schematic representation of an eukaryotic promoter region	72

3.2	Oligonucleotide primer sites for the analysis of the 5'-end of the CA125 gene	76
3.3	CA125 genomic structure	82
3.4	Analysis of 1kb upstream of reference CA125 mRNA sequence for TFBSs	83
3.5	Identification of an ERE in the proximal promoter region of the CA125 gene	84
3.6	Amplification of products from CA125 exons 1 and 2 by RT-PCR	86
3.7	Genomic and protein sequence of CA125 5'-UTR derived from the NCBI database	87
3.8	Amplification of the 5' and 3' terminals of the CA125 gene	88
3.9	CA125 specific 5'-RACE reaction	89
3.10	Genomic and protein sequence of CA125 5'-UTR derived from the NCBI database	90
3.11	Schematic representation of sequential upstream primer positions and fragment sizes (bp)	91
3.12	PCR amplification of the sequence upstream of the 5'-UTR extension	92
3.13	Upstream EST analysis	94
3.14	RT-PCR amplification spanning CA125 5' coding region and EST AA633839	95
3.15	Upstream putative promoter constructs	96
3.16	PCR amplification of nested promoter fragments from genomic DNA	97
3.17	Genomic and protein sequence of CA125 5'-UTR derived from the NCBI database	98
3.18	Endogenous luciferase activity of the CA125 proximal promoter constructs	99
3.19	Identification of the oestrogen receptor subunits ER α and ER β in HPMC by Western blot analysis	
3.20	Luciferase activity of the CA125 proximal promoter constructs	

	in response to retinoic acid and 17 β -oestradiol stimulation	102
Chapter 4:	The regulation of CA125 expression during inflammation	114
4.1	Introduction	115-116
4.2	Methods	117-120
4.2.1	Analysis of CA125 production by HPMC	
4.2.2	Analysis of CA125 regulation in response to IL-1 β stimulation	
4.2.2.1	Analysis of CA125 transcription	
4.2.2.2	Analysis of CA125 cell surface expression	
4.2.2.3	Analysis of CA125 cell surface secretion	
4.2.2.4	Analysis of CA125 promoter activity	
4.2.3	Analysis of CA125 regulation in response to IL-6/sIL-6R stimulation	
4.2.3.1	Analysis of CA125 transcription	
4.2.3.2	Analysis of CA125 cell surface expression	
4.2.3.3	Analysis of CA125 cell surface secretion	
4.2.3.4	Analysis of CA125 promoter activity	
4.2.4	Analysis of MCP-1 concentration in response to IL-1 β and IL-6/sIL-6R stimulation	
4.3	Results	121-134
4.3.1	Analysis of CA125 production by HPMC	
4.3.2	Analysis of CA125 regulation in response to IL-1 β stimulation	
4.3.2.1	Analysis of CA125 transcription	
4.3.2.2	Analysis of CA125 cell surface expression	
4.3.2.3	Analysis of CA125 cell surface secretion	
4.3.2.4	Analysis of CA125 promoter activity	
4.3.3	Analysis of CA125 regulation in response to IL-6/sIL-6R stimulation	
4.3.3.1	Analysis of CA125 transcription	
4.3.3.2	Analysis of CA125 cell surface expression	

- 4.3.3.3 Analysis of CA125 cell surface secretion
- 4.3.3.4 Analysis of CA125 promoter activity
- 4.3.4 Analysis of MCP-1 concentration in response to IL-1 β and IL-6/sIL-6R stimulation

4.4 Discussion 135-139

Tables

- 4.1 Oligonucleotide primers used in RT-PCR experiments 118

Figures

- 4.1 Western Blot analysis of CA125 production by HPMC 121
- 4.2 HPMC expression of CA125 in response to IL-1 β 122
- 4.3 Densitometric analysis of CA125 gene expression in response to IL-1 β stimulation 123
- 4.4 Optimization of the OC125 antibody concentration for mesothelial cell CA125 staining 124
- 4.5 Control of mesothelial cell CA125 cell surface expression in response to IL-1 β stimulation 125
- 4.6 Cell surface secretion of CA125 from HPMC in response to IL-1 β stimulation 126
- 4.7 Luciferase activity of the CA125 proximal promoter constructs in response to IL-1 β stimulation 127
- 4.8 HPMC expression of CA125 in response to IL-6/sIL-6R stimulation 128
- 4.9 Densitometric analysis of CA125 gene expression in response to IL-6/sIL-6R stimulation 129
- 4.10 Control of mesothelial cell CA125 cell surface expression in response to IL-6/sIL-6R stimulation 130
- 4.11 Change in HPMC CA125 cell surface secretion in response to IL-6 and sIL-6R stimulation 131

4.12	Luciferase activity of the CA125 proximal promoter constructs in response to IL-6/sIL-6R stimulation	132
4.13	MCP-1 production by HPMC in response to IL-1 β and IL-6/sIL-6R stimulation	134
Chapter 5:	The potential role of CA125 in mesothelial cell repair	140
5.1	Introduction	141-144
5.2	Methods	145-146
5.2.1	The effect of exogenous CA125 on mesothelial wound healing	
5.2.2	The effect of CA125 blocking on mesothelial wound healing	
5.2.3	Examination of CA125 shedding in response to high and low levels of glucose degradation products (GDP) present in peritoneal dialysis fluid (PDF)	
5.2.4	Statistical analysis	
5.3	Results	148-153
5.3.1	The effect of exogenous CA125 on mesothelial wound healing	
5.3.2	The effect of CA125 blocking on mesothelial wound healing	
5.3.3	Examination of CA125 shedding in response to high and low levels of glucose degradation products (GDP) present in peritoneal dialysis fluid (PDF)	
5.4	Discussion	154-157
Appendix I		158
	CA125 effluent levels in response to low GDP dialysis solutions	
Appendix III		159
	HPMC wound closure in response to Gambrosol [®] and Gambrosol-trio [®]	

Figures		
5.1	The effect of PD on the peritoneal mesothelium	141
5.2	Time dependant closure of an <i>in vitro</i> wounded human peritoneal mesothelial cell monolayer	142
5.3	Analysis of HPMC rate of wound closure	145
5.4	The effect of exogenous CA125 on the rate of HPMC re-mesothelialization	149
5.5	The effect of exogenous OC125 on the rate of HPMC re-mesothelialization	151
5.6	The effect of GDPs on HPMC CA125 shedding	152
Chapter 6:	General Discussion	160
Appendix I		170-174
	siRNA knockdown of mesothelial cell GAPDH expression	
Tables		
6.1	Oligonucleotide primers used in siRNA (RT-PCR) analysis	170
Figures		
6.1	The potential role of CA125 in re-mesothelialization as a response to GDP levels in the dialysed peritoneum	165
6.2	Potential involvement of CA125 in re-mesothelialization in response to peritonitis induced injury	166
6.3	Optimisation of GAPDH knockdown in HPMC	171
6.4	Optimisation of GAPDH siRNA concentration in HPMC	173
6.5	Analysis of GAPDH expression 48 hours after siRNA transfection using quantitative PCR	174
References		175-201

Chapter 1

Introduction

1.1 Established Renal Failure

Established renal failure (ERF) occurs as the result of permanent deterioration of the renal function (usually expressed as glomerular filtration rate (GFR)). Normal GFR in adults is in the region of 80-130ml/min for males and 70-120 ml/min for females. Thirty five percent of newly diagnosed cases of ERF per year occur as a direct result of diabetes. Other causes include hypertension, primary and secondary glomerulopathies, cystic and interstitial renal diseases and obstructive uropathy [Pastan and Bailey, 1998].

Currently, the preferred treatment for ERF, in most individuals, is kidney transplantation. Unfortunately lack of donor kidneys and transplant failure (kidney rejection) limits the effectiveness of this treatment [Vale *et al*, 2005]. Both haemodialysis and peritoneal dialysis (PD) can be used to replace the excretory function of the kidney and therefore used to treat ERF [Pastan and Bailey, 1998].

The prevalence of ERF is increasing at a rate of approximately 8% per year. In Wales alone, 120 new patients are being accepted for long-term dialysis each year. Such treatment is associated with a significant impairment in quality of life and therefore poses considerable social and economic consequences [Pastan and Bailey, 1998][Vale *et al*, 2005].

1.1 Peritoneal Dialysis

1.1.1 Background

Peritoneal dialysis is now an established form of therapy in the management of ERF. First attempts to use peritoneal dialysis as a treatment for ERF were made by Wear and co-workers in 1938 [Wear *et al*, 1938]. In 1959 a simplified method of intermittent irrigation of the peritoneal cavity using a disposable catheter and commercially made PD fluids was developed by Maxwell and colleagues [Gokal and Mallick, 1999]. CAPD became a viable alternative to haemodialysis 19 years later, in 1978, when Moncrief and

Popovich showed its adequacy as a treatment for kidney failure in a long-term clinical trial [Popovich *et al*, 1978].

At present more than 35% of the ERF population in the United Kingdom are treated using PD [Vale *et al*, 2005]. Due to its effectiveness as a treatment PD has now outstripped haemodialysis worldwide [Prichard, 2005] and is generally accepted as the better form of treatment. These potential advantages can be attributed to its slower decrease in residual renal function and its adaptability to suit patient requirements [Fenton *et al*, 1997].

1.1.2 The Technique

The human peritoneal membrane functions as a semi-permeable membrane and hence can be used as a dialysis organ [Vale *et al*, 2005]. Haemodialysis depends on hydrostatic pressure to remove waste products from the body, whereas, peritoneal dialysis utilises the peritoneum as a semi-permeable membrane across which ureamic waste products and water are removed via the physiological processes of diffusion, convective transport and osmosis [Gokal and Mallick, 1999].

In practice, PD is performed in a closed system composed of the peritoneal cavity, a long-term catheter anchored in subcutaneous tissue and a plastic container of peritoneal dialysis fluid (PDF) [Gokal and Mallick, 1999]. A typical treatment will consist of 4 exchanges of 2-2.5 litres of dialysis fluid per day [Pastan and Bailey, 1998]. The composition of the dialysis fluid creates an osmotic and chemical gradient between the dialysis fluid and the blood capillaries of the peritoneum. During the period of dwell, solute transport occurs across the peritoneal membrane. Uremic metabolites move along a chemical gradient from the blood into the dialysate in a process known as hydrostatic ultrafiltration. Excess water is removed along the osmotic gradient by a process known as osmotic ultrafiltration [Chaimovitz, 1994]. The dialysis solution is then drained from the peritoneal cavity and the cycle is repeated. Various techniques and regimes have now emerged that enhance these transport characteristics [Gokal and Mallick, 1999], although the efficiency largely depends on the available vascular surface area [De Vriese, 2002].

1.1.3 Complications of PD

Due to the bioincompatible nature of conventional peritoneal dialysis fluid, major problems occur that limit its effectiveness as a treatment of ERF. These include the loss of the peritoneal integrity, and therefore a decrease in its ability to function as a dialysing organ [Williams *et al*, 2003][Davies *et al*, 1996]. In addition, the presence of an indwelling catheter provides a portal for microbial entry and the associated episodes of peritonitis (intra-peritoneal inflammation) that occur significantly impact on patient and technique survival [Davies *et al*, 1996][Pastan and Bailey, 1998][Gokal and Mallick, 1999][Troidle, 2003].

1.1.3.1 PDF biocompatibility

The poor biocompatibility of dialysis fluids has a detrimental effect on the effectiveness of peritoneal dialysis as a treatment. During the heat sterilization of the dialysis fluid prior to infusion, harmful breakdown products of glucose (glucose degradation products) are formed by the breakdown of glucose into low-molecular-weight aldehydes such as 3DG-acetaldehyde and formaldehyde [Witowski *et al*, 2001]. During long-term exposure GDPs have been shown to be cytotoxic to the peritoneum causing morphological changes in the peritoneal membrane and down regulation of the peritoneum's defence against infection [Duwe *et al*, 1981][Williams *et al*, 2004]. *In vitro* studies have also shown that GDPs retard the mesothelialization of HPMC, the layer of cells covering the peritoneum [Morgan *et al*, 2003]. Recent advances in the development of new, improved, more biocompatible dialysis fluids (containing less GDPs and with improved buffer system) have resulted in an improvement in the preservation of the peritoneal cell function and are thus promising for the future of long-term peritoneal dialysis [Rippe *et al*, 2001][Mortier *et al*, 2004][Williams *et al*, 2004][Witowski *et al*, 2004].

1.2.3.2 Peritonitis

Peritonitis is the most common serious complication of PD and a major reason for treatment failure. It presents with abdominal pain, fever and a characteristic cloudy peritoneal dialysate (cloudy bag). The condition is diagnosed if the effluent contains more than 100 white blood cells/ μl of which 50% must be polymorphonuclear cells (PMN) [Pastan and Bailey, 1998]. Episodes of peritonitis have been shown to be a risk factor in ultrafiltration failure and cause morphological damage to the peritoneum [Davies *et al*, 1996] including thickening of the peritoneal membrane (Figure 1.1) and loss of mesothelial cells from the peritoneum.

The main site of infection of the peritoneal cavity is through the lumen of the catheter. The main cause of infection is believed to be touch contamination during dialysis exchange. Over 70% of episodes are caused by gram-positive skin commensals such as *Staphylococcus epidermidis*. Gram-negative infections e.g. *Escherichia coli*, may be the result of catheter contamination but are more commonly caused by direct infection from the gut. Less common but more clinically severe fungal peritonitis accounts for between 2-10% of all episodes [Greig *et al*, 2003]. Treatment is usually through self-administered intra-peritoneal antibiotics with up to 80% of episodes being treated at home [Pastan and Bailey, 1998]. The incidence of peritonitis is now approximately 0.5 episodes per patient per year but varies greatly depending on the patient and country. In response to bacterial insult a host defence mechanism is activated within the peritoneum, as discussed in greater detail in section 1.4.

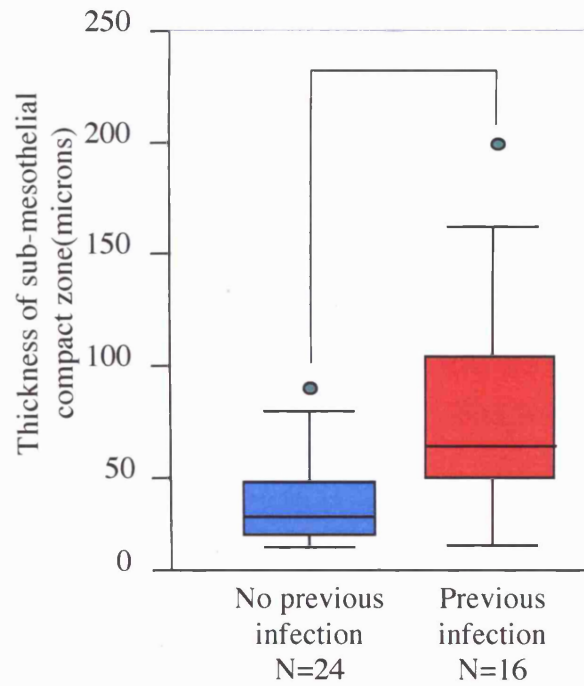


Figure 1.1 Thickness of the sub-mesothelial compact zone (microns) in PD patients with no previous infections versus patients with one or more previous episodes of infection. For each box plot median values are represented by the line within the box. The box presents 50% of the values (the 25th and 75th centiles), with the bars presenting the highest and lowest values, excluding outliers (●). (Unpublished data taken from the Biopsy Registry Study Group).

1.3 The Peritoneal Cavity

1.3.1 Anatomy

The peritoneum is the largest continuous serous membrane in the body. It forms a closed sac in males and an open sac in females (due to the free ends of uterine tubes opening directly into the peritoneal cavity). It can be divided into three anatomical regions. The parietal portion of the membrane lines the parietes (anterior, lateral and posterior abdominal walls, the pelvis and the underside of the diaphragm). The visceral portion of the membrane covers the viscera (intra-peritoneal organs and the mesentery). The peritoneal membrane also covers a fold in the peritoneal wall known as the greater omentum bursa that is situated behind the stomach and adjoining structures [Grey, 1918].

1.3.2 The peritoneal membrane

The original histological description of the peritoneum is credited to von Recklinghausen over 100 years ago [Witz *et al*, 2001]. Anatomically the peritoneal membrane consists of two distinct layers: 1) a simple epithelial monolayer, known as mesothelium and 2) its underlying connective tissue (Fig 1.2). These two layers are separated by an intervening discontinuous basement membrane (BM) that supports the mesothelium [Nagy and Jackman, 1998]. The basement membrane is a thin laminar network composed of proteoglycans, type IV collagen, and glycoproteins such as laminin. The mesothelial cells (MC) overlaying the basement membrane are thought to play a major role in its production and turnover [Nagy and Jackman, 1998].

Beneath the mesothelium and the basement membrane lies a layer of connective tissue, or sub-mesothelial basal lamina, known as the compact zone. This zone is composed of extracellular matrix molecules such as collagen I, collagen III, laminin, fibronectin and hyaluronic acid [Witz *et al*, 2001]. The compact zone acts as a selective cellular barrier preventing the fibroblasts in the connective tissue from making contact with the mesothelial cells. The trafficking of cells and macromolecules across the peritoneal membrane is also regulated by the sub-mesothelial compact zone. Proteoglycans within

the ECM form a gel like substance containing pores of various size and charge density and thus functions as a molecular sieve. The peritoneal sub-mesothelial layer also has an aqueous layer that facilitates the passage of water, electrolytes, nutrients, hormones and waste products between the blood capillaries and the fibroblasts, macrophages and dendritic cells that reside within the ECM [Nagy and Jackman, 1998]. The movement of water is also facilitated by the presence of aquaporin water channels (AQP1 and AQP3) that are expressed on mesothelial cells of the peritoneum, endothelium of capillaries and on host capillary venules [Marples, 2000][Szeto *et al*, 2005].

Blood vessels are found throughout the entire peritoneal membrane (Figure 1.2), although they are most commonly located at the junction of the compact zone and underlying adipose tissue [Williams *et al*, 2002] and function to supply and remove molecules to and from the tissues and organs of the abdominal cavity [Nagy and Jackman, 1998]. A lymphatic system is also present within both the visceral and parietal membranes. This network of lymphatic vessels functions to maintain the small volume of fluid (normally around 50ml) present in the peritoneal cavity and also plays a role in host defence by removing foreign bodies that might enter the peritoneal cavity [Nagy and Jackman, 1998].

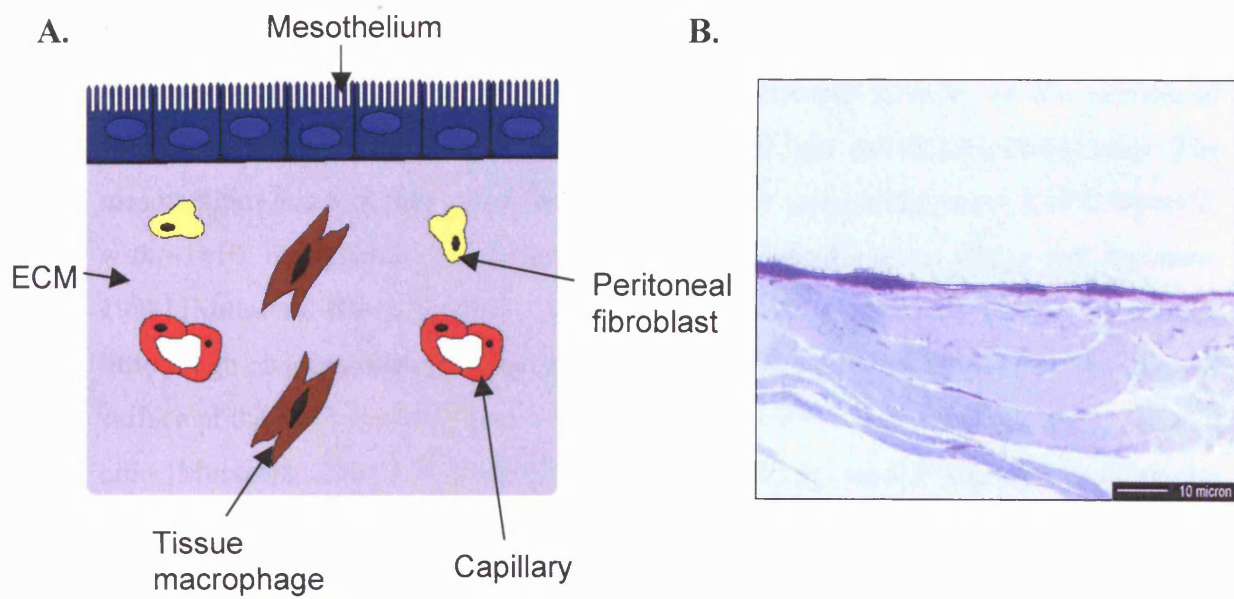


Figure 1.2 Structure of the peritoneal membrane. (A) Cross section of the peritoneal membrane shown schematically and (B) Cross section of the peritoneal membrane from a normal patient using light microscopy (taken from the peritoneal biopsy registry [Williams *et al*, 2003]).

1.3.3 The Mesothelium

The mesothelium covers both the parietal and visceral surfaces of the peritoneal membrane and is composed of a single resident cell type called mesothelial cells. The mesothelium has a cobble-stone like appearance (as seen in Appendix I of Chapter 2) with $\sim 1 \times 10^9$ mesothelial cells covering $\sim 1\text{-}2\text{m}^2$ peritoneal surface [Nagy and Jackman, 1998] [Mutsaers, 2004]. Typically, mesothelial cells are $\sim 25\mu\text{m}$ in diameter and contain little rough endoplasmic reticulum and a poorly developed golgi apparatus. The luminal surface of the cell has a well-developed microvilli border and also displays the occasional cilia [Mutsaers, 2004]. Individual mesothelial cells are packed together in epithelial sheets by anchoring junctions composed of adherens junctions and desmosomes that attach individual cells to their neighbours and mesothelial cells to the basement membrane respectively. These junctions have particular importance in development of cell polarity and the establishment of a semi-permeable diffusion barrier. Gap junctions mediate the passage of chemicals and electrical signals from one cell to another [Nagy and Jackman, 1998].

The mesothelium is a slowly renewing tissue with 0.16%-0.5% of mesothelial cells undergoing mitosis at any one time although this rate is greatly increased if the mesothelium is stimulated with injury. Mesothelial cells are unique from other epithelial type cells as re-growth occurs solely at the wound edge as a movement of sheets of cells. Like other epithelia mesothelial cells can also be induced to trans-differentiate from an epithelial phenotype to a mesenchymal phenotype under certain conditions (e.g. by TGF- β or IL-1 β) and this process is thought to contribute to the changes in peritoneal membrane structure and function during PD [Yanez-Mo *et al*, 2003]. The major function of the mesothelium is to maintain homeostasis within the peritoneal cavity. The important functions of the mesothelium can be seen in Table 1.1. Human peritoneal mesothelial cells also play a major role regulating the inflammatory response to injury or peritoneal infection (discussed in section 1.4).

Table 1.1 Important functions of the mesothelium

Function	Process
Protective barrier and non-adhesive surface.	-Production of hyaluronic acid (HA) to act as lubricant and form pericellular coat [Yung <i>et al</i> , 1996].
Antigen presentation and host defence	-HPMC express adhesion molecules such as ICAM-1 important in leukocyte recruitment [Clayton <i>et al</i> , 1998] -HPMC are the major site of cytokine production during inflammation [Topley <i>et al</i> , 1993].
Coagulation and fibrinolysis	-HPMC have an important role in fibrin deposition and removal to prevent peritoneal adhesions. -HPMC release plasminogen activators (uPA and tPA) that participate in the fibrinolytic cascade. -HPMC release plasminogen activator inhibitors (PAI) that aid fibrin deposition. [Sitter <i>et al</i> , 1995]
Tissue repair and extracellular matrix (ECM) remodelling.	-HPMC have the migratory capacity to migrate and therefore facilitate wound repair [Leavesley <i>et al</i> , 1999]. -HPMC synthesise ECM components such as collagen types I and III [Harvey <i>et al</i> , 1983]. -HPMC regulate ECM turnover by secreting matrix metalloproteinases and tissue inhibitors of metalloproteinases [Martin <i>et al</i> , 2000].

1.3.4 Alterations in the peritoneal membrane

Over the initial 3 to 5 year period of dialysis, PD is generally considered to be an efficient therapy for renal failure. This efficiency, however, appears to be limited to this time period with a majority of patients switching to haemodialysis in the long term due to the failure of PD as a treatment. The main cause of treatment failure is the decline in the ability of the peritoneal membrane's capacity to act as an ultrafiltration membrane. This loss of ultrafiltration accounts for the discontinuation in approximately 16% of all peritoneal dialysis patients and the transfer to hemodialysis [Krediet, 1999]. Years of exposure to bio-incompatible dialysis fluids and repeated episodes of peritonitis progressively damage the peritoneal membrane by causing structural changes that ultimately result in loss of the membrane's function as a dialysing organ [Devuyst *et al*, 2002][Williams *et al*, 2003].

Many studies have shown that time on PD is directly related to the extent of the morphological changes of the peritoneal membrane and the loss of ultrafiltration [Davies *et al*, 1996][Williams *et al*, 2002][Williams *et al*, 2003]. An increased thickening of the sub-mesothelial compact zone (Figure 1.3), vascular degeneration and fibrosis can be observed in the peritoneal membrane of patients on long term peritoneal dialysis [Williams *et al*, 2003]. Other changes occur such as the loss of mesothelial cells from the peritoneal membrane as shown by a decrease in the number of mesothelial cells in 50% of PD patients [Unpublished data, Biopsy registry]. This loss may in turn be reflected in a decrease in effluent cancer antigen 125 (CA125) levels as seen in other studies [Ho-Dac-Pannekeet *et al*, 1997][Visser *et al*, 1995]. Cellular changes also occur such as the loss of typical HPMC morphology (loss of cuboid shape) and down regulation of intercellular adhesion molecules that ultimately leads to fibrosis of the peritoneal membrane [Yanez-Mo *et al*, 2003]. The culmination of these changes are directly linked to ultrafiltration failure.

The majority of research over the past 5 years has been focused on the development of new more biocompatible PD fluids in order to try and lessen their pathophysiological role

in loss of membrane function. These studies have identified acidic pH, high concentrations of lactate and glucose and the presence of glucose degradation products (GDPs) as the main factors in the limited biocompatibility of PD fluids [Witowski *et al*, 2004]. The development of new sterilization processes in order to reduce GDP formation as well as the use of improved buffered PDFs have been shown to significantly increase the preservation of the peritoneal membrane during long term PD [Liberek *et al*, 1993][Witowski *et al*, 1995][Witowski *et al*, 2001][Williams *et al*, 2004].

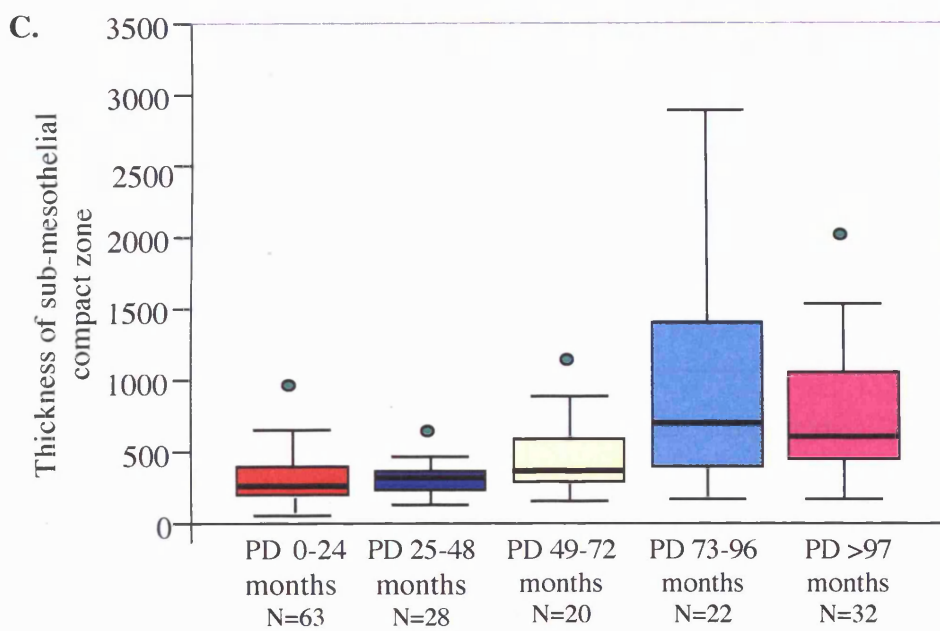
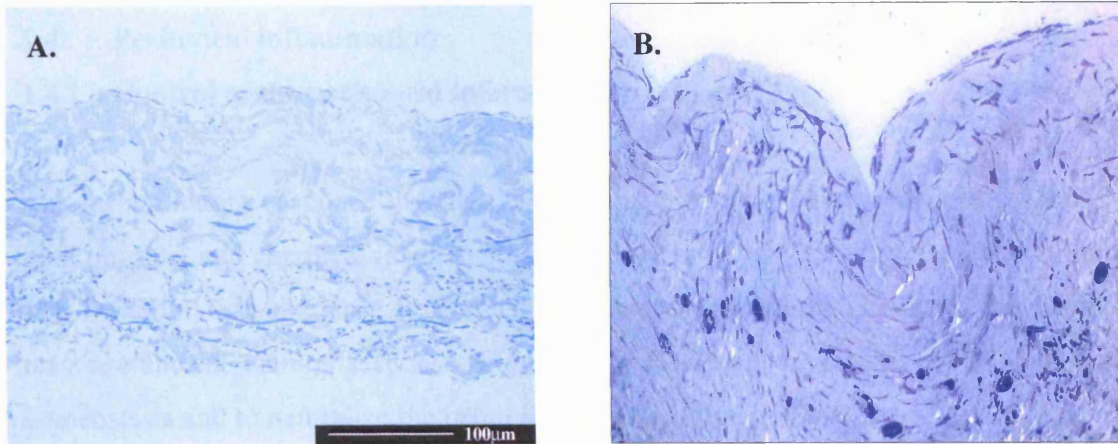


Figure 1.3 A comparison of cross sections of peritoneal membrane taken from a patient at the start of therapy (A) and a long term PD patient (B) shows a loss of mesothelium from the membrane surface, as well as a thickening of the sub-mesothelial compact zone, due to increased matrix deposition. (C) Progressive thickening of the peritoneal membrane over time during peritoneal dialysis. Thickness of sub-mesothelial compact zone shown in microns. (Data taken from the Biopsy Registry Study Group [Williams *et al*, 2003]).

1.4 Peritoneal inflammation

1.4.1 Control of the peritoneal inflammatory response

The inflammatory response involves a co-ordinated sequence of events in response to both physical and chemical insult such as bacterial infection or injury caused by trauma. The inflammatory response is divided into two components. These are the humoral response and the cellular response (Figure 1.4). Both pathways work to maintain tissue homeostasis and to neutralize the insult [Lewis and Holmes, 1993].

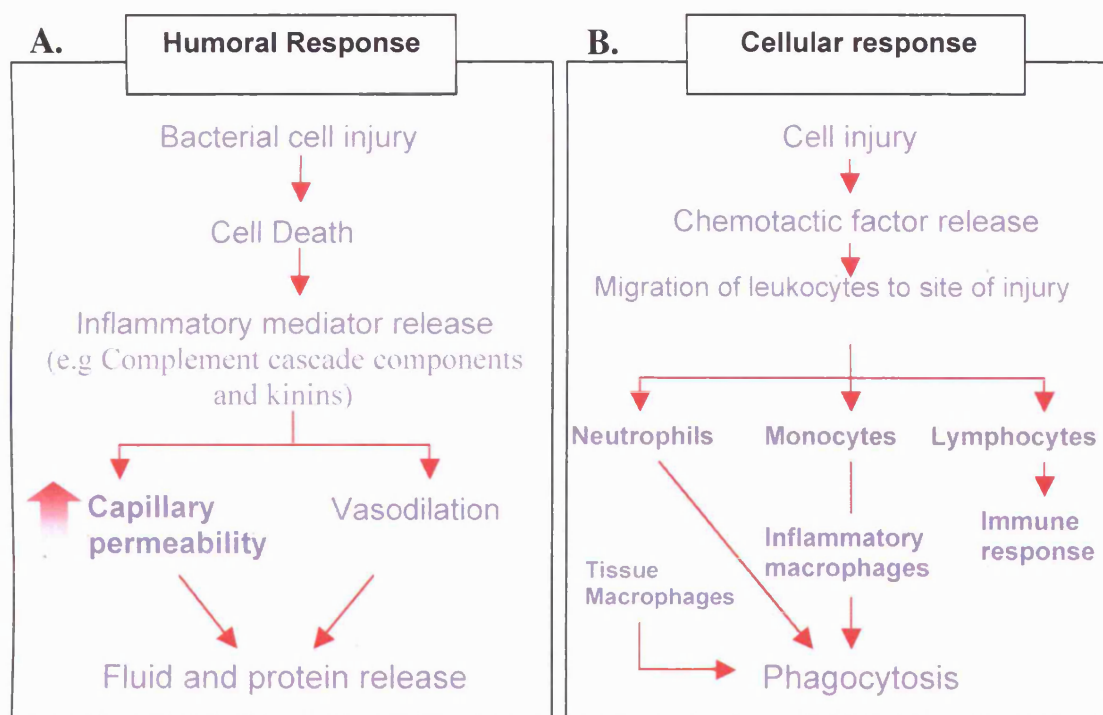


Figure 1.4 The humoral (A) and cellular (B) components of the inflammatory response. (Adapted from [Lewis and Holmes, 1993]).

Peritoneal infection is characterized by pain, the appearance of a cloudy dialysate indicative of the massive influx of polymorphonuclear cells (>85%) into the peritoneal cavity [Topley, 1995] and a time dependant increase in CA125 dialysate levels (Figure 1.5) [Ho-Dac-Pannekeet *et al*, 1995]. The inflammatory response is orchestrated by

resident cell populations of the peritoneum and the cytokine network is able to coordinate the infiltration of leukocytes into the peritoneum [Topley, 1995].

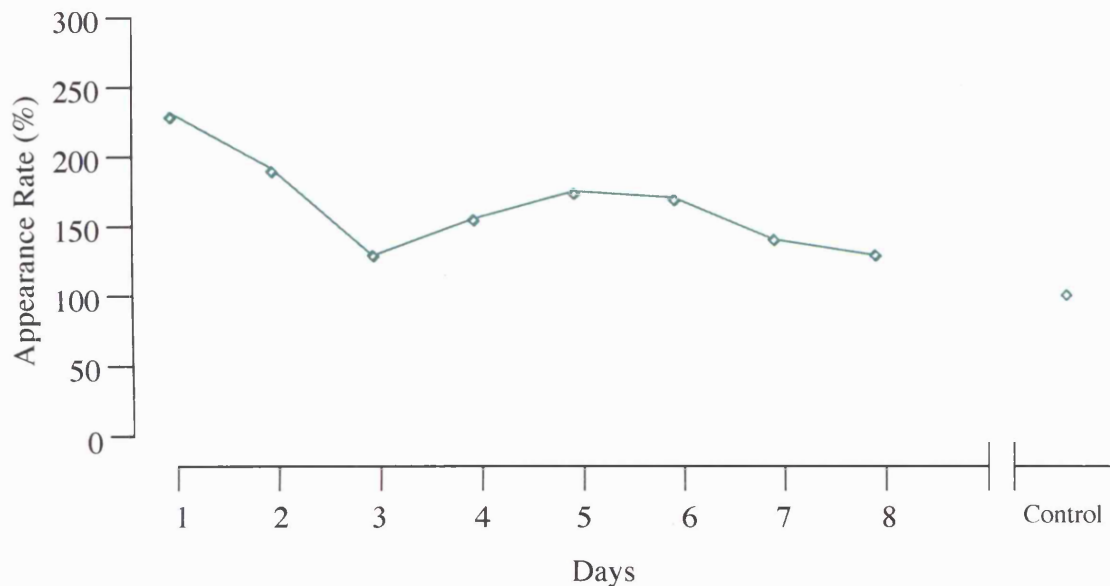


Figure 1.5 CA125 levels during peritonitis. The appearance rate of CA125 in peritoneal dialysate during peritonitis, shown as percentage of the normal CA125 control value (Taken from [Ho-Dac-Pannakeet *et al*, 1995]).

HPMC are the most abundant cell type in the peritoneal cavity and play an integral role in the orchestration of the inflammatory response in the peritoneum. After HPMC the most abundant cell type in the peritoneal cavity is the peritoneal macrophages ($PM\Phi$). These cells appear to be the first line of defence against invading organisms [De Souza *et al*, 1985]. $PM\Phi$ play major roles in the phagocytosis of invading micro-organisms and contribute to the production of inflammatory mediators [Topley and Williams, 1994]. Bacterial activation of resident macrophages results in the initiation of the innate immune response and immune cell recruitment [Brauner *et al*, 1996].

1.4.2 The cytokine network of the peritoneum

As seen in Figure 1.6, upon exposure to invading pathogens, PM Φ are activated which causes them to release the pro-inflammatory cytokines IL-1 β and TNF α [Douvdevani *et al*, 1994]. These cytokines then direct the resident HPMC monolayer to release high levels of IL-8 and express the cell surface adhesion molecule ICAM-1 [Allan *et al*, 2005]. This event results in the recruitment of neutrophils directly from the capillaries of the peritoneal membrane. As the number of resident HPMC outweigh the number of PM Φ there is an amplification of the inflammatory response at this step that is fundamental to the resolution of inflammation [Topley and Williams, 1994][Hurst *et al*, 2001].

Regulation of leukocyte trafficking in the peritoneal cavity is dependant on the specific release of chemokines by the mesothelium. These chemokines are small (7-10 KDa in monomeric form) and are characterized by the arrangement of conserved cysteine motifs within the N-terminus of their amino acid structure. Within the CXC sub-family, the presence of a glutamine-leucine-arginine (ELR) motif before the first of two conserved cysteine residues (separated by another amino acid, X) [Clark-Lewis *et al*, 1991][Clark-Lewis *et al*, 1993][Clark-Lewis *et al*, 1995] confers selectivity in recruiting neutrophils (whereas non-ELR-CXC chemokines confer selectivity to lymphocytes). In CC chemokines the two conserved cysteine residues lay next too each other and are all chemotactic for monocyte/macrophages and T Cells [Valente *et al*, 1988].

In addition to IL-8 production the cytokine IL-6 is also released by HPMC in response to IL-1 β and TNF α stimulation [Topley *et al*, 1993]. Circulating IL-6 can then complex with the circulating soluble IL-6 receptor (produced by neutrophils) allowing the autocrine stimulation of the peritoneum [Jones *et al*, 2005]. This action results in the down regulation of the CXC (IL-8) cytokine gradient and expression of CC (MCP-1) chemokines favouring the infiltration of mononuclear cells and activation of pro-apoptotic genes in neutrophils. Essentially the IL-6/sIL-6R complex results in a switch of the leukocyte population of the peritoneal cavity and the switch from innate to acquired

immunity (Figure 1.7)[Hurst *et al*, 2001][McLoughlin *et al*, 2004][McLoughlin *et al*, 2005].

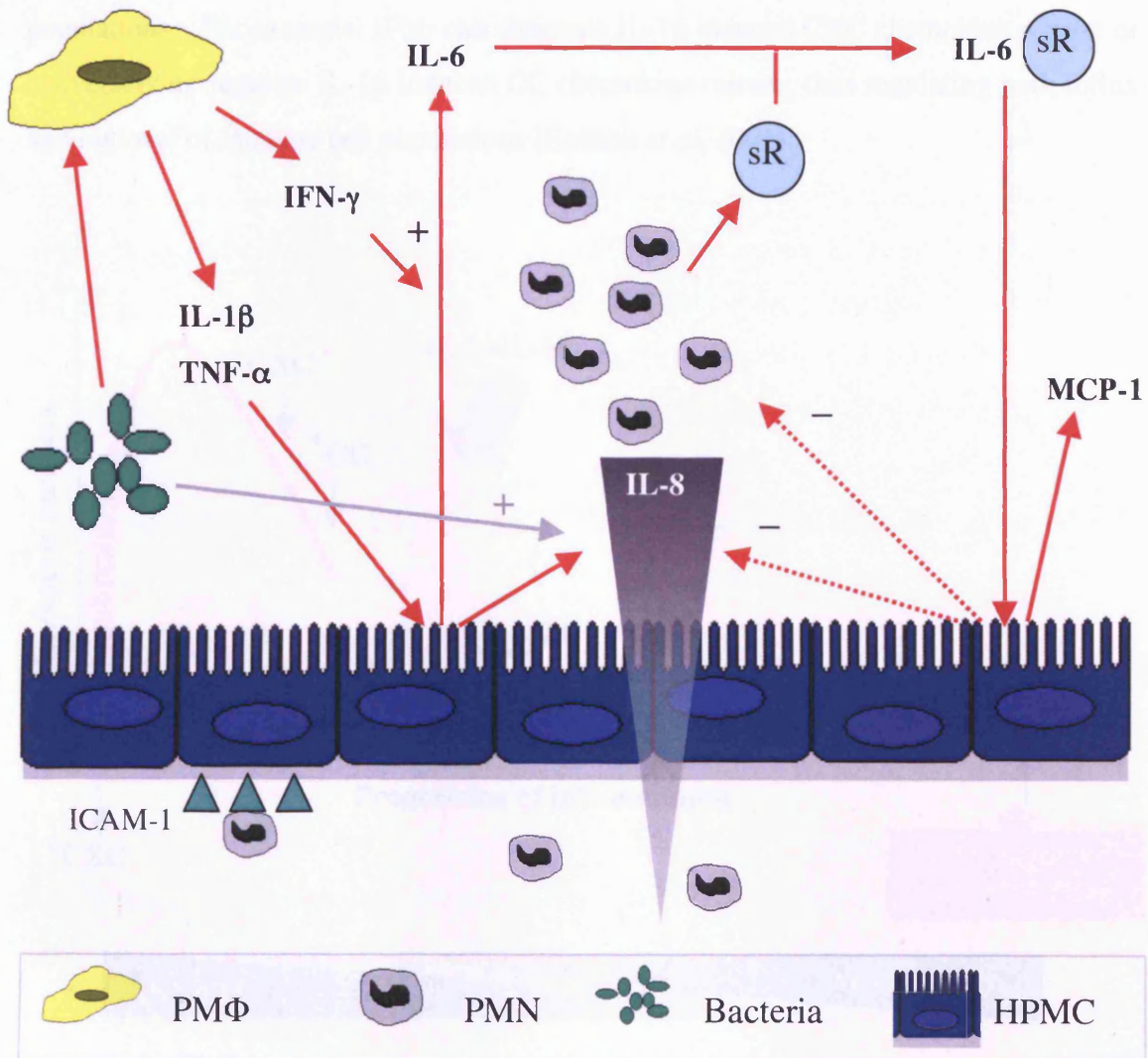


Figure 1.6 The cytokine network in peritoneal inflammation. Invading microorganisms cause the release inflammatory mediators such as IL-1 α , TNF- β and IFN- γ from peritoneal macrophages. This results in the release of IL-6 from resident HPMC that binds with its soluble receptor (released by recruited polymorphonuclear cells) to induce chemokine release by HPMC resulting in the recruitment of leukocyte cell populations to the site of infection.

Under normal acute inflammation, $\text{IFN}\gamma$ also plays an important role in the trafficking of different cell populations to the site of infection, by regulating the release of CXC and CC cytokines (Figures 1.6 and 1.7) and by directing apoptosis in infiltrating cell populations. For example, $\text{IFN}\gamma$ can attenuate $\text{IL-1}\beta$ induced CXC chemokine release or conversely up-regulate $\text{IL-1}\beta$ induced CC chemokine release, thus regulating both influx and removal of immune cell populations [Robson *et al*, 2001].

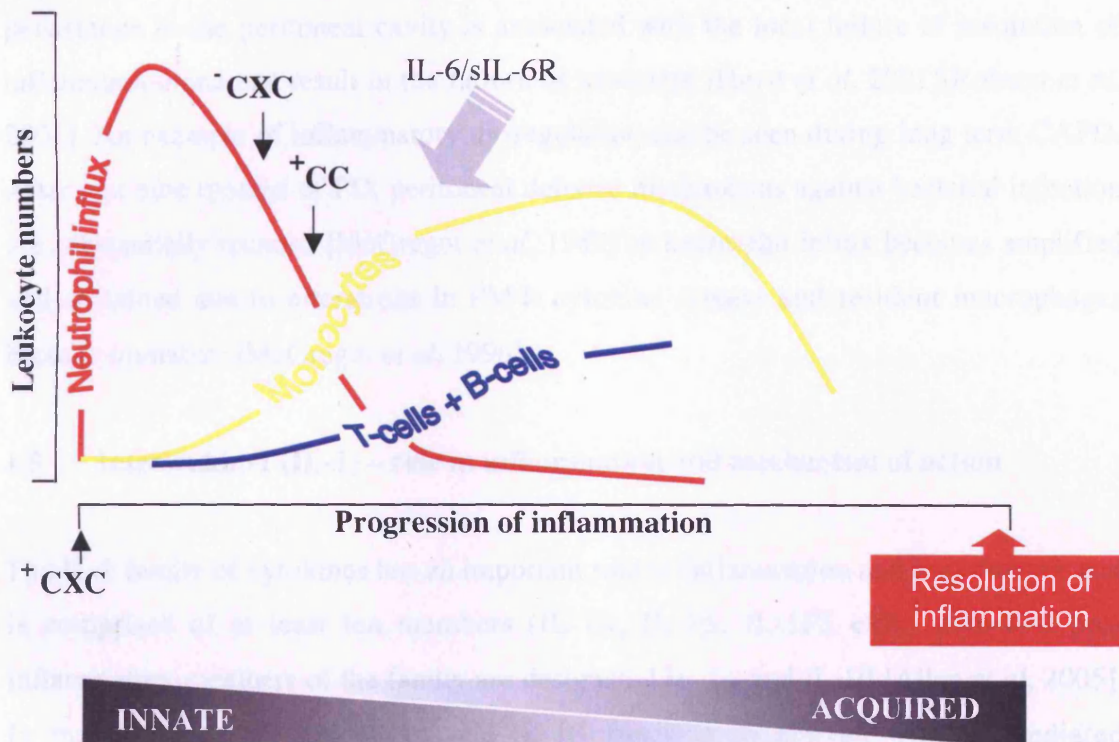


Figure 1.7 The sequence of events leading to resolution of peritoneal infection by resident and recruited cell populations.

HPMC themselves play an important role in the activation of the inflammatory response. As mentioned earlier, HPMC release IL-8 and express cell surface adhesion molecules in response to $\text{PM}\Phi$ activation. In addition to this, HPMC show an identical action in response to direct stimulation with the pathogen itself, as well as the release of

chemokines such as MCP-1 and RANTES. These events lead to the rapid accumulation of neutrophils and mononuclear cells in the first 24 hrs of infection [Topley *et al*, 1996].

1.4.3 Resolution of peritoneal inflammation

Resolution of inflammation is key to the host's successful response to peritonitis. The recruitment of leukocytes to the peritoneum is obviously beneficial to the host in the initial stages of infection, in order to remove the invading pathogen but leukocyte persistence in the peritoneal cavity is associated with the local failure of resolution of inflammation and can result in the failure of treatment [Hurst *et al*, 2001][Robson *et al*, 2001]. An example of inflammatory dysregulation can be seen during long term CAPD. After just nine months of PD, peritoneal defence mechanisms against bacterial infection are substantially reduced [McGregor *et al*, 1989] as neutrophil influx becomes amplified and sustained due to alterations in PM Φ cytokine release and resident macrophages become immature [McGregor *et al*, 1996].

1.5 Interleukin-1 (IL-1) – role in inflammation and mechanism of action

The IL-1 family of cytokines has an important role in inflammation and host defence and is comprised of at least ten members (IL-1 α , IL-1 β , IL-1F5 etc). The two pro-inflammatory members of the family are designated IL-1 α and IL-1 β [Allan *et al*, 2005]. In the peritoneal cavity, IL-1 α and IL-1 β function to activate HPMC mediated chemokine production that can orchestrate the recruitment of immune cells to the site of infection/injury.

IL-1 α and IL-1 β expression is up-regulated in response to various stimuli such as endotoxins, produced by invading micro-organisms, lipopolysaccharide (LPS) or TNF α , either through transcriptional up-regulation or by mRNA stabilization [Douvdevani *et al*, 1994]. Despite being encoded by different sized genes, the two have high sequence homology and are both synthesised as large precursor molecules from many cell types of the peripheral and central immune system, such as monocytes [Allan *et al*, 2005],

epidermal cells, endothelial cells and fibroblasts [Dinarello, 2002]. In the cytosomal compartment of these IL-1 producing cells, the IL-1 α precursor molecule (Pro-IL-1 α) is biologically active and is cleaved by an enzyme called calpain to produce a mature protein, whereas, pro-IL-1 β is biologically inactive and requires caspase-1 cleavage to produce an active 17 KDa protein [Dinarello, 2005]. The mechanism of IL-1 cell release has not yet been fully defined. Proposed mechanisms include release by micro-vesicle shedding, release through secretory lysosomes and release by cell lysis [Allan *et al*, 2005].

Both IL-1 α and IL-1 β exert similar biological effects. IL-1 α or IL-1 β binding to a membrane type 1 IL-1 receptor (IL-1R1) allows the association with the IL-1 receptor accessory protein (IL-1RacP) and the formation of a complex capable of intracellular signalling [Cullinan *et al*, 1998]. The IL-1 receptors belong to the Toll-like receptor family (TLR) that have a major role in immune response. This family of receptors are characterized by the presence of a Toll-IL-1 receptor (TIR) domain that trigger a series of intricate signalling events, such as MyD88 [O'Neill, 2003], TRAF-2 and IRAK-1 recruitment and I κ B degradation [Rayet *et al*, 1999][Celec, 2004] that results in the activation of nuclear factor- κ B (NF- κ B) [Stylianou *et al*, 1992] and stress related mitogen activated protein kinases (MAPKs) [Allan *et al*, 2005]. This leads to the transcription of many inflammatory responsive genes such as the CXC chemokine IL-8 [Hoffman *et al*, 2002], cytokines such as IL-6 [Berghe *et al*, 2000], adhesion molecules like ICAM-1 [Allan *et al*, 2005] and the multifunctional acute phase protein called C-reactive protein (CRP) [Voleti and Agrawal, 2005].

1.6 Interleukin-6 (IL-6) – role in inflammation and mechanism of action

IL-6 is a multifunctional cytokine that plays a central role in host defence due to its potent ability to induce the acute phase inflammatory response [Berghe *et al*, 2000]. IL-6 is commonly described as both a pro- and anti-inflammatory cytokine due to its ability to block pro-inflammatory cytokine expression and promote the expression of IL-1 receptor antagonist [Jones *et al*, 2001][Hurst *et al*, 2001]. IL-6, therefore, facilitates the switch

from innate to acquired immunity by orchestrating chemokine-directed attraction and apoptotic clearance of leukocytes [McLoughlin *et al*, 2004]

IL-6 belongs to a family of cytokines whose members act via a receptor complex containing the signal transducing protein gp130. A key feature in the regulation of the IL-6 response is the identification of a soluble IL-6 receptor (sIL-6R) that can bind to IL-6 to produce a complex capable of stimulating cellular responses, such as proliferation and activation of the inflammatory response [Jones *et al*, 2001]. sIL-6R itself is present in two distinct isoforms. One isoform is produced from the proteolytic cleavage of the membrane bound receptor (PC) and the other is produced from differential IL-6R mRNA splicing (DS). Both isoforms have been shown to elicit common cellular events through gp130 activation [Jones *et al*, 2001][McLoughlin *et al*, 2004].

IL-6 can also activate cells through a membrane bound IL-6 receptor (IL-6R) with the central regulation of IL-6 mediated responses occurring through the binding of sIL-6R. Cells lacking the cognate IL-6R can still be activated by the IL-6/sIL-6R complex due to its ability to interact with the ubiquitously expressed 130 KDa signal-transducing glycoprotein (gp130) in a process termed IL-6 trans-signalling. The first event in IL-6 signalling involves the homodimerization of the ligand-receptor complex to gp130 that is able to trigger activation of gp130-associated cytoplasmic tyrosine kinases (JAK1, JAK2 and TYK2) that subsequently cause the phosphorylation of STAT1 and STAT3. Monomeric STAT subunits can then form homo- and hetero-dimers and translocate to the nucleus where they can initiate expression of specific genes [Heinrich *et al*, 1998][Heinrich *et al*, 2003] such as RANTES and MCP-1, in order to promote a sustained mononuclear cell population [McLoughlin *et al*, 2005].

1.7 Cancer Antigen 125

1.7.1 CA125 in Ovarian Cancer

Ovarian cancer is the 5th most common form of cancer and accounts for 5% of all female malignancies. Latest statistics suggest that 1 in 55 women will develop cancer of the ovaries at some point during their life. When diagnosed at an early stage the patient has a 5 year survival of 70%, whereas, those who are diagnosed at a later stage of the disease have a 5 year survival rate of 20%, hence underlining the need for an efficient tool for the diagnosis of early stage ovarian cancer [Whitehouse and Solomon, 2003].

CA125 was first described in a study carried out on the OVCA433 by Bast and his colleagues in 1981 [Bast *et al*, 1981]. His group developed a murine monoclonal antibody, named OC125, that reacted with the OVCA433 cell line from a patient suffering with cystadenocarcinoma of the ovaries. The antibody was found to react with an antigenic determinant on the surface of the ovarian epithelial tumors. The antigenic determinant was named Cancer Antigen 125 (CA125) and was subsequently found to be produced by other tumours such as malignant tissue of the lung and breast [Jacobs and Bast, 1989],

Serum analysis of CA125 levels in patients suffering with ovarian cancer using a CA125 immunoradiometric assay showed that 80% had elevated levels (>35 U/ml) when compared with normal patients (<35U/ml) thus indicating CA125's potential as a diagnostic tool [Bast *et al*, 1983]. Elevations in CA125 serum levels are also associated with advanced or untreated endometrial cancer [Ziomet *et al*, 1996]. Since its first identification, 26 antibodies have been described that recognize CA125. These antibodies can be separated into two groups, either OC125 like- or M11 like- antibodies. Competition studies showed M11 binding is not inhibited by OC125, suggesting they bind to different epitopes on the CA125 molecule [Nustad *et al*, 1996]. This allowed the development of a double determinant sandwich assay in which M11 acts as the capture antibody and OC125 acts as the detection antibody. This assay shows much less variation than the original assay and is the current assay used in the diagnosis of ovarian

cancer. These commercially available kits are now commonly used to monitor the disease's progression and regression as well as the recurrence of the condition [Kenemans *et al*, 1993]. For example, doubling or halving of the CA125 serum levels in patients can be indicative of progression or regression of the malignancy. After treatment serum levels of less than 35 U/ml indicate successful resolution of the disease whereas the disease is still present in 95% of patients with levels above 35U/ml. Recurrence of the disease after treatment completion is commonly preceded by a significant increase in CA125 levels sometimes up to a year before the actual recurrence [Kenemans *et al*, 1993]. Other markers of ovarian carcinoma have been identified such as human kallikrein 6, osteopontin and claudin 3, but to date CA125 remains the most effective and reliable signal for the detection of ovarian cancer [Rosen *et al*, 2005]. Although, more recent data using gene array technology has suggested that the efficiency of malignancy detection may be significantly increased if many markers are used in combination [Lu *et al*, 2004].

1.7.2 CA125 in Peritoneal Dialysis

CA125 was also found to be expressed in normal tissues of the pancreas, kidney, colon, the surface of eye and the peritoneum [Loy *et al*, 1992][Argueso *et al*, 2003]. Interest in CA125 expression in the peritoneal cavity is related to the search for markers that iterate the status of the peritoneal membrane. Mesothelial cells were shown to be the major CA125 producing cells of the peritoneum [Koomen *et al*,1994][Zeillemarker *et al*, 1994][Epiney *et al*, 2000] and as a result CA125 has been adopted as a marker of HPMC mass and integrity [Visser *et al*, 1995][Ho-Dac-Pannekeet *et al*, 1997].

During peritoneal dialysis, CA125 can be found in fluids from the peritoneal cavity. Studies in the measurement of CA125 effluent levels of patients undergoing PD, as well as *in vitro* studies, show that it is constitutively produced and secreted by mesothelial cells (Figure 1.8(A)) and therefore, it has been suggested that it can be used diagnostically as a marker of mesothelial mass and of mesothelial cell integrity [Visser *et al*, 1995]. CA125 levels in the effluent of PD patients show a decrease over treatment

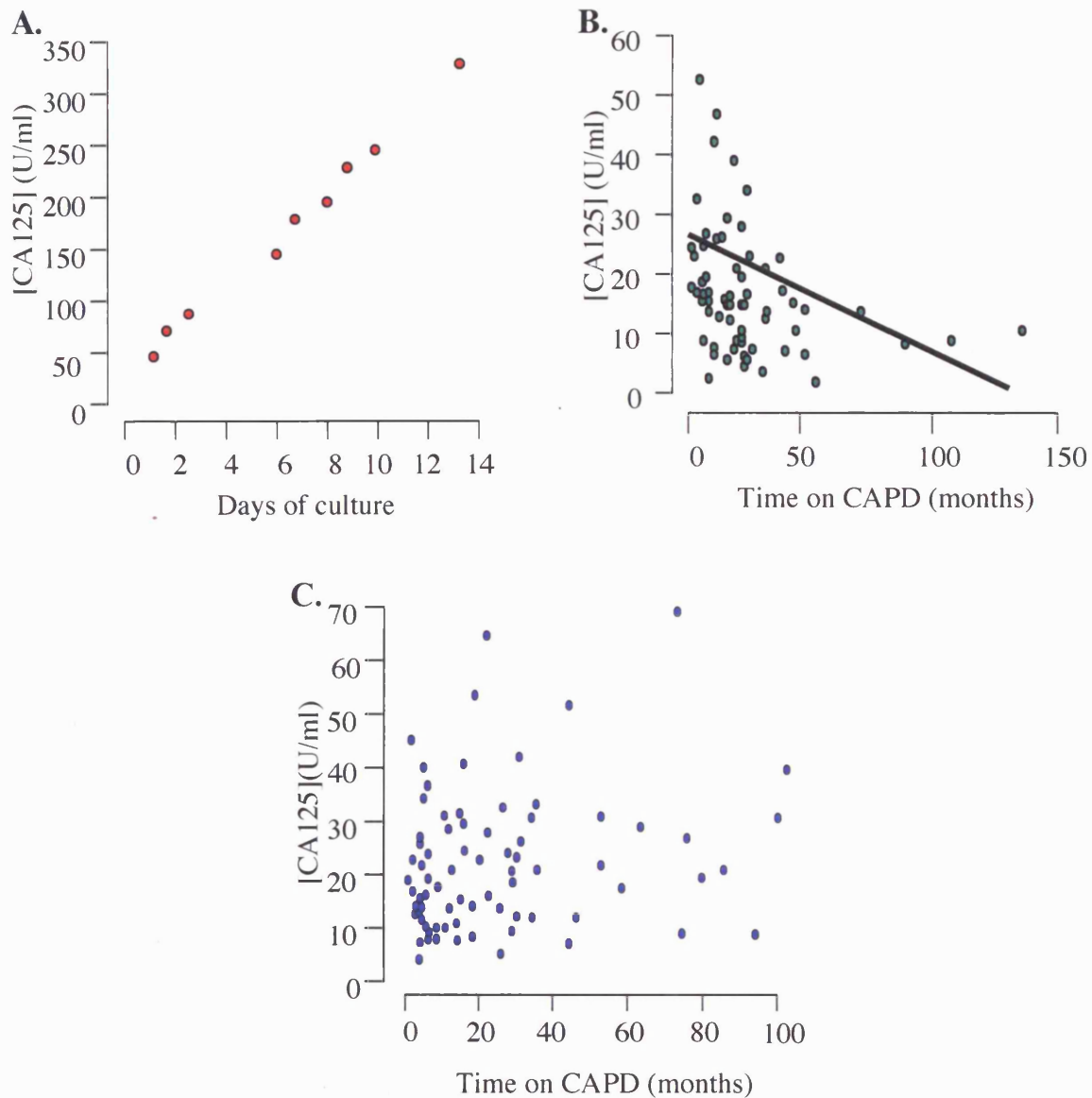


Figure 1.8 Constitutive expression of CA125. (A) Graph illustrating the positive correlation between CA125 concentration and the duration of HMPC cell culture (Taken from [Visser *et al*, 1995]). (B) Graph illustrating the reduction of CA125 effluent levels during long-term continuous ambulatory peritoneal dialysis (taken from [Ho-Dac-Pannekeet *et al*, 1997]). (C) Graph showing no correlation between CA125 concentration and the duration of treatment (taken from [Lai *et al*, 1997]).

time (Figure 1.8(B)) suggesting that the loss of mesothelial cell mass correlates to the membrane dysfunction in PD patients [Ho-Dac-Pannekeet *et al* 1997][Sanusi *et al*, 2001]. Further evidence is provided by the positive correlation between the number of HPMC in the peritoneal effluent and the CA125 concentration [Koomen *et al*, 1994][Visser *et al*, 1995]. Nevertheless these data remain contentious since Lai and his colleagues were unable to produce this data in a study of similar size (Figure 1.7(C)) [Lai *et al*, 1997], which may indicate that CA125 is a marker of homeostasis within the peritoneal cavity and reflects more than just mesothelial cell mass.

1.7.3 PDF biocompatibility

The use of CA125 as a marker of peritoneal “health” is reinforced by studies comparing dialysis fluid compatibility in medium term clinical trials [Breborowicz *et al*, 2005][Topley *et al*, 2005]. In summary, the use of more biocompatible dialysis fluids (containing less glucose degradation products and improved buffer systems (i.e. neutral pH)) during PD results in elevated CA125 effluent levels after 6 months [Williams *et al*, 2004][Rippe *et al*, 2001][Jones *et al*, 2001]. The improved biocompatibility of the PDFs also result in functional and morphological improvements to the peritoneal membrane and mesothelium [Devuyst *et al*, 2002] and therefore it is still not clear whether an increase in CA125 simply reflects a more intact mesothelium or contributes directly to function. Studies carried out in a human mesothelial cell model showed that high glucose concentrations inhibit mesothelial cell proliferation, suggesting osmotic solutes may contribute to the poor biocompatibility of PDFs [Breborowicz *et al*, 1992]. More recently, it has been shown that the GDP content of PD fluid has a significant impact on CA125 concentrations found in effluent PD fluid. The lower the GDP content the higher the CA125 concentration found in the effluent [Williams *et al*, 2004].

However, CA125 has not been shown unequivocally to be a predictor or marker of the health of the mesothelium. Other studies discredit CA125 as a marker of peritoneal health suggesting that the variability between patient samples is too large to gain a positive correlation between CA125 concentration and mesothelial mass. This study

suggested that the observed levels of CA125 produced is a combination of the amount of cells present as well as their ability to produce the antigen, which can be effected by factors such as patient age and can therefore, not be used as a marker of mesothelial cell mass [Brebrowicz *et al*, 2005].

1.7.4 CA125 in peritonitis

As outlined in section 1.4, peritonitis and its associated inflammation are frequent complications of peritoneal dialysis. CA125 effluent levels can be seen to be modulated during an episode of peritonitis (Figure 1.5) [Ho-Dac-Pannekeet *et al*, 1995] with some studies reporting a 3.5-fold increase in CA125 levels in effluent levels during an episode of peritonitis aswell as a 7-fold increase in serum level within 2 months of the inflammatory incident, therefore, indicating CA125 as a marker of inflammation [Bastani and Chu, 1995]. Other studies suggest the increase in CA125 levels after peritonitis is caused by the release of intracellular CA125 as a result of mass mesothelial cell death [Visser *et al*, 1995].

The regulation of CA125 in peritoneal inflammation is poorly understood and there is much confusion about its role during inflammation. Some publications have shown that pro-inflammatory cytokines such as IL-1 β have no effect on CA125 expression by mesothelial cells [Visser *et al*, 1995]. In the various ovarian cancer cell lines tested in a separate study, IFN- α , IFN- β , IFN- γ , TNF- α and TGF- β were found to have little or no effect on CA125 expression [Imbert-Marcille *et al*, 1994], thus providing further evidence for the constitutive nature of CA125's expression and therefore suggest that CA125 can be used as a marker of cell mass. Conversely, some other conflicting publications have shown that IL-1 β can induce [Zeillemarker *et al*, 1994] or down-regulate CA125 cell surface secretion [Zeimet *et al*, 1996] and therefore, can no longer be thought of as a marker of mesothelial cell mass.

In order to understand how CA125 fulfils its potential biological roles it is essential to understand how its expression and secretion are regulated under defined conditions. To

date it is not known if its production is regulated by growth phase, cell damage or following direct stimulation of pro-inflammatory cytokines or growth factors known to be present in the peritoneal cavity during dialysis.

1.8 The molecular status of CA125

1.8.1 The protein

CA125 is a high molecular weight, highly glycosylated multi-subunit glycoprotein with a carbohydrate content of 77% (sialic acid, fucose, manose, galactose, N-acetylgalactosamine and N-acetylglucosamine) [Yin and Lloyd, 2001] and is predominantly a surface expressed molecule, although it can be found intracellularly (in the cytoplasm) and in the extracellular matrix of producing cells [O'Brien *et al*, 1991]. The use of various antibodies has resulted in the detection of varying molecular weights ranging from 68Kd to 1000Kd [Yin *et al*, 2002]. SDS page polyacrylamide gel analysis using the antibody OC125 gives rise to a band of approximately 200Kd, thought to represent the protein core of the CA125 molecule [Davis *et al*, 1986]. It has been suggested that the form of CA125 found in serum might be a degraded product from a larger molecule produced in the peritoneal cavity [Nustad *et al*, 1998] and may even be present as a complex of adhering CA125 molecules [O'Brien *et al*, 1998].

1.8.2 CA125 is a mucin type glycoprotein

A monoclonal antibody specific for CA125, VK-8, was used to purify the antigen from the ovarian cancer cell line OVCAR-3. The purified antigen displayed characteristics typical of a mucin type glycoprotein [Lloyd *et al*, 1997]. These include: 1/ A highly glycosylated molecule (77% w/w) dominated by galactose and N-acetylglucosamine, 2/ A protein rich moiety rich in serine, threonine and proline molecules, 3/ Predominant glycosylation of serine and threonine residues and 4/ Predominantly O-linked glycans [Lloyd *et al*, 1997][Wong *et al*, 2003]. Further evidence for CA125's inclusion in to the mucin group of glycoproteins stems from similarities in the deduced amino acid sequence

of MUC16 and the sequence of isolated peptides from CA125, along with the subsequent correlation between MUC16 and CA125 mRNA expression [Yin *et al*, 2001].

1.8.3 CA125 proposed structure

The proposed structure of the antigen can be seen in Figure 1.9. CA125 has a short cytoplasmic domain containing a transmembrane domain, a glycosylated extracellular domain and a large amino terminal domain. The extracellular structure contains a 156 amino acid repeat sequence (upwards of 60 repeats) that displays epitopes for both OC125 and M11 binding. Each repeat has a conserved methionine residue at position 24, thought to be involved in antibody binding, and two conserved cysteine residues, 19 amino acids apart, indicating the possible presence of a disulphide loop structure [O'Brien *et al*, 2001][Wong *et al*, 2003]. NMR spectroscopic analysis of the repeat structure indicates that each repeat contains a SEA domain composed of two α helices and four β anti-parallel strands [Maeda *et al*, 2004]. The carboxy-terminal domain has a short cytoplasmic tail made of 256 amino acid residues, possibly containing a glycan-phosphatidylinositol (GPI) anchor [Nagata *et al*, 1991].

1.8.4 Molecular Weight

This extraordinarily large moiety appears to be composed of at least 22,152 amino acids of which 12,068 constitute the amino terminal domain and approximately 10,000 residues representing the 60+ repeat domains. A complete molecule of this magnitude would have a molecular weight of approximately 2.5 million daltons and a potential glycosylated molecular weight of more than double that [O'Brien *et al*, 2002].

1.8.5 Cell surface secretion

CA125 has a proteolytic cleavage site 50 amino acid residues up from its trans-membrane domain [O'Brien *et al*, 2002] but little is known about the specific pathway in which CA125 is released from the cell surface. Work carried out on the WISH amnion human

cell line suggests that the release of CA125 requires both serine or threonine and tyrosine phosphorylation which may act as a signal for the proteolytic cleavage of CA125 from the cell surface. It has also been suggested that removal of CA125 from the cell may be mediated through a pathway involving the plasminogen-plasmin activator, tPA [Fendrick *et al*, 1997] or the EGF signal transduction pathway [Konishi *et al*, 1994][O'Brien *et al*, 1998].

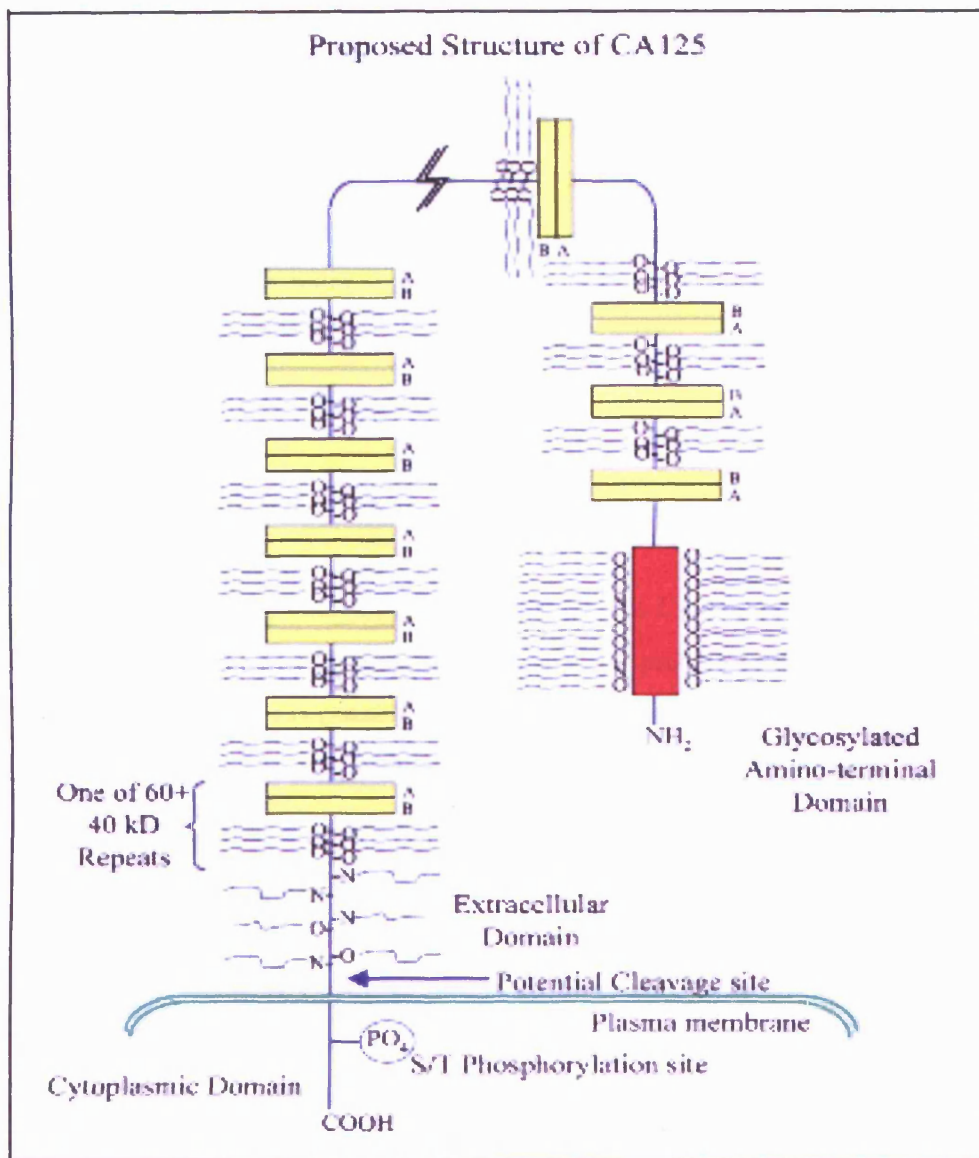


Figure 1.9 Proposed structure of the CA125 antigen (Taken from [O'Brien *et al*, 2001]).

1.9 The Gene

1.9.1 Initial characterization

The earliest attempt to characterize the CA125 gene resulted in the identification of NBR1 as a CA125 candidate gene. This gene was identified by screening an OVCA432 lambda ZAP cDNA library with a polyclonal antibody raised to the CA125 antigen and was subsequently found to be located on chromosome 17q21.1, the same genomic region as the BRCA1 gene [Brown *et al*, 1996][Whitehouse and Solomon, 2003]. The sequence of the gene recovered was found to be void of any transmembrane domain motif sequences and when expressed as an epitope-tagged construct appeared to be expressed in cytoplasmic and perinuclear locations. It was suggested that NBR1 may code for just part of the CA125 complex but it was more likely that the antibody raised to CA125 cross reacted with an epitope on NBR1, indicating that NBR1 is not a candidate gene for CA125 [Whitehouse and Solomon, 2003].

1.9.2 Cloning of the CA125 gene

Progress in understanding the molecular nature of the CA125 gene was hampered by difficulties in cloning the gene. This was until Lloyd and his group screened a lambda ZAP cDNA library from OVCAR-3 cells and discovered a 5797bp clone containing a stop codon and poly (A) sequence (but no 5' initiation sequence) [Yin and Lloyd, 2001]. This work suggested that CA125 was in fact a mucin gene (MUC16).

Further progress was made, later that same year, when a group from the University of Arkansas used controlled CNBr cleavage of the antigen to produce fragments of approximately 40Kd, which were subsequently sequenced in an attempt to elucidate CA125 gene structure. This study indicated that production of CA125 required a transcript of more than 35,000 bases [O'Brien *et al*, 2001]. Interestingly, this data was later proved incomplete by the same group who identified an extension to the N-terminal domain that doubled the size of the CA125 antigen [O'Brien *et al*, 2002]. Therefore, the most recent data shows that the CA125 gene occupies over 134,000bp of genomic DNA,

has a transcript of 67,000 bases and is positioned on chromosome band 19p13.2, assigned to cosmids AC008734 and AC016584 in the genome database [Hovig *et al*, 2001]. Little else is known about the gene with regards to its expression and regulation.

1.10 Function of CA125

1.10.1 Lubricating molecule

The function of CA125 is an area that attracts a great deal of speculation due to the lack of understanding of the antigen's regulation and expression. Its use as a biological marker of the status of the peritoneal mesothelium is well documented, as well as its use as a target for the monitoring of ovarian cancer onset and recurrence but these "uses" give little clue to its actual biological function.

A major step in the understanding of its function came when it was identified as a mucin type molecule [Yin and Lloyd, 2001]. Typically, mucins function as lubricating molecules on the surface of epithelial cells and also act as signal transducers allowing the binding of a vast array of proteins to their extensive structure [Gum, 1992][Verma *et al*, 1994]. Given the size of the CA125 antigen it seems likely to be involved in a number of functions in parallel. Due to the nature of the molecule and its cell surface expression, CA125 is thought to have a role as a lubricating molecule preventing cell-cell adhesions of opposing membranes of the peritoneum (although there is no clear evidence for this function) [Hardardottir *et al*, 1990]. Further evidence for this biological function is provided by CA125's apparent lubricating function on the ocular surface epithelium of the eye [Hori *et al*, 2004] and the inhibited adhesion of various cancer cell lines to CA125 coated plates *in vitro* [Gaetje *et al*, 2002].

1.10.2 Mesothelin binding and cellular adhesion

Like CA125, mesothelin is a surface molecule expressed in the mesothelial cell lining of body cavities and in many tumour cells [Rump *et al*, 2004]. An antibody, Mab K1, was first used to identify a 69-kDa precursor that is proteolytically processed into a 40kDa

membrane-tethered form called mesothelin and a 30kDa secreted form known as megakaryocyte potentiating factor (MPF) [Chang and Pastan, 1996][Chowdhury *et al*, 1998]. Soluble forms of mesothelin and MPF are detectable in the sera of patients with ovarian cancer, indicating its potential use as another marker for the diagnosis of ovarian cancer and monitoring its response to therapy [Scholler *et al*, 1999]. Mesothelins biological function remains poorly understood although it is implicated as having a role in cellular adhesion [Chang and Pastan, 1996].

Work carried out by Rump and his colleagues in 2004 showed that the polypeptides encoding the mesothelin molecule are matched to portions of the CA125. In addition to this, they showed a specific affinity for the binding of CA125 to mesothelin, along with the co-expression of CA125 and mesothelin in advanced stage ovarian cancer. Binding studies monitoring the binding of OVCAR-3 cells to an endothelial cell monolayer expressing mesothelin showed that CA125/mesothelin binding mediates the binding of the two cell types. Given his findings, Rump speculated that CA125 might contribute to the metastasis of ovarian cancer in the mesothelium via mesothelin binding [Rump *et al*, 2004].

1.10.3 Galectin binding and export

Galectins are a family of animal lectins that all possess the same carbohydrate binding affinity for β -galactosidase and conserved consensus sequence elements in their carbohydrate binding sites [Liu *et al*, 2002]. The biological functions of galectins include the regulation of cell adhesion, cell proliferation and cell death [Brewer, 2002]. Recent evidence has also implicated galectins to be important regulators of immune cell homeostasis. For example, Galectin-1 is widely expressed by cells of the central and peripheral immune compartments including macrophages and activated B-cells and has many functions including the inhibition of T-cell proliferation as well as the induction of cell cycle arrest and apoptosis in these cells [Rabinovich *et al*, 2002].

In 2002, Seelenmeyer and her group established that CA125 functions as a counter receptor for galectin binding, as both soluble and membrane-associated forms of CA125, derived from HeLa cell line lysates, were able to bind to galectins with high efficiency. This binding was found to be dependant on β -galactose-terminated, O-linked oligosaccharide chains of CA125 and seemed preferential to galectin-1 [Seelenmeyer *et al*, 2003]. FACS analysis showed that the HeLa cell lines producing endogenous CA125 had ten times more galectin-1 bound to their cell surface compared to a CHO cell line that is CA125 deficient. Interestingly, the cell surface binding capacity for galectin-1 was shown to be equal in both the HeLa and CHO cell lines, as was the galectin-1 expression levels, suggesting that CA125 maybe involved in the regulation of galectin-1 transport to the cell surface and therefore be part of the immune response to inflammation.

1.11 AIM OF THESIS

1.11.1 Aim

The literature has identified CA125 as a marker of HPMC mass/integrity in the peritoneum. During peritoneal dialysis CA125 effluent levels can be seen to change but it is unclear whether this is a reflection of the state of the mesothelium or due to alterations in the regulation of CA125 expression. The aims of the thesis were to examine the regulation of CA125 at the level of transcription by detailed analysis of the promoter region.

Peritonitis is a common occurrence in some patients on peritoneal dialysis and is a common cause of technique failure in these patients. The role of CA125 during the associated inflammatory process may be important in understanding its amplification and/or resolution. Therefore, this study was also aimed at identifying the potential biological roles for CA125 during the inflammatory state by studying its regulation at the level of transcription, surface expression and cell surface secretion in response to classic inflammatory mediators. Additionally, this study attempts to further elucidate the biological function of CA125 by examining its role in a HPMC wound healing model and by using siRNA technology to knock out CA125 expression in these primary cells.

1.11.2 Scope of the thesis

Chapter 3 details the reconstruction of the CA125 gene using a variety of computational methods such as use of the Biotechnology Information (NCBI) database (<http://www.ncbi.nlm.nih.gov>) and the internet based Cis-element cluster finder (Cister) programme (<http://zlab.bu.edu/~mfrith/cister.shtml>). These data were corroborated using laboratory based methods such as Polymerase Chain Reaction (PCR) and 5'-Rapid Amplification of cDNA Ends (5'-RACE). In addition, the proximal promoter region was tested for transcriptional capability using luciferase reporter gene technology.

Chapter 4 investigates HPMC regulation of CA125 expression during disease conditions using an *in vitro* model of inflammation. Changes in the transcriptional regulation, cell surface expression and cell surface secretion of CA125 were analysed using RT-PCR, flow cytometry (FACS) and Radioimmunoassay (RIA), respectively, in response to IL-1 β and IL-6/sIL-6R stimulation.

Chapter 5 examines the biological function of CA125 using a HPMC wound healing model. Time-lapse photography was used to analyse the rate of wound closure of mechanically scratched HPMC monolayers in response to the addition of exogenous CA125 and exogenous OC125 antibody. This chapter also investigates the potential relationship between the CA125 levels observed in the effluents of PD patients and the level of GDPs present in the dialysis fluids used.

Chapter 2

Methods and Materials

2.1 COMPUTATIONAL BASED METHODS

2.1.1 CA125 *in silico* gene reconstruction

cDNA sequences for CA125 were retrieved from the national centre for biotechnology information (NCBI) database at <http://www.ncbi.nlm.nih.gov>. Using the program BLAST (<http://www.ncbi.nlm.nih.gov/blast/>)[Altschul *et al*, 1997] genomic clones for CA125 were also retrieved. BLAST2 alignment software (<http://www.ncbi.nlm.nih.gov/blast/b12seq/b12.html>)[Tatusova *et al*, 1999] allowed direct alignment of the cDNA sequences with the gDNA sequences. These data were corroborated using the University of California Santa Cruz (UCSC) genome browser (<http://genome.cse.ucsc.edu/cgi-biun/hgGateway>).

2.1.2 Identification of putative transcription factor binding sites

The CA125 proximal promoter region was screened for the presence of TFBS's using the internet based Genomatrix suite (<http://genomatrix.de/cgi-bin/eldorado/main.pl>) and the internet based Cis-element cluster finder (Cister) programme (<http://zlab.bu.edu/~mfrith/cister.shtml>) using standard default parameters. The Estrogen Responsive Element Finder (<http://research.i2r.a-star.edu.sg/promoter/ERE-V2b/cgi/ere/pl>) was used to identify oestrogen responsive elements in proximal promoter sequence in accordance with Tang's method [Tang *et al*, 2004].

2.2 CELL CULTURE

2.2.1 Reagents

All chemicals were purchased from Sigma-Aldrich Co, Ltd (Gillingham,UK) unless otherwise stated. All chemicals were of analytical grade or higher.

2.2.2 Isolation and culture of human peritoneal mesothelial cells

Human peritoneal mesothelial cells (HPMC) were isolated from greater omentum tissue obtained from consenting patients undergoing elective abdominal surgery using an adapted version of Stylianou's original method [Stylianou *et al*, 1990]. Briefly, small pieces of omentum tissue (5cm²) were washed in sterile PBS (Gibco, Invitrogen Ltd, Paisley, UK) and transferred to 15ml of a trypsin/EDTA (0.1% w/v trypsin and 0.02% w/v EDTA) mixture and incubated for 15 mins at 37°C with continuous rotation. HPMC were then harvested by centrifugation of the digested tissue at 800g for 6 minutes. Pelleted cells were then suspended in growth medium.

2.2.3 HPMC growth conditions

HPMC were grown in Earles salt medium M199 (Gibco) containing 10% fetal calf serum (Hyclone, Perbio Science Ltd, Cranlington, Uk) supplemented with 100µg/ml penicillin, 100µg/ml streptomycin, 2mM glutamine (Gibco), 5µg/ml insulin, 5µg/ml transferrin and 0.4µg/ml hydrocortisone. Cell monolayers were then grown (incubated at 37°C, 5% CO₂) in T25 Falcon culture flasks (Becton Dickinson, Oxford, UK) until confluent. Primary cultures typically attained confluence in 3-5 days. All experiments were performed on cells of passage two.

2.2.4 Characterization of HPMC

2.2.4.1 HPMC Morphology

The morphology of monolayer cultures of HPMC was examined using an inverted light microscope (Axiovert 25, Carl Zeiss Ltd, Hertfordshire, UK). Confluent HPMC were typically polygonal in shape having approximately 5 sides and displaying the classical “cobblestone” appearance as seen in Appendix I. Cells adopting this morphology were growth arrested (section 2.2.8) and used in various experiments.

2.2.4.2 Immunohistochemistry

HPMC grown to confluence (first passage) on 8-well glass chamber slides (Gibco) were washed in PBS before they were fixed and permeabilized by addition of cold (4°C) acetone/methanol (1:1 v/v) for 5 minutes at room temperature (RT). The fixative was then removed and the cultures allowed to air dry. The cells were subsequently washed in 0.9% bovine serum albumin (BSA) in PBS (w/v) before the addition of the primary antibody (incubated for 45 minutes in a humidified chamber). Following staining with the primary antibody the cells were washed a further 3 times in 0.9% BSA/PBS (w/v) before incubation with a Fluorescein-conjugate (FITC) secondary antibody for 45 minutes in a dark humidified chamber. After a final wash the cells were mounted in PBS/glycerol (1.9% v/v) and viewed/photographed under a Leitz Orthoplan fluorescence microscope (Leica UK Ltd, Milton Keynes, UK). The antibodies used are listed below (Table 2.1).

Table 2.1 Antibodies used for the characterization of HPMC

Antibody	Sub-class	Optimal dilution	Supplier
Anti-Human cytokeratin 18 (clone CY 90)	IgG1, kappa	1:800	Dako Cytomation Ltd, Ely, UK.
Anti-swine vimentin	IgG1, kappa	1:10-1:25	Dako Cytomation Ltd, Ely, UK.
Anti-myosin (smooth and skeletal)	IgG	1:10	Sigma-Aldrich Co Ltd, Gillingham, UK.
Anti-human desmin	IgG1, kappa	1:50-1:100	Dako Cytomation Ltd, Ely, UK.
Anti-human Factor VIII (clone F8/F9)	IgG1, kappa	1:25-1:50	Dako Cytomation Ltd, Ely, UK.
FITC-conjugated rabbit anti-mouse	Immunoglobulins	1:20-1:40	Dako Cytomation Ltd, Ely, UK.
FITC-conjugated anti-rabbit	IgG	1:16-1:32	Sigma-Aldrich Co Ltd, Gillingham, UK.

2.2.5 Human Kidney (HK) 2 Cells

HK-2 cells are human proximal tubule cells transformed with the human papilloma virus 16 E6/E7 genes that retain the functional characteristics of fully differentiated proximal tubular cells [Ryan *et al*, 1994]. HK-2 cells were purchased from American Type Culture Collection (LGG Promochem, Teddington, UK).

2.2.6 HK-2 Growth conditions

HK-2 cells were grown in a 1:1 mix (v/v) of D-MEM:F-12 medium (Gibco/BRL Life Technologies Ltd) supplemented with 20 mM HEPES (Gibco), 2mM L-glutamine (Gibco), 5µg/ml insulin, 5µg/ml transferrin, 5ng/ml sodium selenite, 0.4µg/ml hydrocortisone and 10% fetal calf serum. Cell monolayers were then grown (incubated at 37°C, 5% CO₂) in T25 Falcon culture flasks until confluent.

2.2.7 Monolayer Sub-culture

On reaching confluence in the primary culture flask, cells were transferred into T75 culture flasks and then into the required experimental culture vessel (e.g. 6 well plate). Firstly the growth media was removed via aspiration and a 1:10 dilution (v/v) of trypsin/EDTA in sterile PBS was added in a volume adequate to submerge the cells. Cell detachment was then monitored via light microscopy (Axiovert 25). Following detachment 10mls of the appropriate growth medium with 10% FCS was added to neutralise the trypsin. This was then transferred to a 50ml centrifuge tube (Greiner Bio-One Ltd, Stonehouse, UK) and spun at 800g for 6 minutes. The supernatant was then removed and the pellet re-suspended in supplemented medium containing 10% FCS which was then dispensed into the new culture vessel. Confluent cells were split in a ratio of 1:3.

2.2.8 Growth Arrest

Prior to each experiment, the growth phase of the cells was synchronised by growth arresting them in serum free supplemented medium M199. Briefly, growth medium was removed and the cells were washed twice in serum free M199 to remove residual FCS before the addition of fresh serum free medium [Floege *et al*, 1990]. Under these conditions, cells remain viable for up to 96 hours and were typically used after 48 hours growth arrest.

2.2.9 Cell Stimulation

HPMC at passage two were grown to confluence in a culture vessel. Following growth arrest the spent medium was removed and the cells were washed in serum free medium. Stimulation was performed by incubation of the cells with the desired stimulus (i.e. IL-1 β , IL-6, retinoic acid, oestrogen) diluted in serum free M199 for varying times and concentrations before analysis.

2.2.10 Oestrogen and Retinoic Acid Stimulation

Cells to be stimulated with oestrogen or all-trans retinoic acid were grown in phenol red free M199 supplemented with 100 μ /ml penicillin, 100 μ g/ml streptomycin, 2mM glutamine, 5 μ g/ml insulin, 5 μ g/ml transferrin, 0.4 μ g/ml hydrocortisone and 10% charcoal/dextran treated FCS (Hyclone). The cells were growth arrested in phenol red free M199 (minus serum) for 48 hours prior to experimentation. This alternative medium was used to reduce the amount of oestrogen and retinoic acid in the system.

2.3 RNA ANALYSIS

2.3.1 Chloroform/Isopropanol RNA extraction

One millilitre of tri-reagent was added per well of a 6 well plate and left for 5 minutes until all cells were lysed. The lysate was then collected in a 1.5ml microcentrifuge tube to which 0.2ml of chloroform was added per 1ml lysate. After mixing by inversion, each sample was left to incubate for 5 minutes to allow the separation of two phases. The samples were then centrifuged at 12000rpm for 15 minutes (4°C, with no braking). The colourless phase was transferred to a clean microfuge tube and the lower phase (and interface) discarded. RNA precipitation was achieved by addition of 0.5ml isopropanol to each sample before storage over night at -20°C. The RNA was pelleted by centrifugation at 12000 rpm for 15 minutes at 4°C. The pellet was then washed by adding 1.5ml of ice cold ethanol, vortexing briefly and centrifuging at 12000 rpm for 15 minutes at 4°C. All traces of ethanol were then removed and the pellet allowed to air dry for approximately 1 hour before re-suspension in 10 μ l of sterile H₂O.

2.3.2 Determination of DNA and RNA concentration

RNA and DNA concentrations were determined by spectrophotometric analysis using a Beckman UV-DU64 spectrophotometer (Beckman Instruments Ltd, High Wycombe, UK). In an appropriate cuvette 1 μ g of RNA or DNA was diluted in 54 μ l of sterile water. The absorbance was read at both 260nm and 280nm. A 260/280 ratio of above 1.8 was

indicative of a sufficiently pure sample. The concentration was calculated using the following formula:

$$[\text{RNA or DNA}] (\mu\text{g/ml}) = \text{Abs}_{260} \times \text{Molar extinction coefficient} \times \text{dilution factor}$$

Molar extinction coefficient for RNA = 40

Molar extinction coefficient for DNA = 50

Dilution factor = 55

An Abs_{260} of between 0.1 -1.0 was required to be in the linear range of the Beer-Lambert law. Samples were diluted where necessary and discarded if $\text{Abs}_{260} < 0.1$.

2.3.3 RNA quantification

RNA integrity was determined by flat bed electrophoresis using a mini gel system (Thermo Life Sciences Ltd, Basingstoke, UK) through a 2% agarose gel (composed of 1g Electrophoresis grade agarose (Ultrapure agarose, GIBCO/BRL), 50ml of 1 X TAE buffer (Promega Ltd, Southampton, UK) and 5 μ l ethidium bromide (5mg/ml). Into a single well, 1 μ g of RNA was loaded along with 5 μ l of loading buffer (15% Ficoll Type 400 (Amersham Biosciences UK Ltd, Chalfont St.Giles, UK) in H₂O, 0.25% Orange G). Visualisation of the gel (Figure 2.1) was carried out using ultra violet light in the ChemiDoc™ Gel documentation system (Bio-Rad Laboratories Ltd, Hemel Hempstead, UK).

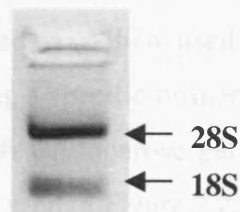


Figure 2.1 A RNA agarose gel (2% w/v) showing the 18S and 28S ribosomal subunits of total RNA (1 μ g) extracted from HPMC. The presence of the two distinct bands is confirmation of non-degraded RNA that is suitable to be used in further experiments.

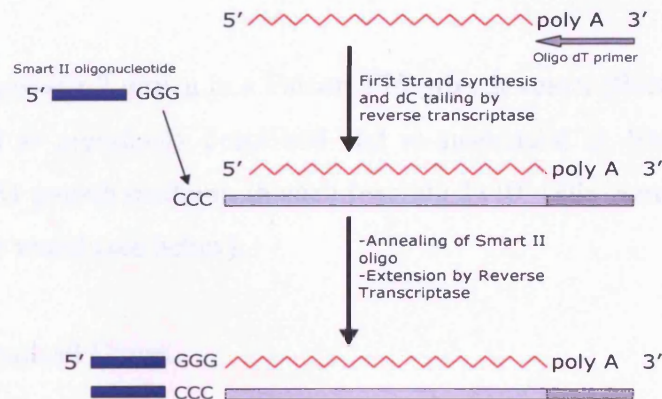
2.3.4 Semi-quantitative RT-PCR

Reverse Transcription was performed using the random hexamer method [Topley *et al*, 1993]. Briefly, 1µg total RNA in a total volume of 20µl comprising 100µM random hexamers (Amersham Biosciences UK Ltd), 5mM dNTPs (Amersham Biosciences UK Ltd), 1 X PCR buffer containing 1.5mM MgCl₂ (Applied Biosystems, Warrington, UK) and 1mM DTT (Invitrogen Ltd) was heated to 95°C for 5 minutes in order to linearise the RNA. Following immediate cooling on ice 40U of recombinant RNAsin ribonuclease inhibitor (Promega Ltd) and 200U Superscript II Rnase H- reverse transcriptase (Invitrogen Ltd) were then added. The RNA was then reverse transcribed by heating to 20°C for 10 minutes, 42°C for 60 minutes, 95°C for 5 minutes and finally 4°C for 2 minutes. Two microlitres of the resulting cDNA was used in each PCR reaction (see section 2.4.1).

2.3.5 5'-Rapid amplification of cDNA ends (5'-RACE)

Firstly, mRNA was isolated from total RNA (75µg) using Oligo (dT)₂₅ Dynabeads (DynaL Biotech, Wirral, UK) in accordance with the manufacturer's protocol. The isolated mRNA was subsequently used in the 5'-RACE reaction using the SMART RACE Kit (BD Biosciences, Oxford, UK). Following the manufacturer's protocol, 3µl of mRNA was reverse transcribed before PCR was used to amplify the resultant cDNA, using the Advantage 2 PCR Kit (BD Biosciences). Briefly, 2.5µl of cDNA was amplified using a specific primer that binds to the RACE 1 site. See appendix II for 5'-RACE PCR conditions. The product generated was then used in a nested PCR reaction (same conditions as described above) using a specific primer that binds at the RACE 2 site. The products were analysed using a 2% w/v agarose gel, by flat bed electrophoresis. The complete RACE mechanism can be seen in Figure 2.2.

A. Mechanism of cDNA synthesis



B. 5'-RACE Polymerase Chain Reaction

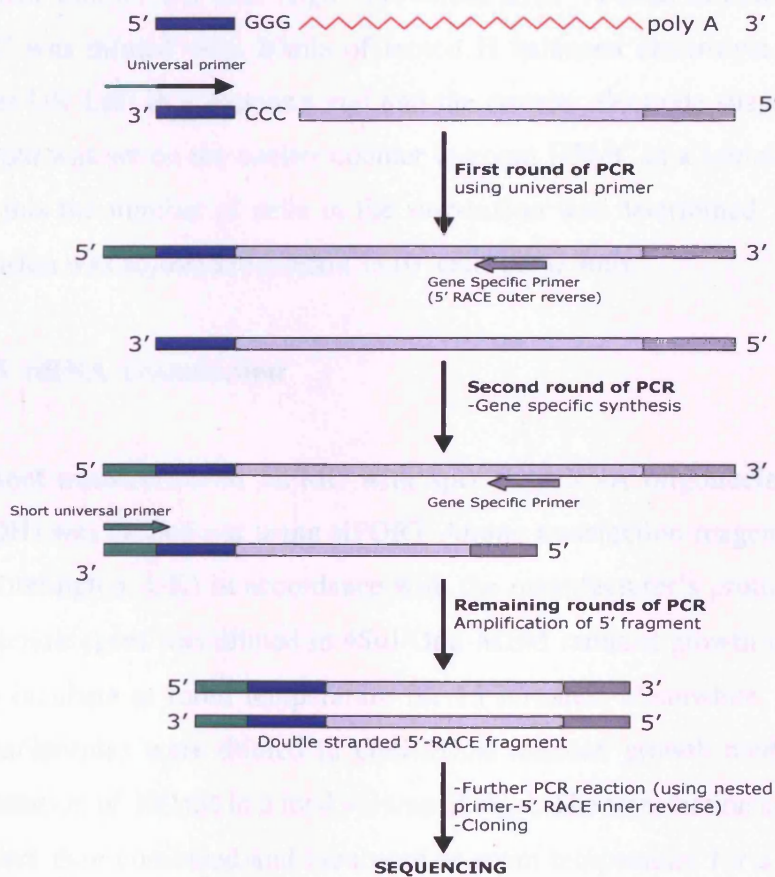


Figure 2.2 5'-RACE Mechanism (adapted from SMART RACE kit protocol (BD Biosciences, Oxford, UK))

2.3.6 RNA Interference

2.3.6.1 Plate layout

HMPc of passage 2 grown in a Falcon T75 growth vessel (Becton Dickinson Ltd) were trypsinized as previously described and re-suspended in 10ml supplemented M199 (+10% FCS) growth medium. In each reaction 1×10^5 cells were added per well of a 12 well culture vessel (see below).

2.3.6.2 Total cell Count

The number of resuspended HMPc was determined using a coulter counter (Z2, Beckman Coulter UK Ltd, High Wycombe, UK). A $20 \mu\text{l}$ sample of the resuspended HMPc was diluted with 20mls of Isoton II balanced electrolyte solution (Beckman Coulter UK Ltd) in a counting vial and the counter electrode suspended in the vial. A threshold was set on the coulter counter to count HMPc in a sample volume of 0.5mls. From this the number of cells in the suspension was determined. The volume of the suspension was adjusted to contain 1×10^5 cells per 0.9mls.

2.3.6.3 siRNA Transfection

Transient transfection of HMPc with specific siRNA oligonucleotides (CA125 and GAPDH) was carried out using siPORT Amine transfection reagent (Ambion (Europe) Ltd, Huntingdon, UK) in accordance with the manufacturer's protocol. Briefly, $5 \mu\text{l}$ of transfection agent was diluted in $45 \mu\text{l}$ Opti-MEM reduced growth medium (Gibco) and left to incubate at room temperature for 15 minutes. Meanwhile, the specific siRNA oligonucleotides were diluted in Opti-MEM reduced growth medium to give a final concentration of 100nM in a total volume of $50 \mu\text{l}$. The transfection agent mix and siRNA mix were then combined and incubated at room temperature for a further 10 minutes. The newly formed transfection complexes ($100 \mu\text{l}$) were dispensed into empty wells of a 12 well culture plate. To each well 1×10^5 HMPc (see 2.3.6.2) were then added, so that the total volume in each well was 1ml. The plate was then rocked gently back and forth,

to evenly distribute the complexes, before the cells were incubated at 37°C with 5% CO₂ for 48 hours. The mechanism of siRNA can be seen in Figure 2.3.

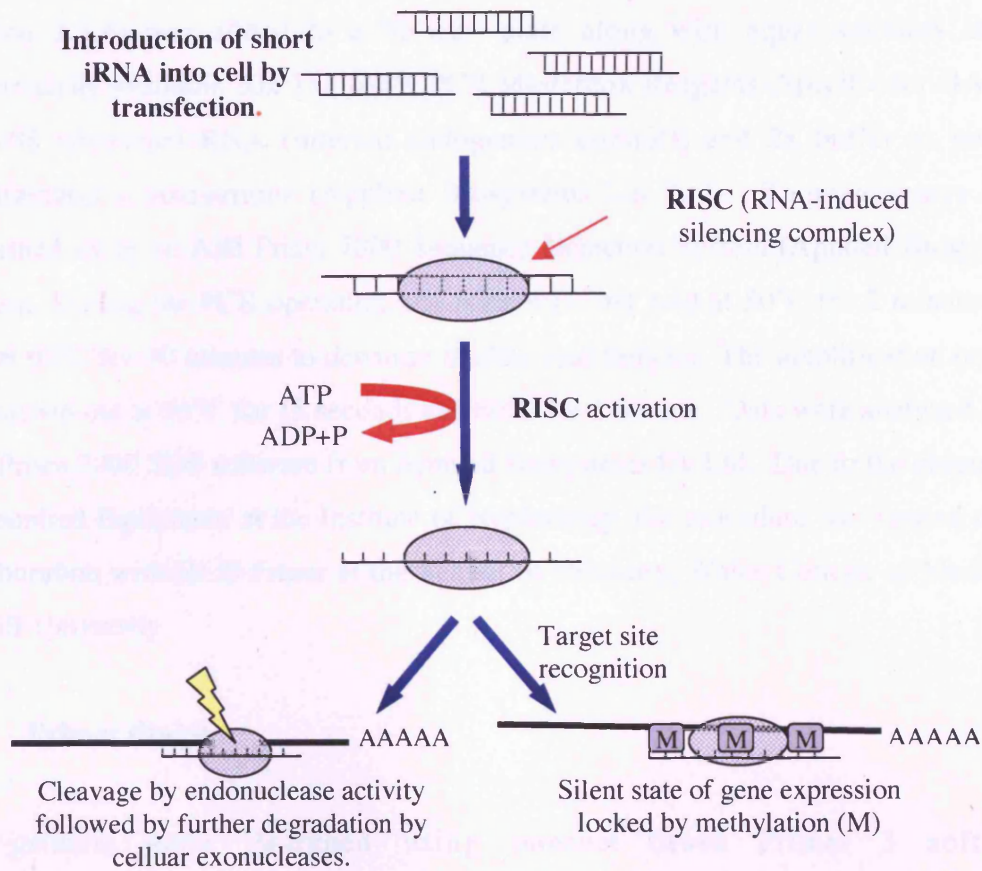


Figure 2.3 Mechanism of gene knockdown by interference RNA (siRNA).

2.4 DNA ANALYSIS

2.4.1 Polymerase Chain Reaction (PCR)

For each 50µl PCR reaction, 2µl of the cDNA generated from the reverse transcription (section 2.3.4) reaction (or 40ng genomic DNA) was used. Each reaction comprised 1 x PCR Buffer containing 1.5mM MgCl₂ (Applied Biosystems), 5mM dNTPs (Amersham Biosciences UK Ltd), 2.5U AmpliTaq Gold (Applied Biosystems UK Ltd) and 1mM oligonucleotide primers. The standard PCR protocol can be seen in Appendix II.

2.4.2 Quantitative Polymerase Chain Reaction

For each 25µl qPCR reaction, 1µl of the cDNA generated from reverse transcription (section 2.3.4) was added to a 96-well plate along with equal amounts of the commercially available 20x Taqman® PCR Mastermix Reagents (Specific for GAPDH and 18S ribosomal RNA (internal endogenous control)) and 2x buffer as per the manufacturer's instructions (Applied Biosystems UK Ltd). Taqman assays were performed using an ABI Prism 7000 Sequence Detection System (Applied Biosystems Uk Ltd). During the PCR operation, the plate was first held at 50°C for 2 minutes and then at 95°C for 10 minutes to denature nucleic acid samples. The amplification process was carried out at 95°C for 15 seconds and 60°C for 1 minute. Data were analyzed using ABI Prism 7000 SDS software from Applied Biosystems Uk Ltd. Due to the absence of the required Equipment at the Institute of Nephrology, the procedure was carried out in collaboration with Dr D Fraser at the School of Dentistry, Wales College of Medicine, Cardiff University.

2.4.3 Primer design

All primers were designed using internet based Primer 3 software (http://frodo.wi.mit.edu/cgi-bin/primer3/primer3_www.cgi) and purchased from Invitrogen Ltd. Primers were designed to have a GC content of 50-60% and a T_M (annealing temperature) of approximately 60°C. All primers (lyophilised upon arrival) were reconstituted in sterile H₂O to give a stock concentration of 200µM.

2.4.4 Sizing of PCR Products

All PCR products were run on a 2% agarose gel. Each gel comprised 2% w/v agarose, 1 X TAE and 5µl ethidium bromide (5mg/ml). 5µl of PCR product was loaded onto the gel along with 5µl of loading buffer (15% Ficoll Type 400 in H₂O, 0.25% Orange G). Typically, the gel was run at 90v for 45-60 minutes. The agarose gels were visualised/photographed using a ChemiDoc™ Gel documentation system

2.4.5 Purification of PCR products

Bands were extracted from an agarose gel using the QIAquick Gel purification kit (Qiagen Ltd, Crawley, UK) in accordance to the manufacturers protocol. Briefly, bands were made visible on a UV transilluminator (GRI, Braintree, UK) where they were cut from the gel and centrifuged at 13000rpm for 5 minutes, through a filter column, in order to remove any traces of agarose. The remaining sample was then mixed with equal volumes of buffer PB (supplied in kit) and passed through a QIAquick spin column by centrifugation (13000rpm for 60 seconds). DNA bound to the column was then washed with 0.75ml ethanol by centrifugation (13000rpm for 60 seconds) and eluted in 50µl sterile H₂O.

2.5 CLONING TECHNIQUES

2.5.1 Cloning of 5'-RACE products

Extracted and cleaned DNA fragments were cloned into a pCR[®]2.1 TOPO sequencing vector (see Appendix III) using a TOPO TA cloning[®] kit (Invitrogen Ltd). A TOPO cloning reaction mixture was set up by mixing 2µl fresh PCR product, 0.5µl salt solution, 0.5µl TOPO vector and 2µl water for a total volume of 5µl. The newly formed vector was then used to transform One Shot *Escherichia coli* (Invitrogen Ltd) as described in section 2.5.3.

2.5.2 Generation of Luciferase promoter constructs

Purified promoter constructs (generated using PCR) were cloned into a modified version of pGL-3 Basic luciferase reporter vector (Promega Ltd) in which the multiple cloning site had been altered to include cleavage sites from other common restriction enzymes (supplied by Dr. P. Buckland, Department of Psychological Medicine, Wales College of Medicine, Cardiff Univeristy). Appendix IV shows the original and modified sequence of the pGL-3 multiple cloning site. Using the restriction enzymes *KpnI* and *SpeI*, 5µg of modified pGL3 vector was digested for 2 hours at 37°C. The digested vector was then

analysed by electrophoresis on a 2% agarose gel before being extracted using the QIAquick gel extraction kit (see section 2.4.5) in accordance with the manufacturer's protocol. Two micrograms of the digested vector was then treated with 2U shrimp alkaline phosphatase (Promega Ltd) in a total volume of 30 μ l. Heating to 65°C for 20 minutes then deactivated the enzyme.

Promoter fragments obtained via PCR were digested using the enzymes outlined in 2.5.5, and purified as previously described. The promoter fragments were then cloned into the digested and dephosphorylated pGL-3 vector using the following reaction mix. 6 μ l Promoter fragment, 2 μ l vector, 1 x ligase buffer and 2000U T4 DNA ligase (New England Biolabs (UK) Ltd, Hitchin, UK) in a total volume of 10 μ l. After incubation at 16°C for 24 hours, One Shot Top 10 *Escherichia coli* (Invitrogen Ltd) were transformed with the recombinant vectors (see section 2.5.3) and grown overnight in a shaking incubator. The vectors were then purified and sequenced as previously described.

2.5.3 Transformation

To each sample, 50 μ l (10^8 cfu/ μ g) One Shot Top 10 *Escherichia coli* cells were added and incubated on ice for 30 minutes. The cells were then heat-shocked by incubating at 42°C for 45 seconds before being placed back on ice for 5 minutes. To the cells, 150 μ l of fresh LB medium (see Appendix V) was added, followed by incubation at 37°C for approximately 90 minutes in an orbital shaker (200rpm). These cells were then plated on to YT Agar (see Appendix V) containing 100 μ g/ml carbenicillin and incubated at 37°C overnight.

2.5.4 Purification of recombinant vectors

From each plate 5 colonies were picked and grown in 5ml YT broth (containing 100Ug/ml carbenicillin) at 37°C overnight. The cells contained within 1.5ml of each cell culture were then pelleted by centrifugation (13,000rpm for 1 min) and the supernatant removed by decanting, leaving approximately 50 μ l residual medium. Pellets were then

re-suspended by brief vortexing before the addition of 300µl of TENS buffer (50 mM Tris [pH 8.0], 20 mM disodium EDTA, 100 mM NaCl, 1% [wt/vol] sodium dodecyl sulfate). The solutions were then mixed by inversion and left to incubate at room temperature for a maximum of 5 minutes before the addition of 150µl 2M sodium acetate. After centrifugation at 13,000rpm for 4 minutes, the supernatants were transferred to a second vessel where 900µl pure ethanol was added. Samples were then centrifuged for a further 4 minutes at 13,00rpm. The pellet formed was then washed a second time as previously described but using 70% ethanol. After the second wash the pellet was allowed to dry at room temperature (inverted tube) and re-suspended in 20µl sterile water.

2.5.5 Screening for presence of inserts

In order to confirm the presence of the desired insert, 5µl of each resultant sample was then digested with the appropriate restriction enzyme, to excise the inserted fragment for 2 hours (See Table 2.2).

Table 2.2 Restriction enzymes used in plasmid screening

Construct	Restriction enzyme
CA125 Promoter	- F100 <i>KpnI</i> and <i>SpeI</i>
	- F500 <i>KpnI</i> and <i>SpeI</i>
	- F1000 <i>KpnI</i> and <i>SpeI</i>
5'-RACE Fragments	<i>EcoRI</i>

These products were then separated by electrophoresis on 2% agarose. Any RNA contamination in the preparations was removed by adding 1µl ribonuclease A (10mg/ml) to the loading buffer. After analysis of the gel, colonies containing the desired promoter fragments were re-picked and grown in 5ml YT broth as previously outlined. The recombinant vector was then harvested using the QIASpin Mini-prep kit (QIAGEN Ltd) in accordance with the manufacturer's instructions. Samples were eluted in 50µl H₂O instead of TE buffer.

2.5.6 Sequence analysis

In order to ensure the identity of the target sequence, all promoter and 5'-RACE constructs were sent for sequence analysis to The Sequencing Service, The University of Dundee, Dundee, UK. 5'-RACE fragments were sequenced in a pCR 2.1 TOPO vector using M13 forward and reverse primers. Promoter constructs were sequenced in the pGL-3 modified vector using RV3 and GL2 primers. The primer sequences can be seen in Table 2.3.

Table 2.3 Sequencing oligonucleotide primers

Primer	Sequence*
M13 forward	GTAAAACGACGCCAG
M13 reverse	CAGGAAACAGCTATGAC
RV3	CTAGCAAATAGGCTGTCCC
GL2	CTTTATGTTTTGGCGTCTTCC

*primer sequences are shown in 5'-3' orientation

2.6 LUCIFERASE ANALYSIS

2.6.1 Plate set up

Confluent 75cm² flasks of HPMC or HK-2 cells were harvested as described previously. After resuspension in the appropriate, supplemented, medium the cells were plated into 6-well plates (2ml per well). Cells were grown to a confluence of ~70% before transfection.

2.6.2 Transient transfection

Transient transfection of HPMC and HK-2 cells was performed using the lipofection agent FuGene 6 (Roche Diagnostics Ltd, Lewes, UK) as this was shown to be the most efficient for HPMC transfection [Ohan *et al*, 2001]. Optimisation experiments on HK-2 cell transfection [Fraser *et al*, 2002] and unpublished experiments on HPMC transfection have previously determined that a ratio of 3:1 (μ l FuGene: μ g DNA) was required for HPMC transfection in 6-well plates (see Appendix V). When the cells reached the required confluence (70%) the growth medium was removed and the cells were washed

in PBS. The cells were then transfected with 1µg of the previously made luciferase *Firefly* promoter constructs (see section 2.5.2) and 1µg of *Renilla* luciferase vector (Promega Ltd) in accordance with the FuGene 6 manufacturer's instructions. The transfection was carried out in growth medium without FCS. After 24 hours the transfection medium was replaced with fresh medium containing the necessary stimulus for the experiment and incubated for a further 24 hours under growth conditions.

2.6.3 Reporter gene analysis in HPMC

The growth medium was removed and the cells were washed with PBS. The cells from each well were then scrapped into 1ml PBS and transferred to 1.5ml microcentrifuge tubes. The cells were then pelleted using centrifugation at 5000rpm for 2 minutes. The supernatant was removed by aspiration and 60µl lysis buffer (supplied in Dual-Glo luciferase assay kit (Promega Ltd)) was added to each sample before vortexing for 10 seconds. The samples were then incubated at room temperature for 15 minutes before 50µl of each sample was transferred to a white luminometric 96-well plate (Thermo Life Sciences). Luciferase activity was then assayed using the Dual-Glo luciferase assay kit as outlined in the manufacturer's protocol. Briefly, 100µl of Luciferase Assay Reagent II (LARII) was added to each sample in the 96-well plate. Immediately after this the luminescence of each well was read for 10 seconds using a luminometer (FLUOSTAR Optima, BMG Labtechnologies GmbH, Offenburg, Germany). Stop and Glo reagent (100µl) was then added and *Renilla* luminescence in each sample was recorded as before.

2.6.4 Reporter gene analysis in HK-2 Cells

The growth medium was removed and the cells were washed in PBS before the addition of 500µl of lysis buffer (supplied in Dual-Glo luciferase assay kit) per well. The cells were then incubated at room temperature for 15 minutes with gentle agitation. Any remaining adhered cells were removed by scrapping and the cell suspension was transferred to 1.5ml microcentrifuge tubes where each sample was vortexed for 10 seconds. Fifty microlitres of each sample was transferred to a white luminometric 96-

well plate. Luciferase activity was then assayed using the Dual-Glo luciferase assay kit, as previously described.

2.7 WESTERN BLOT

2.7.1 Gel preparation

Appropriate percentage SDS-polyacrylamide running gels were used for all Western blotting experiments dependant on protein of interest (see figure below for all gel compositions). Gels were made using a large vertical apparatus (Bio-Rad Laboratories Ltd). Firstly a SDS-polyacrylamide block gel was poured to form a 1cm layer at the bottom of the gel, once polymerised the running gel was added before addition of the stacking gel. All gels were left to polymerise over night.

Table 2.4 Western gel compositions

	Stacking Gel	Running Gel		10% Block Gel
		3%	7.5%	
H ₂ O	6.1ml	6.35ml	4.85ml	4ml
Tris	2.5ml (pH6.8)	2.5ml (pH8.8)	2.5ml (pH8.8)	2.5ml (pH8.8)
SDS (10%)	100µl	100µl	100µl	100µl
Acrylamide (30%)	1.3ml	1ml	2.5ml	3.34ml
APS	50µl	50µl	50µl	50µl
Temed	10µl	5µl	5µl	5µl

2.7.2 Sample preparation and electrophoresis

Each sample (supernatant (section 2.7.3) or cell lysate (section 2.7.4)) was loaded on to the gel in a 2:1 mix (v/v) with sample loading buffer (60mM Tris (pH 6.8), 30% glycerol, 3mM EDTA, 3% SDS, 0.01% bromophenol blue and 5% β-mercaptoethanol) after heating at 95°C for 5 minutes. Samples were then vortexed and centrifuged briefly before loading on a gel submerged in 1 x running buffer (30g/L Tris, 144g/L glycine and 10g/L SDS made up in H₂O). The size of the target protein was calibrated by the addition of

20µl of high molecular weight protein marker (Amersham Biosciences UK Ltd) to a separate well. The gel was then run at 80v (4°C) until the loading buffer reached the end of the gel.

2.7.3 Supernatant sample preparation

Supernatants were collected for cell monolayers and spun for 10 minutes at 3000rpm in a Vivaspin concentrator centrifuge tube (Vivascience, Epsam, UK) according to the manufacturer's instructions.

2.7.4 Cell lysate sample preparation

Cells lysate samples were collected from HPMC monolayers by the addition of 200µl of cell lysis buffer (mix of 0.5% NP-40 in Tris buffered saline (pH 5.5) and 2% protease inhibitor cocktail) followed by incubation at RT for 15 minutes. Cell debris was pelleted via centrifugation at 13000rpm for 1 minute and the cell lysate removed.

2.7.5 Protein concentration estimation

The protein concentration of each sample was determined using the Bio-Rad protein assay (Bio-Rad Laboratories Ltd). Sample protein concentration was determined by direct comparison with BSA standards diluted in PBS, ranging from 0-10µg/ml. Appropriately diluted standards and samples (100µl) were loaded in duplicate in to a flat-bottomed 96 well plate (Microlite II, Thermo life Sciences) followed by the addition of an equal volume of 40% dye binding reagent (Bio-Rad Laboratories Ltd). The absorbance of each sample was read (600nm) using the Dynex Revalation 96-multiwell plate reader (Thermo Life Sciences Ltd).

2.7.6 Transblotting

The gel was removed from the vertical slab apparatus and equilibrated in 1x Transfer buffer (25mM Tris, 192mM glycine, 20% methanol in H₂O) for 10 minutes with a nitrocellulose transblotting membrane (Hybond ECL, Amersham Biosciences Ltd). Both gel and membrane were placed between a layer of filter papers and plastic wool pads and assembled into the transblotting apparatus (Bio-Rad Laboratories Ltd). Transblotting was performed with cooling (4°C) at 90v for approximately 2 hours.

2.7.7 Blocking and antibodies

Following the transblotting stage the membrane was blocked in 5% w/v non-fat powdered milk in PBS Tween 20 (0.2%) for 1 hour. This was followed by 5 washes in PBS Tween (0.2%) over 1 hour. The primary antibody was diluted 1:100 in 5% non-fat powdered milk/PBS Tween 20 (0.2%) for a total volume of 20ml per membrane. The membrane was incubated at 4°C overnight, with gentle rocking. Following five further washes in PBS Tween (0.2%), a relevant horseradish peroxidase-conjugated secondary antibody (diluted 1 in 1000) in 5% non-fat powdered milk/0.2% PBS Tween was added and the membrane incubated at RT for 1 hour, with rocking.

2.7.8 Detection

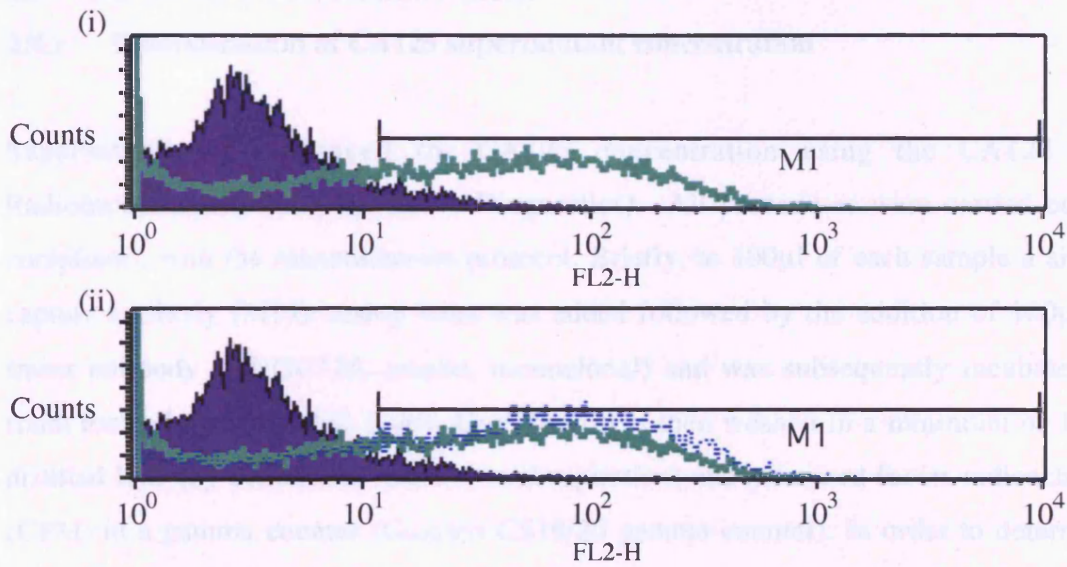
Following 5 washes in 0.2% PBS Tween 20 over a 2 hour period, the blot was developed on high performance autoradiography film (Amersham Biosciences Ltd) using the ECL chemiluminescence system (Amersham Biosciences Ltd) in accordance with the manufacturer's protocol. The exposure time was dependant on each specific experiment.

2.8 FACS ANALYSIS




2.8.1 CA125 HPMC surface expression

HPMC were removed from the culture flask using 1:10 mix (v/v) of trypsin/EDTA in PBS. Medium M199 with 10% FCS was added to neutralise trypsin activity. The cells were then centrifuged at 800g for 6 minutes and the supernatant removed by aspiration. The mesothelial cell pellet was then resuspended in FACS buffer (PBS containing 10mM EDTA, 15mM sodium azide and 1% BSA) and transferred to a 96 well plate (100µl per well). To each sample 100µl (0.4µg/ml) of monoclonal antibody OC125 (Fujirebio Diagnostics, Toyama, Japan) was added and incubated at 4°C for 30 minutes. The antibody concentration was defined as shown in Figure 4.3 of chapter 4. The cells were then washed by centrifugation at 800g for 6 minutes, removing the supernatant and re-suspending in 250µl FACS buffer. This was carried out for a maximum of three washes. After the third wash the pellet was re-suspended in 100µl of secondary antibody (1/100 dilution, rat anti-mouse IgG PE, Becton-Dickinson Ltd), and incubated at 4°C for 30 minutes. The wash procedure was then repeated. At the end of the last wash the cells were re-suspended in 250µl FACS buffer and transferred to FACS tubes. A total of 10000 cells for each sample were counted on the FACS calibur 4CA cell sorter (Becton Dickinson Ltd) using the FL2-PE detector. HPMC void of antibody staining and HPMC stained with only secondary antibody were used as controls to ensure that no non-specific binding was present. Data was analysed using Cell Quest-pro software (see Figure 2.4).

A. Fluorescence Intensity Histogram



M1: Fluorescence intensity gate. Defines the % surface expression of specific cell surface antigen (Boxed values-Histogram Statistics).

-  : Negative staining population
-  : Positive Control Staining population (no cell stimulation, 48 hours)
-  : Positive staining population (cell stimulation, 48 hours)

B. Histogram Statistics

File: 25.2.3.009
 Gate: No Gate
 Total Events: 10000

Acquisition Date: 25-Feb-03
 Gated Events: 10000

	Marker	Events	% Gated	% Total
	All	10000	100.00	100.00
48 hour control-no stimulation	M1	10000	81.92	81.92
48 hour- stimulated	M1	10000	88.48	88.48

**6.56%
change in
Expression**

Figure 2.4 Calculation of percentage shift in positively stained cells.

A(i) Histogram demonstrating the shift of positively stained cells into M1 compared to the negatively stained cells. A(ii) Histogram showing the shift in expression of a surface expressed antigen between stimulated and unstimulated cells. B. Histogram statistics provide a value for the % change in staining/expression for a specific antigen.

2.9 RADIOIMMUNOASSAY (RIA)

2.9.1 Determination of CA125 supernatant concentration

Supernatants were assayed for CA125 concentration using the CA125 (II) Radioimmunoassay kit (Fuji-Rebio Diagnostics). All procedures were carried out in compliance with the manufacturers protocol. Briefly, to 100 μ l of each sample a single capture antibody (M11) coated bead was added followed by the addition of 100 μ l of tracer antibody (125 I OC125, mouse, monoclonal) and was subsequently incubated at room temperature for 20 \pm 2 hours. Each bead was then washed in a minimum of 15ml distilled H₂O (by continuous addition and aspiration) and measured for its radioactivity (CPM) in a gamma counter (Gamby CS10/20 gamma counter). In order to determine unknown CA125 concentrations, a standard curve was constructed by plotting average CPM versus CA125 concentration of the standards supplied by the manufacture (Figure 2.5).

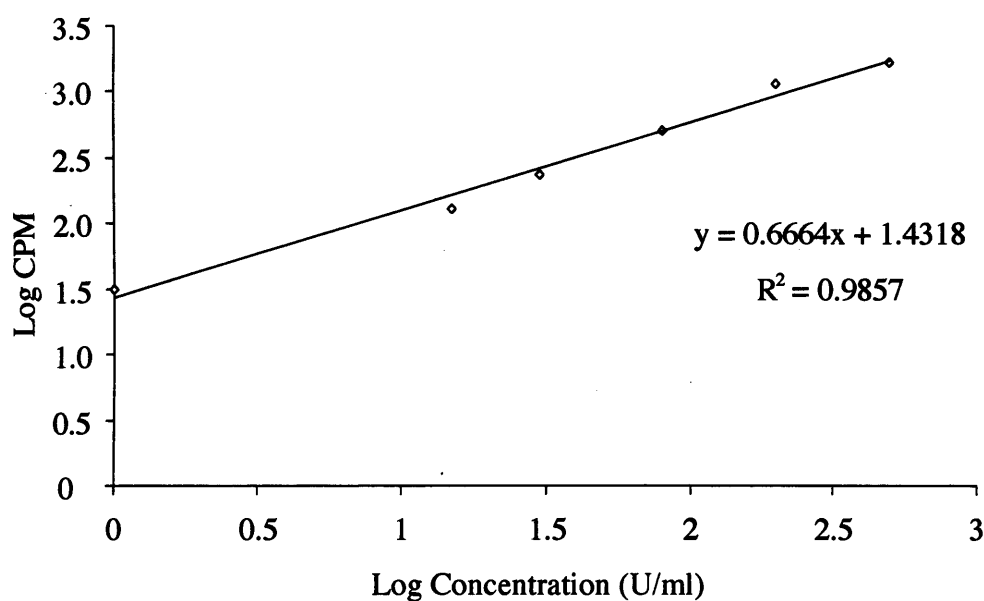


Figure 2.5 Calibration curve showing Log of CPM versus Log of CA125 Concentration.

2.10 ENZYME-LINKED IMMUNOSORBENT ASSAYS (ELISA)

2.10.1 MCP-1 ELISA

Supernatant samples were assayed for MCP-1 concentration in accordance with the BD OptEIA™ Human MCP-1 ELISA set protocol. Briefly, each well of a 96 well micro-titre plate (Immulon 4HBX, Thermo Life Sciences Ltd) was coated by the addition of 100µl anti-human MCP-1 monoclonal capture antibody and incubated overnight. The plate was then washed 3 times with the provided wash buffer on a wellwash 4 automatic plate washer (Thermo Life Sciences Ltd) before blocking via a 2 hour incubation with 200µl/well assay diluent. After a further 3 washes with wash buffer 100µl of each standard sample and control was added into an appropriate well and left for 2 hours at room temperature (1:20 dilution of the working samples was used). Each well was then washed 5 times in wash buffer before 100µl working detection solution (biotinylated anti-human MCP-1 monoclonal antibody and avidin-horseradish peroxidase conjugate) was added to each well and left for 1 hour at RT. This was then followed by a further series of washes. 100µl of substrate solution was then added to each well and incubated in the dark for a maximum of 30 minutes (without sealing the plate). To stop the reaction 50µl of stop solution (2M H₂SO₄) was swiftly added to each well. The absorbance of each sample was read (450nm) using the Dynex Revalation 96-multiwell plate reader. MCP-1 concentrations were deduced using the logarithmic relationship between the standards (pg/ml) and their absorbances (450nm).

2.10.2 IL-8 ELISA

Supernatant samples were assayed for IL-8 concentration in accordance with the BD OptEIA™ Human IL-8 ELISA set protocol. Briefly, each well of a 96 well micro-titre plate was coated by the addition of 100µl anti-human IL-8 monoclonal capture antibody and incubated overnight. The plate was then washed 3 times with the provided wash buffer on a Wellwash 4 automatic plate washer before blocking via a 2 hour incubation with 200µl/well assay diluent. After a further 3 washes with wash buffer, 100µl of each standard, sample and control was added into an appropriate well and left for 2 hours at

room temperature (1:30 dilution of the working samples was used). Each well was then washed 5 times in wash buffer before 100µl working detection solution (biotinylated anti-human IL-8 monoclonal antibody and avidin-horseradish peroxidase conjugate) was added to each well and left for 1 hour at RT. This was then followed by a further series of washes. 100µl of substrate solution was then added to each well and incubated in the dark for a maximum of 30 minutes (without sealing the plate). To stop the reaction, 50µl of stop solution (2M H₂SO₄) was swiftly added to each well. The absorbance of each sample was read (450nm) using the Dynex Revalation 96-multiwell plate reader. IL-8 concentrations were deduced using the logarithmic relationship between the standards (pg/ml) and their absorbances (450nm).

2.11 TIME LAPSE PHOTOGRAPHY

2.11.1 Scratch wounding of HPMC monolayer

HPMC were grown to confluence and growth arrested as described in section 2.2.8. The monolayer was then wounded with a single scratch using a sterile 1ml pipette tip (tarstedt Ltd, Leicester, UK), without damaging the plastic base. This resulted in a linear wound approximately 0.5 – 0.6 mm in width (removing approximately 4% of the HPMC monolayer). The wounded monolayers were then washed with M199 medium, to remove any detached cells and cellular debris. Cells were then incubated with test or control solution for defined time periods. For experimental procedures, solutions were prepared with M199 containing 2mmol/L N-2-hydroxyethylpiperazine-N'-2ethanesulfonic acid (HEPES)(Gibco) to ensure a pH of 7.4 was maintained throughout the experiment.

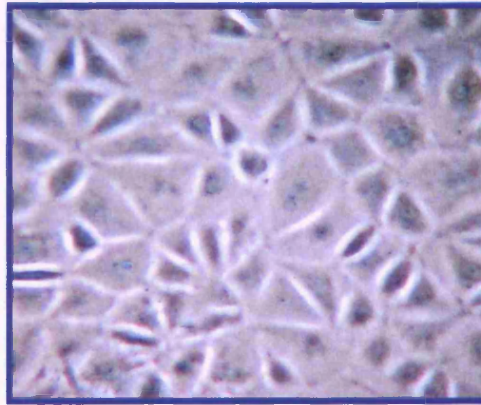
2.11.2 Assessment of wound closure by time-lapse photography

The nude area in each well was identified microscopically and the co-ordinates recorded for subsequent data capture. Wound closure or HPMC migration was monitored using an Axiovert 100M inverted microscope fitted with a XY automated scanning stage and incubator (Carl Zeiss Ltd, Welwyn Garden City, UK). The incubator was maintained at 37°C with 5% CO₂ using a heated insert and vertical airflow. At 1 hour intervals images

were captured from a defined position in each well using a 2.5x Objective on an Orca C5985 digital video camera (Hamamatsu Photonics Uk Ltd, Welwyn Garden City, UK). Images were analysed using Openlab version 3.0.8 on a Macintosh G4 computer (Improvision Ltd, Coventry, UK). The rate of wound closure was calculated by measuring the reduction in denuded area (in pixels) at 60 minutes intervals until the wound was completely closed. Rate of HPMC wound closure (pixels/hour) was determined by measuring the area of the wound at each time point.

APPENDIX I

Characterization of HPMC



Confluent monolayer of HPMC showing typical polygonal shape and “classic” cobblestone appearance.

B. APPENDIX II

1. 5'-RACE PCR protocol

-94°C for	3 minutes	(Denaturation step)		
-94°C for	1 minute		} 15 cycles	
-64°C for	1 minute*			
-72°C for	3 minutes			
-94°C for	1 minute		} 10 cycles	* Decreases by 2°C every 5 cycles
-58°C for	1 minute			
-72°C for	3 minutes			
-72°C for	10 minutes	(Final extension step)		

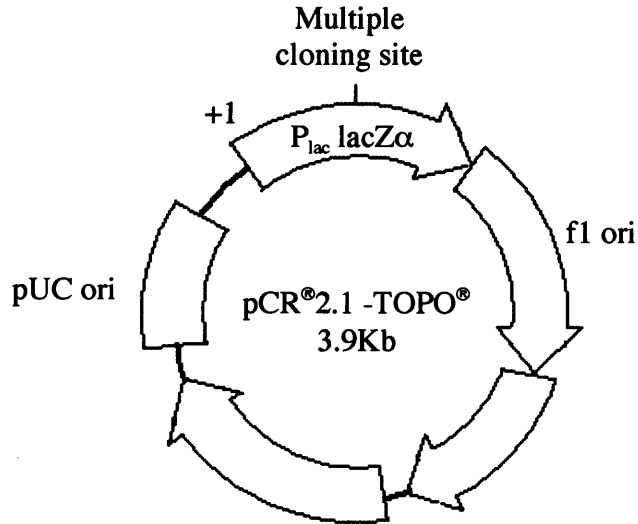
2. Standard PCR protocol

-94°C for	2 minutes			
-94°C for	0.5 minutes		} 26–36 cycles (dependant on primers used)	
-55°C for	1 minute			
-68°C for	1 minute			
-68°C for	15 minutes			

All PCR reactions were carried out in a GeneAmp PCR System 9700 Thermo-cycler (Applied Biosystems Ltd).

APPENDIX III

1. pCR[®]2.1 -TOPO[®] sequencing vector Map



2. pCR[®]2.1 -TOPO[®] Multiple cloning site

CAGGAAACAGCTATGAC CCAAGC TACCGA GCTCG--GAT CCACTA
 M13 Reverse primer *HindIII* *KpnI* *SacI* *BamHI* *SpeI*

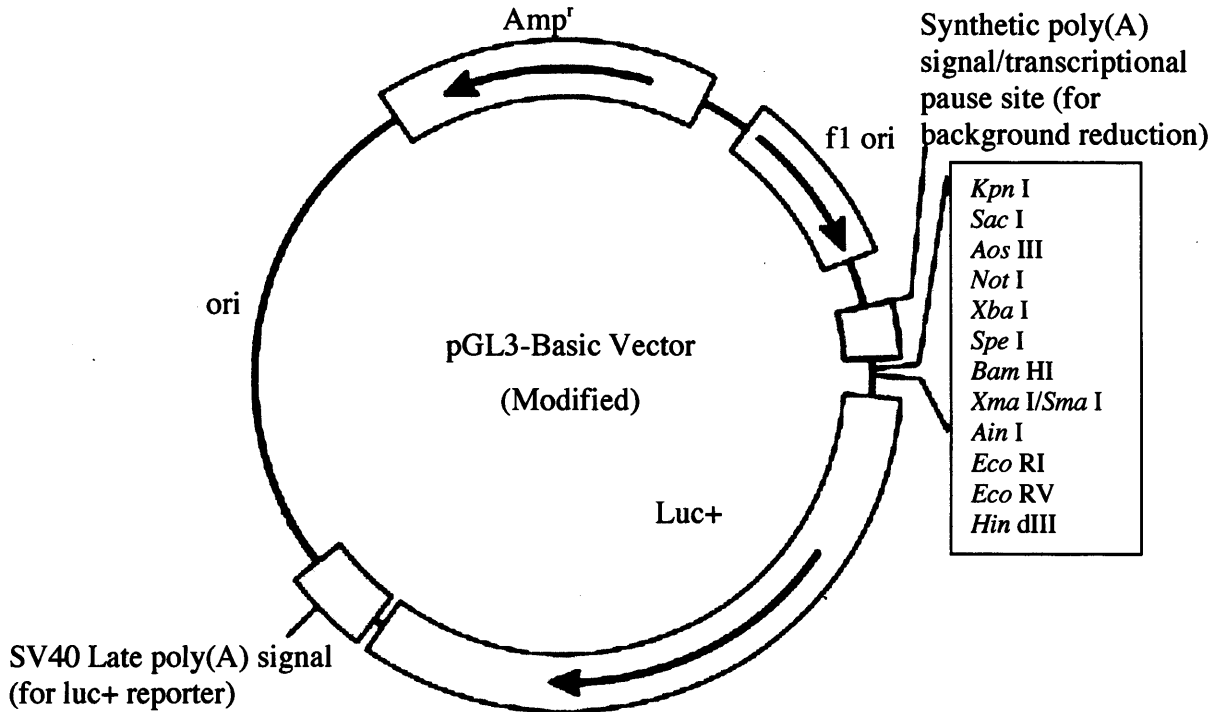
GTGCTG TGGAAT **PCR PRODUCT** TGGAAT GATATC ACACTG
BstXI *EcoRI* *EcoRI* *EcoRV* *BstX I*

GGCGGC CGCTCG GCATCT CATCTA GCCCAA
NotI *XhoI* *NsiI* *XbaI* *Apal*

CCTATAGTGAGTCGTATTA CTGGCCGTCGTTTAC
 T7 promoter M13 Forward (-20) primer

APPENDIX IV

1. pGL3 basic (Modified) Vector Map



2. pGL3 basic (Modified) Multiple cloning Sites

• **pGL-3 Basic**

GGTACC GAGCTC TT ACGCGT GCTAGC---CCGGG CTCGAG---ATCT
KpnI *SacI* *MluI* *NheI* *SmaI* *XhoI* *BglII*

GCGATCTAAGT AAGCTT
 HindIII

• **pGL-3 Basic (Modified)**

GGTACC GAGCTC CA CCGCGG TG GCGGCC GC TCTAGA ACTAGT
KpnI *SacI* *AoaIII* *NotI* *XbaI* *SpeI*

GGATCC CCCGGG CTGCAG GAATTC GAT|ATC AAGCTT
BamHI *SmaI* *PstI* *EcoRI* *EcoRV* *HindIII*

APPENDIX V

1. LB Medium

10g Bacto-tryptone

5g Bacto-yeast extract

5g NaCl

1L Deionised H₂O

pH 7.5

2. LB Agar Plates

1g Bacto-tryptone

0.5g Bacto-yeast extract

0.5g NaCl

0.8g Bacto-agar

0.1L Deionised H₂O

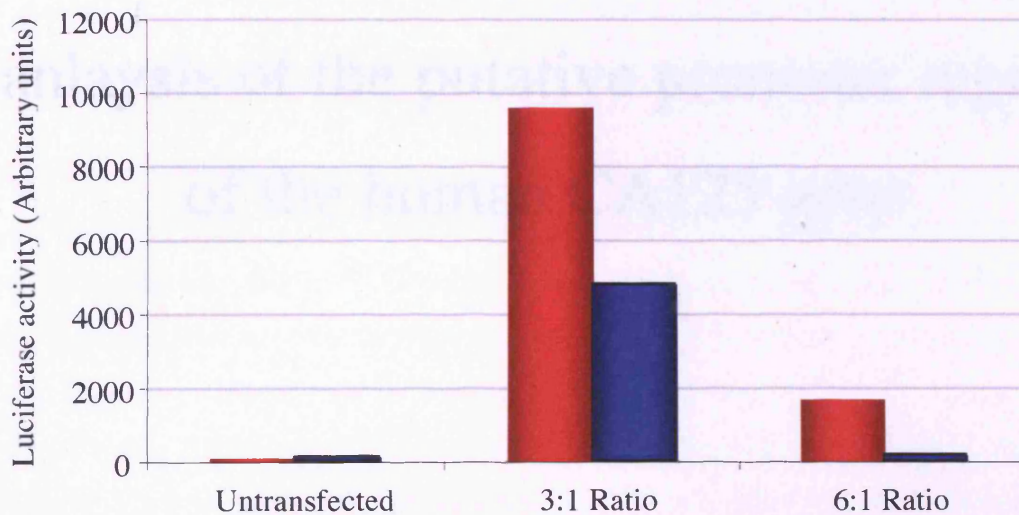
Autoclaved agar was allowed to cool before the addition of carbenicillin (100µl/ml).

Molten agar was then poured into 90mm petri-dishes.

APPENDIX V

Optimisation of HPMC transfection conditions

HPMC were transfected with $1\mu\text{g}$ *Renilla* vector using varying ratios of μl FuGene: μg DNA described in 2.6.2. Transfected HPMC were then analysed for luciferase activity as described in 2.6.3. The experiment was carried out on mesothelial cells demonstrating approximately 70% or 100% confluence.



Optimisation of HPMC transfection conditions and confluency using FuGene 6 transfection reagent. Red bars = 70 % confluent HPMC, Blue bars = 100% confluent HPMC.

These data indicate that HPMC should be transfected with μl FuGene: μg DNA of 3:1 at 70% confluency.

Chapter 3

**Elucidation of the genomic structure and
analysis of the putative promoter region
of the human CA125 gene**

3.1 INTRODUCTION

Numerous studies have identified and used CA125 as a diagnostic tool to detect the onset and recurrence of ovarian cancer [Bast *et al*, 1983] and have suggested a possible role for the molecule as a marker of mesothelial cell mass in the dialyzed peritoneum [Zeillemarker *et al*, 1994][Visser *et al*, 1995][Ho-Dac-Pannekeet *et al*, 1995]. However, studies concerning the regulation of CA125 by mesothelial cells, under homeostasis, have produced contradictory results [Imbert-Marcille *et al*, 1994][Zeillemarker *et al*, 1994][Visser *et al*, 1995][Zeimet *et al*, 1996] and the control of expression of CA125 by HPMC remains poorly understood.

CA125 expression is not confined to the mesothelial cells of the peritoneal cavity; organs such as the pancreas, kidney, colon and the eye also express the antigen [Loy *et al*, 1991][Argueso *et al*, 2003]. Studies examining CA125 regulation in these other cell types may, therefore, provide data relevant to the control of its expression in the peritoneum. A recent study examining the ocular surface of the eye showed that CA125 expression may be regulated by retinoic acid (RA) at the level of transcription and translation [Hori *et al*, 2004]. In addition, a role for RA in the regulation of CA125 in various cervical and ovarian adenocarcinoma cells lines has been suggested [Nakai *et al*, 1993][Langdon *et al*, 1998][Xu *et al*, 2005], while analysis serum levels has shown that CA125 expression in females can be modulated by oestrogen [Nonogaki *et al*, 1991][Karabacak *et al*, 2002].

The fundamental processes controlling gene expression are conventionally simplified by considering the transcription of a single gene in a specific cell type and at a specified time, although clearly these events do not occur in isolation [Smale and Kadonaga, 2003]. Approximately 30,000 genes are encoded by the human genome and their regulation will depend on the specific cellular context under consideration. To date, very little is known of the mechanisms controlling the transcription of the CA125 gene in any cell type.

Transcriptional regulation of gene expression is mediated by the promoter region which typically extends 250bp upstream and 50bp downstream of the transcription initiation

start site (TIS) as seen in Figure 3.1 [Strachan and Read, 1999]. Within this region, the core promoter encompasses the TIS and extends approximately 45bp upstream and 40bp downstream from this site [Strachan and Reed, 1999]. A variety of DNA control elements may be present in this core region, where they serve to bind the RNA polymerase II basal transcription complex, prior to the initiation of gene transcription. These include the “TATA” box, which binds the Transcription Factor IID (TFIID) complex, the BRE element that binds TFIIB, the transcription initiation site (TIS) and the down stream promoter element (DPE) [Smale and Kadonaga, 2003].

In addition to the core promoter region, the upstream proximal promoter region may also contribute to the control of gene expression and does so most frequently via recognition sequences known as transcription factor binding sites (TFBSs). Transcription factors are typically small proteins that can bind to these specific DNA motifs in order to modulate transcription via the core promoter and to act as transcriptional mediators. Common examples of these sequences are CCAAT boxes for nuclear factor-1 (NF-1) binding and GC boxes which bind specificity protein (Sp)1 and Sp3 [Lewin, 2000].

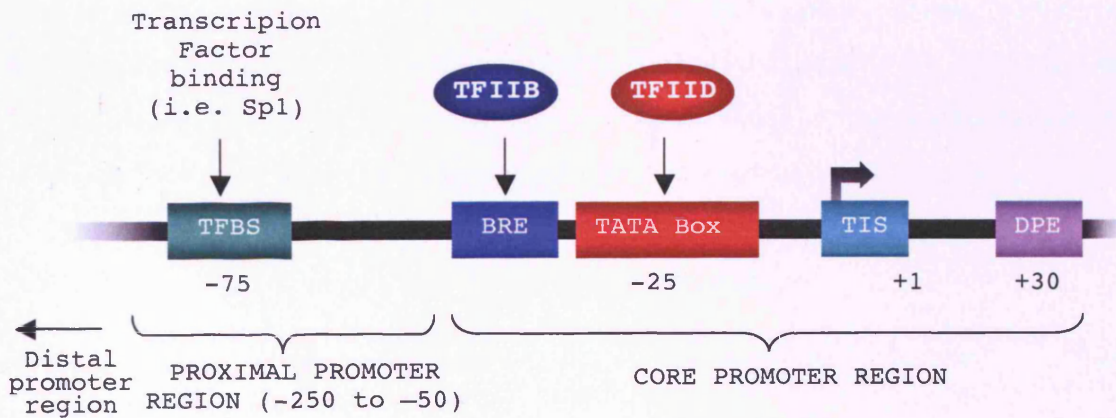


Figure 3.1 Schematic representation of an eukaryotic promoter region.

To understand the mechanisms involved in the regulation of CA125 expression, knowledge of the genomic structure of the CA125 gene including the TIS and upstream promoter sequences was essential. At the start of this project, as discussed in section 1.9.1, previous attempts to clone the entire CA125 cDNA had been unsuccessful [Brown *et al*, 1996][Whitehouse and Solomon, 2003]. However, over the duration of this project further progress was reported and it is now known that the CA125 gene maps to 19p13.2, spans over 134 kb of genomic DNA and encodes a full length transcript of approximately 67 kb [Yin and Lloyd, 2001][O'Brien *et al*, 2001][O'Brien *et al*, 2002].

At the beginning of this study, the CA125 genomic sequence was accessible via cosmid sequences AC008734 and AC016584. In order to better understand the function and transcriptional regulation of the CA125 gene, the genomic structure was reconstructed *in silico*. The 5' end of the coding region was then examined in greater detail, in order to identify the CA125 TIS, the upstream proximal promoter region and the regulatory sequences within this region. Cloned proximal promoter luciferase reporter constructs were then tested for their ability to drive transcription of the reporter gene under endogenous and defined conditions.

3.2 METHODS

3.2.1 *In silico* reconstruction of the human CA125 gene

The genomic structure of the human CA125 gene was reconstructed by combining a variety of *in silico* methods discussed in sections 2.1.1.

3.2.2 *In silico* analysis of the proximal promoter region for transcription factor binding sites

The sequence upstream of the CA125 coding region was analysed for putative TFBSs using internet-based software as described in 2.1.2.

3.2.3 Amplification of transcribed products from CA125 exon 1 and 2 from total RNA

On the basis of these *in silico* data, RT-PCR was carried out using specific primers (Table 3.1) to amplify expressed products from CA125 exons 1 and 2. Firstly, HPMC total RNA was extracted and reverse transcribed as described in section 2.3. PCR was then carried out as described in section 2.4.1. The products of the amplification were visualized and sized by flat bed agarose gel electrophoresis as outlined in 2.4.4.

Table 3.1 CA125 exon 1 and 2 oligonucleotide primers

Primer pair	Sense-strand sequence	Anti-sense strand sequence	Product size
RT-PCR-5'	CACCCTGAGAAATTTGGAGTT	CACGATTGCACCTGTAGATGTC	256bp
RT-Exon2	CTGTCTCTTCTCCACAGAACC	GGAACAGTTGTTTCTGGAGTC	334bp

All primers are in 5'-3' orientation

The position of all primers specific to the 5' end of the CA125 gene used in this chapter can be seen in Figure 3.2 (page 76). Genomic *in silico* data were used to design these primers using internet based software as described in 2.4.3.

3.2.4 Analysis of CA125 terminal expressed sequences from purified mRNA

mRNA was purified from HPMC total RNA using Oligo (dT)₂₅ Dynabeads as described in section 2.3.5. RT-PCR was then used to analyse the expression of CA125 mRNA termini using the primers shown in Table 3.2 and Figure 3.2.

Table 3.2 CA125 mRNA termini oligonucleotide primers

Primer pair	Sense-strand sequence	Anti-sense strand sequence	Product size
RT-PCR- 3'	ACTGGCTCGGAGAGTAGACAGA	CACTGTTGCTGGACGTTGTATT	288bp
CA125 R	GGAGAGGGTTCTGCAGGGTC	GTGAATGGTATCAGGAGAGG	400bp
RT-PCR-5'	CACCCTGAGAAATTTTGGAGTT	CACGATTGCACCTGTAGATGTC	256bp

All primers are in 5'- 3' orientation

The gene specific primers shown in Table 3.3 and Figure 3.2 were designed for use in 5'-rapid amplification of cDNA ends (5'-RACE) analysis to identify upstream expressed CA125 sequence, as shown in 2.3.5.

Table 3.3 5'-RACE oligonucleotide primers

Primer pair	Inner primer	Outer primer
5'-RACE	TCCATGCTGAAACCCTCAGGCCT	GGTCATCTTCTCCCACCCGCTCCT

All primers are in 5'- 3' orientation

The 5'-RACE products were cloned into PCR 2.1 TOPO sequencing vector (Appendix III-chapter 2) as described in 2.5.1 and sequenced (section 2.5.6). RT-PCR from cDNA and PCR from gDNA with additional primers (Table 3.4 and Figure 3.2) were used in

further analysis of upstream expressed CA125 sequences. Amplification products were sized and visualised as described in 2.4.4.

Table 3.4 CA125 upstream analysis oligonucleotide primers

Primer pair	Sense-strand sequence	Anti-sense strand sequence (PR)	Product size
P1	TCCTTTCTCTCCCTGAGATTTG	TTCTTAGACCTCCATCCAGAGG	223bp
P2	TGCAGACACTGAGAATCCGTTA	TTCTTAGACCTCCATCCAGAGG	317bp
P3	GATCTCAAACCTCCCAACCTC	TTCTTAGACCTCCATCCAGAGG	521bp
P0	TGAGATTTGGTCTTCTCAATTA	TTCTTAGACCTCCATCCAGAGG	210bp

All primers are in 5' - 3' orientation

Expressed sequence tag (EST) sequences upstream of the CA125 locus were identified using the UCSC Genome Bioinformatics internet site (<http://genome.cse.ucsc.edu/>). Specific primers were designed (Table 3.5) spanning the 5' terminus of CA125 exon 1 and the most proximal upstream EST (AA633929, for EST sequence see appendix I). RT-Exon2 primers (Table 3.1) specific to CA125 mRNA were used as a positive control.

Table 3.5 EST analysis oligonucleotide primers

Primer pair	Sense-strand sequence (EST F)	Anti-sense strand sequence	Product size
RT-EST1	AGCACATTTCCCCTGTGATAAG	TGTGTCTAGAAGAGCTGCCGTA	163bp
RT-EST2	AGCACATTTCCCCTGTGATAAG	TTCTTAGACCTCCATCCAGAGG	296bp

All primers are in 5' - 3' orientation

3.2.5 Amplification and analysis of the putative CA125 proximal promoter transcriptional activity *in vitro*

Three nested fragments spanning the putative proximal promoter region were then amplified (Table 3.6 and Figure 3.2) from gDNA (section 2.4.1), sized (section 2.4.4) and purified from an agarose gel (section 2.4.5).

Table 3.6 Nested CA125 promoter construct oligonucleotide primers

Construct	Sense-strand sequence	Anti-sense strand sequence (FR)
F100	CCGGTACCGAGAGAGAGGATCATTAAAGACATGA	CCACTAGTGACCTGGGAAAACCTGTGTCTA
F500	CCGGTACCGCTCTTATTACCCATGCTGGAG	CCACTAGTGACCTGGGAAAACCTGTGTCTA
F1000	CCGGTACCCACACTGAGCATTAGTCCATC	CCACTAGTGACCTGGGAAAACCTGTGTCTA

All primers are in 5'-3' orientation

Red=*KpnI* restriction site, Blue = *SpeI* restriction site

These nested promoter fragments were then cloned into a pGL3-modified vector (Appendix IV-chapter 2) as described in section 2.5, and the clones were screened for the presence of the desired fragments using enzymatic digestion (section 2.5.5) followed by sequencing (section 2.5.6). Luciferase assays were carried out as described in section 2.6.

3.2.6 Analysis of CA125 promoter activity in response to retinoic acid and oestrogen stimulation

HPMC expression of the oestrogen receptor (ER) was verified by Western blot (as described in section 2.7) using a rabbit anti-oestrogen receptor antibody (Zymed Labs Inc;Invitrogen Ltd). HPMC were transfected with the putative promoter constructs as described in section 2.6.2. Each construct was then assayed for transcriptional activity in HPMC stimulated for 24 hours with either 10 nmoles of all-trans retinoic acid or 100 nmoles of 17 β -Oestradiol using the luciferase assay described in 2.6. For each promoter construct the luciferase activity was normalised to the negative control promoterless pGL-3 vector. To ensure the system was responsive to RA and oestrogen stimulation, MCP-1 (section 2.10.1) and IL-8 (section 2.10.2) assays were carried out on the supernatants from the luciferase experiments.

3.2.7 Statistical analysis of luciferase assays

All data are presented as mean [\pm standard error of the mean (SEM)] on the assigned number of independent experiments (n) performed on averaged duplicate samples for each experiment. Statistical significance was determined using the two-way ANOVA in SPSS v11.5 for Windows. Where appropriate, analysis was undertaken using a non-parametric statistical test (Friedman Test using SPSS v11.5 for Windows). Differences were considered significant when $p < 0.05$.

3.3 RESULTS

3.3.1 *In silico* reconstruction of the human CA125 gene

While computational prediction of gene structures has improved significantly over the last few years, accurate identification of promoter regions has yet to be optimised. Therefore, a combination of *in silico* and *in vitro* methodologies were used to reconstruct the CA125 genomic structure. The CA125 reference cDNA sequence was compared with high-throughput genomic sequences available via the NCBI database (<http://www.ncbi.nlm.nih.gov>). From these findings the CA125 genomic structure was reconstructed and the upstream putative proximal promoter sequence identified. Table 3.7 shows the predicted sizes of each component of the CA125 genomic structure and Figure 3.3 shows a schematic representation of the CA125 genomic and cDNA structure.

Several cDNA sequences for CA125 were retrieved (date: Jan 2002) from the NCBI database (www.ncbi.nih.gov/):

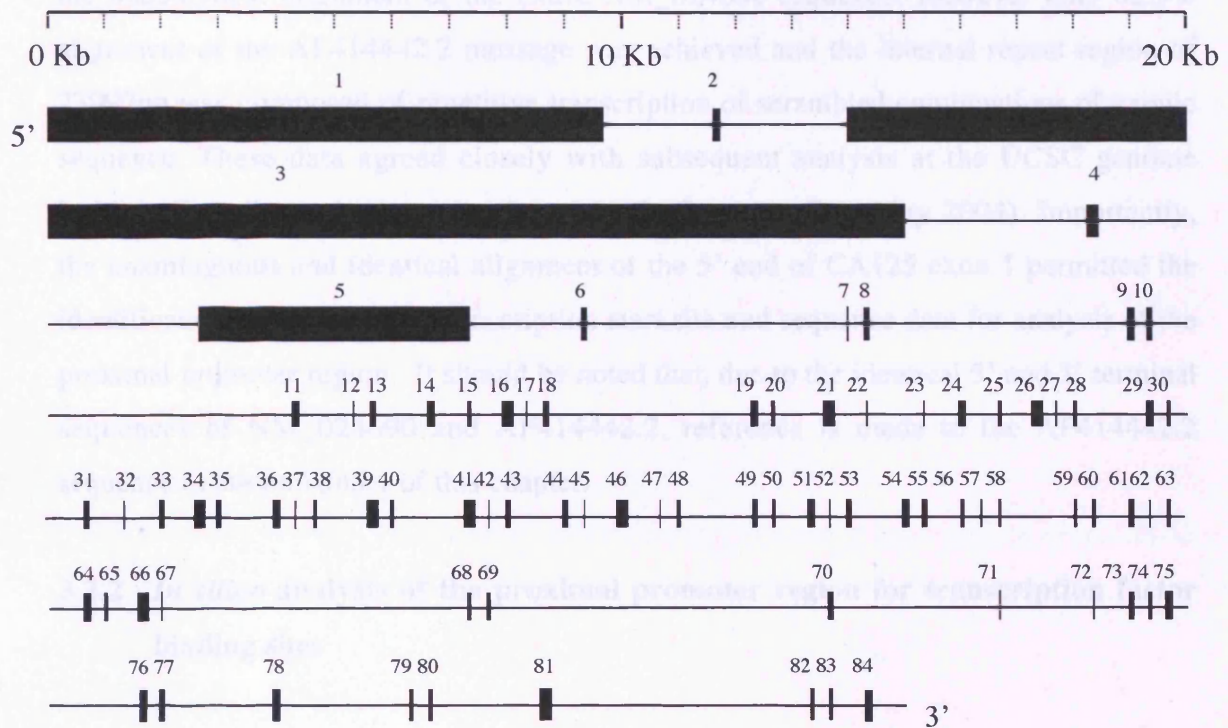
- AF361486 Homo sapiens mucin 16 (MUC16) mRNA, partial cds (5797bp).
- AF414442.1 Homo sapiens ovarian cancer related tumour marker CA125 mRNA, complete cds (35350bp).
- AF414442.2 Homo sapiens ovarian cancer related tumour marker CA125 mRNA, complete cds (66765bp).

The most complete mRNA sequence currently available for CA125 throughout this study was AF414442.2 which comprised of a very large mRNA of 66.765Kb that encoded a theoretical CA125 protein of 22152 amino acids. BLAST (www.ncbi.nlm.nih.gov/blast/) analysis using this sequence retrieved genomic clones AC016584 and AC008734. BLAST2 alignment software (www.ncbi.nlm.nih.gov/blast/bl2seq/bl2.html) was used to align the AF414442.2 mRNA sequence with these genomic clones. In December 2005, after this study had been completed, the database curators merged the exonic sequences to form a composite CA125 reference mRNA sequence, NM_024690. A comparison of the structure of these CA125 mRNAs is shown in Figure 3.3B.

Table 3.7 Predicted sizes of the introns and exons of the CA125 genomic structure using data gathered from the UCSC genome browser database.

exon	size (bp)	intron	size (bp)	exon	size (bp)	intron	size (bp)
1	9479	1	1784	43	66	43	720
2	105	2	2585	44	125	44	230
3	21696	3	1824	45	68	45	612
4	114	4	3991	46	173	46	629
5	4680	5	2102	47	36	47	259
6	36	6	5010	48	66	48	1178
7	36	7	243	49	122	49	205
8	60	8	4339	50	68	50	619
9	128	9	311	51	173	51	312
10	68	10	4834	52	36	52	256
11	153	11	648	53	66	53	1264
12	36	12	258	54	125	54	227
13	65	13	900	55	68	55	582
14	126	14	532	56	173	56	331
15	68	15	592	57	36	57	261
16	163	16	329	58	66	58	1161
17	36	17	261	59	124	59	226
18	66	18	2949	60	68	60	624
19	131	19	221	61	173	61	331
20	68	20	607	62	36	62	253
21	173	21	349	63	66	63	1096
22	36	22	259	64	122	64	207
23	66	23	713	65	68	65	596
24	125	24	236	66	173	66	330
25	68	25	614	67	36	67	5672
26	173	26	329	68	125	68	97
27	36	27	258	69	68	69	4715
28	61	28	914	70	173	70	2904
29	127	29	235	71	36	71	1526
30	70	30	600	72	51	72	779
31	184	31	327	73	122	73	90
32	36	32	258	74	68	74	148
33	66	33	946	75	173	75	2157
34	125	34	237	76	131	76	355
35	68	35	973	77	68	77	1724
36	173	36	315	78	149	78	2248
37	36	37	257	79	152	79	328
38	66	38	935	80	68	80	2063
39	125	39	253	81	167	81	4255
40	68	40	921	82	42	82	322
41	183	41	328	83	80	83	783
42	36	42	256	84	187		

A. Genomic DNA structure of CA125



B. Comparison of the NM_024690 and AF41442.2 sequence mRNA structures

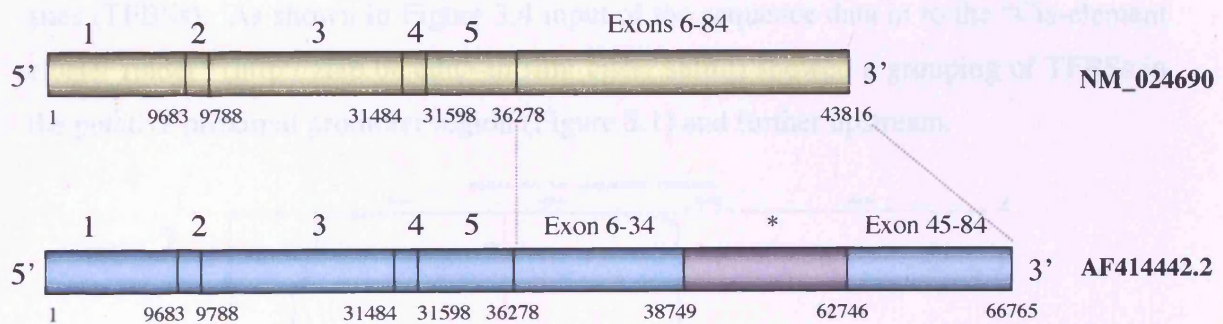


Figure 3.3 CA125 genomic structure. (A) Schematic representation of the genomic structure of the CA125 gene. Exons are represented as black rectangles and introns are represented as thin black lines. (B) Comparisons of the reference sequences NM_024690 and AF41442.2 mRNA structures. The disordered region (*) comprised repetitive sequence that could not be ordered in the mRNA structure due to sequencing ambiguities from AF414442.2.

As can be seen in Figure 3.3A, the *in silico* reconstruction of the CA125 gene resulted in the unequivocal alignment of the entire NM_024690 sequence. However only 62.5% alignment of the AF414442.2 message was achieved and the internal repeat region of 23997bp was composed of repetitive transcription of scrambled combinations of exonic sequence. These data agreed closely with subsequent analysis at the UCSC genome browser (<http://genome.cse.ucsc.edu/cgi-bin/hgGateway>: Date:May 2004). Importantly, the unambiguous and identical alignment of the 5' end of CA125 exon 1 permitted the identification of the putative transcription start site and sequence data for analysis of the proximal promoter region. It should be noted that, due to the identical 5' and 3' terminal sequences of NM_024690 and AF414442.2, reference is made to the AF414442.2 sequence in the remainder of this chapter.

3.3.2 *In silico* analysis of the proximal promoter region for transcription factor binding sites

Using available internet based software (as described in 2.1.2) the 1kb of sequence directly upstream of the TIS of AF414442.2 was analysed for transcription factor binding sites (TFBSs). As shown in Figure 3.4 input of the sequence data in to the “Cis-element cluster finder” (<http://zlab.bu.edu/~mfrith/cister.shtml>) showed a grouping of TFBSs in the putative proximal promoter region (Figure 3.1) and further upstream.

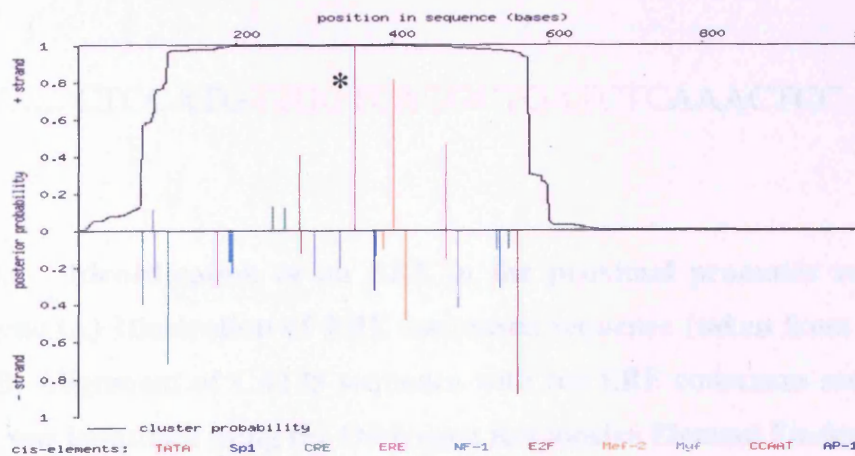


Figure 3.4 Analysis of the 1kb upstream of reference CA125 mRNA sequence AF414442.2 (3' to 5') for TFBS's using “Cister” internet based software.

Figure 3.4 shows a cluster of transcription factor binding sites in the putative CA125 promoter region sequence providing indirect confirmatory evidence of promoter identification. Interestingly, considering the involvement of CA125 in ovarian cancer, this analysis identified the presence of three EREs (oestrogen responsive elements) having probability/matches of 0.99, 0.46 and 0.28. The ERE showing the highest probability/match of the identified consensus sequences is highlighted with * in Figure 3.4. Of the three EREs, only the presence, sequence and position of the ERE showing the highest probability/match (0.99) was corroborated using other internet based TFBS identification programs such as the Genomatrix Matinspector (<http://genomatrix.de/cgi-bin/eldorado/main.pl>) [Quandt *et al*, 1995] and the Oestrogen Responsive Element Finder (Figure 3.5) (<http://research.i2r.a-star.edu.sg/promoter/ERE-V2b/cgi/ere/pl>) as outlined in Tang's method for the identification of oestrogen responsive genes [Tang *et al*, 2004]. The CA125 sequence identified showed 83% identity with the consensus sequence.

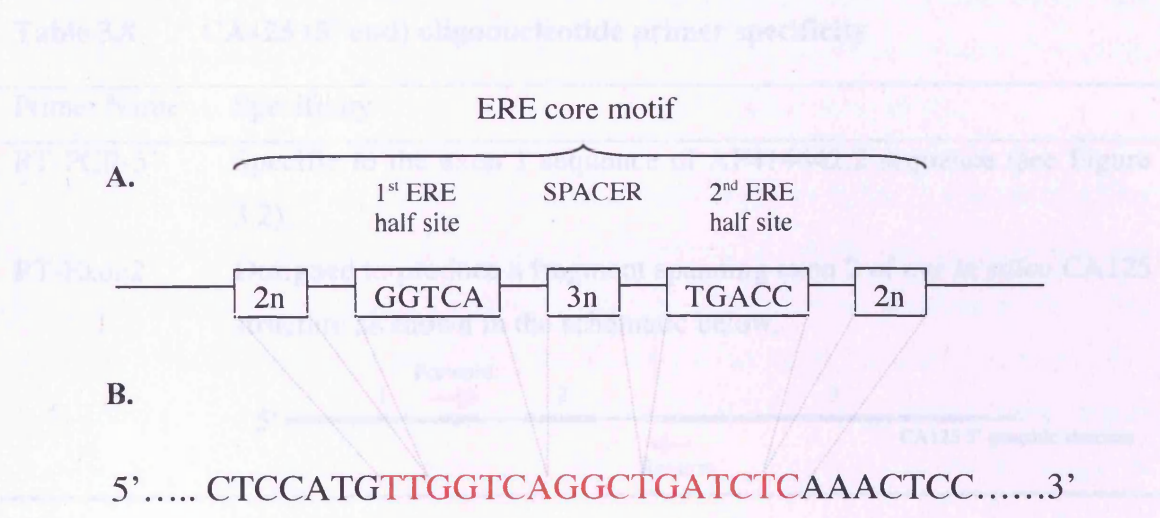


Figure 3.5 Identification of an ERE in the proximal promoter region of the CA125 gene (A) Illustration of ERE consensus sequence (taken from [Tang *et al*, 2004]). (B) Alignment of CA125 sequence with the ERE consensus sequence. This sequence was identified using the Oestrogen Responsive Element Finder [Tang *et al*, 2004].

As described in section 3.1, previous studies have indicated that human peritoneal mesothelial cells are RA responsive [Kim *et al*, 1987]. Analysis of the CA125 proximal promoter sequence using the internet based TFBS identification program [Quandt *et al*, 1995] identified a RAR binding site. This sequence (5' TGGTCA) corresponded closely to the steroid receptor core motif 5'-PuGG(T/A)CA [Mader *et al*, 1993] suggesting that the CA125 response to RA may be mediated via this site. The position of the ERE and RAR can be seen in Figure 3.7(page 87).

3.3.3 Amplification of the CA125 5' region

After *in silico* reconstruction of the CA125 gene, pairs of oligonucleotide primers were designed for analysis of the 5' end of the gene and of CA125 exon two. The specificity of each primer pair is described in Table 3.8.

Table 3.8 CA125 (5' end) oligonucleotide primer specificity

Primer Name	Specificity
RT-PCR-5'	Specific to the exon 1 sequence of AF414442.2 sequence (see Figure 3.2).
RT-Exon2	Designed to produce a fragment spanning exon 2 of our <i>in silico</i> CA125 structure as shown in the schematic below.

In order to detect the 5' end of the reference CA125 cDNA sequence and to verify our *in silico* data, as well as testing for gDNA contamination, RT-PCR was carried out using the primers described in Table 3.8.

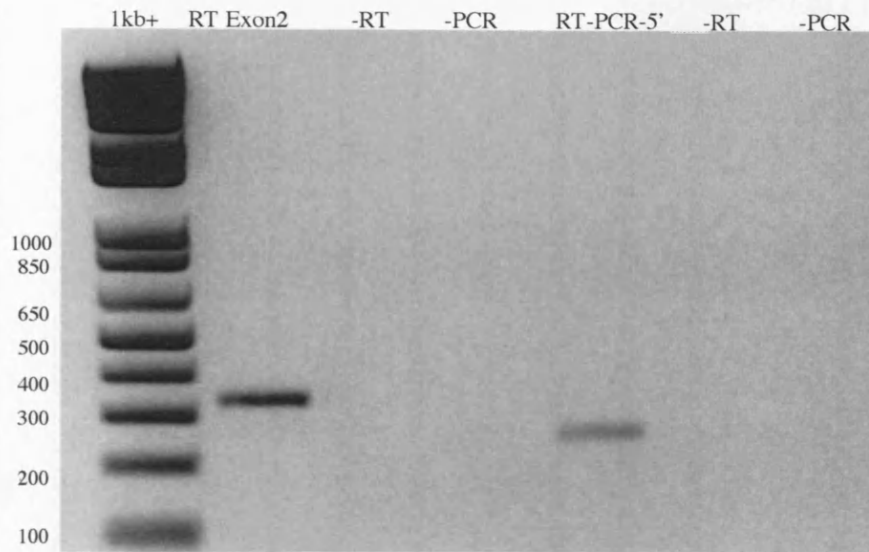


Figure 3.6 Amplification of products from CA125 exons 1 and 2 by RT-PCR. -RT = negative control for reverse transcription, -PCR = negative control for PCR. Double stranded DNA markers are given (1kb+) with their sizes in bp.

As shown in Figure 3.6, an RT-PCR product of predicted size (256bp) was obtained for the RT PCR-5' primers. This confirmed the expression of CA125 exon 1 in HPMC and suggested that the very large AF414442.2 mRNA sequence was complete at its 5' end although amplification from total RNA produced a weak exon 1 specific band. An RT-PCR product of correct size was also obtained for the RT Exon 2 primers (334bp) which corroborated our existing *in silico* CA125 5' gene structure and no evidence of amplification of larger products from contaminating gDNA was observed. The *in silico* genomic and protein sequence can be seen in Figure 3.7.

Further inspection of the putative CA125 5'-UTR sequence revealed that the 5' end of the AF414442.2 mRNA sequence was in-frame with respect encoding amino acids, as illustrated in Figure 3.7. Furthermore, the 5' end of AF414442.2 and the adjacent upstream nucleotides resembled a consensus intron/exon boundary sequence (5'-AG-3') [Zhang, 1998] as highlighted in grey in Figure 3.7. The possibility therefore remained that AF414442.2 comprised only protein coding sequence, and that the transcription initiation start site (TIS) lay further upstream. Nevertheless, a sequence was identified 15 bp further upstream which showed identity with the TIS consensus sequence motif (YYANWYY where Y=Pryrimidine, W=A or T) [Smale, 1997][Smale and Kadonaga, 2003] as shown in Figure 3.10 (page 90).

3.3.4 Analysis of the 5' terminal expressed sequence

mRNA isolated from HPMC total RNA was used as a template for RT-PCR with primers specific to the 3' and 5' termini of the CA125 gene (RT-PCR-3' and RT-PCR-5' primers, Table 3.2) as well as primers specific for the repeat region of the gene (CA125 R primers, Table 3.2). These analyses were performed to confirm that a complete CA125 mRNA (Figure 3.8) was recovered from a purified mRNA template. Once again, however, the exon-1 specific fragment amplified weakly.

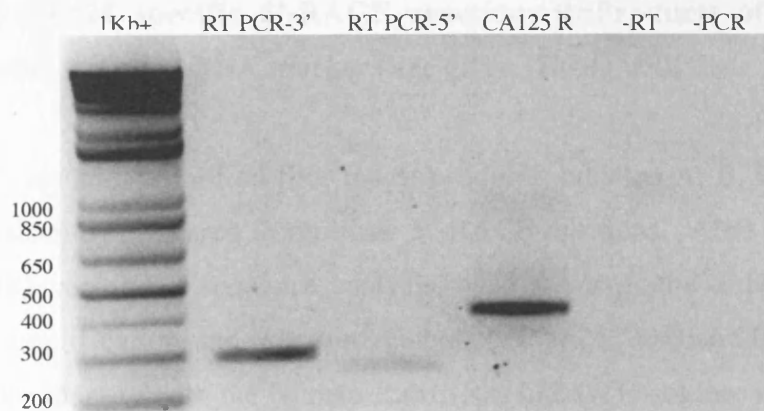


Figure 3.8 Amplification of the 5' and 3' terminals of the CA125 gene. -RT = negative control for reverse transcription, -PCR = negative control for PCR. Double stranded DNA markers are given (1kb+) with their sizes in bp.

RT-PCR products of predicted size were obtained for all the primers suggesting that the CA125 message synthesised by HPMC's was complete with respect to AF414442.2. 5'-RACE was then carried out on the same mRNA sample in order to identify additional expressed sequence at the 5' end of the gene (Figure 3.9).

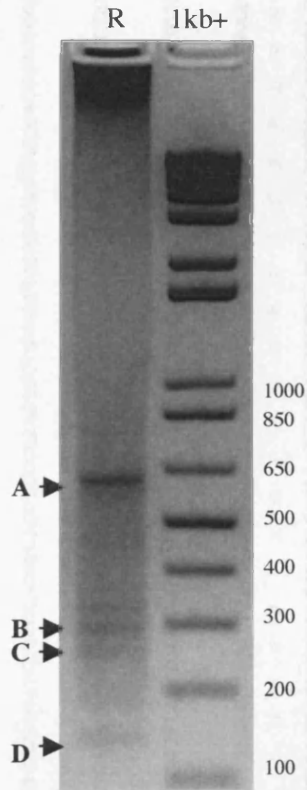


Figure 3.9 CA125 specific 5'-RACE reaction. R=Products of the 5'-RACE reaction. Double stranded DNA markers are given (1kb+) with their sizes in bp.

The 5'-RACE reaction amplified four major products, labelled A, B, C and D (Figure 3.9), that consistently appeared in replicate 5'-RACE reactions. After cloning into the PCR 2.1 TOPO vector and sequence analysis, band A was found to be the product of non-specific amplification and was not related to CA125. A BLAST search showed strong sequence identity with the Human Rab1 (Ras like GTPase) receptor. Band D was truncated and contained no additional 5' sequence. Bands B and C contained a 9 base extension to the 5'-UTR as shown in Figure 3.10. 5'-RACE sequence data can be seen in Appendix I.

The additional 5'-UTR sequence retrieved through the 5'-RACE reaction contained an in-frame stop codon (TAG). This represented a block to the translation of any sequence further upstream. Together with the identification of a nearby consensus TIS motif, these combined data suggested that the CA125 proximal promoter region lay immediately upstream of the AF414442.2 sequence, as shown in Figure 3.10. RT-PCR was carried out (Figure 3.12(i)) using nested primers spanning the region upstream of the 5'-UTR extension (Figure 3.11) to identify any further upstream expressed sequences. Using identical reaction conditions, a control amplification from gDNA was carried out to ensure reaction condition and primers were functional (Figure 3.12(ii)).

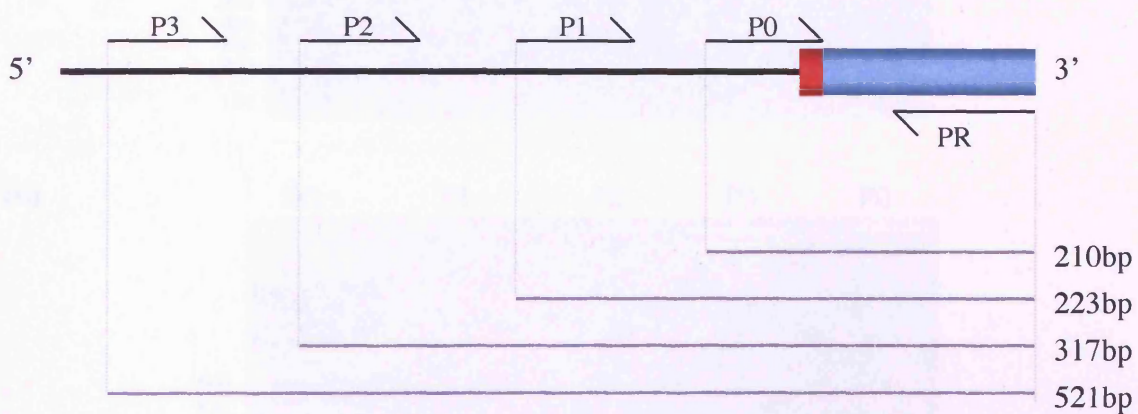


Figure 3.11 Schematic representation of sequential upstream primer positions and fragment sizes (bp). The red block represents the extended RACE sequence.

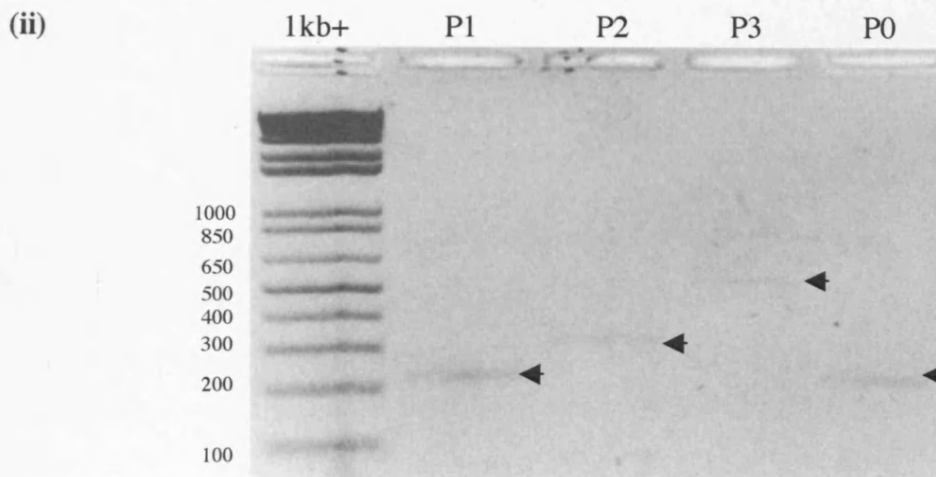
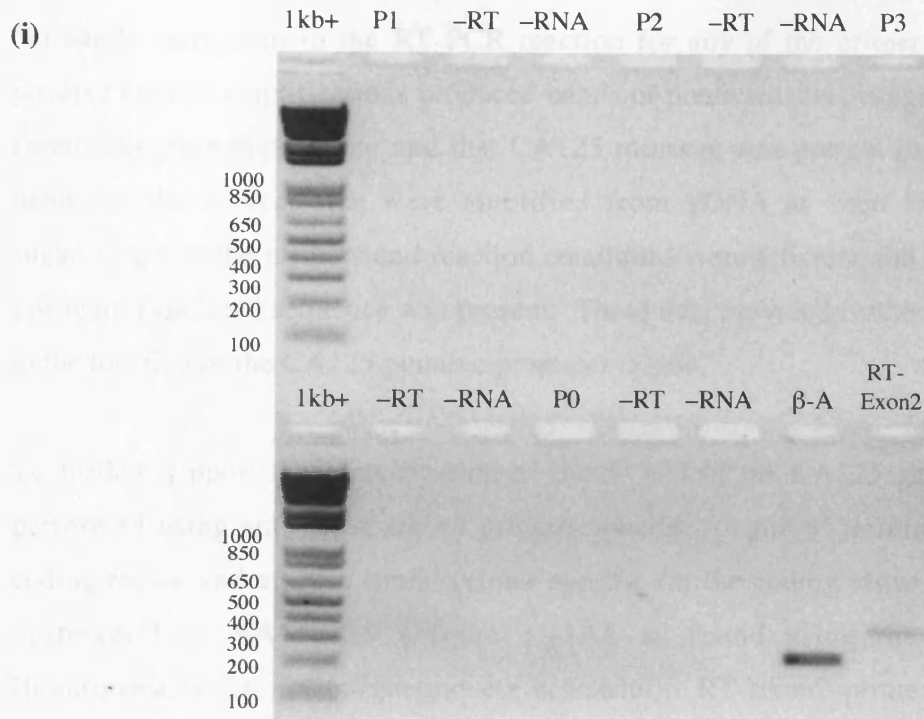


Figure 3.12 PCR amplification of the sequence upstream of the 5'-UTR extension.
(i) PCR amplification from HPMC cDNA. β -A = Positive β -Actin control for PCR. RT-Exon2 = Positive control for the CA125 message. -RT = Negative control for reverse transcription. -PCR = Negative control for PCR (ii) PCR amplification from HPMC gDNA. Double stranded DNA markers are given (1kb+) with their sizes in bp.

No bands were seen in the RT-PCR reaction for any of the primer pairs used. Both positive control amplifications produced bands of predicted size, suggesting the reaction conditions were appropriate and that CA125 message was present in the sample. Four bands of the correct size were amplified from gDNA as seen in Figure 3.12(ii), suggesting that the primers and reaction conditions were efficient and that no additional upstream expressed sequence was present. These data provided further indirect evidence to the location of the CA125 putative promoter region.

To further support the identification of the 5' end of the CA125 gene, RT-PCR was performed using anti-sense strand primers specific for the 5'-terminus of the CA125 coding region and a sense strand primer specific for the coding sequence of the nearest upstream EST AA633929 (Figure 3.13A), as found using the UCSC Genome Bioinformatics Site (<http://genome.cse.ucsc.edu/>). RT-Exon2 primers were used as a positive control in the experiment (Figure 3.13B).

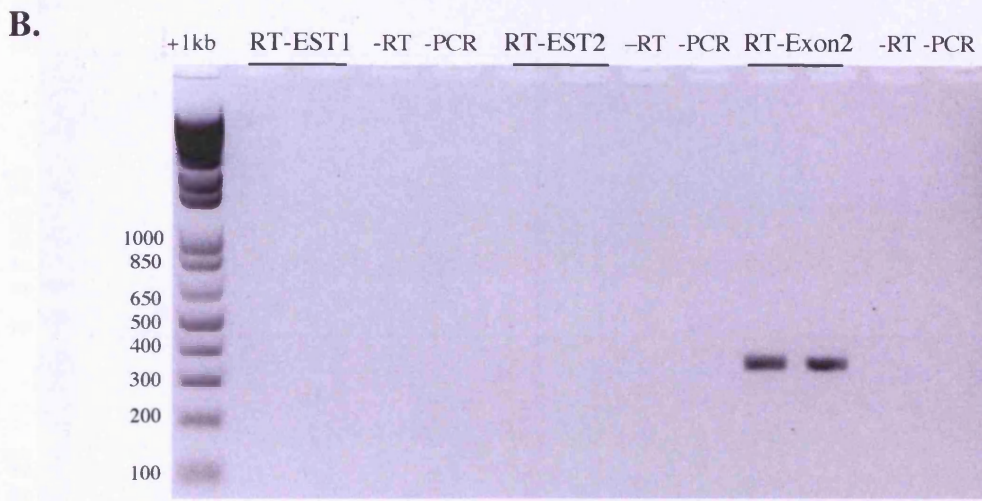
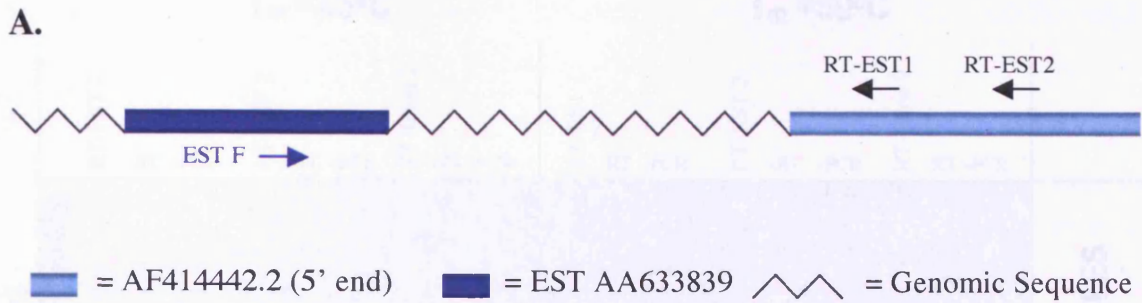


Figure 3.13 Upstream EST analysis. (A) Locations of oligonucleotide primers used in amplification of CA125 the 5' end (AF414442) and the EST (AA633839) immediately upstream of AF414442.2. (B) RT-PCR Amplification spanning CA125 5' coding region and EST (AA633839). -RT = negative control for reverse transcription, -PCR = negative control for PCR. Double stranded DNA markers are given (1kb+) with their sizes in bp.

Figure 3.13B suggests that the EST AA633839 is not expressed as part of the CA125 message as no bands were produced using the RT-EST1 and RT-EST2 primers. Bands of the correct size were amplified using the RT-Exon2 primers indicating the CA125 message was transcribed in the reverse transcription process. In order to substantiate these data the same experiment, as shown in 3.13, was carried out using lower annealing temperatures and varying cycle numbers (Figure 3.14).

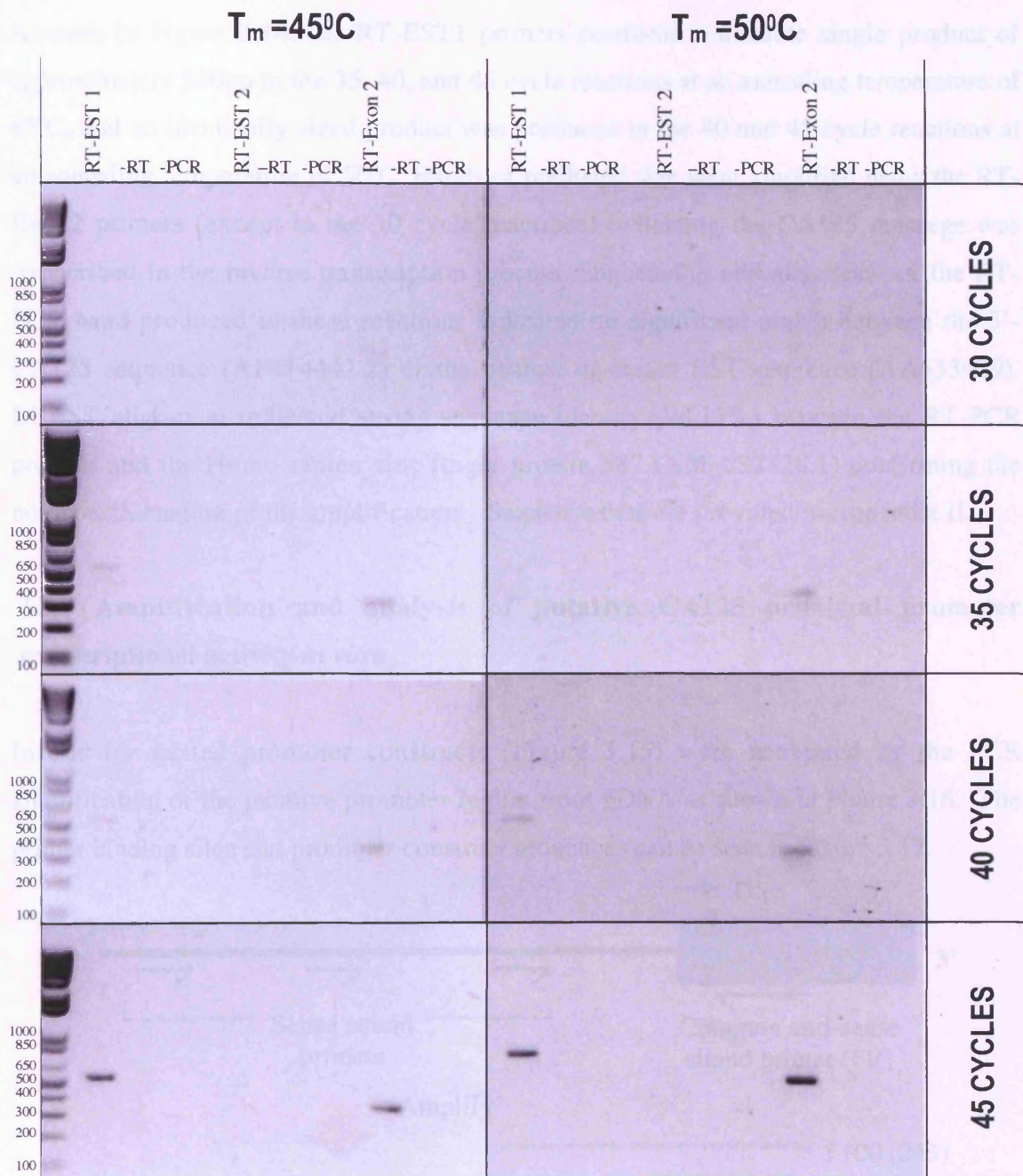


Figure 3.14 RT-PCR amplification spanning CA125 5' coding region and EST AA633839 at varying annealing temperatures (T_m) of 45°C and 50°C and a range of amplification cycles. -RT = negative control for reverse transcription, -PCR = negative control for PCR. Double stranded DNA markers are given (1kb+) with their sizes in bp.

As seen in Figure 3.14, the RT-EST1 primers produced a discrete single product of approximately 550bp in the 35, 40, and 45 cycle reactions at an annealing temperature of 45°C, and an identically sized product was produced in the 40 and 45 cycle reactions at an annealing temperature of 50°C. Bands of predicted size were amplified using the RT-Exon2 primers (except in the 30 cycle reactions) indicating the CA125 message was transcribed in the reverse transcription process. Sequencing and alignment of the RT-PCR band produced in these reactions indicated no significant match between the 5'-CA125 sequence (AF414442.2) or the nearest upstream EST sequence (AA633929). BLAST alignment indicated strong sequence identity (98.17%) between the RT-PCR product and the Homo-sapien zinc finger protein 587 (NM_032828.1) confirming the non-specific nature of the amplification. Sequence data are provided in Appendix II.

3.3.5 Amplification and analysis of putative CA125 proximal promoter transcriptional activity *in vitro*

Inserts for nested promoter constructs (Figure 3.15) were generated by the PCR amplification of the putative promoter region from gDNA as shown in Figure 3.16. The primer binding sites and promoter construct sequences can be seen in Figure 3.17.

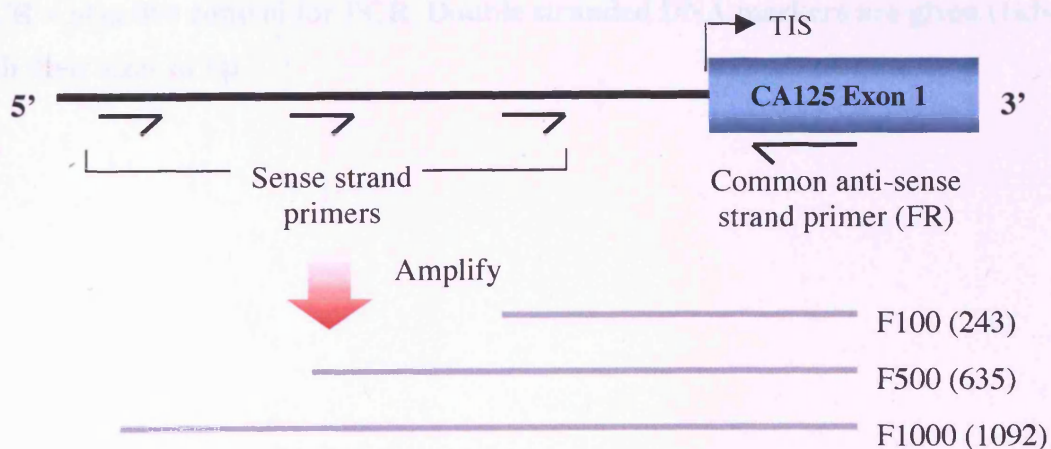


Figure 3.15 Upstream putative promoter constructs. (A) Schematic for the generation of nested PCR fragments for the CA125 core promoter region. Three nested fragments were generated; F100, F500 and F1000. Actual nested fragment sizes are shown in bp.

The anti-sense primer was tailed with a *SpeI* (ACTAGT) restriction site and the sense strand primers were tailed with *KpnI* (GGTACC) restriction sites to aid cloning into the pGL-3 luciferase vector. In each case, amplification of discrete single products of predicted size suggests that amplification was successful.

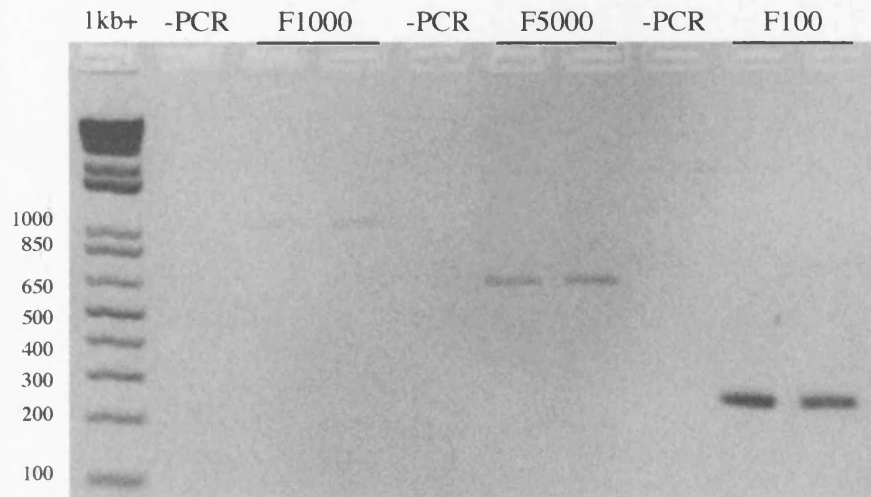


Figure 3.16 PCR amplification of nested promoter fragments from genomic DNA. Expected sizes for each fragment: P100 (258bp), P500 (645bp), F1000 (1194bp). -PCR = negative control for PCR. Double stranded DNA markers are given (1kb+) with their sizes in bp.

The anti-sense primer was tailed with a *SpeI* (ACTAGT) restriction site and the sense strand primers were tailed with *KpnI* (GGTACC) restriction sites to aid cloning into the pGL-3 luciferase vector. In each case, amplification of discrete single products of predicted size suggests that amplification was successful.

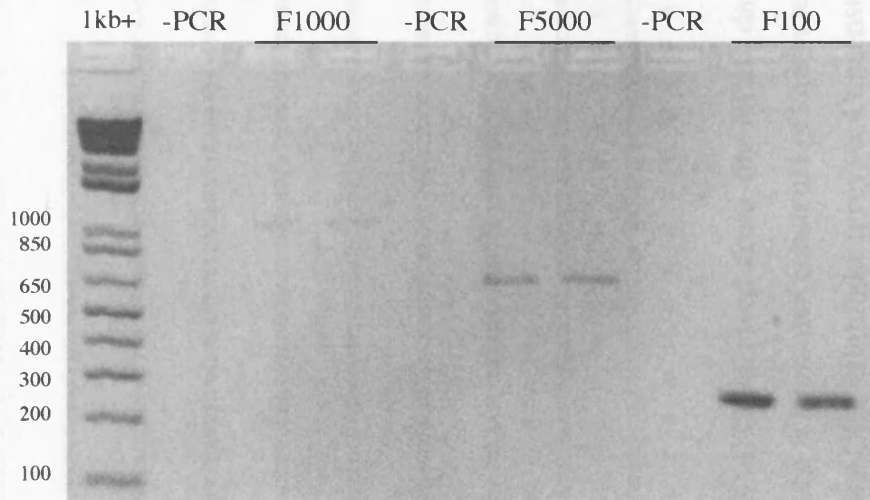


Figure 3.16 PCR amplification of nested promoter fragments from genomic DNA. Expected sizes for each fragment: P100 (258bp), P500 (645bp), F1000 (1194bp). -PCR = negative control for PCR. Double stranded DNA markers are given (1kb+) with their sizes in bp.



Figure 3.17 Genomic and protein sequence of the CA125 5'-UTR derived from the NCBI database. Blue = Translation start site from AF414442.2, Purple = Stop codon, Green = Promoter construct primer sites, Bold = ERE, Underlined = RARE, Red = Additional expressed sequence (5'-RACE), Highlight (grey) = Consensus Intron-Exon boundary motif, Highlight (yellow) = Sequence showing high identity with the consensus TIS motif.

Each construct was then assayed for endogenous transcriptional activity using the luciferase assay described in 2.6. This was carried out in primary human mesothelial cells (HPMC) and a human kidney cell line (HK-2). For each promoter construct the luciferase activity was normalised to the negative control promoterless pGL-3 vector as shown in Figure 3.18.

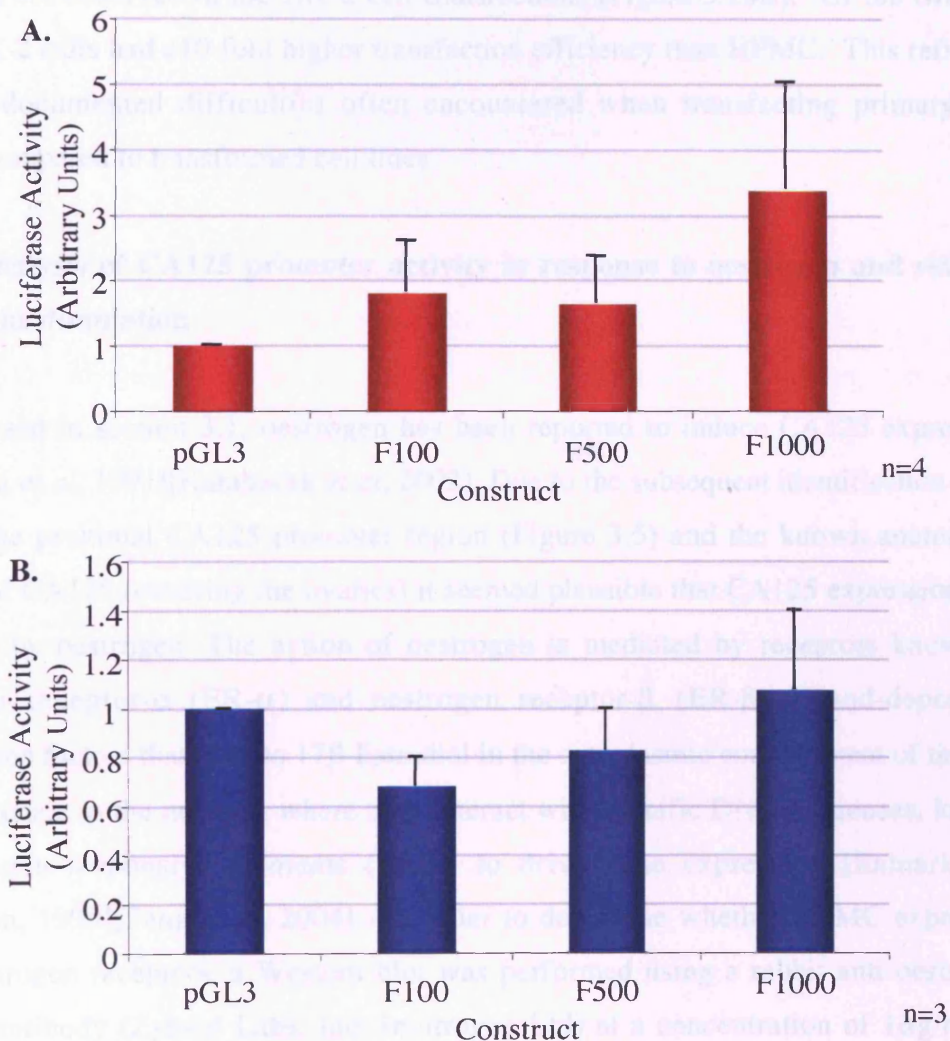


Figure 3.18 Endogenous luciferase activity of the CA125 proximal promoter constructs and pGL-3 control construct in (A) primary HPMC and (B) HK-2 cells. Luciferase activity is expressed as the magnitude of normalized luciferase activity relative to the promoterless negative control (pGL-3). 'n' refers to the number of independent experiments.

As seen in Figure 18A, there was no significant change in luciferase activity between the F100, F500 and F1000 HPMC transfected constructs. Interestingly, the F1000 promoter construct showed a trend towards an increase ($p=0.097$) in promoter activity when compared with the promoterless control vector in HPMC as seen by an approximate 2-fold increase in activity when compared to the promoterless control construct. This same trend was not observed in the HK-2 cell transfections (Figure 3.18B). Of the two cell types, HK-2 cells had a 10-fold higher transfection efficiency than HPMC. This reflected the well documented difficulties often encountered when transfecting primary cell cultures compared to transformed cell lines.

3.3.6 Analysis of CA125 promoter activity in response to oestrogen and retinoic acid stimulation

As discussed in section 3.1, oestrogen has been reported to induce CA125 expression [Nonogaki *et al*, 1991][Karabacak *et al*, 2002]. Due to the subsequent identification of an ERE in the proximal CA125 promoter region (Figure 3.5) and the known anatomical location of CA125 (covering the ovaries) it seemed plausible that CA125 expression was regulated by oestrogen. The action of oestrogen is mediated by receptors known as oestrogen receptor- α (ER- α) and oestrogen receptor- β (ER- β); ligand-dependent transcription factors that bind to 17 β -Estradiol in the cytoplasmic compartment of the cell and translocate to the nucleus, where they interact with specific DNA sequences, known as oestrogen responsive elements (ERE), to drive gene expression [Enmark and Gustafsson, 1999][Tang *et al*, 2004]. In order to determine whether HPMC expressed these oestrogen receptors, a Western blot was performed using a rabbit anti-oestrogen receptor antibody (Zymed Labs. Inc; Invitrogen Ltd) at a concentration of 1 μ g/ml on HPMC cell lysates (Figure 3.19).

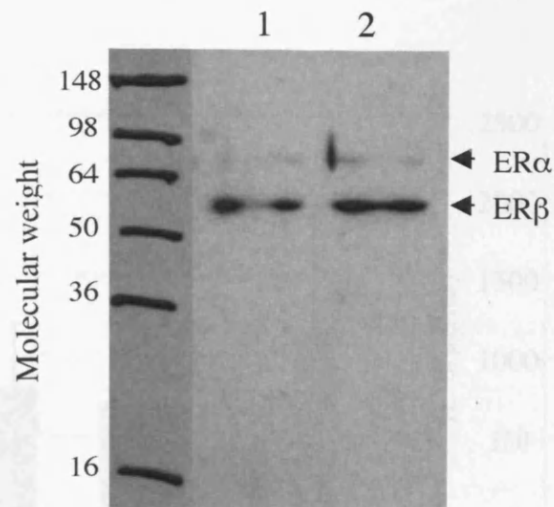


Figure 3.19 Identification of the oestrogen receptor subunits ER α and ER β in HPMC by Western blot. 20 μ g of total protein extracted from HPMC was run in lanes 1 and 2. Lanes 1 and 2 represent HPMC cultured from different patients. Molecular weight markers are given in kDa.

Western blot analysis identified two distinct bands. These bands corresponded to the alpha and beta subunits of the oestrogen receptor [Enmark and Gustafsson, 1999], having molecular weights of 67kDa and 55kDa respectively, and suggested that HPMC were oestrogen responsive cells.

In addition, as outlined in section 3.1, CA125 expression may also be regulated by retinoic acid (RA) [Nakai *et al*, 1993][Langdon *et al*, 1998][Hori *et al*, 2004][Xu *et al*, 2005]. RA acts through retinoic acid receptors (RARs) that undergo a conformational change when bound to the RA ligand. This complex then orchestrates the transcription of specific genes via DNA responsive element binding (RARE) [Bastein *et al*, 2004]. Therefore, using our previously described luciferase assay system, primary HPMC were tested for their ability to drive the transcription of the luciferase reporter gene in the presence of optimal concentrations of all-trans retinoic acid (100nmoles)[Hori *et al*, 2004] or 17 β -oestradiol (100 nmoles)[Garmy-Susini *et al*, 2004].

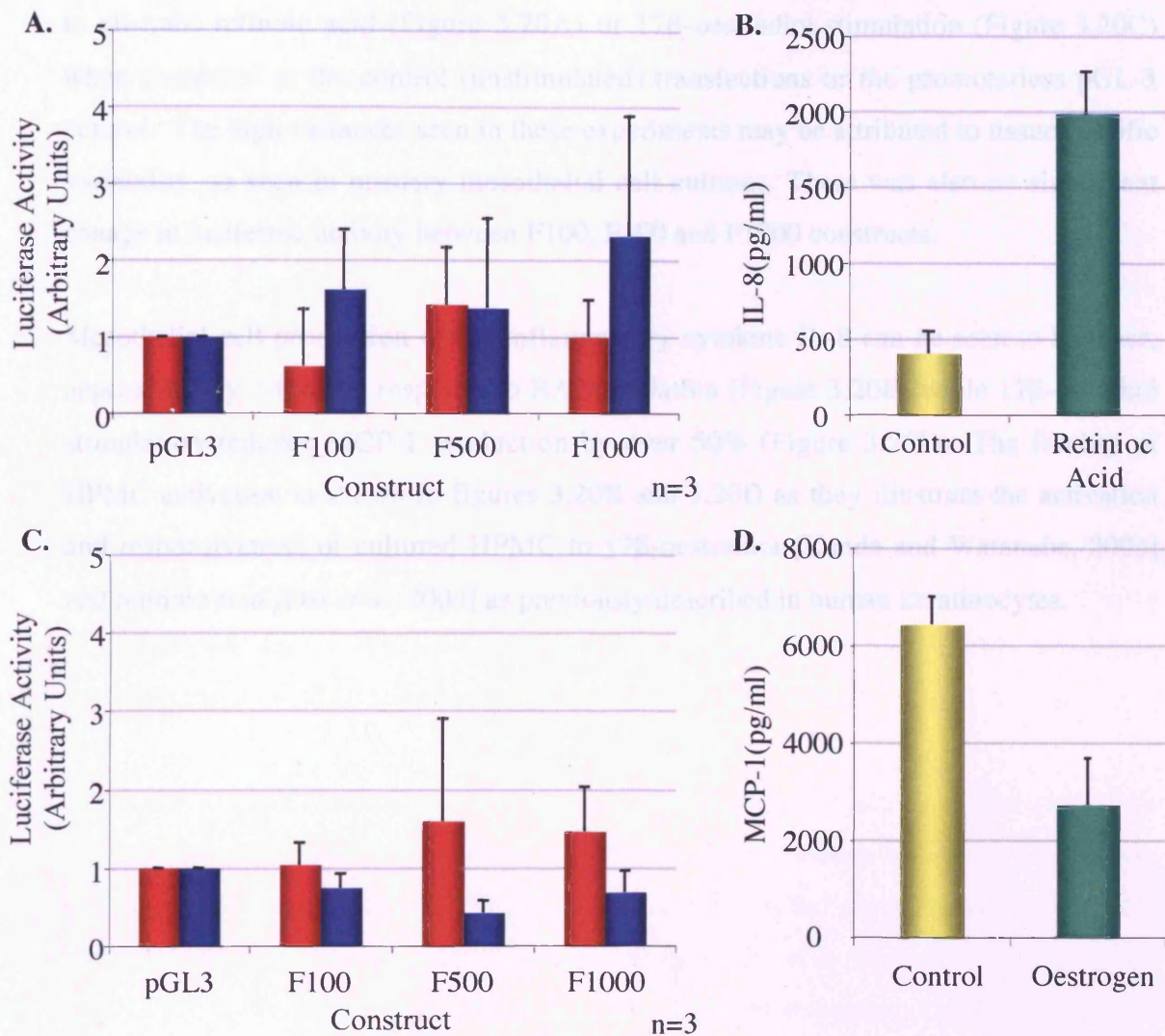


Figure 3.20 Luciferase activity of the CA125 proximal promoter constructs and pGL-3 control vector in response to retinoic acid and 17β -oestradiol stimulation. (A) Blue = retinoic Acid stimulation (10 nmoles), Red = Control. (C) Blue = 17β -oestradiol (100 nmoles), Red = Control. Luciferase activity is expressed as the magnitude of normalized luciferase activity relative to the promoterless negative control (pGL-3). (B) IL-8 concentrations of supernatant samples acquired from RA stimulation. (D) MCP-1 concentrations of supernatant samples acquired from 17β -oestradiol stimulation. 'n' refers to the number of independent experiments.

No statistically significant change was seen in any of the promoter constructs in response to all-trans retinoic acid (Figure 3.20A) or 17 β -oestradiol stimulation (Figure 3.20C) when compared to the control (unstimulated) transfections or the promoterless pGL-3 control. The high variances seen in these experiments may be attributed to tissue specific variability, as seen in primary mesothelial cell cultures. There was also no significant change in luciferase activity between F100, F500 and F1000 constructs.

Mesothelial cell production of the inflammatory cytokine IL-8 can be seen to increase, approximately 3-fold, in response to RA stimulation (Figure 3.20B) while 17 β -estradiol stimulation reduces MCP-1 production by over 50% (Figure 3.20D). The fidelity of HPMC activation is shown in figures 3.20B and 3.20D as they illustrate the activation and responsiveness of cultured HPMC to 17 β -oestradiol [Kanda and Watanabe, 2003] and retinoic acid [Dai *et al*, 2004] as previously described in human keratinocytes.

3.4 DISCUSSION

The genomic structure of the CA125 gene has been elucidated for the first time. A combination of *in silico* and *in vitro* methodologies were used, as previously described during the characterisation of the N-methyl-D-aspartate glutamate receptor [Williams *et al*, 2002]. Thus the >65kb mRNA sequence, AF414442.2, that was available at the beginning of this project, was used to identify clones containing intact gDNA sequence by BLAST analysis. Alignment of these mRNA and gDNA sequences using BLAST2 was then used to deduce the genomic structure of the CA125 gene. The genomic sequence upstream of CA125 exon 1 thus represented the putative promoter region. Luciferase analysis of nested PCR amplified fragments from this region was subsequently performed to investigate the transcriptional regulation of this large surface expressed mucin. Promoter analysis of several other members of the mucin gene family has been described previously [Gum *et al*, 1997][Van Seuning *et al*, 2000][Chen *et al*, 2001][Perrais *et al*, 2001][Gum *et al*, 2003][Shekels *et al*, 2003].

The reconstructed genomic structure of the CA125 gene indicated the presence of 84 exons within the genomic structure that occupied approximately 134 kb of the genome and produced a transcript of 66.765 kb. Due to a large tandem repeat region in the central region of the message, unambiguous sequence alignment was restricted to the 5' and 3' ends of mRNA sequence AF414442.2. The recently released composite reference CA125 mRNA sequence NM_024690 is not internally repetitive and is aligned completely and unambiguously with gDNA from chromosome 19p13.2. The existence of this ambiguous large repeat region did not allow accurate reconstruction of the repeat domain but may partly explain the high variability in the reported molecular size of CA125 RNA transcripts [O'Brien *et al*, 2001] and protein molecules [Fendrick *et al*, 1997][Nustad *et al*, 1997]. These findings are consistent with gene structure studies on other mucin genes, such as *MUC1* and *MUC5AC*, that also identified tandem repeat domains within their structures that permit the synthesis of variably sized molecules by tandem repeat polymorphisms [Spicer *et al*, 1991][Escande *et al*, 2001].

After closer inspection of the 5' end of the *in silico* CA125 genomic sequence, it became apparent that the 5' untranslated region (UTR) was in-frame with respect to amino acid encoding, suggesting that the TIS (transcription initiation start site) was further upstream. The 5' terminal sequence of exon 1 also resembled an intron-exon boundary [Zhang, 1998], providing further evidence that there may be more expressed sequence upstream. Bearing in mind that many 5' truncated mRNA sequences have been deposited on public access databases [Coleman *et al*, 2002][Casadei *et al*, 2003] and in order to identify the CA125 TIS, 5'-RACE was used to identify any further upstream expressed sequence. 5'-RACE analysis identified 9bp of additional, previously unidentified, expressed sequence (with regard to AF414442.2) at the 5'-end of the CA125 gene as seen in Figures 3.9 and 3.10. The additional sequence included an in-frame stop codon (TAG) and thus represented a barrier to translation of any upstream sequences. Critically, since the first methionine codon encoded by mRNA AF414442.2 coincided with the predicted translation start site of CA125, this provided strong evidence that the sequence upstream of this site was non-coding.

As seen in Appendix I, identical sequences were recovered for bands B and C. This result was unpredicted since the size of these bands appears to be different in Figure 3.9 (Band B≈300bp, Band C≈260bp). This discrepancy was attributed to the accidental repeated cloning of the same band. Since the predicted size of the larger band B was consistent with the observed size of the DNA fragment cloned and sequenced it was apparent that the larger of the two fragments had been cloned. This is consistent with 5'-RACE sequence data from the analysis of the human *HAS* gene family that show smaller 5'-RACE bands may represent truncated forms of full-length mRNAs [Monslow *et al*, 2004]. It was therefore assumed that band C was either a 5'-truncated CA125 specific sequence or a product of non-specific amplification.

Further analysis of the 5' sequence located a motif (5'-TGAGATTT-3') with high identity to the TIS consensus motif, YYANWYY (Y=Pyrimidine, W=A or T) [Smale, 1997], positioned 6bp upstream from the additional RACE sequence (Figure 3.10). This provided strong evidence that the TIS and the promoter region of the CA125 gene had

been identified. The absence of a downstream promoter element (DPE) or TATA box core promoter consensus motifs [Smale and Kadonaga, 2003] in the surrounding sequence does not detract from the possibility that this is promoter sequence as many other genes [Smale, 1997] including MUC3A [Gum *et al*, 2003] and CD80 [George *et al*, 2006] do not have DPEs or TATA box motifs in their promoter regions. In addition, the absence of RT-PCR products amplified between AF414442.2 and EST AA633830 (Figures 3.13 and 3.14), the absence of RT-PCR products using any of the nested upstream fragments tested in Figure 3.12 and the cluster of TFBS present in the sequence (Figure 3.4) suggested that the CA125 TIS and proximal promoter had been identified and that the 5'-upstream flanking region constitutes the CA125 promoter region.

The sequence directly upstream of the CA125 TIS was amplified and analysed for transcriptional activity using a dual-luciferase assay system. Initially, the endogenous promoter activity of each promoter construct in HK-2 cells and primary HPMC was examined by testing their ability to drive the transcription of the luciferase gene. In HK-2 cells none of the constructs produced a significant increase in luciferase output when compared to the promoterless control. HK-2 cells were originally selected for use in this system due to their ease of transfection, as shown previously [Monslow *et al*, 2004]. Subsequent analysis showed that HK-2 cells do not express CA125 (see appendix III), rendering them unsuitable for this system in any capacity other than acting as a negative control for the HPMC analysis.

When the CA125 promoter constructs were transfected into primary HPMC cells, a trend towards an increase in luciferase output was observed using the F1000 promoter construct that was not observed in the HK-2 cell transfections. This vector displayed an approximate 2-fold increase in activity compared to that of the other constructs, demonstrating its endogenous promoter activity. As seen in Figure 3.2, the difference between the F1000 and F500 promoter construct sequence is the existence of an extensive polypyrimidine tract region approximately 385bp in length. Although considerably larger than other simpler repeat regions described in the literature, some studies have shown the regulation of genes such as VEGF [Sun *et al*, 2005] and human c-ets-2 [Mavrothalassitis

et al, 1990] by polypyrimidine/purine repeat regions in their promoter regions thus indicating a possible mechanism by which the CA125 promoter regulates gene expression. This represents, along with the cloning of larger promoter constructs, a target for future work in order to further understand the mechanisms involved in the regulation of CA125 transcription.

As mentioned previously, the F1000 construct displayed a 2-fold increase in promoter activity when compared to the promoterless control vector. This activity is substantially less than that reported for promoter constructs from mucin gene *MUC6* which displayed an 80-fold increase in activity compared to control vectors [Sakai *et al*, 2005]. However, analysis at a different mucin locus demonstrated that the transcriptional regulation of these genes varies. Thus, the promoter of the highly expressed cell surface *MUC1* showed only a 5-fold increase over control values [Thathiah *et al*, 2004]. The CA125 data described above suggest that the low-level endogenous promoter activity of the F1000 fragment is sufficient for the constitutive expression of this very large protein.

As seen in Figure 3.20, though not statistically significant, stimulation of transfected HPMC with RA resulted in an approximate 2-fold increase in the luciferase activity of the F1000 construct, while stimulation with 17β -oestradiol resulted in approximate 3- and 2-fold inhibitions of the F500 and F1000 constructs luciferase activity, respectively. These data suggest that CA125 transcription may be up regulated through the RARE motif, possibly via a mechanism involving the polypyrimidine repeat region due to the specific induction of the F1000 construct. It is also possible that CA125 mRNA synthesis might be down regulated through the ERE motif, in a mechanism similar to that described in other studies examining the complement-3 (C3) promoter [Harrington *et al*, 2003] and the CRH-BP promoter [Van De Stolpe *et al*, 2004], as indicated by the reduced activity of both F500 and F1000 constructs. The above findings are consistent with previous studies on the regulation of CA125 by retinoic acid [Nakai *et al*, 1993][Hori *et al*, 2004] but disagree with previous reports regarding the effects of oestrogen [Nonogaki *et al*, 1991][Karabacak *et al*, 2002]. Additionally, the profile of luciferase activity observed for control transfections in these experiments, appears to be inconsistent with the endogenous

activity displayed in Figure 3.18A, possibly due to an altered response of HPMC to the phenol red free M199 medium and charcoal/dextran treated FCS in which they were grown [Garmy-Susini *et al*, 2004]. Statistical significance was not achieved in these experiments, possibly due to the highly variable and notoriously difficult process of transfecting primary HPMC demonstrated by a maximal primary HPMC transfection efficiency of 1% reported elsewhere [Ohan *et al*, 2001]. Additional replicate experiments would possibly allow improved definition of the observed changes, nevertheless, the level of modulation displayed by the CA125 promoter region matches the observed magnitude of induction seen in CA125 expression shown in our *chapter 4* studies (<45% increase) and in other *in vitro* [Zeillemarker *et al*, 1994][Zeimet *et al*, 1997] and *in vivo* [Jones *et al*, 2001][Williams *et al*, 2004] CA125 studies.

Chromatin architecture may have a profound impact on transcription including ERE and RAR dependent gene activation. As previously described, ligand binding induces a conformational change in the receptor complex (dimer) that allows translocation into the nucleus and association with specific response element motifs (section 3.3.2) in the target DNA sequence thus promoting transcription via specific interactions with the core polymerase apparatus [Klinge, 2001][Bastein *et al*, 2004]. Additionally, upon stimulation, conformational changes to the receptor allow the recruitment of a protein complex that has the ability to modify DNA-histone interactions, possibly via acetylation of specific histone lysine residues, rendering the DNA more accessible to the transcriptional machinery [Sanchez *et al*, 2002][Clayton *et al*, 2006]. Mindful of the influence of chromatin modification on the transcriptional process from genomic DNA, it is worthy of note that these factors were absent from our *in vitro* system. Therefore the results obtained using pGL-3 luciferase reporter constructs containing CA125 promoter inserts may not accurately represent the native regulation of CA125 mRNA synthesis *in vivo*.

In conclusion, having successfully reconstructed and characterised the CA125 5' flanking sequence, we demonstrated that the CA125 promoter has low-level endogenous activity. This is consistent with the regulation of this large, highly expressed, gene whose production has previously been shown to have a low magnitude of modulation

[Zeillemarker *et al*, 1994][Zeimet *et al*, 1997][Jones *et al*, 2001][Williams *et al*, 2004]. Data has been provided suggesting that the regulation of CA125 transcription may occur through the polypyrimidine repeat region, as well as through retinoic acid receptors and oestrogen receptors present in the proximal promoter region. The low levels of modulation of CA125 expression shown in this work is further highlighted in *chapter 4* of this thesis where IL-1 β and IL-6 trans-signalling can be seen to induce CA125 expression levels consistent with our present findings. The regulation of CA125 at the level of transcription remains far from clear. This work serves to highlight the need for the repeated examination of the CA125 promoter region in response to RA and Oestrogen, and ultimately, the need for the generation of functional murine knockout models in order to progress our understanding of the regulation and function of CA125.

APPENDIX I

5'-Race Sequence data (5'-3')

Band A Non-specific to CA125

CAAATTTAGGGGGGGCGAAATTGGGGCCCTCTAGATGCATGCTCGAGCGGCCGCCAGTGTGATGG
ATATCTGCAGAATTCGCCCTTAGGAGCGGGTGGGAGAAGATGACCACCAGGGTGGCTCCCAGCAC
CCAGAAGACGGCCGAGCCCGCACCAGCCAGCCAGAAGAAGGGGAAGGAGATGCCTCCAGCCAGAG
CATACTGATGCGCTGGGCTCACCTCTCGGCCAAAGAGCACAAGCTTGGACTCCAAGGTGCGCAGA
TAGAGAATGTAACAGGCGCCGAAAAAGACAGCCAGAGCCACCAGCAACATAGGGGACGTCACCAC
ACAGTACAGGATGAGGCCAGGAACACGAACACATAGTTGCTCTGGTAGTACTCCACGTTGCGTA
CGAGGCGCTGGCACAGCTCTCCCAGGTTGCGGGGCCGTGAGAAGCGCTGCTGGTCCACGAAGGTG
CTCCAGGGCCGGATGGCCGCGCGGCCGCTCCAGCCACTCCCGGCCTGCACCGGAGGGAATCAG
CTTCGGCAGCAGGGTCGTGCCGCTCAGCCCTTCCGCCTCGGCATCTTTCTGCTGGTCCTTCTGCG
CTGCCATGTCTGCGTCGTGAGGGGGGAGCTGCTGTCCCCGCTACTCTGCGTTGATACTACTGCT
TGCCCTATAGTGAGTCGTATTAGAAGGCGAATTCAGCACACTGGCGGCCGTTACTAGTGGATCC
GAGCTCGGTACCAAGCTTGGCGTAATCATGGTCATAGCTGTTTCTGTGTGAAATTGTTATCCGC
TCACAATTCACACAACATACGAGCGAGCATAAAGTGTAAGCCTGGGGTGCCTATGAGTGACTA
CTCACATAGTGCGTGCGCTCACTGCCGCTTTCAGTCGGAAACTGTCTTGCACTGCATTATGATCG
CCACGCCGGGAAAGGCGTTGCGATTGGGGCCTTCCGCTTCCGCTCATGATCGTGGCCTGAGTT
CGTGCGGGGAGGGTTACGCTTCTCAGCGGTAACCGTTTGAATCGTACAGAACTTGCAAGGCCGAG
GCACTACGGCCTTCGTTTCAGGTCCCCTGGATCAATCGCCT

Band B (233 bp) 9 bp Extension


CTCAATTAGAAGCGTTGTACAATTCGCCAACCTCCATACATACGGCAGCTCTTCTAGACACAGG
TTTTCCCAGGTCAAATGCGGGGACCCAGCCATATCTCCCACCCTGAGAAATTTTGGAGTTTCAG
GGAGCTCAGAAGCTCTGCAGAGGCCACCCTCTCTGAGGGGATTCCTTAGACCTCCATCCAGAGG
CAAATGTTGACCTGTCCATGCTGAAACCCTCAGGCCT


Band C (233 bp) 9 bp Extension

CTCAATTAGAAGCGTTGTACAATTCGCCAACCTCCATACATACGGCAGCTCTTCTAGACACAGG
TTTTCCCAGGTCAAATGCGGGGACCCAGCCATATCTCCCACCCTGAGAAATTTTGGAGTTTCAG
GGAGCTCAGAAGCTCTGCAGAGGCCACCCTCTCTGAGGGGATTCCTTAGACCTCCATCCAGAGG
CAAATGTTGACCTGTCCATGCTGAAACCCTCAGGCCT

Band D (85 bp) Truncated

AGAGGCCACCCTCTCTGAGGGGATTCTTCTTAGACCTCCATCAGAGGCAAATGTTGACCGTTCCA
TGCTGAAACCCTCAGGCCT

 = Additional 5'RACE sequence

 = 5'RACE Gene specific primer

APPENDIX II

A. Predicted composite sequence (5'-3') of CA125 (AF414442.2) and EST (AA633929)

EST F →
AGCACATTTCCCCTGTGATAAGTACCTTCTCATCTCTCAGGGCCCTCCTTAAATATTACCTCCTA
TGAGAAGTCTTCCCTGATGACTCTATGGAAAATTATGCTTCTCTCTCAATTAGAAGCGTTGCACA
ATTCCCCAACCTCCATACA TACGGCAGCTCTTCTAGACACA ← RT-EST 1
AGGTTTTCCAGGTCAAATGCGGG
GACCCAGCCATATCTCCACCCTGAGAAATTTGGAGTTTCAGGGAGCTCAGAAGCTCTGCAGA
GCCCACCCTCTCTGAGGGGATTC TTCTTAGACCTCCATCCAGAGG ← RT-EST 2

■ = Upstream EST sequence (AA633929) ■ = CA125 5'-end sequence (AF414442.2)

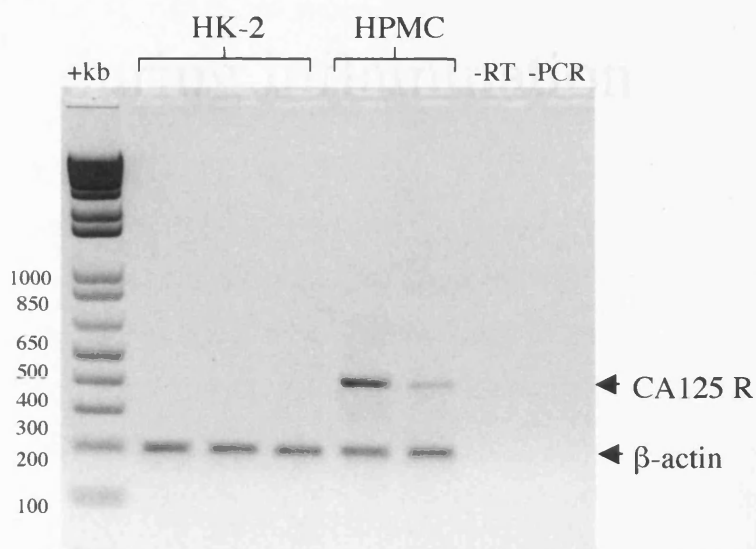
B. Nucleotide sequence (5'-3') of RT-PCR band produced using the RT-EST1 primers

CCCCCTTCCTGTTGGAACCTTTGGCCTGATGTTTGAATGAGGTTACCCTTTTGACCAAAAAGATT
TCCACATTCTCTACACTCATAAGGCCCTTCTCCAGTGTGAACACGCTGATGGCTAATAAGGCTG
CCCTTCTGACTAAAAGATTTCCCGCACTCCTCACAGGGATAAGCTGTCTGTCCAGTGTGGACTCG
CTGATGTTGAATAAGGCTGCTCTTTCGACTATAAGATTTCCCACTCTCCACAATCATAAGGTC
CTTTTGCAGTGTGATCTCGCTGATGATTACTGAAGCTGACATATCTGCTAAAGGATTTCCACAA
TCACTGCACACATAACATCCATCTCTAGTGAAAAGTTTCTGGTGTGGAATAACTGAGTGTTTGGT
GGAGAGGGCTTATGAGCGTAGAGAATACGGGTAATTACTTAGGTCAATCCCGGAAAGATA

APPENDIX III

CA125 expression by HK-2 cells *versus* HPMC

RT-PCR was carried out on RNA extracted from HK-2 cells (as in sections 2.3, 2.4.1 and 2.4.4) using primers specific for the repeat region of the CA125 gene (CA125 R, Table 3.2) and β -actin. The same amplification was carried out on RNA extracted from HPMC as a positive control.



Specific amplification of the CA125 repeat region by RT-PCR in HK-2 cells and HPMC. -RT = negative control for reverse transcriptase, -PCR = negative control for PCR. Double stranded DNA markers are given (1kb+) with their sizes in bp.

Bands of predicted size were amplified from HPMC total RNA suggesting the reaction conditions were optimal for CA125 specific amplification. No bands were amplified for HK-2 cell RNA suggesting HK-2 cells do not express CA125.

4.1 INTRODUCTION

The introductory chapter of this thesis has described the inflammatory cascade that takes place, locally, in the peritoneal cavity in response to dialysis fluid driven injury or to invasion by micro-organisms (Sections 1.4, 1.5 and 1.6). Presently it is not known how CA125 expression is regulated during the inflammatory response or how the antigen may itself contribute to this process. Previous studies have provided sharply contrasting results relating to the control of CA125 expression during inflammation. CA125 effluent levels have been shown to increase during and after episodes of peritonitis [Ho-Dac-Pannakeet *et al*, 1995][Bastani and Chu, 1995] but it is not known whether this is a result of alterations to the mesothelium or a direct result of the modulation of HPMC CA125 production by inflammatory mediators. In 1995, Visser *et al* reported that CA125 expression by HPMC did not appear to be controlled by the inflammatory cytokines (i.e. IL-1 β) and thereby postulated that CA125 was only expressed in a constitutive manner [Visser *et al*, 1995]. This data was in conflict with other studies that showed the modulation of CA125 expression by IL-1 β and other pro-inflammatory cytokines [Zeillemarker *et al*, 1994][Zeimet *et al*, 1996]. However, to add further confusion to the situation, Zeillemarkers study indicated an increase in CA125 secretion while Zeimet's study documented a decrease in CA125 shedding in response to the same pro-inflammatory cytokines.

Currently, we know very little about the mechanisms involved in the control of CA125 expression under normal conditions. To date, no studies have investigated the mechanisms involved in the transcriptional control of the gene (as we have attempted in chapter 3). Present evidence indicates that CA125 is predominantly a surface expressed antigen that can be shed although it's exact biological function remains unknown. The structure of the protein core suggests that the molecule has a proteolytic cleavage site allowing its release from the cell surface [O'Brien *et al*, 2002] and SEA domains that allow the subsequent cleavage of the released molecule [Maeda *et al*, 2004][Palmai-Pallag *et al*, 2005] but little is understood about the specific pathways involved in this

process. In order to investigate these unknown mechanisms we must first understand how CA125 is regulated under defined conditions.

As previously described, HPMC play a key role in the coordination and control of the inflammation [Topley, 1995]. Work carried out at this Institute has shown that in response to IL-1 β stimulation, HPMC release IL-6. This in turn binds to its soluble receptor (sIL-6R) and induces the release of chemokines from resident HPMC for the subsequent recruitment of leukocyte populations [Topley *et al*, 1993][Topley *et al*, 1996][McLoughlin *et al*, 2004]. Using an *in vitro* HPMC model we have demonstrated that the addition of IL-1 β drives the early phase of the inflammatory response [Topley *et al*, 2003] and that IL-6/sIL-6R will trigger the later resolution phase of the response [McLoughlin *et al*, 2004] in primary human mesothelial cells. In this chapter we use this *in vitro* model of inflammation to re-evaluate how CA125 expression is regulated during inflammation by examining CA125's control at the level of transcription, cell surface expression and the subsequent release from the cell surface in response to IL-1 β and IL-6/sIL-6R stimulation.

4.2 METHODS

All HPMC for the subsequent experiments were harvested from consenting patients undergoing elective abdominal surgery and grown into confluent monolayers as discussed in sections 2.2. All cells were growth arrested for 48 hours in serum free M199 prior to stimulation. In this chapter, the n number given for each experiment refers to the number of individual omental isolations (from separate donors) on which experiments were performed.

All data are presented as mean [\pm standard error of the mean (SEM)] of the assigned number of independent experiments (n) performed on averaged duplicate samples for each experiment. Data were analysed using two-way ANOVA on SPSS v11.5 for Windows. For Figure 4.13 significance was determined using the Student T-test (Excel for Mac[®]). Differences were considered significant when $p < 0.05$.

4.2.1 Analysis of CA125 production by HPMC

HPMC cell lysate and supernatant samples were prepared as described in section 2.7.3 and 2.7.4 respectively. A Western blot was then performed as outlined in section 2.7. Primary antibody; Anti-CA125 OC125 (purchased from Fuji-Rebio Diagnostics Inc), Secondary antibody; Anti-mouse HRP (Santa-Cruz Biotechnologies; Antigen Bioclear Uk Ltd, Calne, UK).

4.2.2 Analysis of CA125 regulation in response to IL-1 β stimulation

4.2.2.1 Analysis of CA125 transcription

Cells were stimulated with recombinant human IL-1 β (R&D Systems Europe Ltd, Abingdon, UK). At 0, 3, 6, 12, 24 and 48 hours the cells were harvested and the RNA extracted as described in section 2.3.1. The total amount of RNA was quantified (section 2.3.2) before it was reverse transcribed (section 2.3.4). The resultant cDNA was then used in a PCR reaction using CA125 specific primers (Table 4.1) as described in section

2.4.1. The PCR products were visualized using ethidium bromide staining following gel electrophoresis (section 2.4.4). Densitometric analysis was carried out using Chemidoc® computer software.

Table 4.1 Oligonucleotide primers used in RT-PCR experiments

Primer pair	Sense-strand sequence	Anti-sense strand sequence	Cycle No
β-Actin	GGAGCAATGATCTTGATCTT	CCTTCCTGGGCATGGAGTCCT	30
CA125 Repeat	GGAGAGGGTTCTGCAGGGTC	GTGAATGGTATCAGGAGAGG	30
HLGP	AACCTCCTTCCCAGAATCCAGG	CCTCTGTGTGCTGCTTCATTGGG	30

All primers are in 5' - 3' orientation

4.2.2.2 Analysis of CA125 cell surface expression

Cells were stimulated with recombinant human IL-1β. At defined time points the cells were harvested, stained and analysed as described in section 2.8.

4.2.2.3 Analysis of CA125 cell surface secretion

Cells were stimulated with recombinant human IL-1β. At defined time points the supernatant samples were collected and centrifuged at 5000g for 3.5 minutes in order to remove any detached cells and cell debris. The supernatants were then assayed for CA125 concentration as described in section 2.9.

4.2.2.4 Analysis of CA125 promoter activity

HPMC were transfected with the putative promoter constructs (section 2.6.2) and stimulated with IL-1β as described in section 2.2.9. Luciferase assays were then carried out using HPMC as discussed in section 2.6.

4.2.3 Analysis of CA125 regulation in response to IL-6/sIL-6R stimulation

4.2.3.1 Analysis of CA125 transcription

Cells were stimulated with recombinant human IL-6 (R&D Systems Europe Ltd) and recombinant human sIL-6R (R&D Systems Europe Ltd). At 0, 3, 6, 12, 24 and 48 hours the cells were harvested and the RNA extracted, as described in section 2.3.1. The total amount of RNA was quantified (section 2.3.2) before it was reverse transcribed (section 2.3.4). The resultant cDNA was then used in a PCR reaction using CA125 specific primers (for primer sequence see Table 4.1) as described in section 2.4.1. The PCR products were visualized using ethidium bromide staining following gel electrophoresis (section 2.4.4). Densitometric analysis was carried out using Chemidoc[®] computer software.

4.2.3.2 Analysis of CA125 cell surface expression

Cells were stimulated with recombinant human IL-6 and recombinant human sIL-6R. At defined time points, the cells were harvested, stained and analysed as described in section 2.8.

4.2.3.3 Analysis of CA125 cell surface secretion

Cells were stimulated with recombinant human IL-6 plus recombinant human sIL-6R. At defined time points, the supernatant samples were collected and centrifuged at 5000g for 3.5 minutes in order to remove any detached cells and cell debris. The supernatants were then assayed for CA125 concentration as described in section 2.9.

4.2.3.4 Analysis of CA125 promoter activity

HPMC were transfected with the putative promoter constructs (section 2.6.2) and stimulated with IL-6/sIL-6R as described in section 2.2.9. Luciferase assays were then performed using HPMC as discussed in section 2.6.

4.2.4 Analysis of MCP-1 concentration in response to IL-1 β and IL-6/sIL-6R stimulation

Growth arrested HPMC were stimulated with IL-1 β and IL-6/sIL-6R (R&D systems). After 24 hours the supernatants were collected and centrifuged at 5000g for 3.5 minutes. The supernatants were then assayed for MCP-1 concentration as described in section 2.10.1.

4.3 RESULTS

4.3.1 Analysis of CA125 production by HPMC

In order to determine the nature and molecular weight of the CA125 antigen being produced by HPMC a Western blot was performed using pooled supernatant (SNT) samples (obtained after 48 hours growth arrest) and cell lysate samples extracted from growth arrested HPMC. The commercially produced CA125 antigen was used as a positive control.

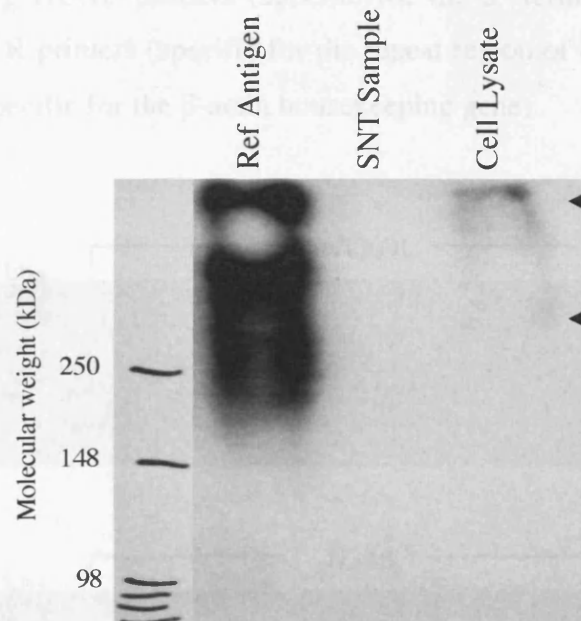


Figure 4.1 Western Blot analysis of CA125 production by HPMC. 20 μ g Total protein was run in each lane. Molecular weights are given in kDa.

As demonstrated in Figure 4.1, CA125 was detected in the HPMC lysates but not in the supernatant samples. Although CA125 is known to be shed from the cell surface of HPMC, these data may simply reflect the large difference seen between the amount of CA125 present within the cell and the amount released from the cell. Figure 4.1 also illustrates that CA125 molecules of varying molecular weights are produced as shown by the diffuse band seen for the reference antigen (between ≈ 200 and 1×10^6 kDa) and for the HPMC lysate sample (between ≈ 1000 and 1×10^6 kDa (arrows)).

4.3.2 Analysis of CA125 regulation in response to IL-1 β stimulation

4.3.2.1 Analysis of CA125 transcription

In order to determine the effect that pro-inflammatory cytokines have on the transcription of the CA125 gene, confluent monolayers of growth arrested HPMC were incubated in the presence or absence of IL-1 β . IL-1 β was used at 100pg/ml, as previous work has shown this to induce sub-maximal activation in HPMC [Topley *et al*, 1993]. As shown in Figure 4.2, at 0, 3, 6, 12, 24 and 48 hours, the cells were analysed for gene expression using HLGP primers (specific for the 5' terminus of the CA125 coding region), CA125 R primers (specific for the repeat region of the CA125 message) and β -actin primers (specific for the β -actin housekeeping gene).

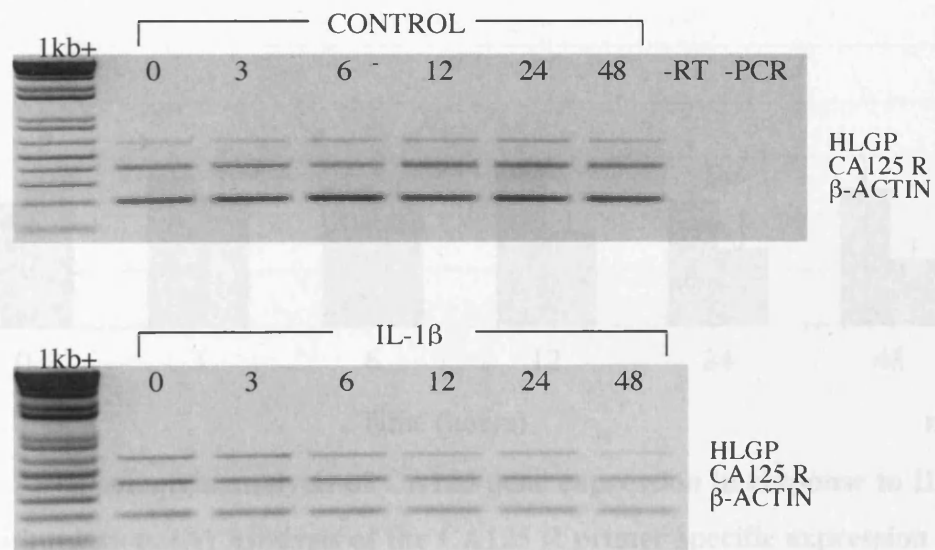


Figure 4.2 HPMC expression of CA125 in response to IL-1 β . Representative agarose gel showing expression levels of the CA125 gene (CA125 R and HLGP) and β -actin in control (un-stimulated) and stimulated (IL-1 β (100pg/ml)) at defined time points. -RT=Negative control for reverse transcription, -PCR=Negative control for PCR.

Semi-quantitative analysis of CA125 transcription was achieved using a ratio of each product compared to the β -actin housekeeping gene, via densitometric analysis (Figure 4.3).

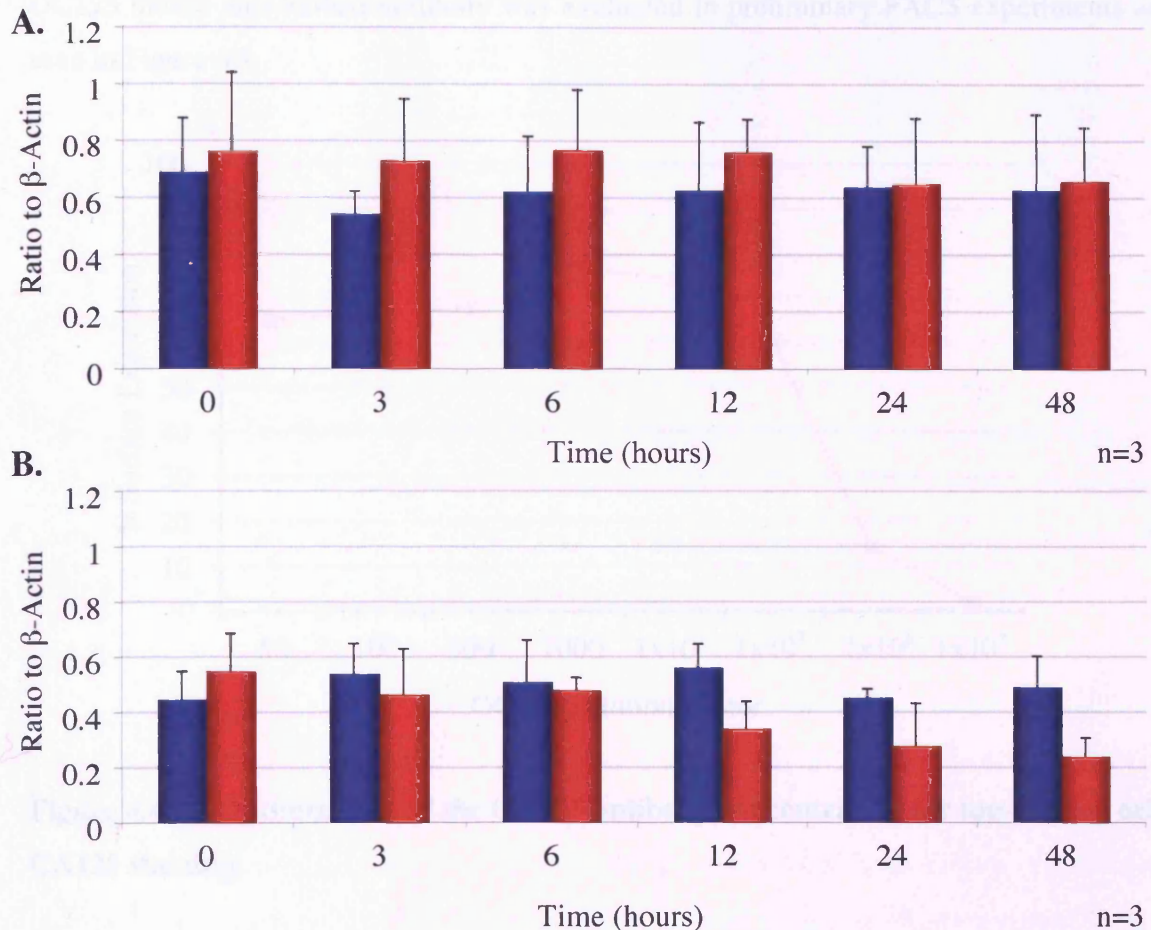


Figure 4.3 Densitometric analysis of CA125 gene expression in response to IL-1 β (100pg/ml) stimulation. (A) Analysis of the CA125 R primer specific expression as a ratio of β -actin. Blue bars = Control, Red bars = IL-1 β (100pg/ml) stimulation. (B) Analysis of the HLGP primer specific expression as a ratio of β -actin. Blue bars = Control, Red bars = IL-1 β (100pg/ml) stimulation. 'n' refers to the number of independent experiments.

As can be seen in Figure 4.3, analysis of CA125 gene expression in response to IL-1 β , using either of the CA125 specific primers, shows no statistically significant change in expression over the 48 hour period when compared to the control expression.

4.3.2.2 Analysis of CA125 cell surface expression

Prior to analysis of CA125 cell surface expression, the optimal concentration of the OC125 mouse anti-human antibody was evaluated in preliminary FACS experiments as seen in Figure 4.4.

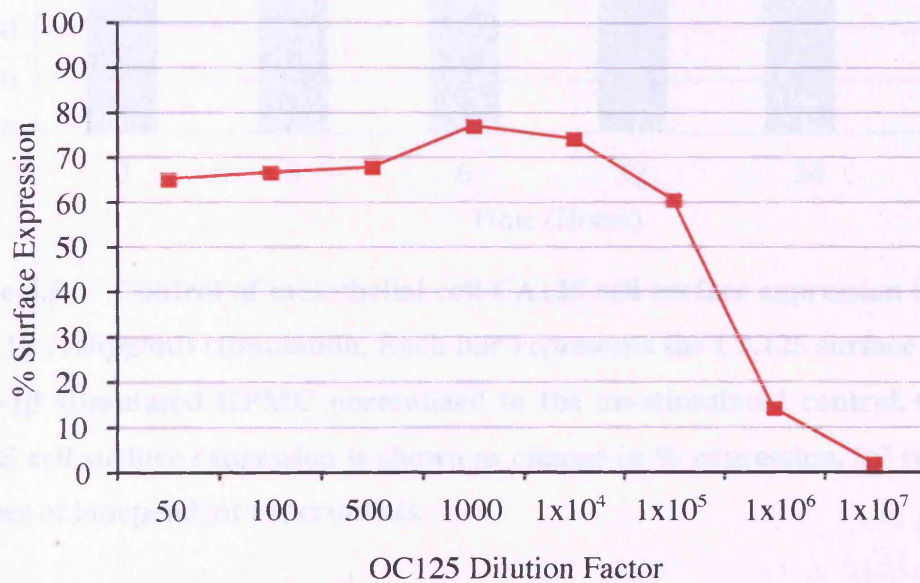


Figure 4.4 Optimization of the OC125 antibody concentration for mesothelial cell CA125 staining.

Figure 4.4 shows that a 1/1000 dilution of the OC125 stock (0.4mg/ml) is the optimal dilution for CA125 staining. Therefore, OC125 was used at 0.4µg/ml for all subsequent FACS experiments. The secondary antibody: Rat anti-mouse IgG-PE was used at 62.5ng/ml as defined in previous experiments.

To determine the effect that IL-1β has on cell surface expression of CA125, confluent growth arrested HPMC were treated with IL-1β (100pg/ml) or control serum free M199 and the surface expression of CA125 was analysed at defined time points using FACS analysis (Figure 4.5).

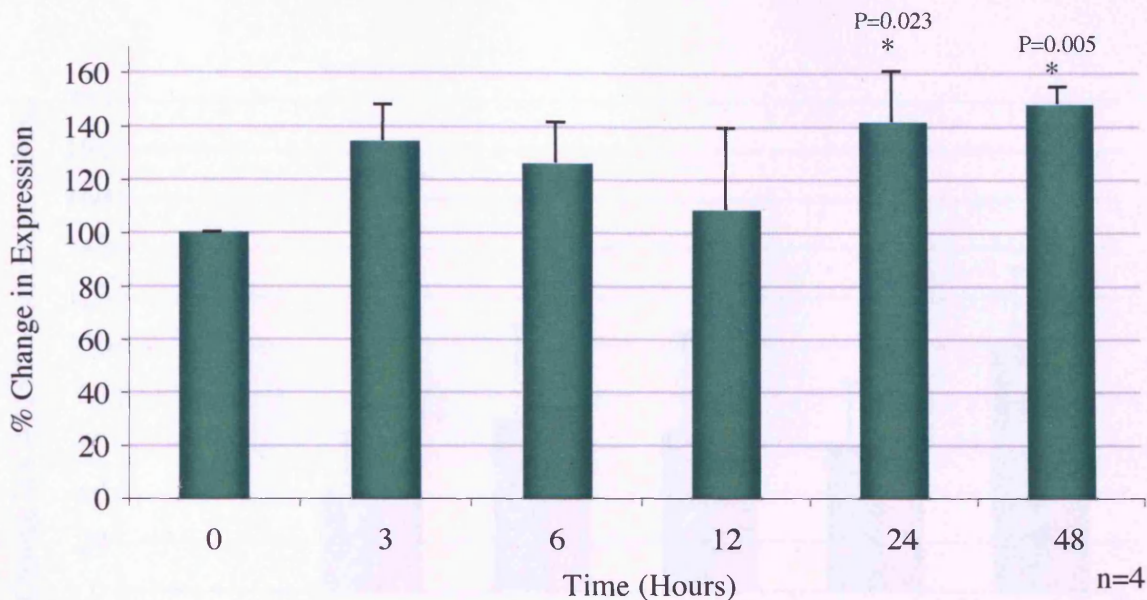


Figure 4.5 Control of mesothelial cell CA125 cell surface expression in response to IL-1 β (100pg/ml) stimulation. Each bar represents the CA125 surface expression of IL-1 β stimulated HPMC normalized to the un-stimulated control. Change in CA125 cell surface expression is shown as change in % expression. ‘n’ refers to the number of independent experiments.

As shown in Figure 4.5, the amount of CA125 expressed on the HPMC cell surface is increased by IL-1 β stimulation in a time dependant manner. When compared to the control cell surface expression, stimulation with IL-1 β can be seen to induce a significant change (\approx 50% increase) in CA125 surface expression after 24 and 48 hours stimulation.

4.3.2.3 Analysis of CA125 cell surface secretion

In order to determine whether a change in surface expression of CA125 was associated with the amount released from the cell surface, HPMC were stimulated with IL-1 β for defined times. At defined time points the supernatant samples for both control (serum free M199) and IL-1 β stimulated cells were collected and analysed for CA125 concentration (Figure 4.6).

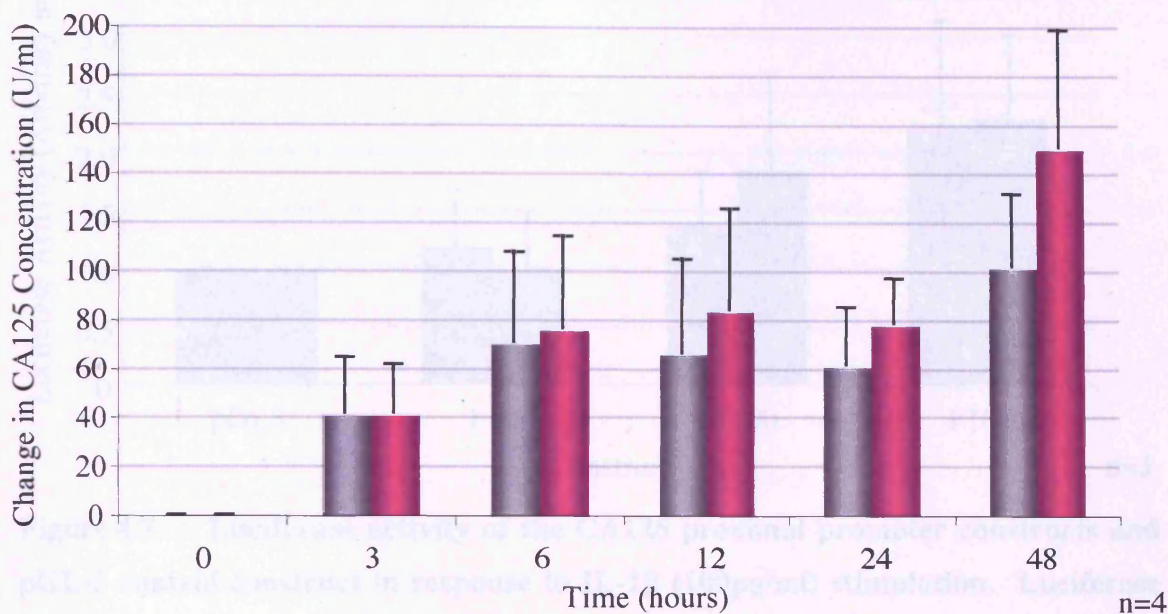


Figure 4.6 Cell surface secretion of CA125 from HPMC in response to IL-1 β stimulation. HPMC were treated with serum free medium (grey) or stimulated with 100pg/ml IL-1 β (pink) and analysed for CA125 concentration at defined time points. Changes in CA125 concentration are shown as a change in concentration compared to the zero hour time point. 'n' refers to the number of independent experiments.

Although not statistically significant, these data indicate a trend in the amount of CA125 released from the surface as observed by an increase in CA125 shedding from the cell surface in response to IL-1 β stimulation after 48 hours when compared to the unstimulated control cells.

4.3.2.4 Analysis of CA125 promoter activity

HPMC were transfected with the putative promoter constructs (see chapter 3) as described in section 2.6.2. Each construct was then assayed for transcriptional activity in HPMC, stimulated for 24 hours in the presence or absence IL-1 β (100pg/ml), using the luciferase assay described in 2.6. For each promoter construct the luciferase activity was normalized to the promoterless control vector, pGL-3.

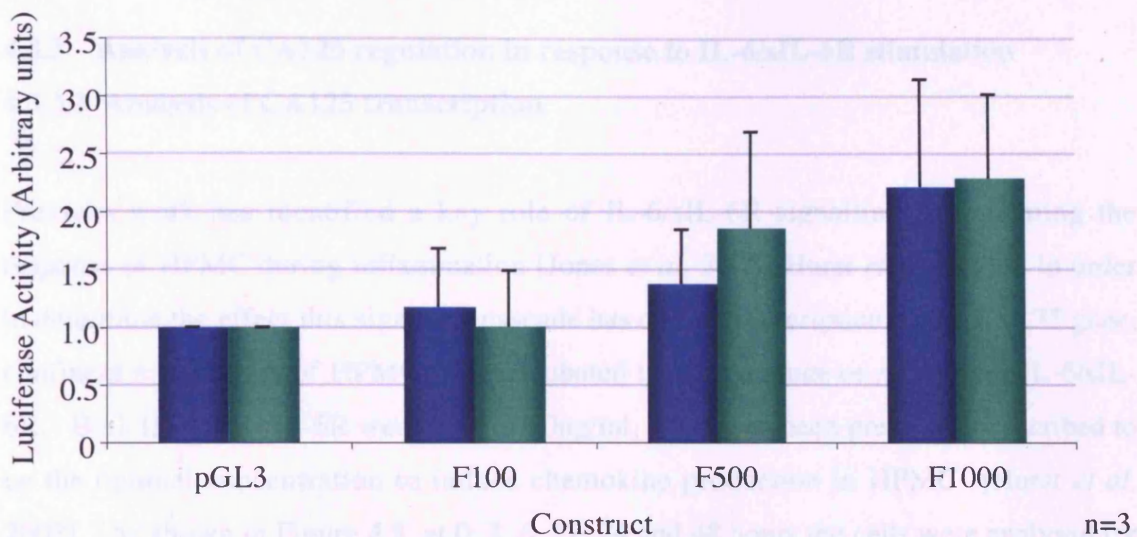


Figure 4.7 Luciferase activity of the CA125 proximal promoter constructs and pGL-3 control construct in response to IL-1 β (100pg/ml) stimulation. Luciferase activity is expressed as the magnitude of normalized luciferase activity relative to the promoterless negative control (pGL-3). Blue bars = Control, Green bars = IL-1 β (100pg/ml) stimulated. 'n' refers to the number of independent experiments.

No significant change was seen in any of the promoter constructs in response to IL-1 β when compared to the pGL-3 control. There was also no significant change in luciferase activity between stimulated F100, F500 and F1000 constructs and the control constructs, although an upward trend was observed for the larger promoter fragments, as seen in our previous promoter experiments in chapter 3. The high variances seen in these experiments may be attributed to tissue specific variability as seen in primary mesothelial cells cultures.

4.3.3 Analysis of CA125 regulation in response to IL-6/sIL-6R stimulation

4.3.3.1 Analysis of CA125 transcription

Previous work has identified a key role of IL-6/sIL-6R signalling in regulating the response of HPMC during inflammation [Jones *et al*, 2005][Hurst *et al*, 2001]. In order to determine the effect this signaling cascade has on the transcription of the CA125 gene, confluent monolayers of HPMC were incubated in the presence or absence of IL-6/sIL-6R. Both IL-6 and sIL-6R were used at 10ng/ml, which has been previously described to be the optimal concentration to induce chemokine production in HPMC [Hurst *et al*, 2002]. As shown in Figure 4.8, at 0, 3, 6, 12, 24 and 48 hours the cells were analysed for gene expression using HLGP primers (specific for the 5' terminus of the CA125 coding region), CA125 R primers (specific for the repeat region of the CA125 coding region) and β -actin primers (specific for the β -actin housekeeping gene).

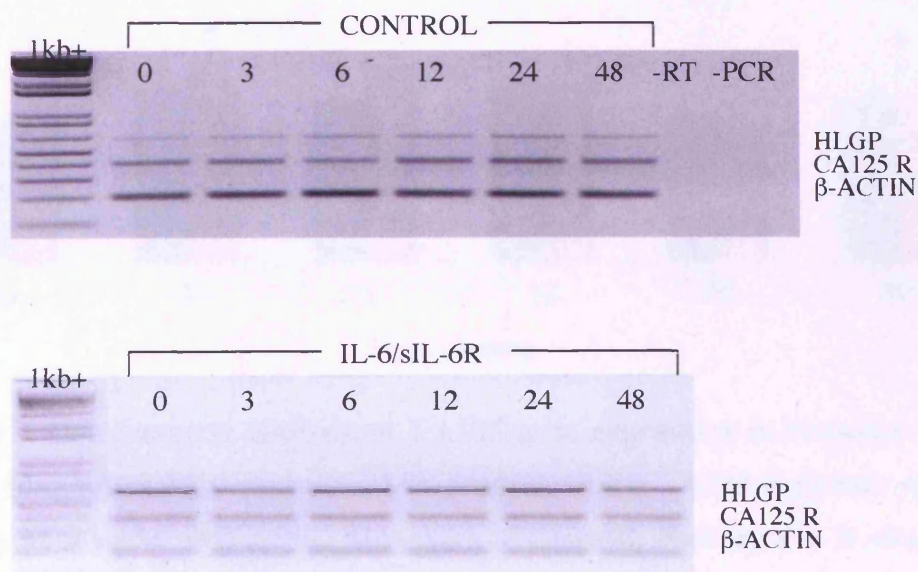


Figure 4.8 HPMC expression of CA125 in response to IL-6/sIL-6R stimulation. Representative agarose gel showing expression levels of the CA125 gene (CA125 R and HLGP) and β -actin in control (un-stimulated) and stimulated IL-6/sIL-6R (10ng/ml each) at defined time points. -RT=Negative control for reverse transcription, -PCR=Negative control for PCR.

Semi-quantitative analysis of CA125 transcription was carried out by determining the ratio of each product compared to the β -actin housekeeping gene via densitometric analysis (Figure 4.9).

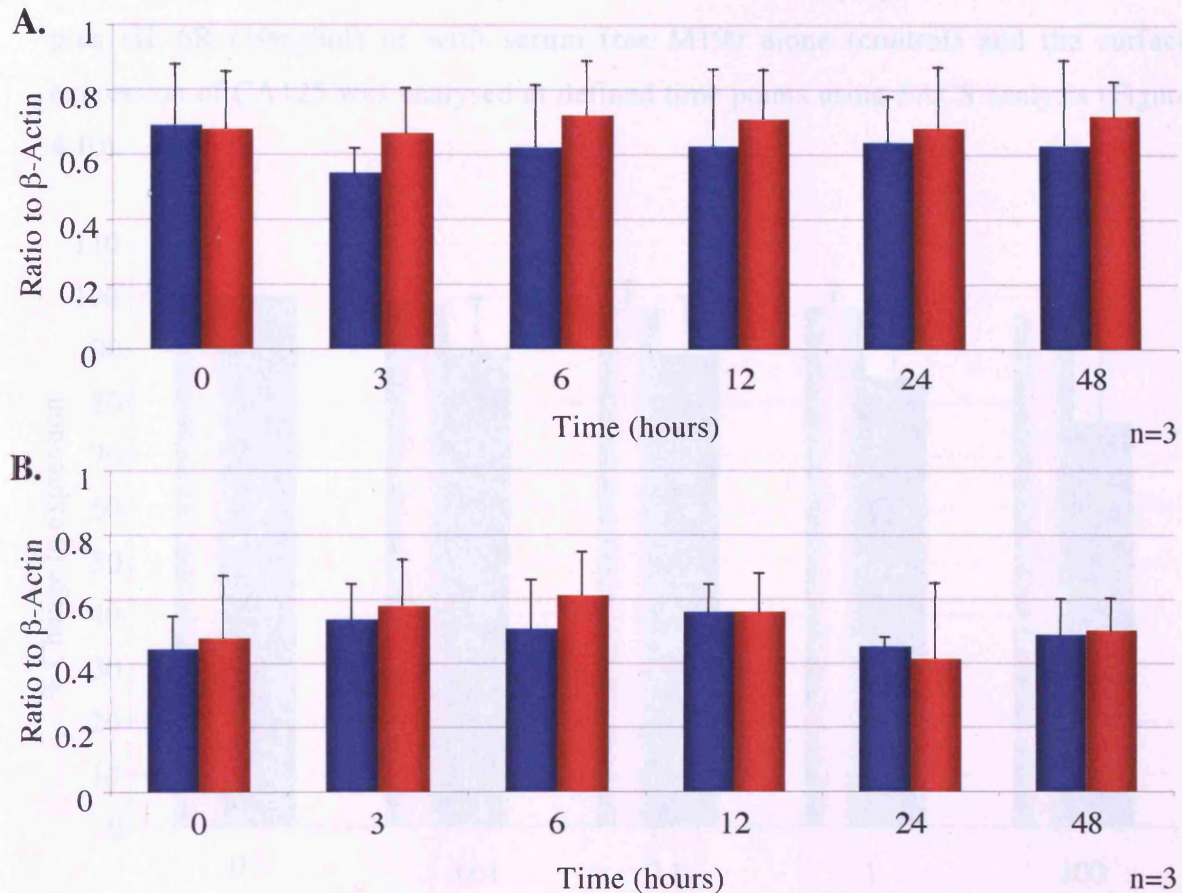


Figure 4.9 Densitometric analysis of CA125 gene expression in response to IL-6/sIL-6R (10ng/ml each) stimulation. (A) Analysis of the CA125 R primer specific expression as a ratio of β -actin. Blue bars = Control, Red bars = IL-6/sIL-6R stimulation. (B) Analysis of the HLGP primer specific expression as a ratio of β -actin. Blue bars = Control, Red bars = IL-6/sIL-6R (10ng/ml) each stimulation. 'n' refers to the number of independent experiments.

As can be seen in Figure 4.9, analysis of CA125 gene expression using the CA125 repeat primers and HGLP primers shows no significant change in CA125 expression over the 48 hour period in response to IL-6/sIL-6R stimulation.

4.3.3.2 Analysis of CA125 cell surface expression

To determine the effect of IL-6/sIL-6R signalling on cell surface expression of CA125 confluent mesothelial cell monolayers were treated with varying concentrations of IL-6 plus sIL-6R (10ng/ml) or with serum free M199 alone (control) and the surface expression of CA125 was analysed at defined time points using FACS analysis (Figure 4.10).

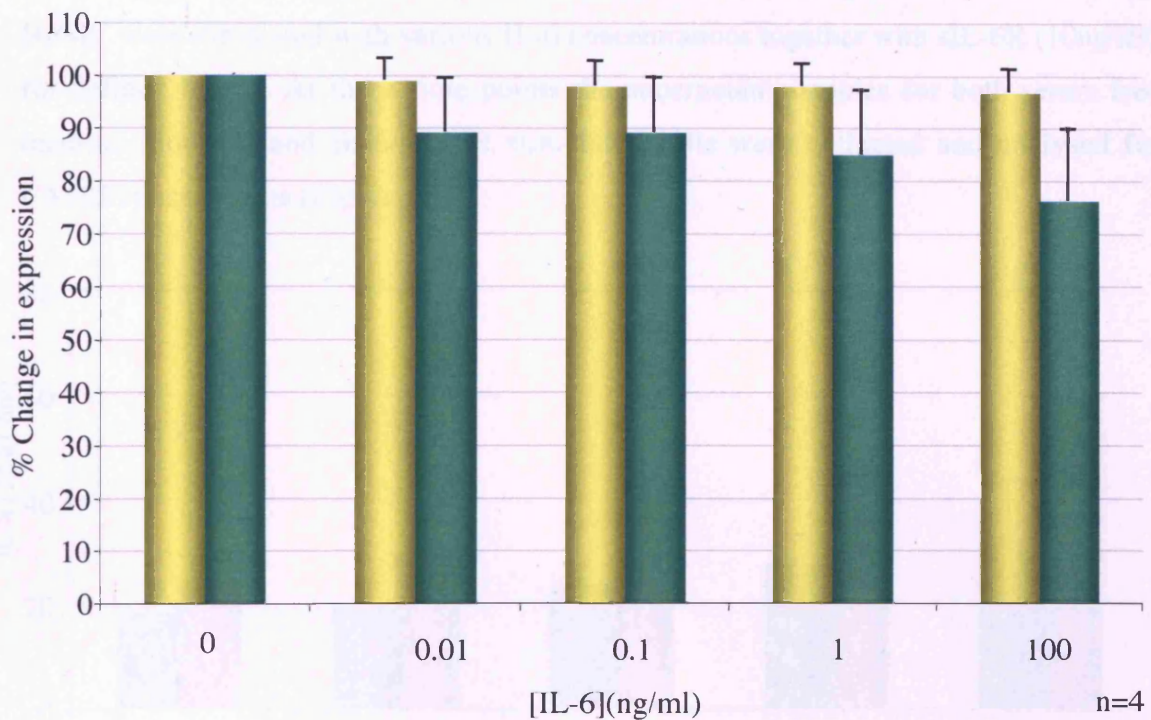


Figure 4.10 Control of mesothelial cell CA125 cell surface expression in response to IL-6 and sIL-6R (10ng/ml) stimulation. Each bar represents the CA125 surface expression of IL-6/sIL-6R stimulated HPMC as normalized to its un-stimulated (0ng/ml) control. Yellow bars = 24 hours stimulation. Green bars = 48 hour stimulation. Changes in CA125 cell surface expression is shown as changes in % expression. 'n' refers to the number of independent experiments.

As seen in the Figure 4.10 after 48 hours stimulation with IL-6 (100ng/ml) and sIL-6R (10ng/ml) there is a trend towards a decrease in expression ($p=0.073$) compared to the

control cells as well as a trend towards a decrease in expression compared to the 24 hour stimulation. This is indicative of a reduction of CA125 expression at the cell surface in response to IL-6/sIL-6R stimulation.

4.3.3.3 Analysis of CA125 cell surface secretion

In order to determine if this IL-6 trans-signalling mediated reduction in surface expression of CA125 was associated with increased shedding from the cell surface, HPMC were stimulated with various IL-6 concentrations together with sIL-6R (10ng/ml) for defined times. At these time points the supernatant samples for both serum free medium (control) and IL-6/sIL-6R stimulated cells were collected and analysed for CA125 concentration (Figure 4.11).

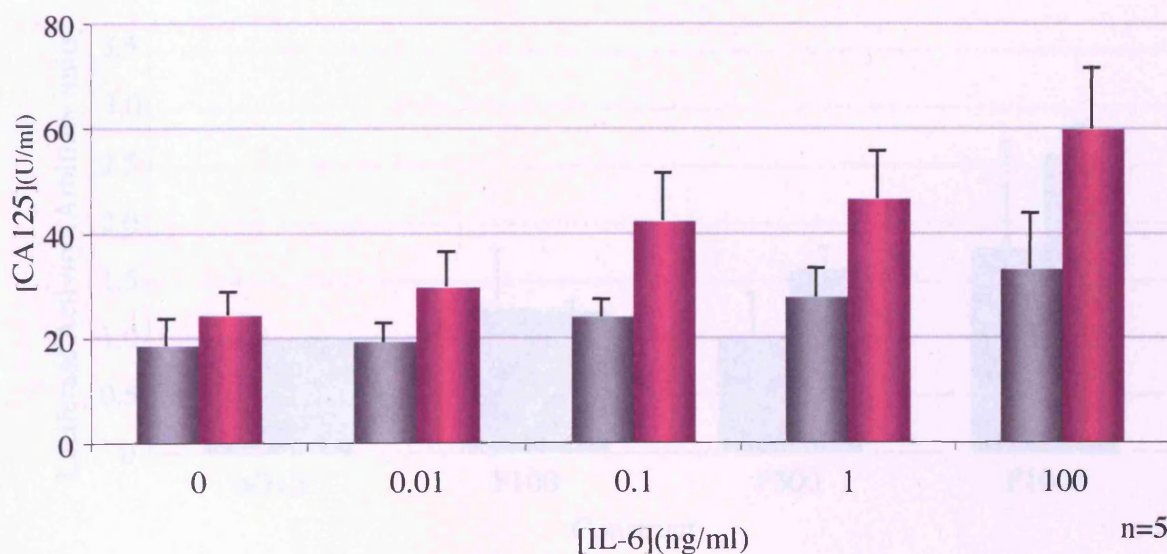


Figure 4.11 Change in HPMC CA125 cell surface secretion in response to IL-6 and sIL-6R [10ng/ml] stimulation. Grey bars = 24 hours, Pink bars = 48 hours. 'n' refers to the number of independent experiments.

Stimulation with IL-6/sIL-6R can be seen to induce a trend towards a dose dependant increase (at 48 hours, 100 ng/ml IL-6, p=0.073) in CA125 released from the cell surface when compared to the un-stimulated controls. IL-6/sIL-6R can also be seen to induce a

trend towards a time dependant increase (100ng IL-6, 24 hour vs 48 hour, $p=0.164$) in CA125 cleavage from the cell surface as shown by the change in the amount of CA125 released from cells stimulated for 24 hours (\approx maximal 1.5-fold increase) and cells stimulated for 48 hours (\approx maximal 3-fold increase).

4.3.3.4 Analysis of CA125 promoter activity

HPMC were transfected with the putative promoter constructs (chapter 3) as described in section 2.6.2. Each construct was then assayed for transcriptional activity in HPMC stimulated for 24 hours with IL-6 (10ng/ml) and sIL-6R (10ng/ml), using the luciferase assay described in section 2.6. For each promoter construct the luciferase activity was normalised to the negative control promoter less pGL-3.

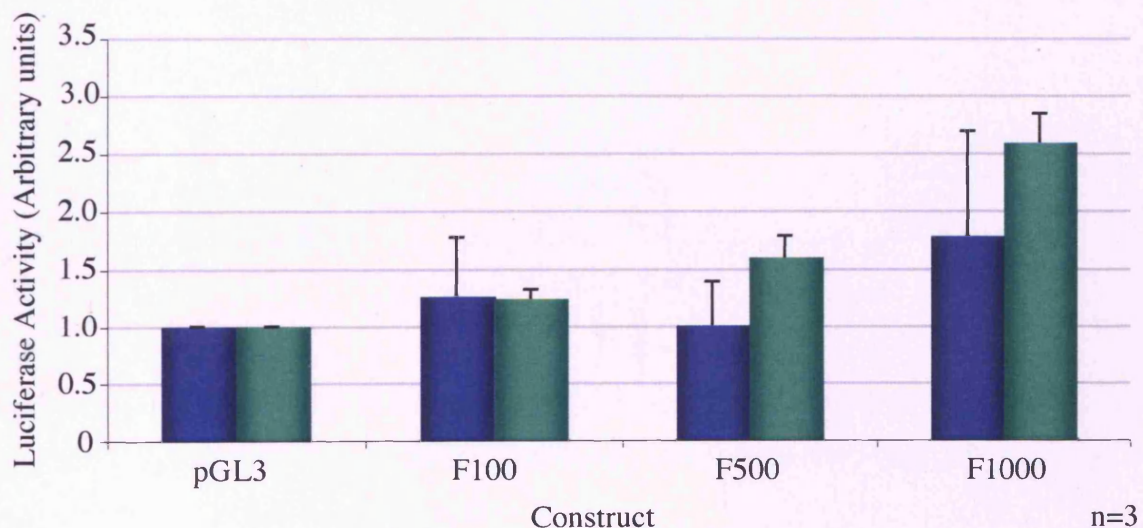


Figure 4.12 Luciferase activity of the CA125 proximal promoter constructs and PGL-3 control construct in response to IL-6 (10ng/ml)/sIL-6R (10ng/ml) stimulation. Luciferase activity is expressed as the magnitude of normalized luciferase activity relative to the promoterless negative control (pGL-3). Blue bars = Control, Green bars = IL-6 (10ng/ml)/sIL-6R (10ng/ml) stimulated. 'n' refers to the number of independent experiments.

No significant change was seen in any of the promoter constructs in response to IL-6/sIL-6R when compared to the pGL-3 control. There was also no significant change in luciferase activity between stimulated F100, F500 and F1000 constructs and the control constructs though the observed trend (i.e. increased activity of larger constructs) remains consistent with our previous luciferase data from chapter 3. The high variances seen in these experiments may be attributed to tissue specific variability as seen in primary mesothelial cells cultures.

4.3.4 Analysis of MCP-1 concentration in response to IL-1 β and IL-6/sIL-6R stimulation

To ensure that the HPMC model, examined in this chapter, was activated under the defined conditions used, MCP-1 assays were performed on supernatants gathered from the experiments. Previous to this work, other studies indicate that MCP-1 production by HPMC *in vitro* is increased in response to IL-1 β and IL-6/sIL-6R stimulation [Li *et al*, 1998].

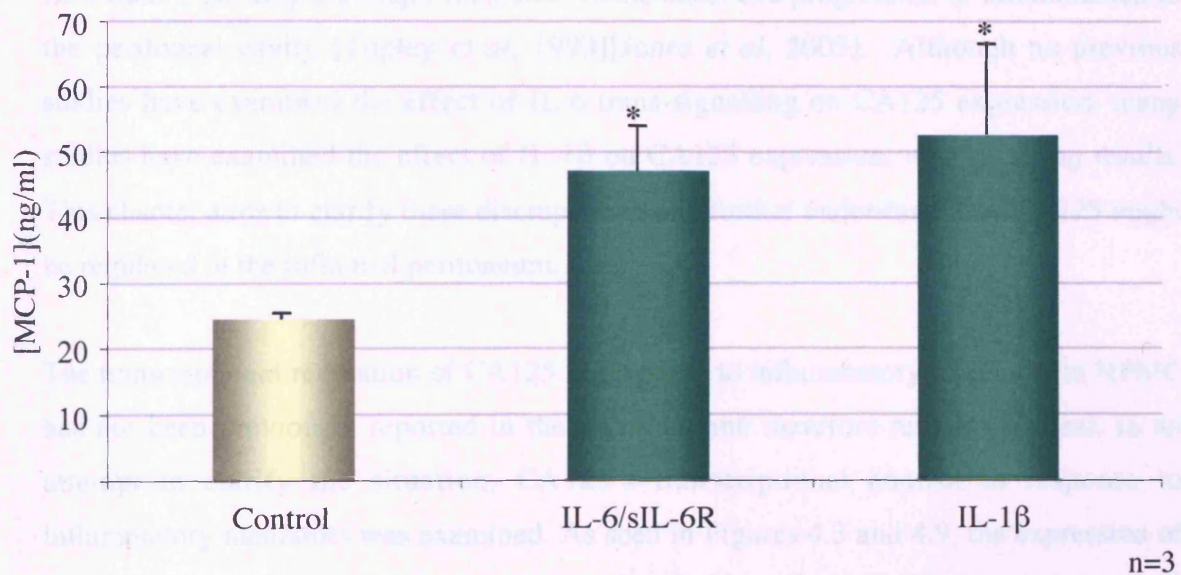


Figure 4.13 MCP-1 production by HPMC in response to IL-1 β (100pg/ml) and IL-6/sIL-6R (10ng/ml each) stimulation after 24 hours incubation. * $p < 0.05$. 'n' refers to the number of independent experiments.

As seen in Figure 4.13 both IL-1 β and IL-6/sIL-6R induced a significant increase in mesothelial cell MCP-1 production after 24 hours, consistent with other studies examining the effect of these inflammatory mediators on MCP-1 production [Li *et al*, 1998][Hurst *et al*, 2002]. This ensured the fidelity of the stimulatory conditions used and illustrates the activation and response of HPMC to the specific stimulations used in the experiments within this chapter.

4.4 DISCUSSION

As documented in many previous studies, CA125 is predominantly a surface expressed antigen that is shed from the surface of the cell by an unknown mechanism [Fendrick *et al*, 1997][O'Brien *et al*, 1998][O'Brien *et al*, 2002]. The current debate regarding CA125 regulation stems from differing opinions as to whether the antigen is constitutively expressed or whether it is specifically secreted and regulated in response to inflammatory mediators and cytokines. As discussed in the introduction to this thesis, both IL-1 β and IL-6 trans-signalling are major mediators in the onset and progression of inflammation in the peritoneal cavity [Topley *et al*, 1993][Jones *et al*, 2005]. Although no previous studies have examined the effect of IL-6 trans-signalling on CA125 expression, many studies have examined the effect of IL-1 β on CA125 expression, with differing results. This chapter aims to clarify these discrepancies and further understand how CA125 might be regulated in the inflamed peritoneum.

The transcriptional regulation of CA125 in response to inflammatory mediators in HPMC has not been previously reported in the literature and therefore remains unclear. In an attempt to clarify the situation, CA125's transcriptional control in response to inflammatory mediators was examined. As seen in Figures 4.3 and 4.9, the expression of the CA125 gene is not significantly altered by IL-1 β or IL-6/sIL-6R stimulation over a period of 48 hours suggesting that CA125 gene is not regulated at the level of transcription in response to these stimuli. The luciferase reporter gene assay developed in chapter 3 allowed further investigation of CA125's transcriptional regulation by IL-1 β and IL-6/sIL-6R. Using this system, CA125 putative promoter luciferase constructs were transfected into primary HPMC and tested for their transcriptional activity in the presence or absence of IL-1 β and IL-6/sIL-6R. Consistent with our previously described data, under control conditions the CA125 promoter showed low level expression (see chapter 3 discussion). As seen in Figure 4.7 and Figure 4.12, the promoter constructs displayed no significant change in transcriptional activity when stimulated with IL-1 β and a small but not significant increase in response to IL-6/sIL-6R stimulation. Nevertheless, these data, in conjunction with our RT-PCR findings, suggest that CA125 expression is probably not

regulated at the level of transcription. Therefore, the changes seen in CA125 production, by inflammatory cytokines, described in the literature [Zeillemarker *et al*, 1994][Ziemet *et al*, 1996] and this chapter, suggest that changes in CA125 expression may result from an alternative level of regulation, i.e. regulation of its surface expression and cleavage from the cell surface potentially by an as yet unknown cleavage enzyme. Such control has previously been observed in the regulation of *MUC1* that is potentially regulated by the ADAM family of proteases [Brayman *et al*, 2004]. Additionally, regulation by mRNA stabilization, as seen in the control of MUC5AC expression [Fischer *et al*, 2002], cannot be excluded as a mode of CA125 regulation although the low rate of turnover demonstrated for CA125 (Chapter 3-Figure 3.18A), the variation in molecular weight and the negligible amount of CA125 released from the cell (compared with the amount sequestered in and on the cell surface), observed from Western blot analysis (Figure 4.1), suggest that CA125 is probably regulated by post transcriptional mechanisms, possibly activated on the surface of HPMC.

Due to the apparent lack of transcriptional regulation of CA125 in response to inflammatory mediators and the suggestion that CA125 expression may be controlled on the cell surface, FACS analysis was utilized as this allowed the examination of the effect IL-1 β and IL-6 signalling on the surface expression of CA125. As seen in Figure 4.5, IL-1 β significantly increased the surface expression of CA125 after 24 and 48 hour (40-50% increase) when compared to the control levels. In contrast to the effect IL-1 β has on CA125 surface expression, IL-6/sIL-6R (Figure 4.10) was observed to cause a reduction in the amount of CA125 expressed on the cell surface after 48 hours (24% decrease). These data suggest that CA125 surface expression can be regulated at both the level of surface expression and a subsequent coordinated increase or decrease in cell surface shedding in response to inflammation. These data further corroborate the theory that CA125 expression can be regulated in response to inflammatory mediators and that this control occurs post-transcriptionally, by a mechanism controlling changes in surface expression.

To further investigate the effect of inflammatory mediators on CA125 regulation, their effect on the amount of antigen released/shed from the cell surface was examined by measuring the CA125 supernatant levels of IL-1 β and IL-6/sIL-6R stimulated growth arrested HPMC monolayers. As seen in Figure 4.6, IL-1 β induced only a small increase in the amount of CA125 shed from the cell surface after 48 hours. Together with the increased expression of CA125 at the cell surface (Figure 4.5), these data suggest that IL-1 β might increase the turnover of CA125 at the cell surface by increasing CA125 expression on the cell surface and subsequently increasing the amount of CA125 that is released by the cell. Furthermore, the secretion of other members of the mucin gene family, such as MUC5AC [Gray *et al*, 2004] and MUC2 [Kim *et al*, 2002] have also been shown to be regulated by this pro-inflammatory cytokine thus suggesting a common control mechanism of mucin expression.

Similar to the effect of IL-1 β , combined stimulation with IL-6 and sIL-6R resulted in a trend towards an increase in the amount of CA125 released from the surface of HPMC (approximate 2 fold increase after 48 hours (Figure 4.11)). Additionally, Figure 4.10 is suggestive of a trend towards a IL-6/sIL-6R induced decrease in CA125 surface expression under identical conditions thus suggesting a possible coordinated reduction in cell surface CA125 levels via increased cell surface shedding. These are the first studies to have examined the effect of IL-6 trans-signalling on CA125 expression and highlight the dependency for further analysis into the mechanisms by which IL-6/sIL-6R may possibly regulate CA125 expression. Interestingly, despite the lack of statistical significance in these data, the observed trends seen in our system are consistent with the ability of IL-6 to induce the expression of other mucins, such as *MUC5B* and *MUC5AC*, in the inflamed trachea [Chen *et al*, 2003]. The induction of these mucins is mediated by similar cellular signalling pathways as seen in the inflamed peritoneum such as the JAK and ERK pathways [Jones *et al*, 2005]. Together, these data suggest that the co-ordinated increase in CA125 cell surface expression in response to IL-1 β and an increased CA125 shedding from the cell surface in response to IL-6 signalling may be a primary mechanism in the regulation of CA125 release. It should be noted that due to the high variability in the observed levels of CA125 measured within this chapter statistical

significance was not achieved. Further definition of the observed effects may be achieved through the repeated analysis of IL-1 β and IL-6 stimulated CA125 expression in additional donor samples.

Although the mechanism by which CA125 is shed from the cell surface is far from understood, it has been suggested that proteolytic cleavage sites present on the CA125 molecule may facilitate its release by cleavage enzymes [Fendrick *et al*, 1997][O'Brien *et al*, 2001]. It therefore seems plausible that the regulation of "enzyme" activity may be responsible for the regulation of CA125 cell surface biology. Mesothelial cells produce a vast number of proteases including metalloproteinase enzymes (MMPs), such as stromelysin [Marshall *et al*, 1993], that may potentially be responsible for the processing of CA125 at the cell surface. MMPs have previously been shown to be active during peritoneal inflammation [Martin *et al*, 2000] and in other organs such as the bowel [Naito *et al*, 2005]. More specifically, expression of many members of the MMP family have been shown to be regulated by IL-1 β and IL-6 during inflammation of the skin [Dasu *et al*, 2003], joints [Fuchs *et al*, 2004] and the peritoneum [Martin *et al*, 2000]. The production and activation of proteolytic enzymes therefore presents a possible mechanism by which CA125 cell surface release may be regulated during inflammation.

No previous studies have examined transcription, cell surface expression or the effect of IL-6 trans-signalling on the regulation of CA125 in a similar manner to this study. The regulation of CA125 production by inflammatory cytokines demonstrated here both corroborates [Zeillemarker *et al*, 1994] and disagrees with other studies [Visser *et al*, 1995][Ziomet *et al*, 1996] regarding the cell surface release of CA125 *in vitro* and may therefore be seen to add further confusion to an already unclear situation. One major issue that differentiates this study from previously published work is the use of an HPMC *in vitro* model that employs a growth arrest period (incubation in FCS free culture medium) in order to not only synchronize the growth phase of the cells prior to stimulation [Floege *et al*, 1990] but to exclude any exogenous stimulatory agents present in FCS, such as cytokines [Parkash, 2001] and growth factors [Nitz *et al*, 2003] that may modulate cell function. Evidence of the importance of the growth arrest period has been

demonstrated in Chapter 3 where both oestrogen and retinoic acid both induce small changes in luciferase activity of our CA125 promoter constructs (Chapter 3, Figure 3.20) in a growth arrested system void of these stimuli [Garmy-Susini *et al*, 2004]. Since both oestrogen and retinoic acid are present in FCS, and considering CA125's apparent modulation by them, it would seem that the use of a non-growth arrested model to examine the inflammatory control of CA125 may be less reliable due to the variable influence of potentially stimulatory agents (of unknown concentration) in the system. This may partly explain the contrasting results observed in the literature regarding CA125 regulation by inflammatory stimuli.

In conclusion, this study clearly indicates the regulation of CA125 by inflammation. More specifically we have demonstrated that IL-1 β increases the expression/turnover of CA125 at the cell surface while IL-6/sIL-6R induces CA125 release from the cell surface. The ability of IL-1 β to increase CA125 surface expression and subsequent temporal increase in the amount of CA125 secreted from the cell surface by IL-6/sIL-6R poses an important question with regard to future work in this area as well as highlighting potential areas of future analysis regarding CA125's regulation by other cytokines known to be involved in the inflammatory response, such as IL-8, TNF- α [Topley *et al*, 1993] and IFN- γ [Robson *et al*, 2001]. Furthermore, we have also gained valuable insight into the possible mechanisms responsible for CA125's regulation by inflammatory cytokines. The lack of inducible transcriptional activity and the subsequent changes in expression and secretion observed at the cell surface suggest that CA125 expression and production is primarily regulated at a level other than transcription. Although we can only speculate at the role of CA125 during inflammation, its apparent regulation at the cell surface, its size, location and the negligible amount of CA125 released from the cell suggest that CA125's normal function resides predominantly on the mesothelial cell surface. Considering this, the function of CA125 is further investigated in chapter 5 where the role of CA125 in HPMC migration and wound healing is examined using our HPMC *in vitro* model.

Chapter 5

The potential role of CA125 in regulating mesothelial cell repair

5.1 INTRODUCTION

Denudation and injury of the peritoneal mesothelium is a frequent finding in biopsies obtained from the peritoneal cavity of PD patients [Williams *et al*, 2002]. Comparison of the mesothelium in peritoneal biopsy samples taken from normal patients and those receiving PD (Figure 5.1) show the separation of the mesothelial cell layer from the underlying stroma, as a result of PD, as well as the loss of mesothelial cell interactions and alterations in morphology [Williams *et al*, 2003]. In addition to exposure to unphysiological dialysis solutions, episodes of peritonitis are also thought to be a major cause of damage and injury to the mesothelium during peritoneal dialysis [Davies *et al*, 1996]. Such injury to the peritoneal mesothelium is thought to disrupt its protective and homeostatic properties and thereby predispose the membrane to fibrotic alterations and its subsequent loss of function as a dialysing organ. The repair or preservation of the mesothelium therefore represents a critical process in the restoration of the integrity of the peritoneal membrane [Yung and Davies, 1998][Yung *et al*, 2000].

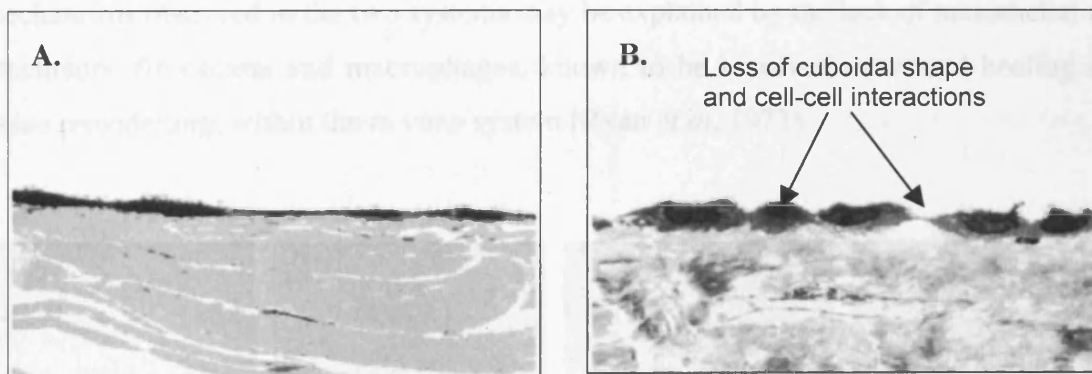


Figure 5.1 The effect of PD on the peritoneal mesothelium. (A) Parietal peritoneum from a normal patient. (B) Parietal peritoneum from a patient treated with peritoneal dialysis (Taken from [Williams *et al*, 2003]).

Prior to the present study the understanding of the wound healing process had been significantly aided by the development of *in vitro* wound healing models that allow the “real time” analysis of the healing process in many cell types, such as epithelial cells of

the nasal passage [Zahm *et al*, 1997] and the small intestine [McCormack *et al*, 1992]. In order to specifically study the process of re-mesothelialization an *in vitro* wounding model was established [Yung and Davies, 1998] in which mechanical (scratch) wounding of HPMC monolayers was performed, allowing the temporal analysis of the progression of the wound closure by time-lapse photography [Yung and Davies, 1998][Yung *et al*, 2000][Morgan *et al*, 2003]. Using this model it was established that HPMC migration was the key process in promoting re-mesothelialization, with cells moving centripetally from the leading edge of the wound to re-cover the denuded area (Figure 5.2). This process was accompanied by an overall increase in HPMC proliferation shown by the evenly distributed proliferating cells throughout the wounded monolayer [Yung and Davies, 1998][Yung *et al*, 2000]. Despite this evidence, the mechanisms involved in healing of the mesothelium following injury remain controversial. Other studies examining mesothelial wound healing *in vivo* have shown that wound healing may occur through different mechanisms involving the detachment, re-attachment and proliferation of mesothelial cells within the wounded surface as opposed to subserosal cell differentiation [Mutsaers *et al*, 2000][Foley-Comer *et al*, 2002]. The different mechanisms observed in the two systems may be explained by the lack of mesothelial cell precursors, fibroblasts and macrophages, known to be involved in wound healing and tissue remodelling, within the *in vitro* system [Ryan *et al*, 1973].

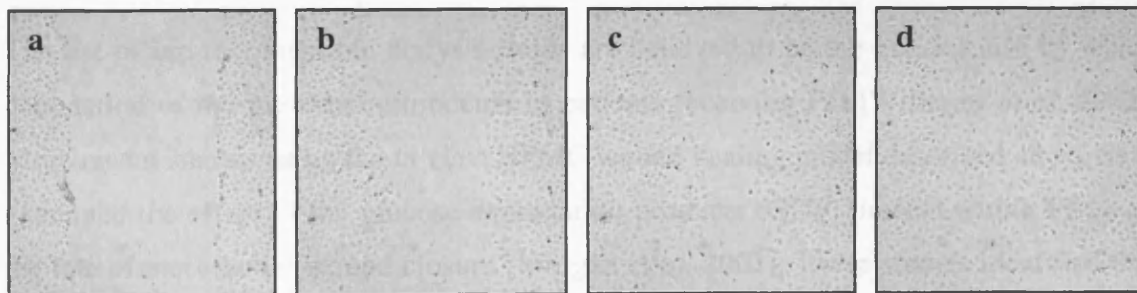


Figure 5.2 Time dependant closure of an *in vitro* wounded human peritoneal mesothelial cell monolayer after a) 0 hours b) 8 hours c) 16 hours and d) 24 hours.

Further analysis of HPMC migration in the *in vitro* model has shown that wounded HPMC monolayers have the ability to repair themselves in the absence of exogenous growth factors suggesting the repair process is a direct response of HPMC to injury. The absence of other cell types, such as macrophages and fibroblasts, within the system also indicates that the wound healing process observed in this system is a direct result of the HPMC response to injury. During this response HPMC have been shown to carry out a number of events such as deposition of their own extracellular matrix components (including laminin and fibronectin) in the wounded area, re-organization of their stress fibres and focal contacts [Yung and Davies, 1998], and the release of signalling molecules such as prostaglandin E₂, PDGF, FGF, EFG and HGF/SF that play important roles in re-mesothelialization [Leavesley *et al*, 1999][Faull *et al*, 2001][Warn *et al*, 2001]. HPMC production of hyaluronan (HA) was also found to be important to this process (especially at the leading edge of the wound) as it is believed to increase cell mobility although its precise function in the wound healing process is not known [Yung *et al*, 2001][Horiuchi *et al*, 2003]. The release of growth factors from disrupted cells or the loss of inhibitory signals through mechanical wounding is thought to be responsible for these cellular responses seen during the repair process. The addition of serum (FCS) to the system induces a significant increase in the rate of wound closure probably due to the action of stimulatory agents, such as EGF and PDGF for example, known to increase the HPMC migration [Yung and Davies, 1998].

The use of bio-incompatible dialysis fluids are believed to be the major cause by which denudation of the mesothelium occurs in patients receiving PD [Williams *et al*, 2002]. More recent studies using the *in vitro* HPMC wound healing model described above have examined the effect of the glucose degradation products (GDP) present within PDFs on the rate of mesothelial wound closure [Morgan *et al*, 2003]. These studies identified that GDPs retard re-mesothelialization of the wounded monolayer suggesting that peritoneal dialysis fluids with improved biocompatibility (i.e. reduced GDPs) may be important in the protection of the mesothelium during PD. As discussed in section 1.7.3, use of these improved PDFs also coincides with an increase in CA125 effluent levels [Rippe *et al*, 2001][Jones *et al*, 2001][Williams *et al*, 2004] thus highlighting a potential association

between CA125 and the process of re-mesothelialization. In this chapter we attempt to analyse CA125's role in this process by examining the effect of exogenous CA125 on our wound healing system. We will also attempt to link our findings to the clinical situation as we further investigate the apparent relationship between the rate of wound healing, CA125 concentration and GDP levels.

5.2 METHODS

5.2.1 The effect of exogenous CA125 on mesothelial wound healing

The effect of adding exogenous CA125 on the rate of mesothelial wound healing was determined by adding M199 containing physiologically relevant concentrations of CA125 antigen (Fuji-Rebio Diagnostic Inc) to the HPMC wound healing model as described in section 2.11.1. All HPMC were growth arrested for 48 hours (section 2.2.8) prior to scratching. Monolayers were incubated and monitored until wound closure. Rate of wound closure (pixels/hour) was determined as shown in Figure 5.3 and discussed in section 2.11.2.

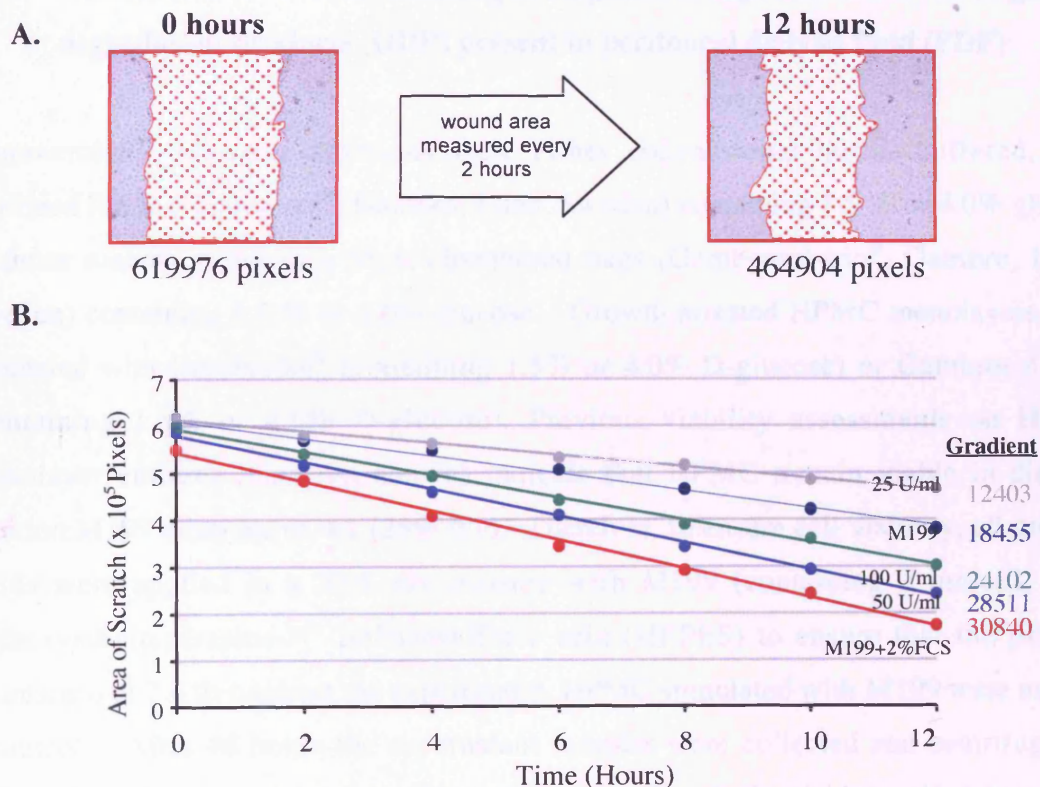


Figure 5.3 Analysis of HPMC rate of wound closure. (A) Image analysis of scratch size in wounded HPMC monolayers, (B) Determination of the rate of wound closure for the first 12 hours of HPMC wound closure. The rate of wound closure is represented by the gradient of the linear portion of the graph. The gradient is shown in pixels/hour.

5.2.2 The effect of CA125 blocking on mesothelial wound healing

The effect that blocking endogenous CA125 activity produced by resident HPMC has on the rate of mesothelial wound healing was determined by the addition of M199 containing defined concentrations (0.04, 0.4 and 4 μ g/ml) of OC125 antibody to the HPMC wound healing model as described in 2.11.1. All HPMC were growth arrested for 48 hours (section 2.2.8) prior to scratching. Monolayers were incubated and monitored until wound closure. Rate of wound closure (pixels/hour) was determined as shown in Figure 5.3 and discussed in section 2.11.2.

5.2.3 Examination of CA125 shedding in response to high and low levels of glucose degradation products (GDP) present in peritoneal dialysis fluid (PDF)

Commercially available solutions were either conventional lactate-buffered, heat sterilized fluids (Gambrosol[®], Gambro, Lund, Sweden) containing 1.5 % or 4.0% glucose or those manufactured in a triple-chambered bags (Gambrosol-trio[®], Gambro, Lund, Sweden) containing 1.5 % or 4.0% glucose. Growth arrested HPMC monolayers were incubated with Gambrosol[®] (containing 1.5% or 4.0% D-glucose) or Gambrosol-trio[®] (containing 1.5% or 4.0% D-glucose). Previous viability assessments on HPMC monolayer cultures (data not shown) indicate that HPMC remain viable in dialysis solution:M199 dilutions of 4:1 (25% v/v). Therefore, to ensure cell viability, all dialysis fluids were applied in a 25% v/v mixture with M199 (containing 2 mmol/L N-2-hydroxyethylpiperazine-N'-2ethanesulfonic acid (HEPES) to ensure that the pH was maintained at 7.4 throughout the experiment). HPMC stimulated with M199 were used as a control. After 48 hours the supernatant samples were collected and centrifuged at 5000g for 3.5 minutes in order to remove any detached cells or cell debris. The supernatants were then assayed for CA125 concentration as described in section 2.9.

5.2.4 Statistical analysis

All wounding experiments were performed in a 24 well plate with random assignment of wells to different treatments. All CA125 supernatant assays were performed in 6 well plates. All data are present as mean [\pm standard error of the mean (SEM)] from the stated number of independent experiments (n) performed on averaged quadruplicate (wounding) or duplicate (CA125 assay) samples with HPMC isolated from different omental donors. All data were analysed using Student's t-test in Excel for Windows. Differences were considered significant when $p < 0.05$.

5.3 RESULTS

5.3.1 The effect of exogenous CA125 on mesothelial wound healing

The observed CA125 concentrations, seen in patient samples, can vary considerably; dependant on factors such as age [Breborowicz *et al*, 2005] and disease phenotypes such as ovarian cancer [Bast *et al*, 1983]. Additionally, as illustrated in Appendix I, peritoneal dialysis has been shown to alter the levels of CA125 seen in the peritoneal cavity dependant on the type of the PD solution used [Rippe *et al*, 2001][Jones *et al*, 2001][Williams *et al*, 2004]. The effect of the CA125 during HPMC wound healing under the observed physiologically relevant CA125 concentrations (i.e. those measured during peritoneal dialysis (12 U/ml to 180 U/ml) based on published data) was examined by the addition of exogenous CA125 antigen to the previously described *in vitro* wound healing model as seen in Figure 5.4. Serum free conditions were used to represent the endogenous rate of HPMC wound closure. Incubation with M199 containing 2% FCS was used as a positive control to ensure the responsiveness of the system to potential rate enhancing stimulations.

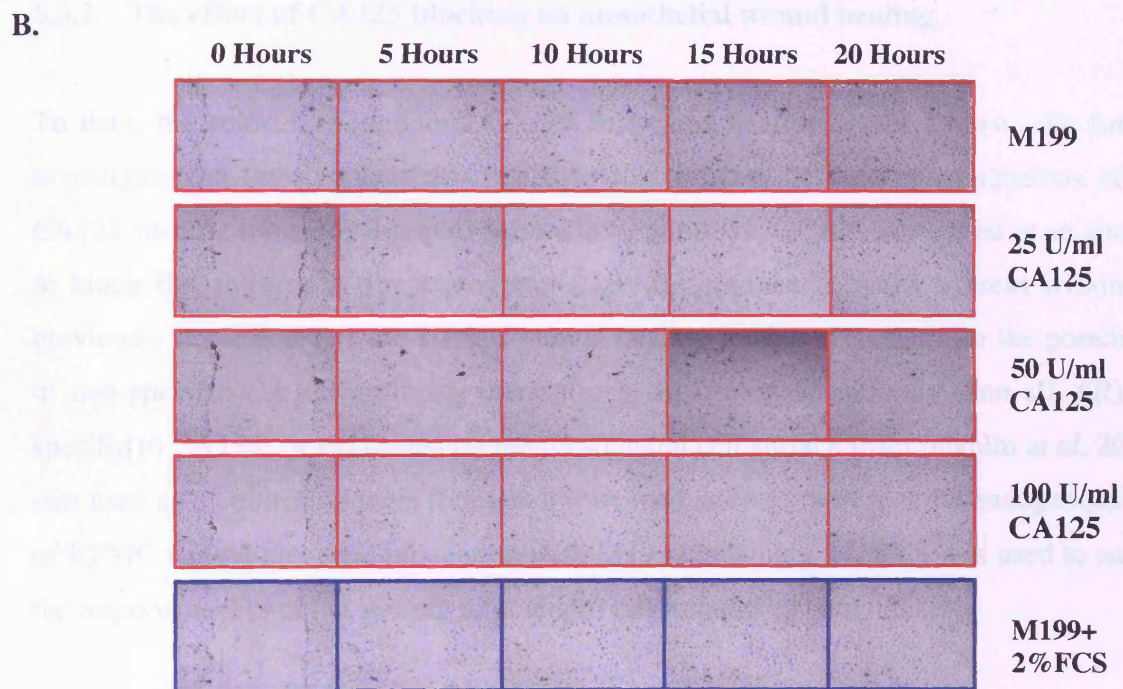
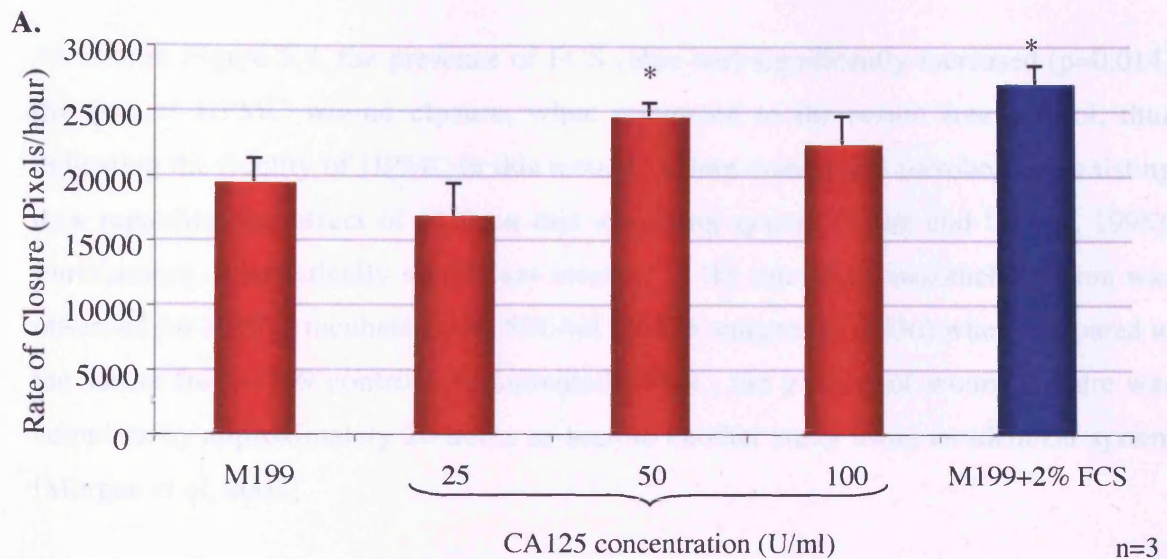


Figure 5.4 The effect of exogenous CA125 on the rate of HPMC re-
mesothelialization. (A) Confluent monolayers of HPMC were mechanically
scratched and incubated with either serum free M199 (negative control), M199
containing CA125 antigen (25, 50 or 100U/ml) or M199 containing 2% FCS (positive
control (blue)). * $p < 0.05$ compared to un-stimulated control, 'n' refers to the
number of independent experiments. (B) Representative images of re-
mesothelialization following scratch wounding in HPMC from above experiment.

As seen in Figure 5.4, the presence of FCS (blue bar) significantly increased ($p=0.014$) the rate of HPMC wound closure, when compared to the serum free control, thus indicating the fidelity of HPMC in this wound healing system and corroborating existing data regarding the effect of FCS on this wounding system [Yung and Davies, 1998]. Furthermore, a statistically significant increase in the rate of re-mesothelialization was observed for HPMC incubated with 50U/ml CA125 antigen ($p=0.036$) when compared to the serum free M199 control. In untreated HPMC, the process of wound closure was complete by approximately 20 hours as seen in another study using an identical system [Morgan *et al*, 2003]

5.3.2 The effect of CA125 blocking on mesothelial wound healing

To date, the role of endogenous CA125 in wound healing is not known. To further investigate the involvement of CA125 in this process defined concentrations of the CA125 specific mouse anti-human monoclonal antibody, OC125, were used in an attempt to block the activity of the endogenous HPMC produced CA125 present within the previously described *in vitro* HPMC wound healing model. To eliminate the possibility of non-specific CA125-antibody interactions, an irrelevant antibody (anti-sIL-6R) not specific to CA125, or expressed on the mesothelial cell surface [McLoughlin *et al*, 2004], was used as a control. Serum free conditions were used to represent the endogenous rate of HPMC wound closure. Incubation with M199 containing 2% FCS was used to ensure the responsiveness of the system to potential rate enhancing stimulations.

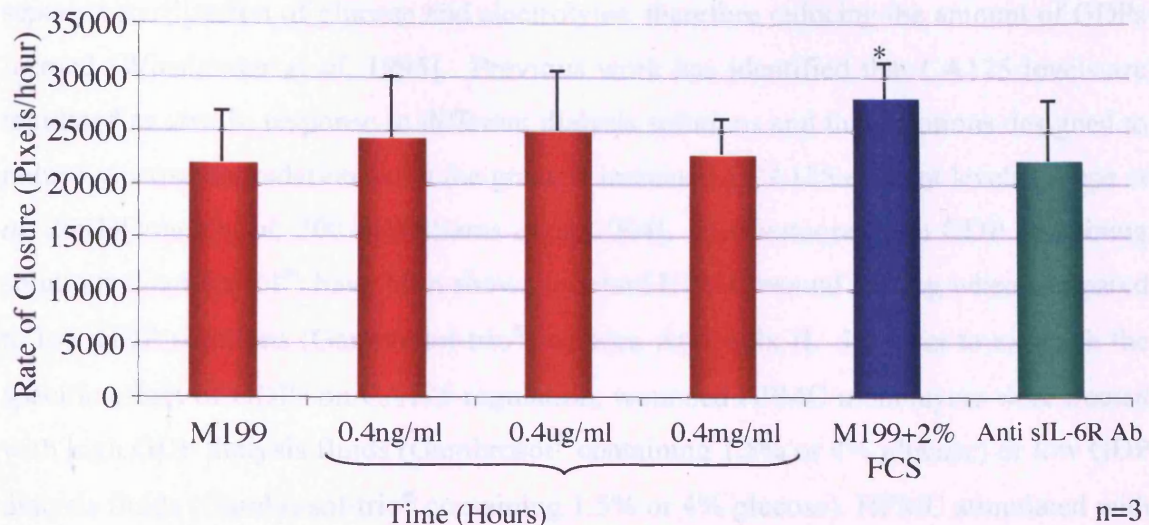


Figure 5.5 The effect of exogenous OC125 on the rate of HPMC re-endothelialization. Confluent monolayers of HPMC were mechanically scratched and incubated with either serum free M199 (negative control), M199 containing OC125 (0.004, 0.04 or 4 μ g/ml), M199 containing 2% FCS (positive control (Blue)) or M199 containing 0.4 μ g/ml anti-sIL-6R antibody (green). * $p < 0.05$ compared to unstimulated M199 control. 'n' refers to the number of independent experiments.

As seen in Figure 5.5, the presence of 2% FCS induced a statistically significant increase in the rate of wound closure when compared to serum free control, thus corroborating existing data regarding the effect of FCS on this wounding system [Yung and Davies, 1998]. The addition of the CA125 specific monoclonal antibody, OC125, did not result in any significant change in the rate of wound closure when compared to the unstimulated control. No significant change in the rate of closure was observed for HPMC incubated with the anti-sIL-6R antibody.

5.3.3 Examination of CA125 shedding in response to high and low levels of glucose degradation products (GDP) present in peritoneal dialysis fluid (PDF)

Heat sterilization of conventional PDFs has been shown to promote the formation of high levels of glucose degradation products from the breakdown of glucose [Kjellstrand *et al*, 1995]. Improved methods of sterilization using a multi-chamber bag system allow the

separate sterilization of glucose and electrolytes, therefore reducing the amount of GDPs formed [Wieslander *et al*, 1995]. Previous work has identified that CA125 levels are regulated *in vivo* in response to different dialysis solutions and that solutions designed to reduce glucose degradation show the greatest increase in CA125 effluent levels [Rippe *et al*, 2001][Jones *et al*, 2001][Williams *et al*, 2004]. Furthermore, high GDP containing solutions (Gambrosol®) have been shown to retard HPMC wound healing when compared to low GDP solutions (Gambrosol-trio®) as seen Appendix II. In order to examine the specific effect of GDPs on CA125 regulation, wounded HPMC monolayers were treated with high GDP dialysis fluids (Gambrosol® containing 1.5% or 4% glucose) or low GDP dialysis fluids (Gambrosol-trio® containing 1.5% or 4% glucose). HPMC stimulated with serum free M199 were used as a control.

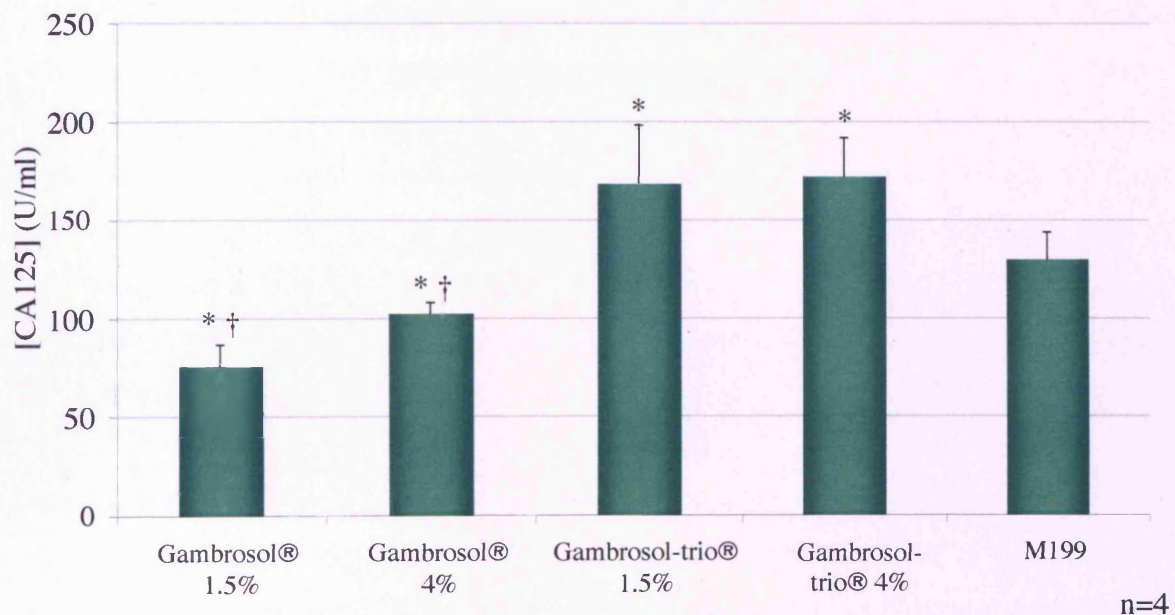


Figure 5.6 The effect of GDPs on HPMC CA125 shedding. Gambrosol® (1.5% or 4% glucose), Gambrosol-trio® (1.5% or 4% glucose) or serum free M199 was applied to confluent HPMC monolayers as a 25% v/v solution in M199. Samples were collected 48 hours after wounding and assayed for CA125 concentration. Cells treated with serum free M199 were used as a control. * $p < 0.05$ compared to M199 control, † $p < 0.05$ compared to low GDP solutions. ‘n’ refers to the number of independent experiments.

Exposure to PDFs containing high GDP concentrations significantly reduces HPMC CA125 secretion, independently of glucose concentration, when compared to the control. In contrast, PDFs containing low GDP concentrations induce a statistically significant increase in CA125 secretion independently of glucose concentration when compared to the control. A significant change in CA125 supernatant concentration is also observed between low and high GDP solutions. This data appears to imply a relationship between GDP levels and HPMC CA125 secretion/shedding during the wounding process.

5.4 DISCUSSION

To date, all of the studies that have examined the biocompatibility of peritoneal dialysis fluids in patients have demonstrated variable increases in CA125 concentrations (up to a maximal 4 fold increase) in the effluent of patients being treated with 'improved' PDFs, containing less glucose degradation products (GDP) and a neutral pH, when compared to more conventional bio-incompatible PDFs [Rippe *et al*, 2001][Jones *et al*, 2001][Williams *et al*, 2003]. Within these studies, the increased CA125 effluent levels are generally interpreted as a reflection of the improved integrity of the mesothelium as a result of reduced damage by more biocompatible dialysis fluids. Although this interpretation is consistent with an increase in the health of the mesothelium [Williams *et al*, 2004] it remains plausible that the changes observed in CA125 effluent levels are a result of altered expression and secretion as a consequence of specific components of the PDF. Therefore, the possibility of an up-regulation of CA125 shedding in response to inflammatory mediators (as demonstrated in chapter 4) induced by the new dialysis fluids remains, although this seems unlikely as levels of inflammatory markers, such as hyaluronic acid [Yung *et al*, 1996][Yamagata *et al*, 1999], have been shown to be reduced in response to the improved dialysis fluids indicative of a reduced inflammatory environment [Williams *et al*, 2004].

In this chapter the ability of the mesothelium to undergo self-repair following injury in response to the increased levels of CA125 observed during the use of biocompatible dialysis fluids was examined. Additionally, examination of CA125 production/shedding by HPMC in response to commercially available dialysis solutions containing low and high concentrations of glucose degradation products will allow understanding of how CA125 may be involved in the wound healing process.

As damage of the mesothelial cell layer of the peritoneal membrane commonly occurs during PD [Williams *et al*, 2003], the effect that physiologically relevant levels of CA125 had on the rate of HPMC wound healing was examined (as seen in section 5.3.1). CA125 concentrations of 25U/ml, 50U/ml and 100U/ml were chosen as these mimicked the

physiologically relevant levels seen in PD patients receiving conventional or more biocompatible formulations (Appendix I). Exogenous CA125 appears to have the effect of increasing the rate of HPMC wound closure when compared to the serum free control. Although the mechanisms by which this observed increase in rate of wound closure are not understood, these data suggest a potential role of CA125 in the process of HPMC migration. It would therefore seem possible that the improved physiology and functionality of the peritoneal membrane observed *in vivo* as a result of the use of improved biocompatible PDFs [Rippe *et al*, 2001][Jones *et al*, 2001][Williams *et al*, 2004] may in part be due to the increased ability of the mesothelium to repair itself in response to normalised CA125 turnover. These observations are consistent with the potential role of other mucins in wound repair as previously reported in other *in vitro* cell models, such as injured bronchial epithelial cells, through their interactions with trefoil factors. The association of mucin molecules with trefoil factors, such as intestinal trefoil factor (ITF), is thought to activate specific cellular pathways (i.e. MAPK) resulting in alterations in cell-cell adhesions that in turn promote cell migration [Kinoshita *et al*, 2000]. The examination of similar signalling pathways in our system may represent a promising area of future work in HPMC research.

As previously discussed, the use of dialysis solutions containing reduced GDP levels is associated with the increase of CA125 peritoneal effluent levels [Rippe *et al*, 2001][Williams *et al*, 2004][Witowski *et al*, 2004]. Prior to this study no work had directly examined CA125's regulation by GDPs although the available *in vivo* data suggested that GDPs may be the PDF component responsible for the observed increase in CA125 effluent levels. As seen in Figure 5.6, the GDP concentration of dialysis fluid has the effect of decreasing the amount of CA125 shed by HPMC suggesting that the changes seen in CA125 peritoneal effluent levels may be the result of repression of CA125 shedding by high GDP concentrations as opposed to CA125 induction by other components present in the fluid. The level of CA125 modulation observed for HPMC treated with Gambrosol-trio[®] compared to that observed for Gambrosol[®] (approximately 2 fold increase) in our *in vitro* system is comparable to the increase seen in the *in vivo* situation [Rippe *et al*, 2001] therefore substantiating our finding in a clinical context. In

addition to this, the re-mesothelialization process has previously been shown to be accelerated by the reduction of GDPs present in PDFs [Morgan *et al*, 2003]. This apparent GDP induced retardation of wound healing and CA125 expression, together with CA125's apparent ability to promote HPMC migration (Figure 5.4) provides further evidence of a potential relationship between CA125 induced re-mesothelialization and the GDP concentrations present during peritoneal dialysis.

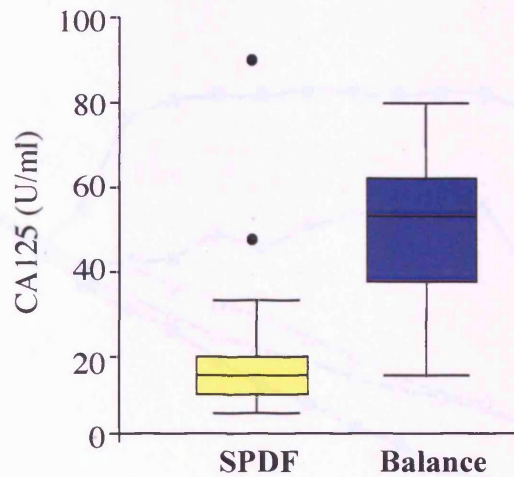
To further examine CA125's involvement in the re-mesothelialization process, OC125 was employed to block the effect of endogenous CA125 activity in the HPMC wound-healing model. As seen in Figure 5.5, the addition of the OC125 had no significant effect on the rate of wound closure when compared to the serum free M199 control suggesting that endogenous CA125 has no function in the wound healing process. To date, nothing is known regarding how OC125 binding might effect CA125's ability to function, and considering no other studies have shown the successful blocking of CA125 activity using OC125 in any system it seems likely that inadequacies within this experimental model may provide a possible explanation for our findings. However, this experiment does serve to highlight the necessity for an improved or new system to study endogenous CA125 function. The blocking of endogenous CA125 using OC125 in a FCS treated model may provide a more meaningful future experiment. Nevertheless, further investigation into CA125's role in cell migration is clearly dependant on the development of a HPMC *in vitro* wound healing model with reduced CA125 expression possibly via the application of siRNA technology.

In conclusion, this chapter demonstrates a role for CA125 in the HPMC wound healing process for the first time although the underlying mechanisms by which CA125 functions remains unclear. Additionally, we have shown that CA125's apparent ability to increase the rate of re-mesothelialization may be directly related to the observed increase in CA125 peritoneal effluent levels seen in response to improved dialysis solutions, shown via the demonstration of CA125's regulation by GDPs in our *in vitro* system. The mechanisms by which GDPs regulates CA125 production/shedding requires further investigation. Furthermore, due to CA125's apparent involvement in the process of

wound healing, the model used in this chapter represents an ideal system for future work in the elucidation of the function of CA125.

APPENDIX I

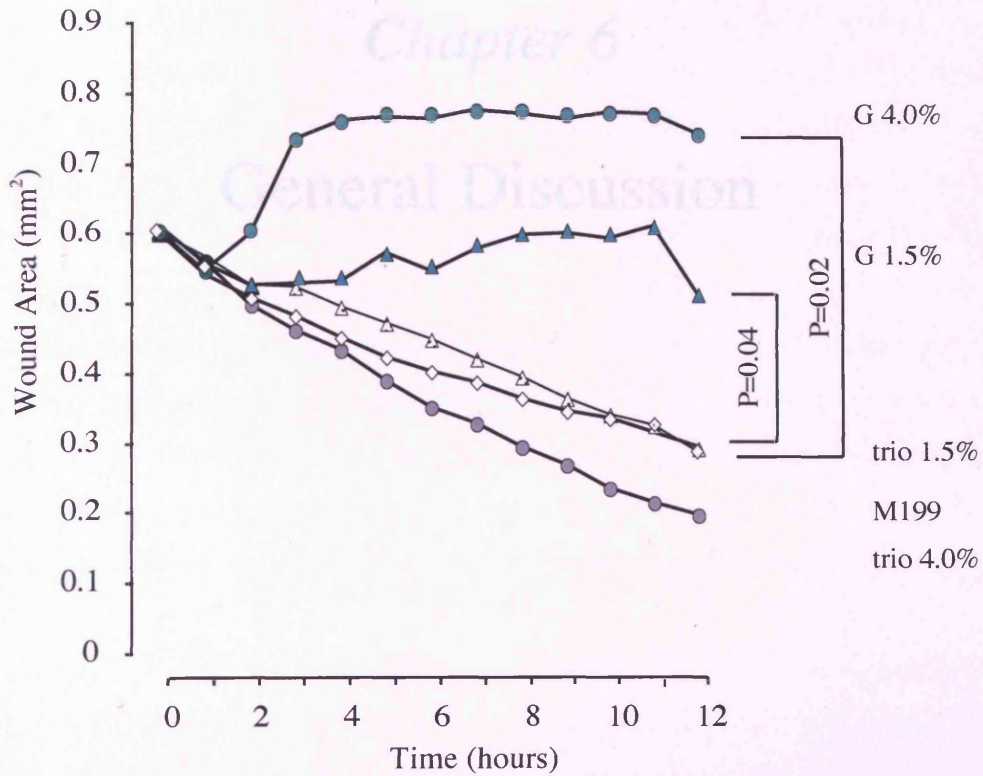
CA125 effluent levels in response to low GDP dialysis solutions



Box plots of effluent CA125 levels (U/ml) for patients treated with a high GDP solution (SPDF) for 12 weeks before treatment with a low GDP solution (Balance) for 12 weeks. CA125 levels were measured at the end of each treatment period. For each box plot median values are represented by the line within the box. The box presents 50% of the values (the 25th and 75th centiles), with the bars representing the highest and lowest values, excluding outliers (●). n=36. (Taken from [Williams *et al*, 2004]).

APPENDIX II

HPMC wound closure in response to Gambrosol® and Gambrosol-trio®



Time course of reendothelialization following scratch wounding in HPMC exposed to Gambrosol® (G) (1.5% and 4.0% glucose), Gambrosol-trio® (Trio) (1.5% and 4.0% glucose) or to control medium (M199). (Taken from [Morgan *et al*, 2003]).

Chapter 6

General Discussion

For the past 25 years the measurement of CA125 has been used as a diagnostic tool for the detection of ovarian cancer [Bast *et al*, 1981][Bast *et al*, 1983]. More recently however, the measurement of aberrant CA125 levels within the peritoneal effluent of patients undergoing PD diverted much attention on to CA125's apparent ability to act as a marker of mesothelial mass/integrity in the peritoneal cavity [Visser *et al*, 1995][Ho-Dac-Pannekeet *et al*, 1997]. The ability to culture HPMC *in vitro* has allowed further analysis of CA125 regulation by these cells and has resulted in a variety of contrasting hypotheses on how CA125 might be regulated in the normal and inflamed peritoneum [Zeillemarker *et al*, 1994][Visser *et al*, 1995][Ziomet *et al*, 1996]. To date, despite CA125's diagnostic value in the monitoring of ovarian cancer and mesothelial cell mass/integrity, the regulation and expression of the CA125 gene, as well as its physiological function, have remained elusive. The aims of this thesis were to investigate the mechanisms controlling transcription of the CA125 gene, to re-evaluate how CA125 expression might be regulated during the inflammatory response and to define a biological function.

Completion of the Human Genome Project generated a large amount of sequence data and allowed the identification and comparison of specific gene sequences, but more importantly, it allowed identification of promoter sequences therefore leading to a better understanding of the transcriptional mechanisms controlling gene expression. At the beginning of this project little work had been carried out on the human CA125 gene. Initial attempts to clone the CA125 gene proved difficult [Yin *et al*, 2001] but the CA125 gene structure was eventually elucidated by O'Brien and his colleagues in 2002 [O'Brien *et al*, 2001][O'Brien *et al*, 2002]. The availability of the CA125 genomic sequence (cosmid sequences AC008734 and AC016584) and the complete mRNA sequence (AF414442.2) allowed the *in silico* reconstruction of the CA125 gene. In this thesis an extra 9bp of expressed sequence were found at the 5' end of the CA125 message and subsequent experiments provided clear evidence that the beginning of the gene and the CA125 promoter region had been located. However, the lack of typical consensus sequence motifs in the immediate up stream sequence, although not uncommon, may pose questions about whether the full gene sequence has been elucidated. Nevertheless, the subsequent analysis of the CA125 promoter region, under resting conditions and in

response to retinoic acid and oestrogen (in primary HPMC) showed that the promoter region was active *in vitro* indicating the successful identification of the CA125 promoter region. These data also substantiated previous studies characterising CA125 as a mucin-like molecule [Yin *et al*, 2001][Yin *et al*, 2002] as our CA125 (or MUC16) promoter constructs displayed a similar magnitude of endogenous promoter activity similar to other surface expressed mucin genes, such as *MUC1* [Thathiah *et al*, 2004], therefore providing further clues to the potential function of CA125 (i.e. as a lubricating molecule).

Although the promoter constructs described in this thesis represent the novel analysis of the CA125 promoter region, many difficulties and problems were presented by this model. Such problems included the transfection of primary cells that express CA125 in order to be certain that the cell type used possessed the transcriptional machinery required to express the antigen, and also allowed comparison with the clinical situation. The use of wild-type cells (HPMC) resulted in low transfection efficiencies in cells that typically express high levels of endogenous CA125 and therefore possibly reducing the sensitivity of the system. Nevertheless, as the use of primary cells in these experiments (i.e. mesothelial cells) allows our observation to be directly relevant to the clinical situation, it would seem that improvement of the transfection efficiencies in this system represents an area of future focus in the analysis of the CA125 promoter region.

Considering the importance of CA125 in the monitoring of ovarian cancer and its more recent adoption as a marker of the viability of the peritoneal mesothelium it seems somewhat surprising that the transcriptional mechanisms regulating CA125's expression remain largely uninvestigated. The controversy that has been ever present in the understanding of CA125 may be attributed to the lack of a basic understanding of how this massive antigen is regulated. Identification of the CA125 promoter region represents a significant step forward in the understanding of this process and will open a gateway to a rapid and better understanding of CA125's function. The immediate impact that the identification of the CA125 promoter region has on understanding the mechanisms involved in CA125's regulation is evident in chapter 4 of this thesis which examines CA125's regulation during inflammation. Analysis of the CA125 promoter constructs, as

well as RT-PCR appears to eliminate transcriptional regulation as a major mechanism regulating CA125's expression during inflammation. The subsequent analysis of CA125's surface expression and shedding in response to inflammatory mediators indicated that the increased turnover of CA125 in response to (the pro inflammatory cytokine) IL-1 β and increased shedding of CA125 in response to IL-6/sIL-6R trans-signalling appears to be a process regulated at the cell surface. Using a growth arrested mesothelial cell culture system [Floege *et al*, 1990] in the absence of interfering growth factors and cytokines has allowed this work to clarify some of the existing discrepancies regarding CA125's regulation by inflammatory cytokines [Zeillemarker *et al*, 1994][Visser *et al*, 1995][Ziemet *et al*, 1996]. It also suggests that the regulation and function of CA125 occurs predominantly on the surface of mesothelial cells and that, as discussed by O'Brien and his colleges [O'Brien *et al*, 1998], cleavage enzymes potentially play a major role in this regulation. It has been suggested that CA125 may function as a lubricant in the peritoneal cavity due to both its anatomical location [Hardardottir *et al*, 1990] and characterisation as a member of the mucin molecule family [Yin *et al*, 2001][Gum, 2002]. We can therefore speculate that increased CA125 production during inflammation may be an attempt to maintain the lubricative layer formed by the mesothelium to preserve gut homeostasis and motility.

Despite CA125's apparent regulation during inflammation (as shown in this study), from a clinical perspective, the argument for the use of CA125 as a marker of mesothelial mass/integrity remains [Ho-Dac-Pannekeet *et al*, 1997][Visser *et al*, 1995]. Although this thesis has to some extent, through the use of a growth arrested and synchronized cell model, partly clarified the existing discrepancies related to CA125 regulation, questions regarding *in vitro* and *in vivo* equivalency of CA125 expression data will ensure this topic remains contentious. Since few studies have investigated changes in CA125 levels seen during peritonitis in patient samples [Ho-Dac-Pannakeet *et al*, 1995], it remains unclear as to whether the changes induced by inflammatory stimuli in our *in vitro* model are comparable with that which is seen in a clinical context. Currently, comparison of *in vitro* and *in vivo* measured CA125 levels in many other studies show that the CA125 appearance rates seen from *in vivo* studies can be 10-30 times lower than those measured

from *in vitro* studies (when one compares data based on defined cell numbers *in vitro* and presumed mesothelial density *in vivo*). These data suggest the *in vitro* environment may not accurately represent the uremic and glucose rich peritoneal cavity where CA125 expression may be suppressed [Topley *et al*, 2005]. Despite this, the observed changes of CA125 modulation seen in chapter 4 (in response to IL-6/sIL-6R trans-signalling), correlate well with the observed magnitude of regulation seen in other *in vitro* and *in vivo* CA125 studies [Zeillemarker *et al*, 1994][Zeimet *et al*, 1997][Jones *et al*, 2001][Williams *et al*, 2004] suggesting that our observations may indeed be relevant to the clinical situation.

The relationship between *in vivo* and *in vitro* CA125 data is further highlighted in chapter 5 of this thesis. As seen in Figure 6.1, previous *in vivo* studies have shown an increase (maximally 3 to 4 fold) in the CA125 effluent levels of patients undergoing dialysis with more biocompatible dialysis solutions, compared to those receiving more conventional solutions. This increase is thought to be in response to lower GDP concentrations present within the newer solutions and is thought to be accompanied by the improved health of the mesothelium [Rippe *et al*, 2001][Jones *et al*, 2001][Williams *et al*, 2004][Witowski *et al*, 2004]. Within these studies we have shown that physiological concentrations of CA125 (i.e. those measurable in patients using new solutions) promote wound healing in our system. Using a similar system we have demonstrated the retardation of CA125 secretion/shedding by high levels of GDPs. Coupled with existing *in vitro* data showing the retardation of HPMC wound healing by solutions containing high levels of GDP [Morgan *et al*, 2003], these data suggest that the improved health of the mesothelium observed in the *in vivo* biocompatibility studies [Rippe *et al*, 2001][Jones *et al*, 2001][Williams *et al*, 2004][Witowski *et al*, 2004] may be as a direct result of peritoneal CA125 levels. It may still be conceivable that adding CA125 to peritoneal dialysis fluids in order to preserve the health of the mesothelium during treatment or inducing its expression may have potential clinical advantage in terms of membrane preservation.

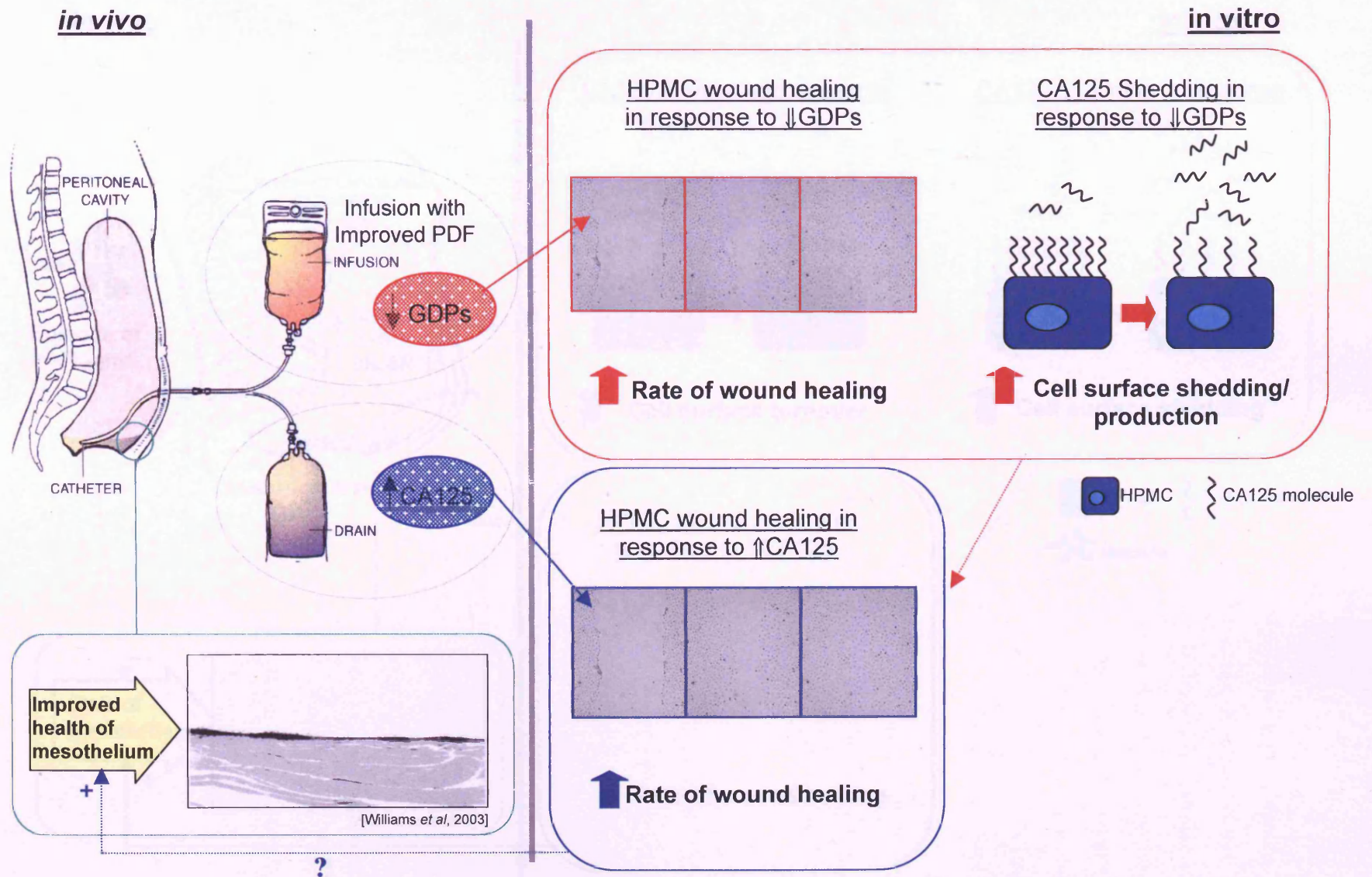


Figure 6.1 The potential role of CA125 in re-mesothelialization as a response to GDP levels in the dialysed peritoneum.

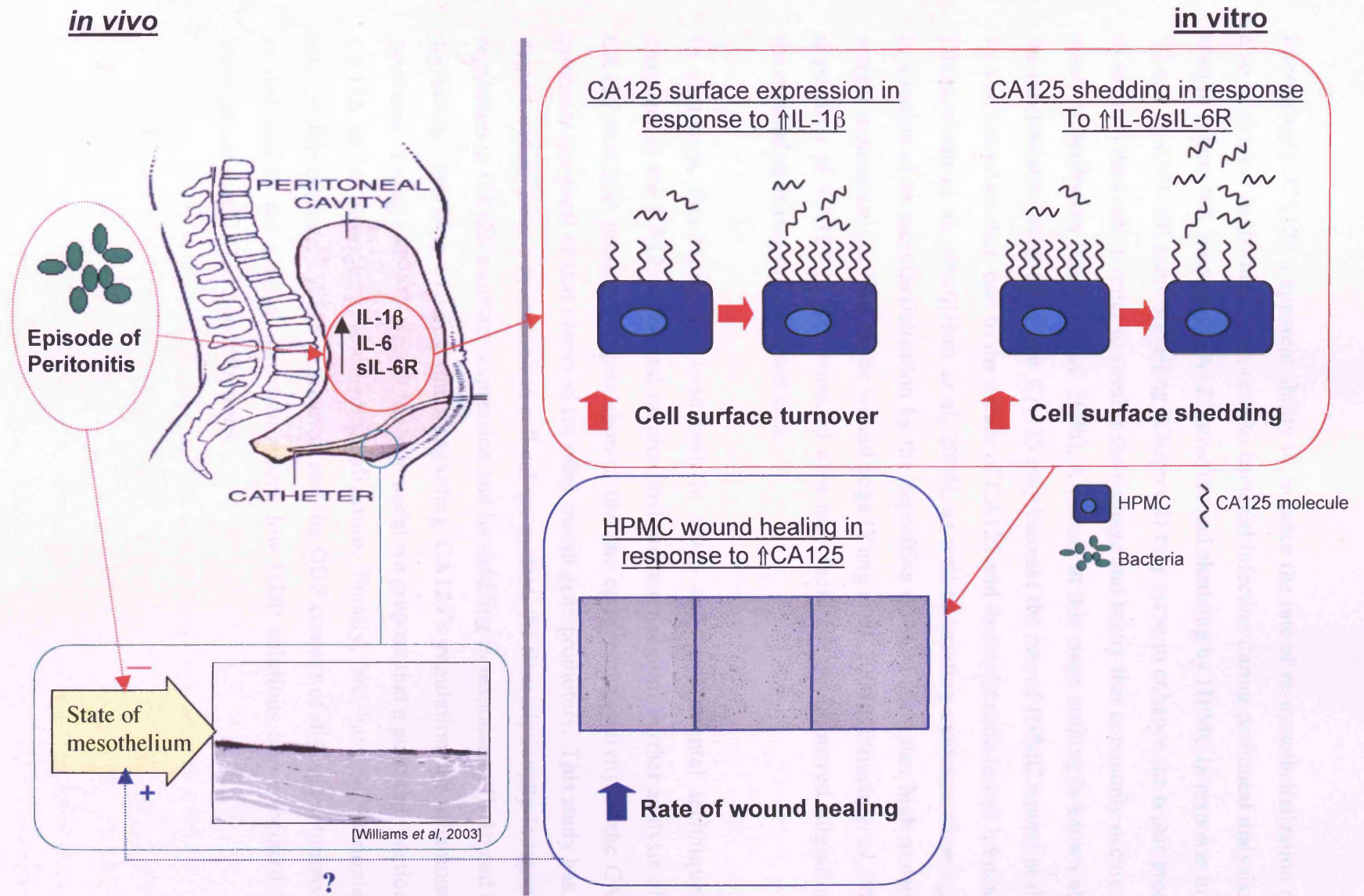


Figure 6.2 Potential involvement of CA125 in re-mesothelialization in response to peritonitis induced injury.

Interestingly, CA125's apparent ability to enhance the rate of re-mesothelialization may also be evident in the host's response to bacterial infection during peritoneal dialysis. As seen in Figure 6.2, increased CA125 turnover and shedding by HPMC in response to IL-1 β and IL-6/sIL-6R trans-signalling (Chapter 4) may serve to enhance the repair process of the mesothelium in order to combat the damage and injury that commonly occurs as a result of peritonitis [Davies *et al*, 1996]. Although at this stage nothing is known about the mechanisms involved in how CA125 may increase the rate of HPMC wound healing, we can speculate that, due to the nature of CA125 and its implication in cell lubrication [Hardardottir *et al*, 1990][Hori *et al*, 2004], as well as existing evidence showing the facilitation of re-mesothelialisation by the deposition of ECM and other high molecular weight molecules (i.e. HA) at the wound edge [Yung *et al*, 2000][Horiuchi *et al*, 2003], deposition of CA125 in the wounded area may facilitate the improved migration of mesothelial cells into the disrupted area.

In summary, this thesis has used both *in silico* and experimental techniques to characterise the CA125 gene and its proximal promoter region. Further analysis of the CA125 proximal promoter region showed that the endogenous activity of the CA125 promoter is typical of that observed for other mucin gene promoters. This study has also demonstrated, using a synchronised cell culture system, the transcriptionally-independent regulation of CA125's surface expression and its shedding in response to IL-1 β and IL-6 signalling clarifying existing ideas regarding CA125's regulation by inflammatory cytokines. Using a HPMC wound healing model we propose that a potential function for CA125 is in promoting re-mesothelialization. Finally, we have substantiated a relationship between CA125 expression and the GDP content of dialysis solutions and related this to the clinical situation where low GDP solutions are associated with increased *in vivo* CA125 concentrations.

Future work

This work provides a preliminary insight into the regulation and function of CA125. The regulation of CA125 shedding by cleavage enzymes is currently not understood and represents an important area of future work for the understanding the regulation of CA125 expression. Examination of CA125's potential as a signalling molecule (as has been seen for other mucin-like molecules) also provides an interesting avenue for future research. For the immediate progression of our understanding of CA125 in peritoneal dialysis further examination of CA125's regulation by GDPs, utilising the CA125 promoter constructs described in this thesis, and CA125's function in HPMC wound healing remains the most likely area of research.

As mentioned throughout this thesis the development of a system displaying “knocked down” or “knocked out” CA125 expression remains a desirable and integral tool for progressing our understanding of CA125 biology. Development of a CA125 full or conditional knockout mouse (non-fatal) would allow for much needed further examination of CA125's function while the development of an *in vitro* system, utilising siRNA technology in order to reduce CA125 expression, may provide a more realistic short term target. As seen in Appendix I, optimization of the knockdown of GAPDH expression in HPMC using this technology was successful, yet, our attempted reduction of CA125 expression in the same system using siRNA oligonucleotides specific for CA125 was unsuccessful due to the lethality of the transfection to HPMC. Should such a system be developed it would facilitate the analysis of CA125's function in HPMC migration through the knockdown of CA125 expression in our *in vitro* wound healing model.

In 1998, O'Brien and his co-authors identified a series of key questions that required addressing including “*the secretory or membrane bound nature of CA125, the function of the CA125 molecule and the elusive CA125 gene*” [O'Brien *et al*, 1998]. Considering these questions it would seem that this thesis has made some advances in the considerable volume of work required to answer these questions. Nevertheless, until the regulation of

CA125 at a molecular level, how and what controls its secretion/shedding and most importantly its biological significance/role are fully defined we will continue to be somewhat in the dark as to CA125's usefulness as a marker of mesothelial integrity.

APPENDIX I

siRNA knockdown of HPMC GAPDH expression

In order to determine the most efficient mode of oligonucleotide transfection a defined number of detached HPMC were transfected with GAPDH siRNA oligonucleotide (Ambion Europe Ltd) or Scrambled (negative control) siRNA oligonucleotide (Ambion Europe Ltd) using FuGene-6 transfection reagent (Roche Diagnostics Ltd, Lewes, UK), NeoFX transfection reagent (Ambion Europe Ltd) or siPORT Amine transfection reagent (Ambion Europe Ltd) as recommended by the manufacturer's protocols (and as discussed in section 2.3.6). RT-PCR (sections 2.3.1-4 and 2.4.1) using primers specific for GAPDH and β -actin (Table 6.1) was then performed to analyse the extent of GAPDH knockdown (Figure 6.3A).

Table 6.1 Oligonucleotide primers used in siRNA (RT-PCR) analysis

Primer pair	Sense strand sequence	Anti-sense strand sequence	Cycle No
β -Actin	GGAGCAATGATCTTGATCTT	CCTTCCTGGGCATGGAGTCCT	30
GAPDH	ATCCACAGTCTTCTGGGTGG	CGAGATCCCTCCAAAATCAA	30

All primers are in 5' - 3' orientation

Semi-quantitative analysis of GAPDH transcription was achieved using a ratio of each product to the β -actin house keeping gene via densitometric analysis (Figure 6.3B).

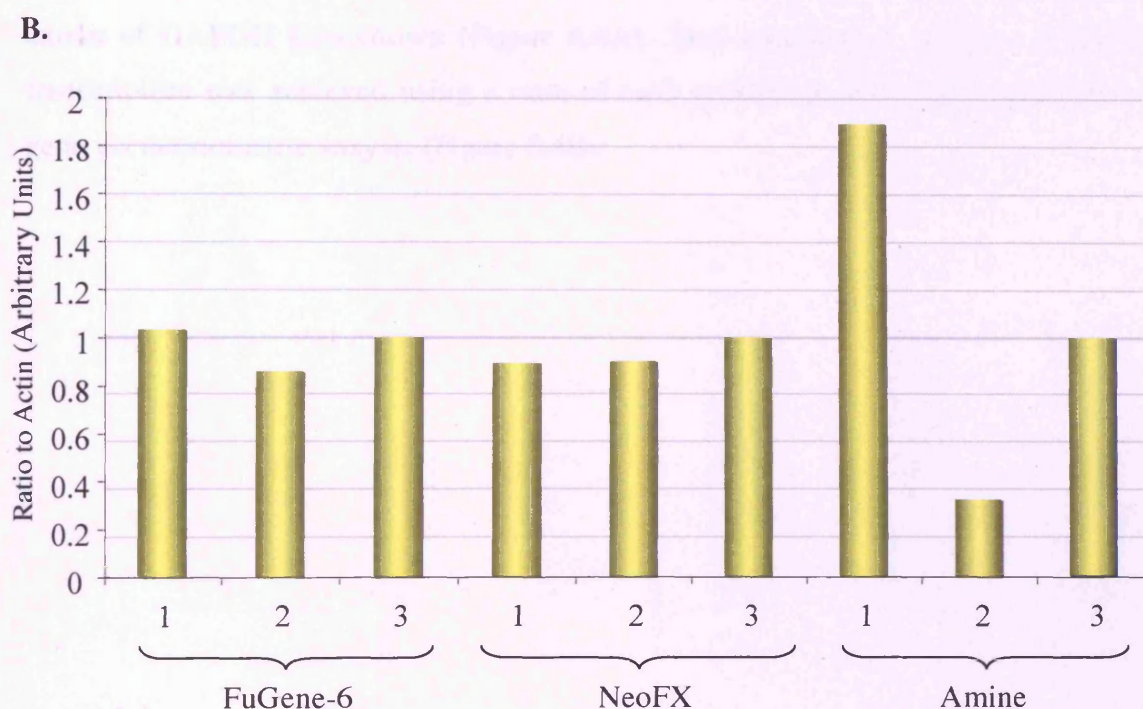
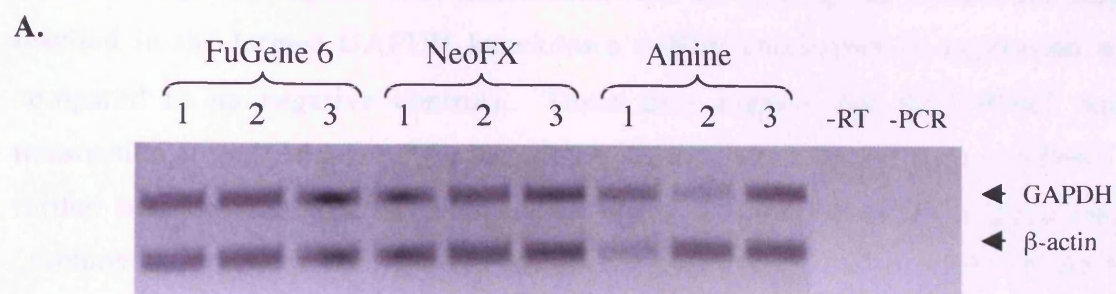


Figure 6.3 Optimisation of GAPDH knockdown in HPMC. (A) Representative gel showing HPMC expression of GAPDH and β -Actin 48 hours after siRNA transfection. HPMC were transfected with either 100nM GAPDH siRNA oligonucleotide¹, 100nM Scramble siRNA oligonucleotide² or no siRNA oligonucleotide³ using either 2 μ l/ml FuGene-6 transfection reagent (FuGene-6), 3 μ l/ml NeoFX transfection reagent (NeoFX) or 5 μ l/ml siPORT Amine transfection reagent (Amine). -RT=Negative control for reverse transcriptase, -PCR=Negative control for PCR. (B) Densitometric analysis of GAPDH expression (as a ratio of β -Actin expression) 48 hours after siRNA transfection.

As can be seen in Figure 6.3B, transfection with siPORT Amine transfection reagent resulted in the largest GAPDH knockdown (~80% knockdown in expression when compared to its negative control). These data suggest that the siPORT Amine transfection reagent is optimal for the siRNA oligonucleotide transfection in HPMC. To further optimize the GAPDH knockdown using siPORT Amine transfection reagent (Ambion Europe Ltd), HPMC were transfected with defined concentrations of GAPDH siRNA oligonucleotide (Figure 6.4). RT-PCR (sections 2.3.1-4 and 2.4.1) using primers specific for GAPDH and β -actin (Table 6.1) was then performed in order to analyse the extent of GAPDH knockdown (Figure 6.4A). Semi-quantitative analysis of GAPDH transcription was achieved using a ratio of each product to the β -actin house keeping gene via densitometric analysis (Figure 6.4B).

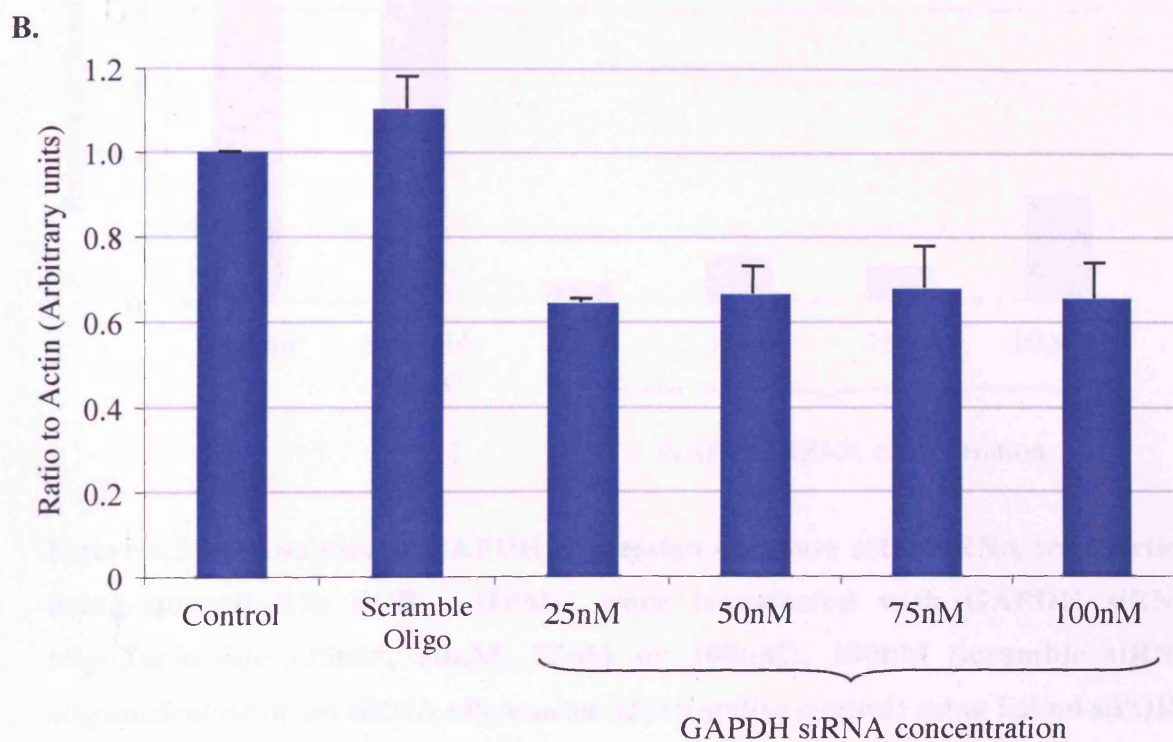
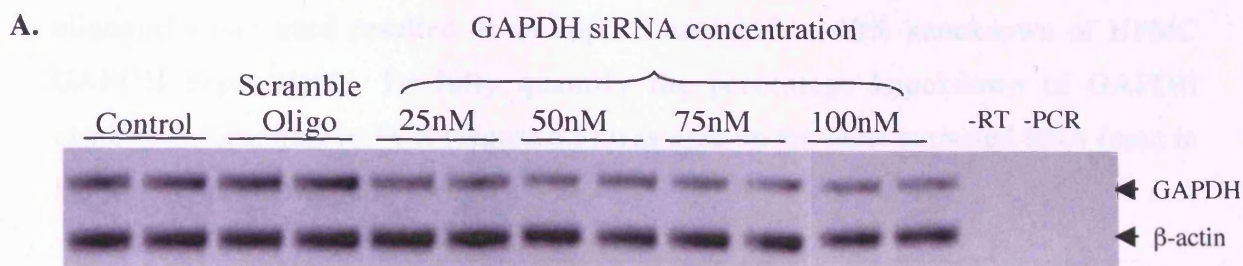


Figure 6.4 Optimisation of GAPDH siRNA concentration in HPMC. (A) Agarose gel showing HPMC expression of GAPDH and β -actin 48 hours after siRNA transfection. HPMC were transfected with either GAPDH siRNA oligonucleotide (25nM, 50nM, 75nM or 100nM), 100nM Scramble siRNA oligonucleotide or no siRNA oligonucleotide (negative control) using 5 μ l/ml siPORT Amine transfection reagent. -RT = Negative control for reverse transcriptase, -PCR = Negative control for PCR. (B) Densitometric analysis of GAPDH expression (as a ratio of β -actin expression) 48 hours after GAPDH siRNA transfection.

As can be seen in Figure 6.4(B), all transfected concentrations of GAPDH siRNA oligonucleotide used resulted in an approximate 35% – 40% knockdown of HPMC GAPDH expression. To fully quantify the percentage knockdown of GAPDH expression, quantitative PCR (Figure 6.5) was used on the same extracted RNA (used in Figure 6.4) as described in section 2.4.2.

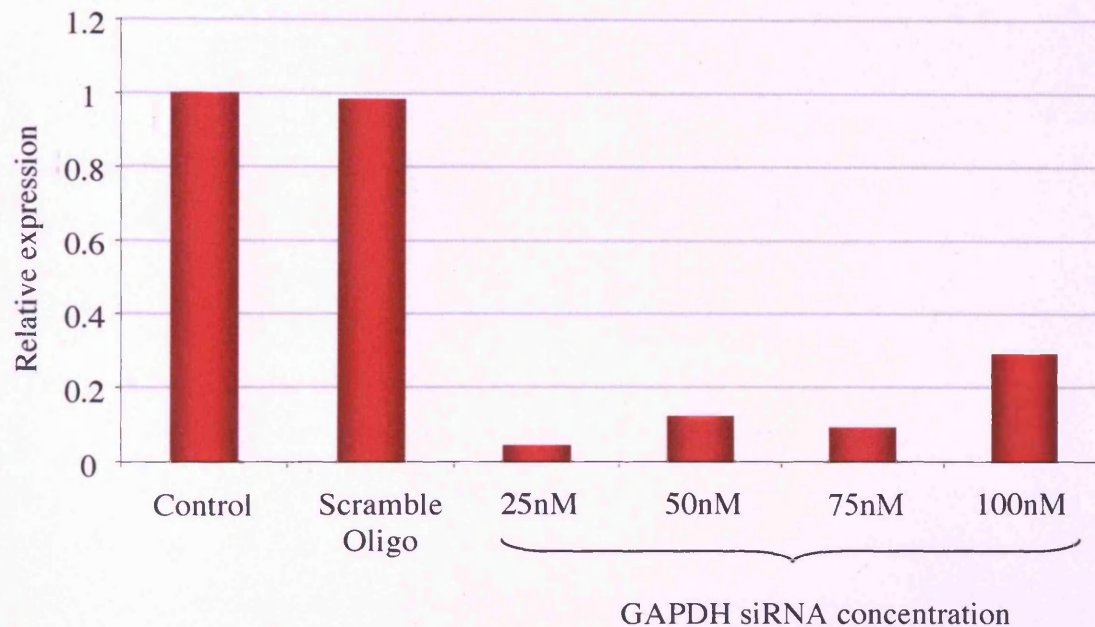


Figure 6.5 Analysis of GAPDH expression 48 hours after siRNA transfection using quantitative PCR. HPMC were transfected with GAPDH siRNA oligonucleotide (25nM, 50nM, 75nM or 100nM), 100nM Scramble siRNA oligonucleotide or no siRNA oligonucleotide (negative control) using 5µl/ml siPORT Amine transfection reagent.

Figure 6.5 shows that transfection of 25nM GAPDH siRNA oligonucleotide resulted in the largest GAPDH knockdown (95% decrease in expression) in HPMC, though all other concentrations tested also induced a high degree of knockdown. These data indicate the successful knockdown of GAPDH expression in primary HPMC.

References

Allan SM, Tyrell PT, Rothwell NJ: Interleukin-1 and neuronal injury. *Nat Rev Immunol* 5(8):629-40, 2005.

Altschul SF, Madden TL, Schaffer AA, Zhang J, Zhang Z, Miller W, Lipman DJ: Gapped BLAST and PSI-BLAST: a new generation of protein database search programs. *Nucleic Acids Res* 25(17):3389-402, 1997.

Argueso P, Spurr-Michoud S, Russo CL, Tisdale A, Gipson IK: MUC16 Mucin is expressed by the human ocular surface epithelia and carries the H185 carbohydrate epitope. *IOVS* 44(6):2487-95, 2003.

Bast RC, Feeney M, Lazarus H, Nadler LM: Reactivity of a monoclonal antibody with human ovarian carcinoma. *J Clin Invest* 68(5):1331-37, 1981.

Bast RC Jr, Klug TL, St John E, Jenison E, Niloff JM, Lazarus H, Berkowitz RS, Leavitt T, Griffiths CT, Parker L, Zurawski VR Jr, Knapp RC: A radioimmunoassay using a monoclonal antibody to monitor the course of epithelial cancer. *The New England Journal of Medicine* 309(15):883-87, 1983.

Bastani B and Chu N: Serum CA-125 level in end-stage renal disease patients maintained on chronic peritoneal dialysis of hemodialysis: The effect of continuous presence of peritoneal fluid, peritonitis, and peritoneal catheter implantation. *Am J Nephrol* 15(6):468-72, 1995.

Bastien J, Rochette-Egly C: Nuclear retinoid receptors and the transcription of retinoid-target genes. *Gene* 328:1-16, 2004.

Berghe WV, Vermeulen L, De Wide G, De Bosscher K, Boone E, Haegeman: Signal transduction by tumor necrosis factor and gene regulation of the inflammatory cytokine interleukin-6. *Biochemical Pharmacology* 60:1185-95, 2000.

Brauner A, Hylander B, Wretling B: Tumor necrosis factor-alpha, interleukin-1 beta, and interleukin-1 receptor antagonist in dialysate and serum from patients on continuous ambulatory peritoneal dialysis. *Am J Kidney Dis* 27(3):402-8,1996.

Brayman M, Thathiah A, Carson DD: MUC1: a multifunctional cell surface component of reproductive tissue epithelia. *Reprod Biol Endocrinol. Review*. 2004.

Breborowicz A, Rodela H, Oreopoulos DG: Toxicity of osmotic solutes on human mesothelial cells in vitro. *Kidney Int* 41(5):1280-5, 1992.

Breborowicz A, Maciej B, Malgorzata P, Alicja P, Dimitros O: Limitations of the CA125 as an index of peritoneal mesothelial cell mass-an *in vitro* study. *Nephron Clin Pract* 100(2):c46-51, 2005.

Brewer CF: Binding and cross-linking properties of galectins. *Biochemica et Biophysica Acta* 1572:255-62, 2002.

Brown MA, Xu C, Nicolai H, Griffiths B, Chambers JA, Black D, Solomon E: The 5' end of the BRCA1 gene lies within a duplicated region of human chromosome 17q21. *Oncogene* 12(12):2507-13, 1996.

Casadei R, Strippoli P, D'Addabbo P, Canaider S, Lenzi L, Vitale L, Giannone S, Frabetti F, Facchin F, Carinci P, Zannotti M: mRNA 5' region sequence incompleteness: a potential source of systematic errors in translation initiation codon assignment in human mRNAs. *Gene* 321:185-93, 2003.

Celec P: Nuclear factor kappa B-molecular biomedicine: the next generation. *Biomedicine & Pharmacotherapy* 58(6-7):365-71, 2004.

Chaimovitz C: Peritoneal Dialysis. *Kidney International* 45(4):1226-40, 1994.

Chang K and Pastan I: Molecular cloning of mesothelin, a differentiation antigen present on mesothelium, mesotheliomas, and ovarian cancers. *Proc Natl Acad Sci* 93(1):136-40, 1996.

Chen Y, Thai P, Zhao YH, Ho YS, DeSouza MM, Wu R: Stimulation of airway mucin gene expression by interleukin (IL)-17 through IL-6 paracrine/autocrine loop. *J Biol Chem* 278(19):17036-43, 2003.

Chen Y, Zhao YH, Di YP, Wu R: Characterization of human mucin 5B gene expression in airway epithelium and the genomic clone of the amino-terminal and 5'-flanking region. *Am J Respir Cell Mol Biol* 25(5):542-53, 2001.

Chowdhury PS, Viner JL, Beers R, Pastan I: Isolation of a high affinity stable single-chain Fv specific for mesothelin from DNA-immunized mice by phage display construction of a recombinant immunotoxin with anti-tumor activity. *Proc Natl Acad Sci* 95(2):669-74, 1998.

Clark-Lewis I, Schumacher C, Baggiolini M, Moser B: Structure-activity relationships of interleukin-8 determined using chemically synthesized analogs. Critical role of NH₂-terminal residues and evidence for uncoupling of neutrophil chemotaxis, exocytosis, and receptor binding activities. *J Biol Chem* 266(34):23128-34, 1991.

Clark-Lewis I, Dewald B, Geiser T, Moser B, Baggiolini M: Platelet factor 4 binds to interleukin 8 receptors and activates neutrophils when its N terminus is modified with Glu-Leu-Arg. *Proc Natl Acad Sci* 90(8):3574-7, 1993.

Clark-Lewis I, Kim KS, Rajarathnam K, Gong JH, Dewald B, Moser B, Baggiolini M, Sykes BD: Structure-activity relationships of chemokines. *J Leukoc Biol* 57(5):703-11, 1995.

Clayton A, Evans RA, Pettit E, Hallett M, Williams JD, Steadman R: Cellular activation through the ligation of intercellular adhesion molecule-1. *J Cell Sci* 111(4):443-53, 1998.

Clayton AL, Hazzalin CA, Mahadevan LC: Enhanced histone acetylation and transcription: a dynamic perspective. *Mol Cell* 23(3):289-296, 2006.

Coleman SL, Hoogendoorn B, Guy C, Smith SK, O'Donovan MC, Buckland PR: Streamlined approach to functional analysis of promoter-region polymorphisms. *Biotechniques* 33(2):412, 414, 416 passim, 2002.

Cullinan EB, Kwee L, Nunes P, Shuster DJ, Ju G, McIntyre KW, Chizzonite RA, Labow MA: IL-1 receptor accessory protein is an essential component of the IL-1 receptor. *J Immunol* 161(10):5614-20, 1998.

Dai X, Yamasaki K, Shirakata Y, Sayama K, Hashimoto K: All-trans-retinoic acid induces interleukin-8 via the nuclear factor-kappaB and p38 mitogen-activated protein kinase pathways in normal human keratinocytes. *J Invest Dermatol* 123(6):1078-85, 2004.

Dasu MR, Barrow RE, Spies M, Herndon DN: Matrix metalloproteinase expression in cytokine stimulated human dermal fibroblasts. *Burns* 29(6):527-31, 2003.

Davies SJ, Bryan J, Phillips L, Russell GI: Longitudinal changes in peritoneal kinetics: the effects of peritoneal dialysis and peritonitis. *Nephrol Dial Transplant* 11(3):498-506, 1996.

De Souza GE, Ferreira SH: Blockade by anti-macrophage serum of the migration of PMN neutrophils into the inflamed peritoneal cavity. *Agents & Actions* 17(1):97-103, 1985.

De Vriese AS: Interesting News in Peritoneal Dialysis. *Nephron* 92(4):763-71, 2002.

Devuyst O, Topley N, Williams JD: Morphological and functional changes in the dialysed peritoneal cavity: impact of more biocompatible solutions. *Nephrol Dial Transplant* 179(3):12-15, 2002.

Dinarello CA: The IL-1 family and inflammatory diseases. *Clin Exp Rheumatol*. 20(S27):S1-13, 2002.

Dinarello CA: Blocking IL-1 in systemic inflammation. *JEM* 201(9):1355-59, 2005.

Douvdevani A, Rapoport J, Konforty A, Argov S, Ovnat A, Chaimovitz: Human peritoneal mesothelial cells synthesize IL-1 α and β . *Kidney International* 46(4):993-1001, 1994.

Duwe AK, Vas SI, Weatherhead JW: Effects of the composition of peritoneal dialysis fluid on chemiluminescence, phagocytosis, and bactericidal activity in vitro. *Infect Immun* 33(1):130-5, 1981.

Enmark E, Gustafsson JA: Oestrogen receptors - an overview. *J Intern Med* 246(2):133-8, 1999.

Epiney M, Bertossa C, Weil A, Campana A, Bischof P: CA125 production by the peritoneum: *in-vitro* and *in-vivo* studies. *Human Reproduction* 15(6):1261-65, 2000.

Escande F, Aubert JP, Porchet N, Buisine MP: Human mucin gene MUC5AC: organization of its 5'-region and central repetitive region. *Biochem J* 358(3):763-72, 2001.

Faull RJ, Stanley JM, Fraser S, Power DA, Leavesley DI: HB-EGF is produced in the peritoneal cavity and enhances mesothelial cell adhesion and migration. *Kidney Int* 59(2):614-24, 2001.

Fendrick JL, Konishi I, Geary SM, Parmley TH, Quirk JG, O'Brien TJ: CA125 phosphorylation is associated with its secretion from WISH Human amnion cell line. *Tumor Biology* 18(5):278-89, 1997.

Fenton SS, Schaubel DE, Desmeules M, Morrison HI, Mao Y, Copleston P, Jeffery JR, Kjellstrand CM: Hemodialysis versus peritoneal dialysis: A comparison of adjusted mortality rates. *Am J Kid Dis* 30(3):334-42, 1997.

Fischer BM, Voynow JA: Neutrophil elastase induces MUC5AC gene expression in airway epithelium via a pathway involving reactive oxygen species. *Am J Respir Cell Mol Biol* 26(4):447-52, 2002.

Floege J, Topley N, Wessel K, Kaever V, Radeke H, Hoppe J, Kishimoto T, Resch K: Monokines and platelet-derived growth factor modulate prostanoid production in growth arrested, human mesangial cells. *Kidney Int* 37(3):859-69, 1990.

Foley-Comer AJ, Herrick SE, Al-Mishlab T, Prele CM, Laurent GJ, Mutsaers SE: Evidence for incorporation of free-floating mesothelial cells as a mechanism of serosal healing. *J Cell Sci* 115(7):1383-9, 2002.

Fraser D, Wakefield L, Phillips A. Independent regulation of transforming growth factor-beta1 transcription and translation by glucose and platelet-derived growth factor. *Am J Pathol* 161(3):1039-49, 2002.

Fuchs S, Skwara A, Bloch M, Dankbar B: Differential induction and regulation of matrix metalloproteinases in osteoarthritic tissue and fluid synovial fibroblasts. *Osteoarthritis Cartilage* 12(5):409-18, 2004.

Gaetje R, Winnekendonk DW, Kaufman AAM: Ovarian cancer antigen CA125 influences adhesion of human and mammalian cell lines in vitro. *Clin Exp Obstet & Gyn* 29(1):34-36, 2002.

Gokal R, Mallick NP: Peritoneal Dialysis. *Lancet* 353(9155):823-8, 1999.

Garmy-Susini B, Delmas E, Gourdy P, Zhou M, Bossard C, Bugler B, Bayard F, Krust A, Prats AC, Doetschman T, Prats H, Arnal JF: Role of fibroblast growth factor-2 isoforms in the effect of estradiol on endothelial cell migration and proliferation. *Circ Res* 94(10):1301-9, 2004.

Gray H: Anatomy of the human body: 20th Edition, *Published by Lea & Febiger* 1825-61, 1918.

Gray T, Coakley R, Hirsh A, Thornton D, Kirkham S, Koo JS, Burch L, Boucher R, Nettekheim P: Regulation of MUC5AC mucin secretion and airway surface liquid metabolism by IL-1beta in human bronchial epithelia. *Am J Physiol Lung Cell Mol Physiol* 286(2):320-30, 2004.

George AA, Sharma M, Singh BN, Sahoo NC, Rao KV: Transcription regulation from a TATA and INR-less promoter: spatial segregation of promoter function. *EMBO J*: Epub ahead of print, 2006.

Greig J, Harkness M, Taylor P, Hashmi C, Liang S, Kwan J: Peritonitis due to the dermatiaceous mold *Exopiala dermatitidi* complicating continuous ambulatory peritoneal dialysis. *Clin Microbiol Infect* 9(7):713-15, 2003.

Gum JR, Hicks JW, Kim YS: Identification and characterization of the MUC2 (human intestinal mucin) gene 5'-flanking region: promoter activity in cultured cells. *Biochem J* 325 (1):259-67, 1997.

Gum JR, Hicks JW, Crawley SC, Dahl CM, Yang SC, Robertson AM, Kim YS: Initiation of transcription of the MUC3A human intestinal mucin from a TATA-less promoter and comparison with the MUC3B amino terminus. *J Biol Chem* 278(49):49600-9, 2003.

Gum JR: Mucin genes and the proteins they encode: Structure, Diversity and Regulation. *Am J Respir Cell Mol Biol* 7(6):557-64, 1992.

Hardardottir H, Parmley TH, Quirk JG, Sanders MM, Miller FC, O'Brien TJ: Distribution of CA125 in embryonic tissues and adult derivatives of the fetal periderm. *Am J Obstet Gynecol* 6(1)1925-31, 1990.

Harrington WR, Sheng S, Barnett DH, Petz LN, Katzenellenbogen JA, Katzenellenbogen BS: Activities of estrogen receptor alpha- and beta-selective ligands at diverse estrogen responsive gene sites mediating transactivation or transrepression. *Mol Cell Endocrinol* 206(1-2):13-22, 2003.

Harvey W, Amlot PL: Collagen production by human mesothelial cells in vitro. *J Pathol* 139(3):337-47, 1983.

Heinrich PC, Behrmann I, Muller-Newen G, Schaper F, Graeve L: Interleukin-6-type cytokine signalling through the gp130/Jak/STAT pathway. *Biochem J* 334(2):297-314, 1998.

Heinrich PC, Behrmann I, Haan S, Hermanns HM, Muller-Newen G, Schaper F: Principles of interleukin (IL)-6-type cytokine signalling and its regulation. *Biochem J* 374(1):1-20, 2003.

Hjelle JT, Miller-Hjelle MA, Dobbie JW: The biology of the mesothelium during peritoneal dialysis. *Peritoneal Dialysis International* 15(7):S13-S23, 1995.

Ho-Dac-Pannekeet MM, Zemel D, Koomen GCM, Struijk DG, Krediet RT: Dialysate markers of peritoneal tissue during peritonitis and in stable CAPD. *Peritoneal Dialysis International* 15(6):217-25, 1995.

Ho-dac-Pannekeet MM, Koopmans JG, Struijk DG, Krediet RT: Restriction coefficients of low molecular weight solutes and macromolecules during peritoneal dialysis. *Adv Perit Dial* 13:72-76, 1997.

Ho-Dac-Pannekeet MM, Hiralall JK, Struijk, Krediet RT: Longitudinal follow-up of CA125 in peritoneal effluent. *Kidney International* 51(3):888-93, 1997.

Hoffman E, Dittrich-Breiholz O, Noltmann H, Kracht: Multiple control of interleukin-8 gene expression. *Journal of Leukocyte Biology* 72(5):847-55, 2002.

Hori Y, Spurr-Michaud S, Russo CL, Argueso P, Gipson IK: Differential regulation of membrane-associated mucins in the human ocular surface epithelium. *Investigative Ophthalmology & Visual Science* 45(1):114-22, 2004.

Horiuchi T, Miyamoto K, Miyamoto S, Fujita M, Sano N, Minamiyama K, Fujimura Y, Nagasawa K, Otsuka C, Ohta Y: Image analysis of remesothelialization following chemical wounding of cultured human peritoneal mesothelial cells: the role of hyaluronan synthesis. *Kidney Int* 64(6):2280-90, 2003.

Hovig E, Rye PD, Warren DJ, Nustad K: CA 125: the end of the beginning. *Tumour Biol* 22(6):345-7, 2001.

Hurst SM, Wilkinson TS, McLoughlin RM, Jones S, Horiuchi S, Yamamoto, Rose-John S, Fuller GM, Topley N, Jones SA: IL-6 and its soluble receptor orchestrates a temporal switch in the pattern of leukocyte recruitment seen during acute inflammation. *Immunity* 14(6):705-14, 2001.

Imbert-Marcille BM, Thedrez P, Sai-Maurel C, Francois C, Auget JL, Benard J, Jacques Y, Imai S, Chatal JF: Modulation of associated ovarian carcinoma antigens by 5 cytokines used as single agents or in combination. *Int J Cancer* 57(3):392-98, 1994.

Jacobs I, Bast RC: The CA 125 tumour-associated antigen: a review of the literature: *Human Reproduction* 4(1):1-12, 1989.

Jones S, Holmes CJ, Krediet RT, Mackenzie R, Faict D, Tranaeus A, Williams JD, Coles GA, Topley N: Bicarbonate/lactate-based peritoneal dialysis solution increases cancer antigen 125 and decreases hyaluronic acid levels. *Kidney International* 59(4):1529-38, 2001.

Jones SA, Houchi S, Topley N, Yamamoto N, Fuller M: The soluble interleukin 6 receptor: mechanism of production and implications in disease. *FASEBJ* 15(1):43-58, 2001.

Jones SA: Directing transition from innate to acquired immunity: defining a role for IL-6. *J Immunol*:175(6):3463-8, 2005.

Kanda N, Watanabe S: 17Beta-estradiol inhibits MCP-1 production in human keratinocytes. *J Invest Dermatol* 120(6):1058-66, 2003.

Karabacak O, Ilgin N, Tiras B, Gursoy R, Himmetoglu O: Influence of exogenous estrogen administration on serum CA-125 originating from the endometrium. *Int J Gynaecol & Obstet* 76(2):169-72, 2002.

Kenemans P, Yedama CA, Bon GG, Von Mensdorff-Pouilly: Ca125 in gynecological pathology-a review. *European journal of obstetrics & gynecology and reproductive biology* 49(1-2):115-24, 1993.

Kim KH, Stellmach V, Javors J, Fuchs E: Regulation of human mesothelial cell differentiation: opposing roles of retinoids and epidermal growth factor in the expression of intermediate filament proteins. *J Cell Biol* 6(2):3039-51, 1987.

Kim YD, Jeon JY, Woo HJ, Lee JC, Chung JH, Song SY, Yoon SK, Baek SH: Interleukin-1beta induces MUC2 gene expression and mucin secretion via activation of PKC-MEK/ERK, and PI3K in human airway epithelial cells. *J Korean Med Sci* 17(6):765-71, 2002.

Kinoshita K, Taupin DR, Itoh H, Podolsky DK: Distinct pathways of cell migration and antiapoptotic response to epithelial injury: structure-function analysis of human intestinal trefoil factor. *Mol Cell Biol* 20(13):4680-90, 2000.

Kjellstrand P, Martinson E, Wieslander A, Holmquist B: Development of toxic degradation products during heat sterilization of glucose-containing fluids for peritoneal dialysis: influence of time and temperature. *Perit Dial Int* 15(1):26-32, 1995.

Klinge CM: Estrogen receptor interaction with estrogen response elements. *Nucleic Acids Res* 29(14):2905-2919, Review, 2001.

Konishi I, Fendrick JL, Parmley TH, Quirk JG Jr, O'Brien TJ: Epidermal growth factor enhances secretion of the ovarian tumor-associated cancer antigen CA125 from the human amnion WISH cell line. *J Soc Gynecol Investig* 1(1):89-96, 1994.

Koomen GCM, Betjes MGH, Zemel D, Krediet RT, Hoek FJ: Cancer antigen 125 is locally produced in the peritoneal cavity during continuous ambulatory peritoneal dialysis. *Peritoneal Dialysis International* 14(2):132-6, 1994.

Krediet RT: The peritoneal membrane in chronic peritoneal dialysis. *Kidney international* 55(1):341-56, 1999.

Lai KN, Lai KB, Szeto CC, Ho KK, Poon P, Lam CW, Leung JC: Dialysate cell population and cancer antigen 125 in stable continuous ambulatory peritoneal dialysis patients: their relationship with transport parameters. *American Journal of Kidney Diseases* 29(5):699-705, 1997.

Langdon SP, Hawkes MM, Hay FG, Lawrie SS, Schol DJ, Hilgers J, Leonard RC, Smyth JF: Effect of sodium butyrate and other differentiation inducers on poorly differentiated human ovarian adenocarcinoma cell lines. *Cancer Res* 48(21):6161-65, 1988.

Leavesley DI, Stanley JM, Faull RJ: Epidermal growth factor modifies the expression and function of extracellular matrix adhesion receptors expressed by peritoneal mesothelial cells from patients on CAPD. *Nephrol Dial* 14(5):1208-16, 1999.

Lewin, B: Genes VII. *Oxford University press*, 2000.

Lewis SL, Holmes CJ: Host defense mechanisms involved in peritonitis. *Perit Dial Int* 13(S2):S295-8, 1993.

Li FK, Davenport A, Robson RL, Loetscher P, Rothlein R, Williams JD, Topley N. Leukocyte migration across human peritoneal mesothelial cells is dependent on directed chemokine secretion and ICAM-1 expression. *Kidney Int* 54(6):2170-83, 1998.

Liberek T, Topley N, Mistry CD, Coles GA, Morgan T, Quirk RA, Williams JD: Cell function and viability in glucose polymer peritoneal dialysis fluids. *Perit Dial Int* 13(2):104-11, 1993.

Liu FT, Patterson RJ, Wang JL: Intracellular functions of galectins. *Biochemica et Biophysica Acta* 1572(2-3):263-73, 2002.

Lloyd KO, Yin BWT, Kudryashov V: Isolation and characterization of ovarian cancer antigen CA 125 using a new monoclonal antibody (VK-8): Identification as a mucin-type molecule. *Int J Cancer* 71(5):842-50, 1997.

Loy TS, Quesenberry JT, Sharp SC: Distribution of the CA 125 in Adenocarcinomas. An immunohistochemical study of 481 cases. *Am J Clin Pathol* 98(2):175-79, 1992.

Lu KH, Patterson AP, Wang L, Marquez RT, Atkinson EN, Baggerly KA, Ramoth LR, Rosen DG, Liu J, Hellstrom I, Smith D, Hartmann L, Fishman D, Berchuck A, Schmandt R, Whitaker R, Gershenson DM, Mills GB, Bast RC Jr: Selection of potential markers for epithelial ovarian cancer with gene expression arrays and recursive descent partition analysis. *Clin Cancer Res* 10(10):3291-300, 2004.

Mader S, Chen JY, Chen Z, White J, Chambon P, Gronemeyer H: The patterns of binding of RAR, RXR and TR homo- and heterodimers to direct repeats are dictated by the binding specificities of the DNA binding domains. *EMBO J* 12(13):5029-41, 1993.

Maeda T, Inoue M, Koshiha S, Yabuki T, Aoki M, Nunokawa E, Seki E, Matsuda T, Motoda Y, Kobayashi A, Hiroyasu F, Shirouzu M, Terada T, Hayami N, Ishizuka Y, Shinya N, Tatsuguchi A, Yoshida M, Hirota H, Matsuo Y, Tani K, Arakawa T, Carninci P, Kawai J, Hayashizaki Y, Kigawa T, Yokoyama S: Solution structure of the SEA domain from the murine homologue of ovarian cancer antigen CA125 (MUC16). *J Biol Chem* 279(13):13174-82, 2004.

Marples D: Aquaporins: roles in renal function and peritoneal dialysis. *Perit Dial Int* 21(2):212-18, 2000.

Marshall BC, Santana A, Xu QP, Petersen MJ, Campbell EJ, Hoidal JR, Welgus HG: Metalloproteinases and tissue inhibitor of metalloproteinases in mesothelial cells. Cellular differentiation influences expression. *J Clin Invest* 91(4):1792-9, 1993.

Martin J, Yung S, Robson RL, Steadman R, Davies M: Production and regulation of matrix metalloproteinases and their inhibitors by human peritoneal mesothelial cells. *Perit Dial Int* 20(5):524-33, 2000.

Mavrothalassitis GJ, Watson DK, Papas TS: Molecular and functional characterization of the promoter of ETS2, the human c-ets-2 gene. *Proc Natl Acad Sci U S A* 87(3):1047-51, 1990.

McCormack SA, Viar MJ, Johnson LR: Migration of IEC-6 cells: a model for mucosal healing. *Am J Physiol* 263(3 Pt 1):G426-35, 1992.

McGregor SJ, Brock JH, Briggs JD, Junor BJ: Longitudinal study of peritoneal defence mechanisms in patients on continuous ambulatory peritoneal dialysis (CAPD). *Perit Dial Int* 9(2):115-9, 1989.

McGregor SJ, Topley N, Jorres A, Speekenbrink AB, Gordon A, Gahl GM, Junor BJ, Briggs JD, Brock JH: Longitudinal evaluation of peritoneal macrophage function and activation during CAPD: maturity, cytokine synthesis and arachidonic acid metabolism. *Kidney Int* 49(2):525-33, 1996.

McLoughlin RM, Hurst SM, Nowell MA, Harris DA, Horiuchi S, Morgan LW, Wilkinson TS, Yamamoto N, Topley N, Jones SA: Differential regulation of neutrophil activating chemokines by IL-6 and its soluble receptor isoforms. *The Journal of Immunology* 172(9):5676-83, 2004.

McLoughlin RM, Jenkins BJ, Grail D, Williams AS, Fielding CA, Parker CR, Ernst M, Topley N, Jones SA: IL-6 trans-signalling via STAT3 direct T cell infiltration in acute inflammation. *Proc Natl Acad Sci* 5(27):9589-94, 2005.

Monslow J, Williams JD, Guy CA, Price IK, Craig KJ, Williams HJ, Williams NM, Martin J, Coleman SL, Topley N, Spicer AP, Buckland PR, Davies M, Bowen T: Identification and analysis of the promoter region of the human hyaluronan synthase 2 gene. *J Biol Chem* 279(20):20576-81, 2004.

Morgan LW, Weislander A, Davies M, Horiuchi T, Ohta Y, Beavis MJ, Braig KJ, Williams JD, Topley N: Glucose degradation products (GDP) retard remesothelialization independently of D-glucose concentration. *Kidney international* 64(5):1854-66, 2003.

Mortier S, Faict D, Schalkwijk CG, La,iere NH, De Vriese AS: Long-term exposure to new peritoneal dialysis solutions: Effects on the peritoneal membrane. *Kidney International* 66(3):1257-65, 2004.

Mustaers SE: The mesothelial cell. *Int J Biochemistry & Cell Biology* 36(1):9-16, 2004.

Mutsaers SE, Whitaker D, Papadimitriou JM: Mesothelial regeneration is not dependent on subserosal cells. *J Pathol* 190(1):86-92, 2000.

Naito Y, Yoshikawa T: Role of matrix metalloproteinases in inflammatory bowel disease. *Mol Aspects Med* 26(4-5):379-90, Review, 2005.

Nagata A, Hirota N, Sakai T, Fujimoto M, Komoda T: Molecular nature and possible presence of a membranous glycan-phosphatidylinositol anchor of the CA125 antigen. *Tumor Biology* 12(5):279-86, 1991.

Nagy JA, Jackman RW: Anatomy and physiology of the peritoneal membrane. *Seminars in Dialysis* 11:49-56, 1998.

Nakai T, Sakahara H, Endo K, Shirato M, Kobayashi H, Hosono M, Saga T, Sakamoto M, Konishi J: Changes in CA125 release and surface expression caused by drugs in uterine cervix adenocarcinoma cells. *Ann Nucl Med* 7(3):133-9, 1993.

Nitz T, Eisenblatter T, Psathaki K, Galla HJ: Serum-derived factors weaken the barrier properties of cultured porcine brain capillary endothelial cells in vitro. *Brain Res* 981(1-2):30-40, 2003.

Nonogaki H, Fujii S, Konishi I, Nanbu Y, Kobayashi F, Mori T: Serial changes of serum CA125 levels during menstrual cycles. *Asia Oceania J Obstet Gyneacol* 17(4):369-78, 1991.

Nustad K, Bast RC Jr, Brien TJ, Nilsson O, Seguin P, Suresh MR, Saga T, Nozawa S, Borner OP, de Bruijn HW, Nap M, Vitali A, Gadnell M, Clark J, Shigemasa K, Karlsson B, Kreutz FT, Jette D, Sakahara H, Endo K, Paus E, Warren D, Hammarstrom S, Kenemans P, Hilgers J: Specificity and affinity of 26 monoclonal antibodies against the CA125 antigen: First report from the ISOBM TD-1 workshop. *Tumour Biol* 17(4):196-219, 1996.

Nustad K, Onsrud M, Jansson B, Warren D: CA125-Epitopes and molecular size. *The International Journal of Biological Markers* 13(4):196-9, 1998.

O'Brien TJ, Raymond LM, Bannon GA, Ford DH, Hardardottir H, Miller FC, Quirk JG: New monoclonal antibodies identify the glycoprotein carrying the CA125 epitope. *Am J Obstet Gynecol* 165(6pt1):1857-64, 1991.

O'Brien TJ, Tanimoto H, Konishi I, Gee M: More than 15 years of CA125: What is known about the antigen, its structure and its function. *The international journal of biological markers* 13(4):188-95, 1998.

O'Brien TJ, Beard JB, Underwood LJ, Dennis RA, Santin AD, York L: The CA125 Gene: An extracellular superstructure dominated by repeat sequences. *Tumor Biology* 22(6):348-66, 2001.

O'Brien TJ, Beard JB, Underwood LJ, Shigemasa K: The CA125 gene: A newly discovered extension of the glycosylated N-terminal domain doubles the size of this extracellular superstructure. *Tumor Biology* 23(3):154-69, 2002.

Ohan J, Gilbert MA, Leseche G, Panis Y, Midoux P, Drouet L: Nonviral gene transfer into primary cultures of human and porcine mesothelial cells. *In Vitro Cell Dev Biol Anim* 37(7):402-7, 2001.

O'Neill LA: The role of MyD88-like adapters in Toll-like receptor signal transduction. *Biochem Soc Trans* 31(3):643-7, 2003.

Palmai-Pallag T, Khodabukus N, Kinarsky L, Leir SH, Sherman S, Hollingsworth MA, Harris A: The role of the SEA (sea urchin sperm protein, enterokinase and agrin) module in cleavage of membrane-tethered mucins. *FEBS J* 272(11):2901-11, 2005.

Parkash O: Presence of cytokines in the serum may affect the in vitro responses of T cells. *Acta Leprol* 12(1):5-6, 2001.

Pastan S, Bailey J: Dialysis Therapy. *N Eng J Med* 338(20):1428-37, 1998.

Perrais M, Pigny P, Ducourouble MP, Petitprez D, Porchet N, Aubert JP, Van Seuningen I: Characterization of human mucin gene MUC4 promoter: importance of growth factors and proinflammatory cytokines for its regulation in pancreatic cancer cells. *J Biol Chem* 276(33):30923-33, 2001.

Popovich RP, Moncrief JW, Nolph KD, Ghods AJ, Twardowski ZJ, Pyle WK: Continuous ambulatory peritoneal dialysis. *Ann Intern Med* 88(4):449-56, 1978

Prichard S: Will peritoneal dialysis be left behind? *Seminars in Dialysis* 18(3):167-70, 2005.

Quandt K, Frech K, Karas H, Wingender E, Werner T. MatInd and MatInspector: new fast and versatile tools for detection of consensus matches in nucleotide sequence data. *Nucleic Acids Res* 23(23):4878-84, 1995.

Rabinovich GA, Baum LG, Tinari N, Paganelli R, Natoli C, Liu FT, Iacobelli S: Galectins and their ligands: amplifiers, silencers or tuners of the inflammatory response. *Trends in Immunology* 23(6):313-20, 2002.

Rayet B, Gelinas C: Aberrant rel/nfkb genes and activity in human cancer. *Oncogene* 18(49):6938-47,1999.

Rippe B, Simonsen O, Heimbürger O, Christensson A, Haraldsson B, Stelin G, Weiss L, Nielsen FD, Bro S, Friedberg M, Wieslander A: Long-term clinical effects of a peritoneal dialysis fluid with less glucose degradation products. *Kidney International* 59(1):348-57, 2001.

Robson RL, McLoughlin RM, Witowski J, Loetscher P, Wilkinson TS, Jones SA, Topley N: Differential regulation of chemokine production in human peritoneal mesothelial cells: IFN-gamma controls neutrophil migration across the mesothelium *in vitro* and *in vivo*. *J Immunol* 167(2):1028-38, 2001.

Rosen DG, Wang L, Atkinson JN, Yinhua Y, Lu KH, Diamandis EP, Hellstrom I, Mok SC, Liu J, Bast RC: Potential markers that complement expression of CA125 in epithelial ovarian cancer. *Gynecologic Oncology* 99(2):267-77, 2005.

Rump A, Morikawa Y, Tanaka M, Minami S, Umesaki, Takeuchi, Miyajima A: Binding of ovarian cancer antigen CA125/MUC16 to mesothelin mediates cell adhesion. *The Journal of Biological Chemistry* 279(10):9190-98, 2004.

Ryan GB, Grobety J, Majno G: Mesothelial injury and recovery. *Am J Pathol* 71(1):93-112, 1973.

Ryan MJ, Johnson G, Kirk J, Fuerstenberg SM, Zager RA, Torok-Storb B: HK-2: an immortalized proximal tubule epithelial cell line from normal adult human kidney. *Kidney Int* 45(1):48-57, 1994.

Sakai H, Jinawath A, Yamaoka S, Yuasa Y: Upregulation of MUC6 mucin gene expression by NFkappaB and Sp factors. *Biochem Biophys Res Commun* 333(4):1254-60, 2005.

Sanchez R, Nguyen D, Rocha W, White JH, Mader S: Diversity in the mechanisms of gene regulation by estrogen receptors. *Bioessays*. 24(3):244-254, Review, 2002.

Sansui AA, Zweers MM, Weening JJ, De Waart DR, Struijk, Krediet RT: Expression of cancer antigen 125 by peritoneal mesothelial cells is not influenced by duration of peritoneal dialysis. *Peritoneal Dialysis International* 21(5):495-500, 2001.

Scholler N, Fu N, Yang Y, Ye Z, Goodman GE, Hellstrom KE, Hellstrom I: Soluble members(s) of the mesothelin/megakaryocyte potentiating factor family are detectable in sera from patients with ovarian carcinoma. *Proc Natl Acad Sci* 96(20):11531-536, 1999.

Seelenmeyer C, Wegehangel S, Lechner J, Nickel W: The cancer antigen CA125 represents a novel counter receptor for galectin-1. *Journal of Cell Science* 116(7):1305-18, 2003.

Shekels LL, Ho SB: Characterization of the mouse Muc3 membrane bound intestinal mucin 5' coding and promoter regions: regulation by inflammatory cytokines. *Biochim Biophys Acta* 1627(2-3):90-100, 2003.

Sitter T, Spannagl M, Schiffel H, Held E, van Hinsbergh VW, Kooistra T: Imbalance between intraperitoneal coagulation and fibrinolysis during peritonitis of CAPD patients: the role of mesothelial cells. *Nephrol Dial Transplant* 10(5):677-83, 1995.

Smale ST, Kadonaga JT: The RNA polymerase II core promoter. *Annu Rev Biochem* 72:449-79, 2003.

Smale ST: Transcription initiation from TATA-less promoters within eukaryotic protein-coding genes. *Biochim Biophys Acta* 1351(1-2):73-88, 1997.

Spicer AP, Parry G, Patton S, Gendler SJ: Molecular cloning and analysis of the mouse homologue of the tumor-associated mucin, MUC1, reveals conservation of potential O-

glycosylation sites, transmembrane, and cytoplasmic domains and a loss of minisatellite-like polymorphism. *J Biol Chem* 266(23):15099-109, 1991.

Strachan T, Read AP: *Human Molecular Genetics 2. Bios Scientific Publishers, 1999.*

Stylianou E, Jenner LA, Davies M, Coles GA, Williams JD: Isolation, culture and characterization of human peritoneal mesothelial cells. *Kidney Int* 37(6):1563-70, 1990.

Stylianou E, O'Neill LA, Rawlinson L, Edbrooke MR, Woo P, Saklatvala J: Interleukin-1 induces NF-kappa B through its type I but not its type II receptor in lymphocytes. *J Biol Chem* 267(22):15836-41, 1992.

Sun D, Guo K, Rusche JJ, Hurley LH: Facilitation of a structural transition in the polypurine/polypyrimidine tract within the proximal promoter region of the human VEGF gene by the presence of potassium and G-quadruplex-interactive agents. *Nucleic Acids Res* 33(18):6070-80, 2005.

Szeto CC, Lai KB, Chow KM, Szeto CYK, Li PKT: The relationship between peritoneal transport characteristics and messenger RNA expression of the aquaporin in the peritoneal dialysis effluent of CAPD patients. *J Nephrol* 18(2):197-203, 2005.

Tang S, Tan SL, Ramadoss SK, Kumar AP, Tang MH, Bajic VB: Computational method for discovery of estrogen responsive genes. *Nucleic Acids Res* 32(21):6212-17, 2004.

Tatusova TA, Madden TL: BLAST 2 Sequences, a new tool for comparing protein and nucleotide sequences. *FEMS Microbiol Lett* 174(2):247-50, 1999.

Thathiah A, Brayman M, Dharmaraj N, Julian JJ, Lagow EL, Carson DD: Tumor necrosis factor alpha stimulates MUC1 synthesis and ectodomain release in a human uterine epithelial cell line. *Endocrinology* 145(9):4192-203, 2004.

Topley N, Jorres A, Luttmann W, Petersen MM, Lang MJ, Thierauch KH, Muller C, Coles GA, Davies M, Williams JD: Human peritoneal mesothelial cells synthesize interleukin-6: induction by IL-1 beta and TNF alpha. *Kidney Int* 43(1):226-33, 1993.

Topley N, Jorres A, Luttmann W, Petersen MM, Lang MJ, Thierauch KH, Muller C, Coles GA, Davies M, Williams JD: Human peritoneal mesothelial cells synthesize interleukin-6: induction by IL-1 beta and TNF alpha. *Kidney Int* 43(1):226-33, 1993.

Topley N, Williams JD: Role of the peritoneal membrane in the control of inflammation in the peritoneal cavity. *Kidney Int Suppl* 48:S71-81, 1994.

Topley N: The cytokine network controlling peritoneal inflammation. *Perit Dial Int* 15(S7):S35-9, 1995.

Topley N: The host's initial response to peritoneal infection: the pivotal role of the mesothelial cell. *Perit Dial Int* 15(2):116-7, 1995.

Topley N, Liberek T, Davenport A, Li FK, Fear H, Williams JD: Activation of inflammation and leukocyte recruitment into the peritoneal cavity. *Kidney Int Suppl* 56:S17-21, 1996.

Topley N, Michael D, Bowen T: CA125: Holy grail or poisoned chalice?. *Nephron Clin Pract* 100(2):52-4, 2005.

Troidle L, Gorban-Brennan N, Kliger A, Finkelstein FO: Continuous Peritoneal Dialysis-Associated Peritonitis: A Review and Current Concepts. *Seminars in Dialysis* 16(6):428-37, 2003.

Vale L, Cody J, Wallace S, Daly C, Campell M, Grant A, Khan I, Donaldson C, MacLeod A: Continuous ambulatory peritoneal dialysis (CAPD) versus hospital or home

haemodialysis of end-stage renal disease in adults (Review), The Cochrane Collaboration, Wiley publishers, 2005.

Valente AJ, Graves DT, Vialle-Valentin CE, Delgado R, Schwartz CJ: Purification of a monocyte chemotactic factor secreted by nonhuman primate vascular cells in culture. *Biochemistry* 27(11):4162-8, 1988.

Van de Stolpe A, Slycke AJ, Reinders MO, Zomer AW, Goodenough S, Behl C, Seasholtz AF, van der Saag PT: Estrogen receptor (ER)-mediated transcriptional regulation of the human corticotropin-releasing hormone-binding protein promoter: differential effects of ERalpha and Erbeta. *Mol Endocrinol* 18(12):2908-23, 2004.

Van Seuningen I, Perrais M, Pigny P, Porchet N, Aubert JP: Sequence of the 5'-flanking region and promoter activity of the human mucin gene MUC5B in different phenotypes of colon cancer cells. *Biochem J* 348(3):675-86, 2000.

Verma M and Davidson EA: Mucin genes: Structure, expression and regulation. *Glycoconjugate Journal* 11(3):172-79, 1994.

Visser CE, Brou-Steenbergen JJE, Beijtes MGH, Koomen GCM, Beelen RHJ, Krediet RT: Cancer antigen 125: a bulk marker for the mesothelial mass in stable peritoneal dialysis patients. *Nephrol Dial Transplant* 10(1):64-9, 1995.

Voleti B and Agrawal A: Regulation of basal and induced expression of C-reactive protein through an overlapping element for OCT-1 and NF- κ B on the proximal promoter. *The Journal of Immunology* 175(5):3386-90, 2005.

Wear JB, Sisk IR, Trinkle AJ: Peritoneal Lavage in the treatment of uremia. *J Urol* 39:53-62, 1938.

Whitehouse C, Solomon E: Current status of the molecular characterization of the ovarian cancer antigen CA125 and implications for its use in clinical screening. *Gynecologic Oncology* 88(1pt2):S152-7, 2003.

Wieslander AP, Deppisch R, Svensson E, Forsback G, Speidel R, Rippe B: In vitro biocompatibility of a heat-sterilized, low-toxic, and less acidic fluid for peritoneal dialysis. *Perit Dial Int* 15(2):158-64, 1995.

Williams JD, Craig KJ, Topley N, Von Rhuland C, Fallon M, Newman GR, MacKenzie RK, Williams GT: Morphological changes in the peritoneal membrane of patients with renal disease. *J Am Soc* 13(2):470-9, 2002.

Williams JD, Craig KJ, Von Ruhland C, Topley N, Williams GT: The natural course of peritoneal membrane biology during peritoneal dialysis. *Kidney International* 64(88):S43-9, 2003.

Williams JD, Topley N, Craig KJ, MacKenzie RK, Pischetsrieder M, Lage C, Passlick-Deetjen: The Euro-balance Trial: The effect of a new biocompatible peritoneal dialysis fluid (balance) on the peritoneal membrane. *Kidney international* 66(1):408-18, 2004.

Williams NM, Bowen T, Spurlock G, Norton N, Williams HJ, Hoogendoorn B, Owen MJ, O'Donovan MC: Determination of the genomic structure and mutation screening in schizophrenic individuals for five subunits of the N-methyl-D-aspartate glutamate receptor. *Mol Psychiatry* 7(5):508-14, 2002.

Witowski J, Topley N, Jorres A, Liberek T, Coles GA, Williams JD: Effect of lactate-buffered peritoneal dialysis fluids on human peritoneal mesothelial cell interleukin-6 and prostaglandin synthesis. *Kidney Int* 47(1):282-93, 1995.

Witowski J, Wisniewska J, Korybalska K, Bender TO, Breborowicz A, Gahl GM, Frei U, Passlick-Deetjen J, Jorres A: Prolonged Exposure to glucose degradation products

impairs viability and function of human peritoneal mesothelial cells. *J Am Soc Nephrol* 12(11):2434-41, 2001.

Witowski J, Korybalska K, Ksiazek K, Wisniewska-Elnur J, Jorres A, Lage C, Schaub TP, Passlick-Deetjen J, Breborowicz A, Grzegorzewska A, Ksiazek A, Liberek T, Lichodziejewska-Niemierko M, Majdan M, Rutkowski B, Stompor T, Sulowicz W: Peritoneal dialysis with solutions low in glucose degradation products is associated with improved biocompatibility profile towards peritoneal mesothelial cells. *Nephrol Dial Transplant* 19(4): 917-24, 2004.

Warn R, Harvey P, Warn A, Foley-Comer A, Heldin P, Versnel M, Arakaki N, Daikuhara Y, Laurent GJ, Herrick SE, Mutsaers SE: HGF/SF induces mesothelial cell migration and proliferation by autocrine and paracrine pathways. *Exp Cell Res* 267(2):258-66, 2001.

Witz CA, Rodriguez IA, Cho S, Centonze VE, Bonewald LF, Schenken RS: Composition of the extracellular matrix of the peritoneum. *J Soc Gynecol Investig* 8(5):299-304, 2001.

Wong NK, Easton RL, Panico M, Sutton-Smith M, Morrison JC, Lattanzio FA, Morris HR, Clark GF, Dell A, Patankar MS: Characterization of the oligosaccharides associated with the human ovarian tumor marker CA125. *The Journal of Biological Chemistry* 278(31):28619-34, 2003.

Xu MJ, Cui Y, Hui N, Liu YJ: Effects of retinoic acid on proliferation and differentiation of a human ovarian carcinoma cell line: 3AO. *Chin Med Sci J* 20(1):51-4, 2005.

Yamagata K, Tomida C, Koyama A: Intraperitoneal hyaluronan production in stable continuous ambulatory peritoneal dialysis patients. *Perit Dial Int* 19(2):131-7, 1999.

Yanez-Mo M, Lara-Pezzi E, Selgas R, Ramirez-Huesca M, Dominguez-Jimenez C, Jimenez-Heffernan JA, Aguilera A, Sanchez-Tomero JA, Bajo MA, Alvarez V, Castro MA, del Peso G, Cirujeda A, Gamallo C, Sanchez-Madrid F, Lopez-Cabrera M:

Peritoneal dialysis and epithelial-to-mesenchymal transition of mesothelial cells. *N Engl J Med* 348(26):403-13, 2003.

Yin BWT and Lloyd KO: Molecular cloning of the CA125 ovarian cancer antigen. *The Journal of Biological Chemistry* 276(29):27371-75, 2001.

Yin BWT, Lloyd KO: Synthesis and secretion of the ovarian cancer antigen CA125 by the human cancer cell line NIH:OVCAR-3. *Tumor Biology* 22(2):77-82, 2001.

Yin BWT, Dnistrian A, Lloyd KO: Ovarian cancer antigen CA125 is encoded by the MUC16 mucin gene. *Int J Cancer* 98(5):737-40, 2002.

Yung S, Coles GA, Davies M: IL -1 beta, a major stimulator of hyaluronan synthesis in vitro of human peritoneal mesothelial cells: relevance to peritonitis in CAPD. *Kidney Int* 50(4):1337-43, 1996.

Yung S, Thomas GJ, Davies M: Induction of hyaluronan metabolism after mechanical injury of human peritoneal mesothelial cells *in vitro*. *Kidney Int* 58(5):1953-62, 2000.

Yung S, Davies M: Response of the human peritoneal mesothelial cell to injury: an in vitro model of peritoneal wound healing. *Kidney Int* 54(6):2160-9, 1998.

Zeillemarker AM, Verbrugh HA, Hoyneck van Papendrecht AGM, Leguit P: CA125 secretion by peritoneal mesothelial cells. *J Clin Pathol* 47(3):263-5, 1994.

Zeimet AG, Marth C, Offner FA, Obrist P, Uhl-Steidl M, Feichtinger H, Stadlmann S, Daxenbichler G, Dapunt O: Human peritoneal mesothelial cells are more potent than ovarian cancer cells in producing tumour marker CA-125. *Gynecologic Oncology* 62(3):384-9, 1996.

Zahm JM, Kaplan H, Herard AL, Doriot F, Pierrot D, Somelette P, Puchelle E: Cell migration and proliferation during the in vitro wound repair of the respiratory epithelium. *Cell Motil Cytoskeleton* 37(1):33-43, 1997.

Zhang MQ: Statistical features of human exons and their flanking regions. *Hum Mol Genet* 7(5):919-32, 1998.